JPL D-7382

Personal Access Satellite System (PASS) Study

Fiscal Year 1989 Results

M. K. Sue, Editor

September 1990

Jet Propulsion Laboratory
California Institute of Technology

The study described in this report was carried out by the Jet Propulsion Laboratory, California Institute of Technology, under NASA Research and Technology Operations Plan 650-60-15 (MSAT-X) for the National Aeronautics and Space Administration.

CONTRIBUTORS

Many individuals made significant contributions to the study, either in the writing of this report or by providing technical input/support. The principal authors for each chapter are listed at the beginning of the chapter. The following individuals are authors/contributors:

P. W. Cramer, Jr. (Section 332)
P. Estabrook (Section 331)
R. E. Freeland (Section 354)
V. Jamnejad (Section 336)
M. Motamedi (Section 339)
F. Manshadi (Section 336)
Y. Rahmat-Samii (Section 336)
M. K. Sue (Section 339)

In addition, B. K. Levitt (Section 331) and K. Dessouky (Section 339) have contributed to some of the work included in this report.

ACKNOWLEDGEMENT

We owe our appreciation to Dr. William Rafferty, JPL Satcom Program Manager, for his guidance and technical input that are both important to this study.

ABSTRACT

JPL is exploring the potential and feasibility of a personal access satellite system (PASS) that will offer the user greater freedom and mobility than existing and currently planned communications systems. Studies performed in prior years have resulted in a strawman design and the identification of technologies that are critical to the successful implementation of PASS. The study efforts in FY'89 have been directed towards alternative design options with the objective of either improving the system performance or alleviating the constraints on the user terminal.

The various design options and system issues studied this year and the results of the study are presented in this report. In addition, to support the PASS study, an in-depth survey was accomplished that focused on commercial IR&D developments of proprietary spacecraft antenna concepts. The results are documented in a separate report, "PASS Spacecraft Antenna Technology Study." This report is intended only for government use, and distribution will be based on written requests to the authors from authorized government agencies. For more information, please contact Robert E. Freeland at (818) 354-3540.

CONTENTS

CHAPTER 1

INTRODUCTION

Miles K. Sue

1.0 BACKGROUND

A recent study by the National Telecommunications and Information Administration (NTIA) has concluded that the 21st century will be the age of information in which the telecommunication infrastructure will be vital to the social and economic well being of our society [1]. To meet the challenge of the coming age, JPL has been performing studies on a personal access satellite system (PASS) for the 21st century. Such a system will advance satellite communications to a truly personal level. It will also augment terrestrial cellular systems by extending services to remote areas. Many innovative services can be supported: direct personal voice and data, personal computer file transfer, database inquiry and distribution, low-rate broadcast (voice, data, and video), telemonitoring and control, and disaster and emergency communications (see Figure 1.1). The long-term objectives of the PASS study are to develop and demonstrate system concepts and high-risk technologies leading to commercialization of a personal satellite communications system at the turn of the century.

The PASS study can be traced back to a 1987 study performed by Signatron under contract to JPL, in which the technical feasibility and potential applications of a high-frequency (20/30 GHz), low-data rate satellite system were identified using small fixed terminals [2]. Subsequent studies further expanded the applications to provide personal communications using compact personal terminals. By early 1989, a strawman system had been designed, and operational constraints and critical technologies had been identified [3,4,5]. Study efforts since then have been directed to refining the strawman design, alleviating operational constraints and providing solutions to some of the challenging problems.

In this chapter, we will first describe the PASS concept and strawman design and then identify the key challenges and possible solutions. Finally, we will summarize our plan for the future. (It should be noted that only key results are presented in this chapter. Detailed discussions are given in subsequent chapters.)

1.1 A BRIEF DESCRIPTION OF THE SYSTEM CONCEPT

PASS is a satellite-based personal communications system that will offer users freedom of access and mobility. Equipped with a user terminal, a subscriber will have, through the satellite, access to a host of voice and data services anywhere in the service area. The system will be capable of handling a range of data rates, starting from less than 100 bps for emergency and other low-rate services,

to 4.8 kbps for voice service, to T1 (1.544 Mbps) for high-rate services and computer file transfer.

The concept of PASS is illustrated in Figure 1.2. The system operator, service providers, and system users or subscribers are the players of the system. The major elements of PASS include one or more satellites; a network management center (NMC); tracking, telemetry and command (TT&C) stations; supplier stations; and user terminals. The satellites serve as a relay between the user and the supplier. The NMC and TT&C stations enable the system operator to control the operation of the system. User equipment includes three major types of user terminals: the basic personal terminal (BPT), the enhanced personal terminal (EPT), and telemonitors. The EPT is similar to today's VSAT terminals. The BPT is a compact personal terminal that will provide users greater freedom and mobility. The telemonitors are used for remote data collection and monitoring.

1.2 A BRIEF SUMMARY OF THE STRAWMAN DESIGN

1.2.1 System Description

The system contains a space segment, a network management center, supplier stations, and a number of user terminals. Services are facilitated by properly linking users and suppliers. The strawman architecture utilizes 142 fixed spotbeams to provide simultaneous, continuous coverage to users in the service area, i.e., CONUS. In addition to these spotbeams, a single CONUS beam is employed to complete the user-to-supplier and/or supplier-to-user links. The uplink frequency is 30 GHz and the downlink frequency is 20 GHz.

Access to the system by suppliers and users will be provided by means of a hybrid Time Division Multiple Access (TDMA)/Frequency Division Multiple Access (FDMA) scheme. A combination of uplink power control and an adjustable data rate is employed to combat rain attenuation. Uplink power control is for the forward link only, whereas a variable data rate is applicable for both directions.

A detailed description of the strawman design is given in [5].

1.2.2 High-Risk Enabling Technologies

Several high-risk enabling technologies have been identified. Some of these technologies are system architecture specific while others are not. The key enabling technologies are

- Low-Cost, Compact, High-Gain Tracking User Antennas
- Low-Cost, Accurate, User Terminal Frequency References
- MMIC Transmitters
- High-Gain, Low-Noise MMIC Receivers
- VLSI-Based Integrated Vocoder/Modem
- Efficient Multiple Access Schemes
- Multi-beam Antenna and Beam-Forming Network

- o Robust and Power-Efficient Modulation and Coding
- o Variable Rate Modem

Timely development and validation of these technologies are essential to the implementation of PASS.

1.2.3 Additional Technological Challenges

In addition to the above high-risk technologies, the strawman design reveals a number of challenges that are vital to the success of PASS. They are as follows [5]:

- o User Terminal Radiation Level
- o System Reliability and Service Quality During Rain
- o Stationary Operations Constraints
- o Nonuniform User Distribution
- o Choice of Frequency

1.3 POSSIBLE SOLUTIONS

The objectives of the FY'89 study are

- o To refine and/or optimize the strawman design by performing tradeoff studies and evaluating alternative design options, and

- o To overcome some of the obstacles identified in previous studies.

A number of studies have been performed to address the above challenges, with the objective of improving system performance, increasing system capacity, alleviating operational constraints, and/or reducing the burden on the spacecraft and user terminals. While many challenges still lie ahead, these studies have brought us one step closer to realizing the benefits of PASS.

1.4 SPREAD SPECTRUM MULTIPLE ACCESS (SSMA)

SSMA has been studied as an alternative multiple access technique because it promises the following benefits:

- o Provide users instant access to the system,
- o Enable ambulatory and even mobile operation by taking advantage of the inherent multipath rejection capability of SSMA, and
- o Increase system capacity by increasing coding gain.

1.4.1 Initial SSMA System Design

Our study effort has focused on direct-sequence SSMA. A system architecture based on code division multiple access (CDMA) has been investigated and documented in Chapter 2 and elsewhere [6]. CDMA is a subset of spread spectrum multiple access (SSMA). For convenience, these two terms are used interchangeably in this report. This system employs spread spectrum (SS) TDMA in the

forward direction and random-access code division multiple access (RA-CDMA) in the return direction. Our initial study indicates that the SSMA system will:

- Have system capacity and hardware complexity similar to the strawman design,
- Enable the user instant access to the system, and
- Result in minimum network control.

1.4.2 An SSMA System Using Powerful Codes

One major disadvantage of CDMA, based on the initial design, is that it will result in a significant increase in bandwidth requirements. One way to alleviate this problem is to employ on-board processing as discussed in Chapter 2, resulting in a much more complex satellite. Due to the large number of channels required, the feasibility of on-board processing is not certain and was not pursued. Another way to alleviate this problem is to take advantage of a property of SSMA that allows more coding gain without increasing the bandwidth. Studies performed after the initial design have indeed indicated that an SSMA system can have system capacity and bandwidth requirements comparable to the strawman system, by taking advantage of more powerful codes (such as rate 1/3, k=9, convolutional code or k=11 super-orthogonal code). Table 1.1, derived from [7], compares the bandwidth requirements and system capacity for CDMA and FDMA systems. The system capacity and bandwidth requirements shown in Table 1.1 were derived under a set of simplifying assumptions and are solely for the purpose of comparing CDMA and FDMA designs. They do not represent the actual system capacity nor the bandwidth requirements for PASS.

1.5 THE USE OF NON-GEOSTATIONARY ORBITS

The potential of non-geostationary orbits for PASS has been examined with the objective of reducing the burden on user terminals. Both elliptical and circular orbits have been examined. Low earth orbits in general have several important advantages over geostationary orbits:

- higher elevation angle and hence less multipath and rain attenuation,
- less space loss, and
- lower launch costs.

The major disadvantages of non-geostationary satellites are

- the large number of satellites required to provide continuous CONUS coverage,
- complicated spacecraft antenna pointing, and
- complex satellite handover.

The non-geostationary orbit study is discussed in Chapter 4. The major advantages and disadvantages are given in the following sections.

1.5.1 Impacts on Rain Attenuation

For a given location, rain attenuation in general is severer at low elevation angles than at high elevation angles. The exact amount depends on the link availability (LA) requirement. Figure 1.3 shows the % of time (P) that a given amount of rain attenuation is exceeded as a function of attenuation at 30 GHz for Portland, Maine with elevation angles as a parameter. P can be interpreted as the cumulative probability and is related to the link availability (LA), i.e., LA (%)= 100-P(%). As indicated in the figure, the attenuation at low elevation angles (near 20 degrees) for 99% availability is about 3 dB higher than that at high elevation angles (above 30 degrees). The difference however is reduced significantly as the link availability decreases. For PASS, which has an availability requirement of 95%-98% (see Section 1.8), non-geostationary satellites will not result in more than 2 dB improvement in rain attenuation.

1.5.2 Impacts on the Number of Required Satellites

Non-geostationary orbits have one major drawback for systems that are required to provide continuous and simultaneous coverage to a large geographical area. Figure 1.4 gives the number of satellites required to provide continuous CONUS coverage as a function of satellite orbits. In calculating the number of satellites, the size of the satellite multibeam antenna is adjusted such that the number of spotbeams required to cover CONUS is fixed at 142 beams. As shown, the number of satellites increases from 1 for the geostationary orbit to 3 for the Molniya orbit, to 8 for a 20,000 km circular orbit, and to almost 50 for a 50,000 km circular orbit.

1.5.3 Recommended Satellite Orbits for PASS

Based on this study, the use of non-geostationary satellites in place of geostationary ones is not recommended for PASS. However, non-geostationary satellites can be used to augment geostationary satellites in order to extend coverage to high-latitude regions, and can be extremely useful for an international personal communications satellite system providing personal communications and position determination services on a global scale.

1.6 INTERBEAM POWER MANAGEMENT

Nonuniform user distribution can significantly reduce the utilization of the satellite resource if not properly accounted for in the design of the satellite; a reduction of 50% or more is possible [5]. While this problem is common to all systems employing multiple spotbeams, the large number of spotbeams and hence small footprints in PASS exacerbates this problem. The mitigation of this problem is essential to the economic viability of PASS. One way to do this is to employ switched/scanning beams to dynamically adapt to traffic variations. The other way is to employ interbeam power management.

1.6.1 Alternative Antenna Coverage Concepts

Different antenna coverage concepts have been studied as a means to effectively mitigate the traffic variation problem. By dynamically varying the dwell times, a system employing scanning/switched beams can effectively adapt to traffic variations. Both scanning/switched beams and hybrid switched/fixed multiple beams have been studied. Results indicate that while these beam concepts can better utilize the satellite resource by adapting to traffic demand, there is an increase in satellite complexity and user terminal eirp. Specifically, the disadvantages are

- o Increased complexity for the antenna beam-forming network,
- o Increased message delays, and
- o Increased user transmitted data rate and radiated power.

The disadvantages have been judged to outweigh the benefits. Therefore, these beam coverage concepts are not recommended.

1.6.2 A Practical Adaptive Power Management Scheme

Another way to mitigate the problem of traffic variations is to incorporate an adaptive power management scheme in the beam-forming network. The basic idea is to design a beam-forming network such that a common set of power amplifiers is shared by all beams. Two techniques have been examined and are summarized in the following subsections (see Chapter 6 for more information).

1.6.2.1 A Hybrid Transponder Concept

The first technique employs a set of hybrids and input filters to enable power sharing and signal routing, and hence interbeam power management. A 4-port hybrid power management scheme is shown in Figure 1.5 as an example. (It is noted that the input filters are not shown in the figure.) This device is composed of 90-degree hybrids and is capable of providing power management for four beams. All signals that are present at the input filter for a given beam (Beam A for example) will be amplified by all amplifiers and transmitted via that beam (Beam A, see Figure 1.5). Because the same set of amplifiers is shared by all beams, the number of carriers (or channels) transmitted from each beam can be changed from 0 to a maximum value by selecting the appropriate carrier frequencies (channels), limited only by the total transmitter power and the input filter bandwidth. (One observation that can be made is that interbeam power management will result in a lower spectrum utility because a larger bandwidth will have to be allocated for each beam in order to accommodate traffic variations.)

1.6.2.2 A Phased-Array Near Field Concept

The second interbeam power management technique examined is principally the same as the first, but utilizes a set of phase

shifters instead of hybrids. This technique is illustrated in Figure 1.6.

1.6.2.3 The Recommended Interbeam Power Management for PASS

While there are advantages and disadvantages, both interbeam power management techniques are technically feasible and are applicable for systems having a limited number of spotbeams. Applying these techniques to PASS, which has 142 spotbeams, however will result in an unmanageably complex beam-forming network. In addition, the frequency reuse capability will be significantly reduced.

As a compromise, a partial interbeam power management scheme is proposed. Instead of interconnecting the 142 beams to achieve full interbeam power management, a nine-beam power management scheme is recommended. This scheme will interconnect 9 spotbeams, each with a distinct frequency assignment, to a set of shared amplifiers. This in effect reduces the traffic variation of 142 beams to a much more manageable 16 (142/9) groups of beams. By properly connecting beams with different user density, traffic variations among the 19 groups of beams can be reduced and hence the effective system capacity can be increased (see Appendix A for more details).

Figures 1.7-1.9 illustrate the nine-beam power management architecture. Figure 1.7 shows the transponder block diagram. Figure 1.8 shows the footprints of the 142 spotbeams and the corresponding frequency assignments. Due to the small footprints, the number of users in a beam can vary drastically from one beam to another. Figure 1.9 illustrates the nine-beam power management architecture. As shown, nine spotbeams each with a distinct frequency assignment are connected together to facilitate interbeam power management.

1.7 USER TERMINAL RADIATION

The current baseline design requires the user terminal to have a transmit antenna gain of about 23 dBi and a 0.17-W transmitter (see Section 1.10.5). Radiation safety is an important issue. Studies have been conducted to ensure that the radiation level complies with established safety standards. The findings are summarized as follows [8].

- The current ANSI standard for frequency above 1.5 GHz is 5 mW per square centimeter averaged over a 6-minute period. This standard includes a safety factor of 10 or more.

- At 30 GHz, the eye, particularly the cornea, is most susceptible to radiation damage due to the lack of blood circulation which drains the deposited heat.

- Independent experiments recently conducted by the USAF School of Aerospace Medicine using cat's eyes have indicated that incident densities up to 100 mW/cm^2 did not cause any harm [9].

Based on these findings, we believe that the radiation safety issue is manageable. By exploiting a combination of transmitter duty cycles (voice activity factor), call duration, antenna gain, and transmitted power, we feel that the safety standard can be complied with. For example, using current user terminal design values (23-dBi transmit antenna, 0.17-W transmitter power, and 14.5-dBW eirp), a 90-second call at 35% duty cycle would produce a peak radiation density of 3.6 mW averaged over a 6-minute period. The peak radiation density occurs at a point on the antenna boresight at a distance about 6 cm from the antenna aperture. The radiation density drops off rapidly as the distance from the aperture increases. The peak radiation density can be further reduced by employing a larger user antenna. If we increase the antenna gain for example from 23 to 25 dBi and maintain the same eirp, the resulting peak radiation level would be reduced to about 1 mW/cm^2, averaged over a 6-minute interval. Appendix B and Chapter 5 address this issue in more detail.

1.8 SYSTEM RELIABILITY AND SERVICE QUALITY

The strawman system as well as the current baseline design employs a combination of uplink power control and an adjustable data rate to combat rain attenuation. Uplink power control is applicable for the uplinks from the suppliers and EPTs. When increased uplink power from the suppliers/EPTs fails to fully compensate for rain degradation, the data rate will be reduced to close the link. No uplink power control will be employed by BPTs due to the limited power capability of the small terminals. Instead, only a variable data rate scheme will be used. During rain, the data rate will be reduced by a factor equal to multiples of 2. These schemes will result in a reduction of service quality or even the termination of certain services during heavy rain. A quantitative assessment of the impacts on service availability has been performed and results are summarized below. (It is noted that there are techniques, such as the use of a processing satellite, that alleviate this problem; however, they have not been actively pursued. On-board processing may not be suitable for PASS due to the large number of single-channel-per-carrier [SCPC] channels.)

1.8.1 Desired Service Availability

Link or service availability is a measure of system performance. Rain attenuation affects the link availability and sufficient rain margin must be provided to maintain a desired link availability. Higher link availability requires a correspondingly large rain margin. Business-oriented and safety-related systems usually require an extremely high availability, i.e., 99.9% or better. A huge rain margin would normally be required for these systems. PASS is mainly to provide personal communications, and consequently can accept a lower service availability. The design goal is to maintain 95% to 98% availability for the basic personal communications services, i.e., 4.8 kbps voice. Accepting a slightly lower availability would significantly reduce the required rain margin, which could result in cost savings and complexity reduction.

1.8.2 Estimated Rain Attenuation

Rain attenuation varies from one location to another. To assess the extent of rain attenuation, five locations in CONUS have been selected for analysis: Seattle, Los Angeles, Mobile, Miami, and Portland (Maine). These locations approximately represent the four corners of CONUS and one southern location. The percentage of time that a given attenuation is exceeded as a function of the attenuation has been computed using a rain model developed by Manning [10]. The resulting data are shown in Figures 1.10 and 1.11 for the uplink frequency (20 GHz) and the downlink frequency (30 GHz), respectively. These figures show that for 98% of the time, the rain attenuation will not exceed approximately 1.0 dB at 20 GHz and 2.5 dB at 30 GHz. For 99.9% of the time, the attenuation will not exceed 20-40 dB.

1.8.3 Estimated Link (Service) Availability

The service availability for the forward and return link has been analyzed in Appendix C in detail. Results show that the current link design provides an estimated 98% availability at 4.8 kbps and about 99% at 2.4 kbps. While these results are based on the limited locations examined, they indicate that the proposed rain compensation technique is adequate for PASS.

Table 1.2 summarizes the estimated rain attenuation, the corresponding degradation on the overall signal-to-noise ratio (SNR), and the proposed compensation techniques.

1.9 CHOICE OF FREQUENCY

The system is designed to operate in the 20/30 GHz bands. While there are advantages, there are a number of issues associated with these bands:

- The wide separation of transmit and receive frequencies may present a technical problem to the design of the user antenna.
- These bands are sensitive to rain attenuation.

A number of studies have been performed to address these issues.

1.9.1 The 20/30 GHz Separation Problem

The wide separation between transmit and receive frequencies raises a question whether separate antennas for transmit and receive will have to be used. The technical feasibility of using the 20/30 GHz bands for PASS has been examined (Chapter 6). Based on studies conducted, we believe that it is technically feasible to use the 20/30 GHz bands, although a band-pair with a smaller separation (such as 20/21 GHz or 20/22 GHz) is preferable.

The 20/21 GHz or 20/22 GHz band-pair has two advantages: (1) easier for the design of user antennas, and (2) lower rain attenuation on

the uplink. Rain attenuation can be significantly different at 20 and 30 GHz, depending on the desired link availability. For the assumed 98% PASS link availability, the difference is small (about 1 dB), as illustrated in Figures 1.12 and 1.13.

Although it is more desirable in terms of antenna designs to have a narrower separation between transmit and receive frequencies, the technical challenges posed by the 20/30 GHz separation are manageable. By using dual resonant radiating elements or interleaved transmit and receive arrays, a single antenna can be designed to operate at these frequencies (Chapter 5). In addition, the wide separation can improve the isolation between the transmit and receive signals. The isolation requirement often is a design driver for the diplexer.

1.9.2 20/30 GHz vs. Lower-Frequency Bands (UHF, L-band, etc.)

The 20/30 GHz bands are more suitable for PASS than lower-frequency bands (UHF, L-band, etc.) for three reasons, as explained in [5]:

- There are ample, unused spectra in the 20/30 GHz bands that will alleviate the spectrum congestion existing in lower-frequency bands, and accommodate future growth.
- These bands have the potential for developing compact user terminals, which are the key to the realization of PASS.
- The use of these bands will enable PASS to benefit from 20/30 GHz technology programs, including the opportunity for an early demonstration of PASS using NASA's ACTS.

One disadvantage of the 20/30 GHz bands is that these frequencies are much more susceptible to rain effects than L- and C-bands, and hence may require a much higher link margin. For PASS-type systems that do not require an extremely high link availability, rain attenuation is manageable based on studies performed.

1.10 SUMMARY OF CURRENT BASELINE SYSTEM DESIGN

The various trade studies performed this year have resulted in some modifications and refinement of the strawman design. These studies also reaffirm some of the decisions on the selection of many of the key features of the strawman system. Only the key features and features that are different from the strawman design are summarized in the following sub-sections. A complete description of the PASS system concept is given in [5].

1.10.1 The Space Segment

The satellite employs fixed multibeams to provide simultaneous, continuous coverage to users in the service area, i.e., CONUS. In addition, the satellite has a single CONUS beam to link suppliers to the satellite. A nine-beam interbeam power management is

employed to mitigate the problem of traffic variations. The transponder block diagram is shown in Figure 1.7.

1.10.2 Multiple Access Scheme

Access to the system by suppliers and users will be provided by means of a hybrid TDMA/FDMA scheme. In the forward direction, suppliers gain access to the system using TDMA. There will be 142 uplink channels at 100 kbps for the BPTs, one for each spotbeam. Each supplier will be assigned to a time slot for each of these channels for transmission of its uplink signals. Signals destined to different users in the same beam will be time multiplexed (TDM) onto a single channel before transmission. The TDMA architecture maximizes the utilization of satellite power in the forward direction, which is severely constrained by the available satellite power. (It should be noted that there is a 300-kbps channel in each beam for the EPTs. The multiple access technique for these high-rate [300-kbps] channels is the same as for the low-rate [100-kbps] channels. The discussion here focuses on the BPT. A more complete description of the entire system is given in [5].)

In the return direction, access to the system by users is provided using narrowband SCPC architecture, and a frequency division, demand assigned multiple access (FD-DAMA) scheme. Each user will be assigned a dedicated channel on a demand assigned basis.

1.10.3 Rain Attenuation Compensation Techniques

As stated earlier, a combination of uplink power control and an adjustable data rate is employed for PASS and the resulting service availability is estimated to be 98% at 4.8 kbps and about 99% at 2.4 kbps.

1.10.4 Operating Frequency

The uplink frequency is in the 30-GHz band and the downlink frequency is in the 20-GHz band. These frequency bands have ample bandwidth and good potential for compact terminals, and allow the early demonstration of system concepts and technology on NASA's ACTS.

1.10.5 Link Budgets

A detailed link budget is shown in Table 1.3 for the return link. This budget is for voice communications using a 4.8-kbps digital voice. This link is designed to provide a 1.0E-3 bit-error rate (BER) with a 3-dB link margin in clear weather. The 1.0E-3 BER is sufficient for providing good quality voice. Data messages generally require a lower BER in order to minimize packet errors. Additional FEC coding therefore will be needed for data messages and will increase the overhead accordingly.

Table 1.4 is a similar link budget for the forward link. Although the signals in the forward direction are time-division multiplexed and normally operate at 100 kbps, the link budget was performed for

a hypothetical voice channel operating at 4.8 kbps. Similar to the return link, the forward link is sized to provide a 3-dB margin during clear weather. Due to the TDM/TDMA architecture, the forward link is designed to provide 1.0E-5 BER, which is adequate for voice and data communications.

1.10.6 System Capacity

Economic viability is a very important factor that will determine whether PASS will be implemented commercially. While there are many factors affecting PASS's economic viability, the significance of system capacity cannot be overstated. Studies have shown that large-capacity systems benefit from economy of scales. Towards that end, the system has been optimized for a higher capacity. Using a high-power commercial satellite bus having a GTO mass of 6500 lbs, the estimated system capacity is equivalent to 7500 duplex voice channels. The capacity is based on the assumption that all user terminals are BPTs (a worst case scenario), and that all traffic is voice, with a voice activity factor of 0.35. The actual capacity depends on the voice and data traffic mix and user equipment mix (i.e., BPT, EPT and telemonitors).

The number of users who can be supported is a function of the traffic model, which is characterized by parameters such as traffic mix, grade of service, and offered traffic. Assuming a typical traffic scenario and including users of EPTs and telemonitors, the number of users who can be served by PASS can easily exceed one million.

1.10.7 Salient Features and Summary of Design Requirements

The salient features of the system are presented in Table 1.5. Design requirements for the satellite and the BPT are given in Tables 1.6 and 1.7.

1.10.8 Alternative System Architecture

The study of multiple access techniques has identified the potential of a spread-spectrum-based architecture. This system would employ TDMA and SSMA in combination with satellite switching.

In the forward direction, the architecture is very similar to the baseline design. Suppliers will access the satellite using a wideband TDMA channel. The satellite received signals will be demodulated, buffered, remodulated, frequency converted, spread by a PN sequence generated on-board the satellite, and transmitted via the spotbeams. The complexity of on-board spreading of 142 signals is within current technology capability and is not expected to result in significant mass and power penalties.

The multiple access technique for the return direction is SSMA. The signal transmitted by each user is spread by a PN sequence as described in Chapter 2.

The spread spectrum signal structure in both the forward and return directions enables full realization of some of the benefits of a spread spectrum system.

1.11 FUTURE PLAN

As currently conceived, PASS is a satellite-based communications system designed to provide a variety of services, ranging from low-rate personal communications to high-rate computer file transfer. The 21st century will be the age of information with the existence of various space and terrestrial telecommunications media. Expansion and advancement of these systems will create fierce competition. This will dictate the integration of space and terrestrial networks and force each to play an optimized role in the telecommunications infrastructure, ultimately benefiting the user. Telecommunications in the 21st century will be characterized by diversity of services, choice of media, and user-transparent, optimized information routing. In recognition of these trends, a two-prong approach has been adopted with the following objectives.

The first objective is to continue the 20/30 GHz PASS system study and technology development with the goal of advancing Ka-band technology in general and Ka-band mobile/personal technology in particular. Technologies targeted for development are user antennas, user terminal components (vocoder/modem, transceiver, MMIC front-end, and frequency reference), modulation and coding, rain compensation techniques, and multiple access schemes. It is our plan to incorporate these technologies into the ACTS mobile terminal (AMT) to the extent possible and conduct a field demonstration using ACTS. The AMT is currently being developed by JPL to demonstrate Ka-band mobile applications.

The expansion of cellular phones suggests they will play a significant role in personal communications in the 21st century. Considering this and other telecommunications trends, the second objective is to specifically address the roles of communications satellites in personal communications and to devise a system concept for an integrated satellite/ground personal communications network. Such a network will provide choice of media and route selection. The key to integrating the characteristically and architecturally different space and terrestrial telecommunications networks lies in compatible networking protocols. The ultimate objective is to devise a system concept capable of providing personal communications to the user using a truly universal personal terminal.

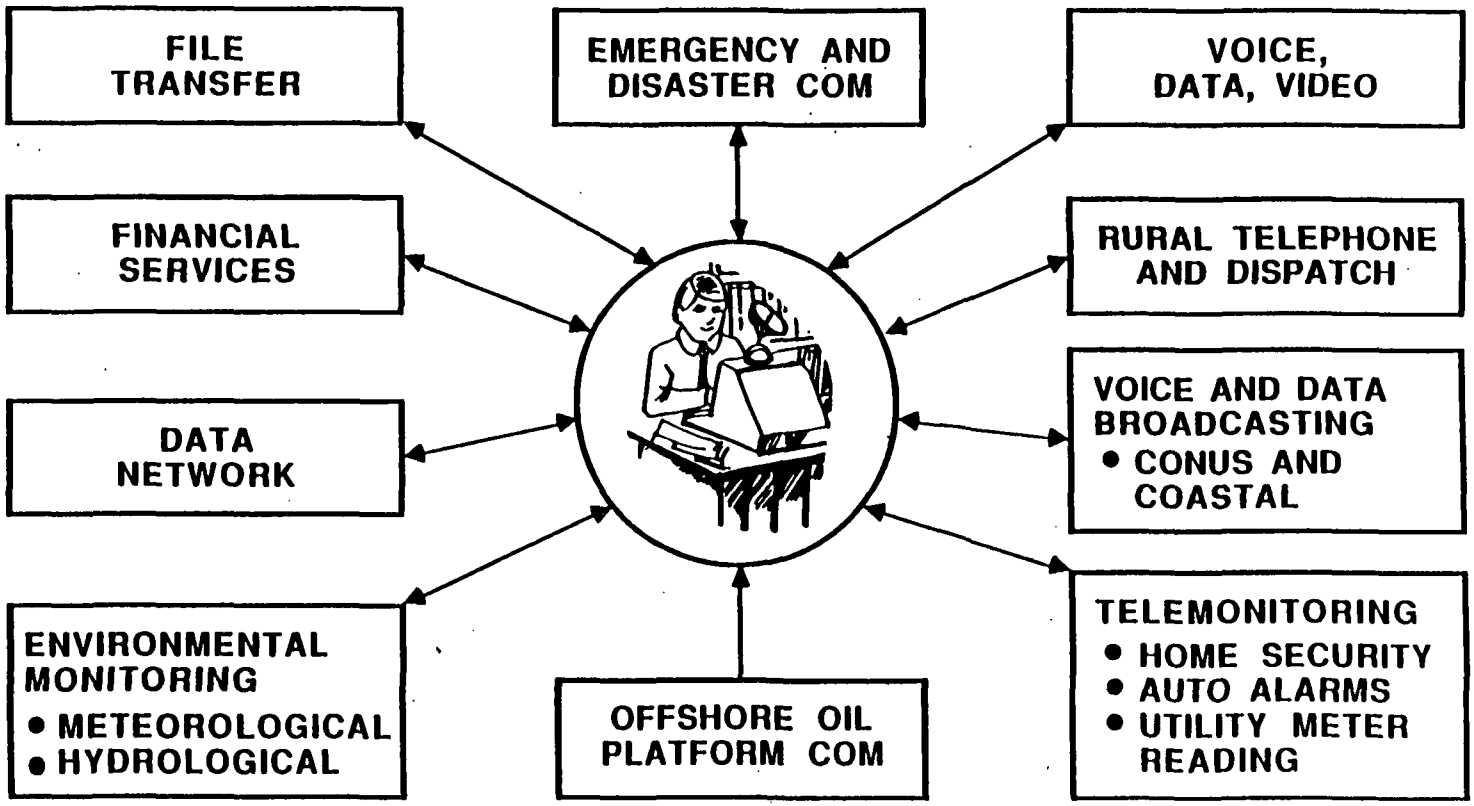

Figure 1.1. Potential Applications for PASS

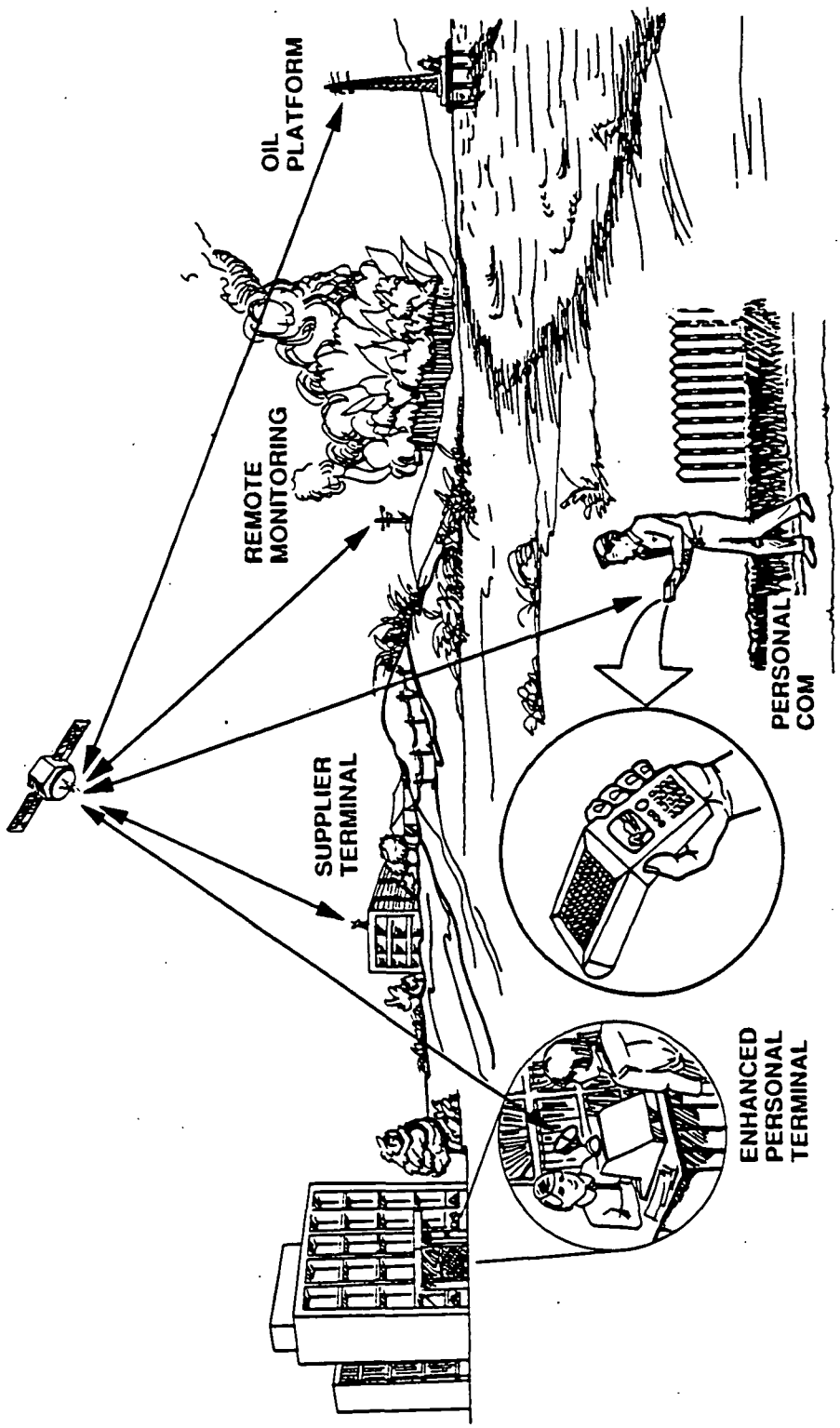

Figure 1.2. PASS Concept

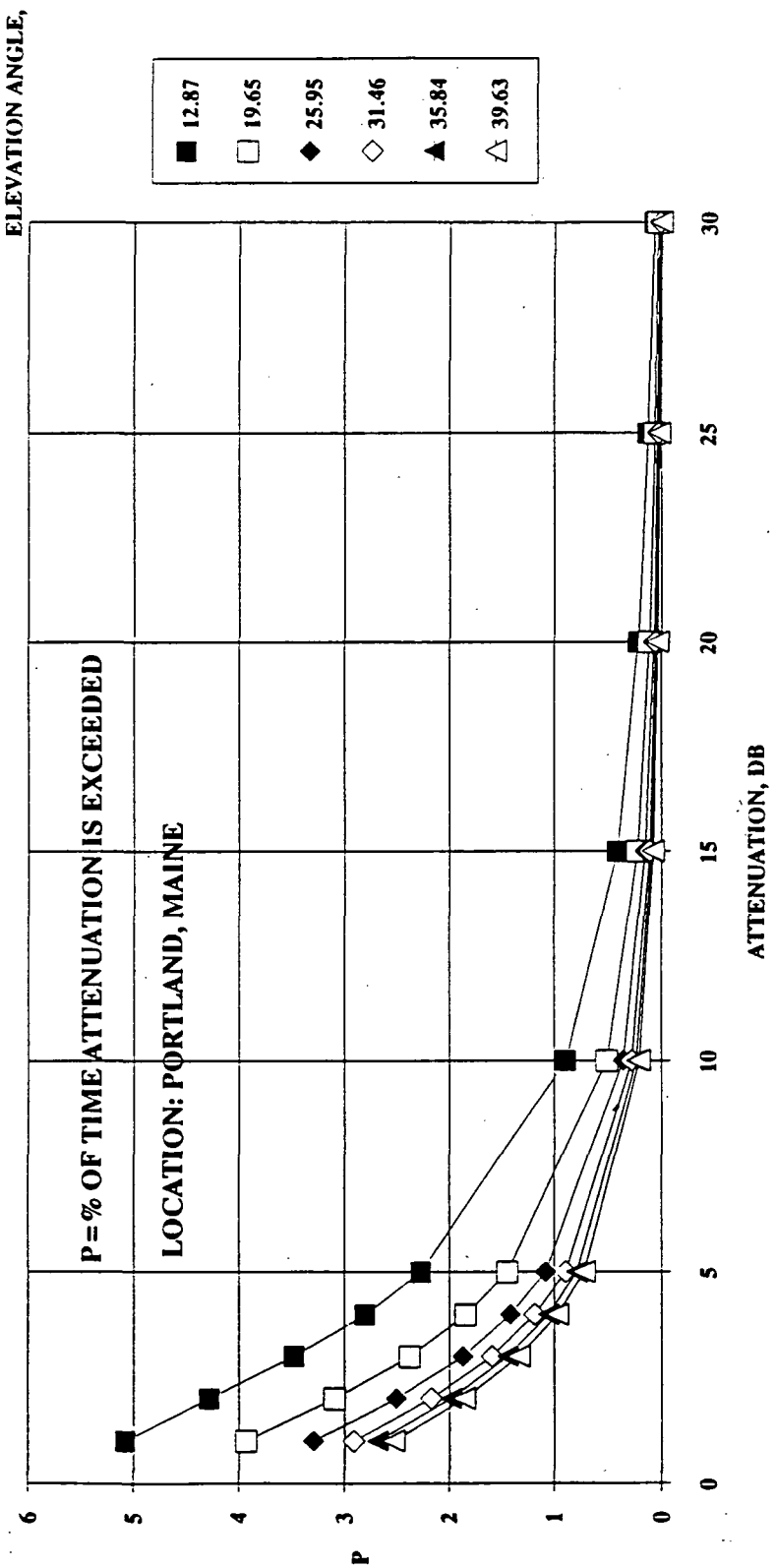

Figure 1.3. Rain Attenuation for Selected Elevation Angles

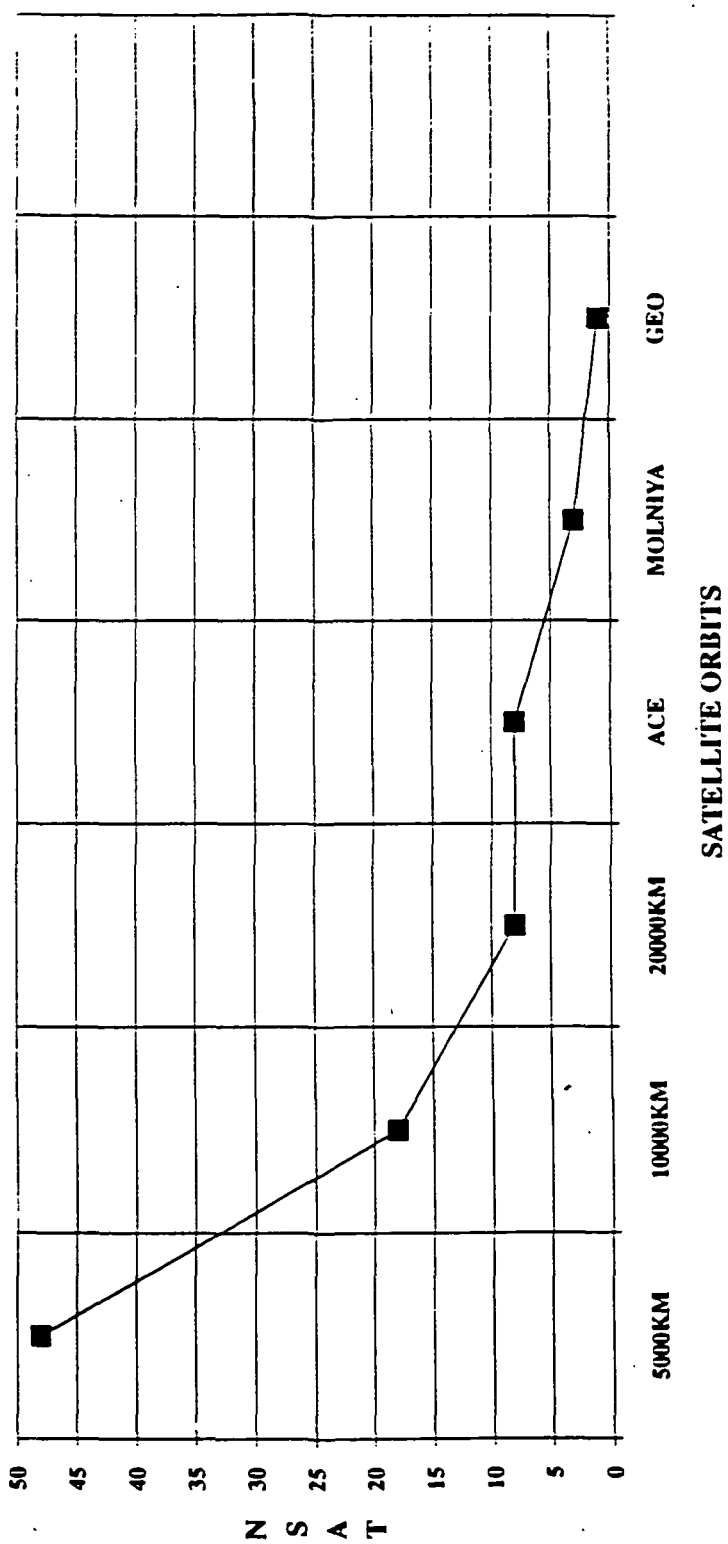

Figure 1.4. Number of Satellites vs. Satellite Orbits for CONUS Coverage (Derived from Chapter 4)

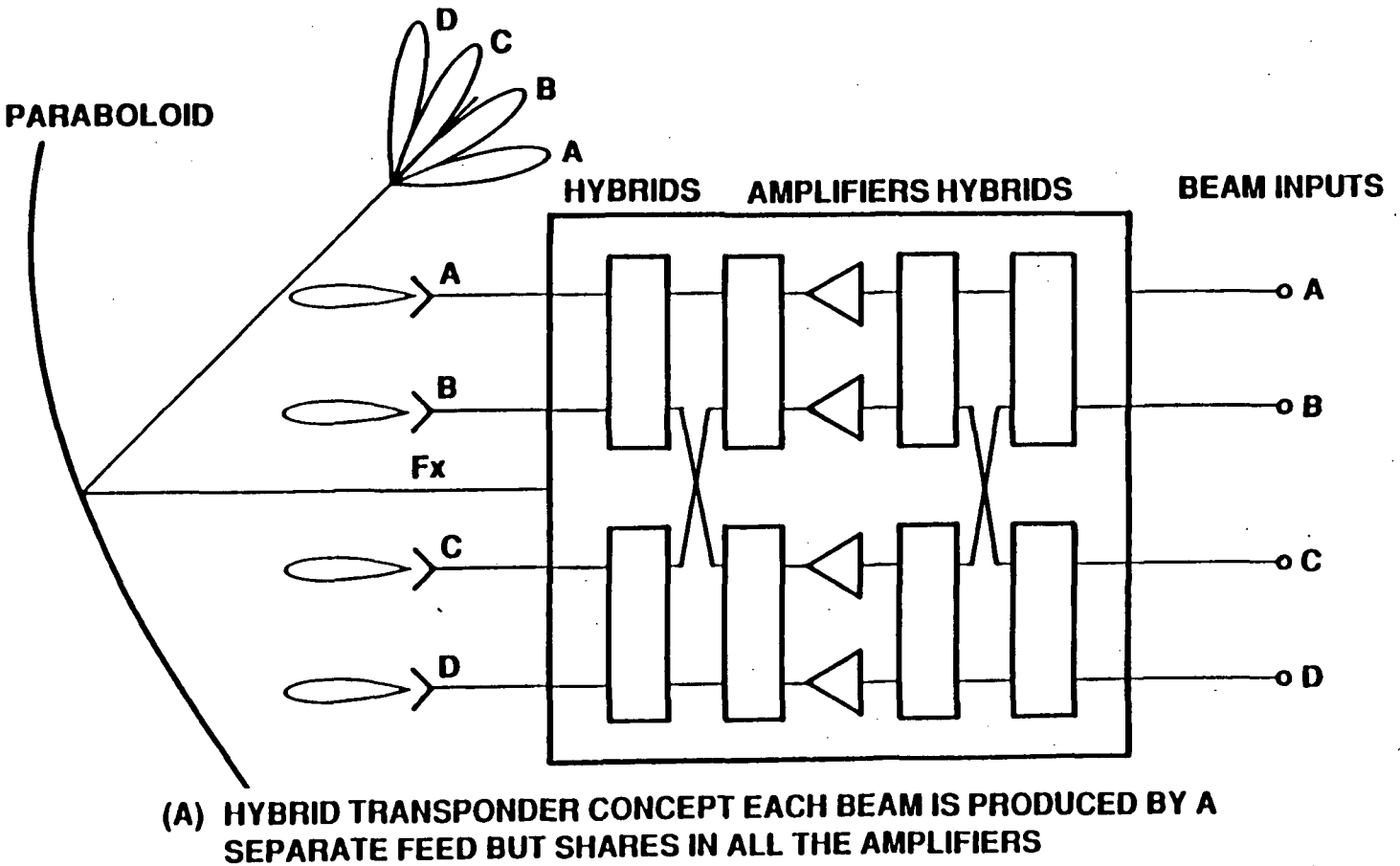

Figure 1.5. A Hybrid Transponder Concept for Interbeam Power Management (Derived from Chapter 6)

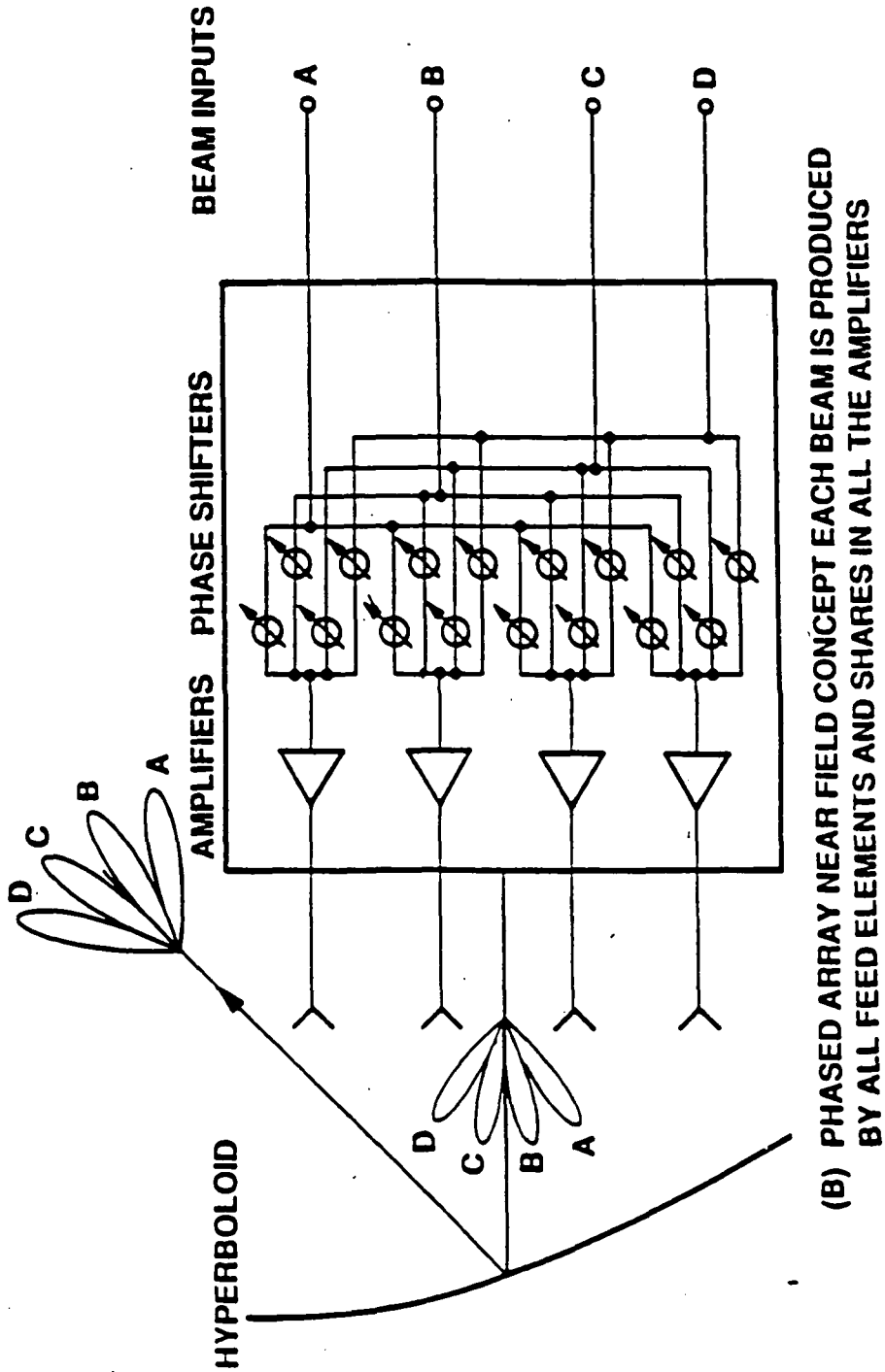

Figure 1.6. A Phased Array Near-Field Concept for Interbeam Power Management (Derived from Chapter 6)

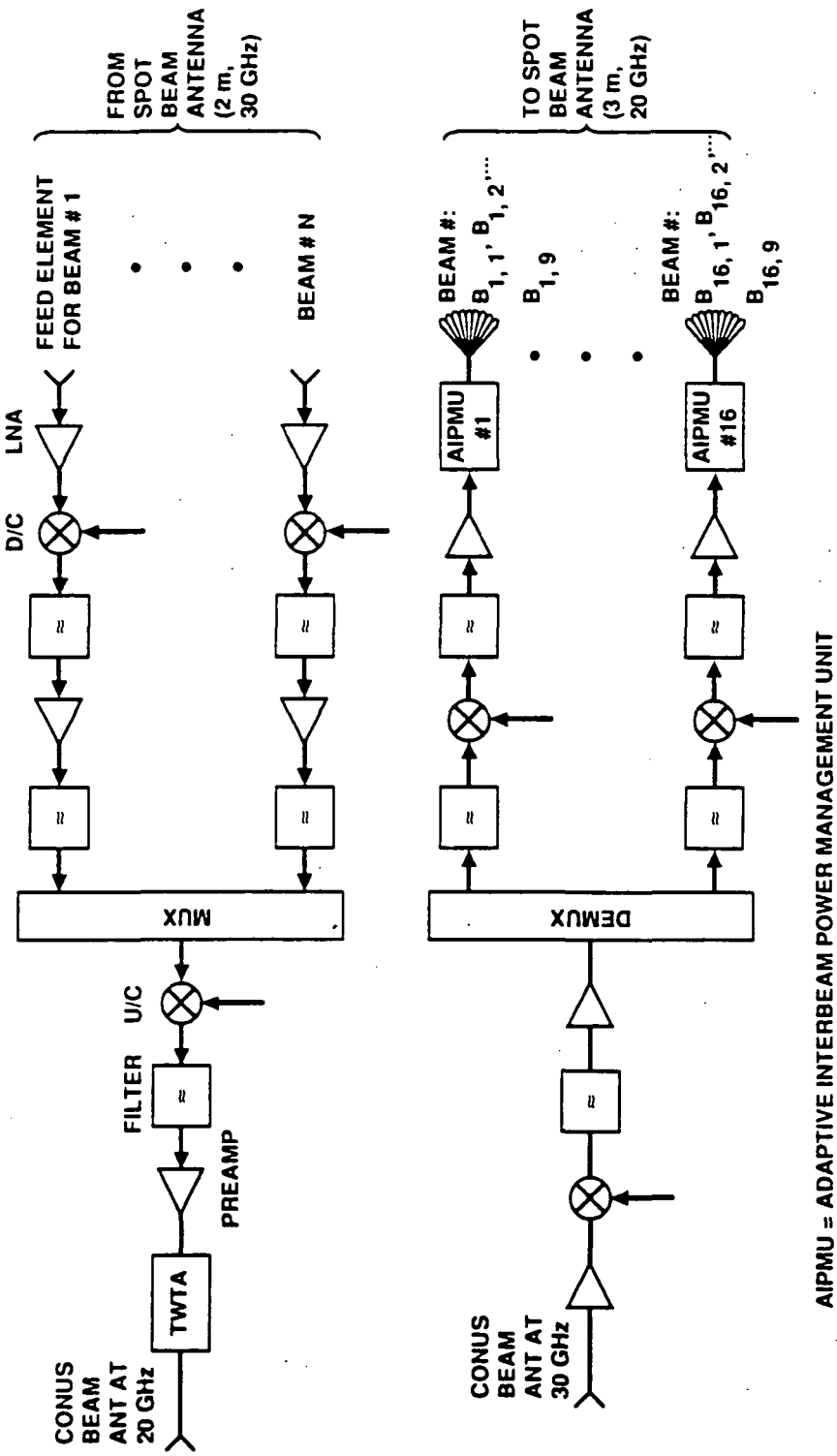

Figure 1.7. Transponder Block Diagram with 9-Beam Interbeam Power Management

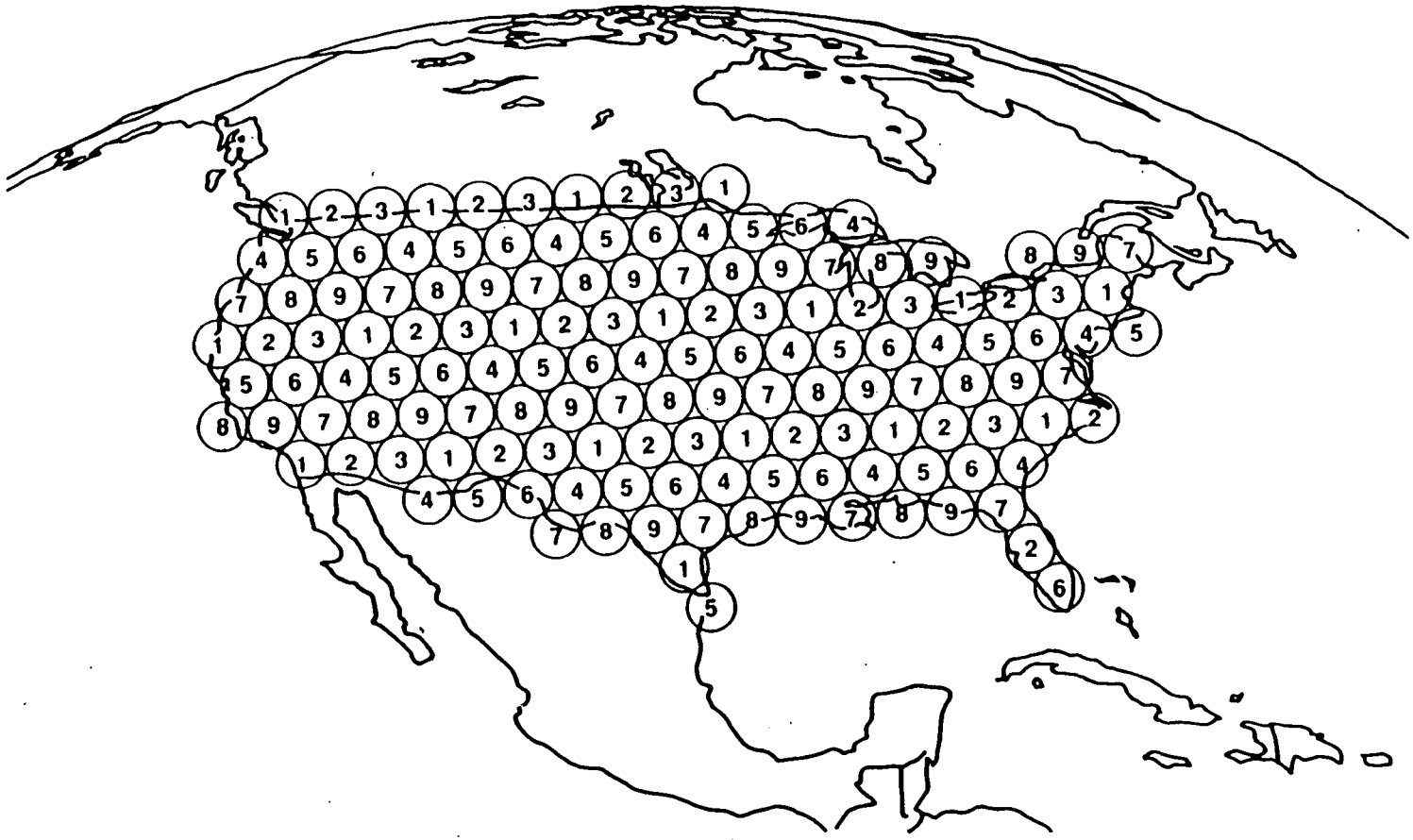

NOTE: NUMBER IN EACH BEAM DENOTES THE FREQUENCY SUBBAND ASSIGNMENT FOR THAT BEAM.

Figure 1.8. Frequency Assignments for the 142 Multiple Spotbeams with 9-Frequency Reuse [Chapter 6]

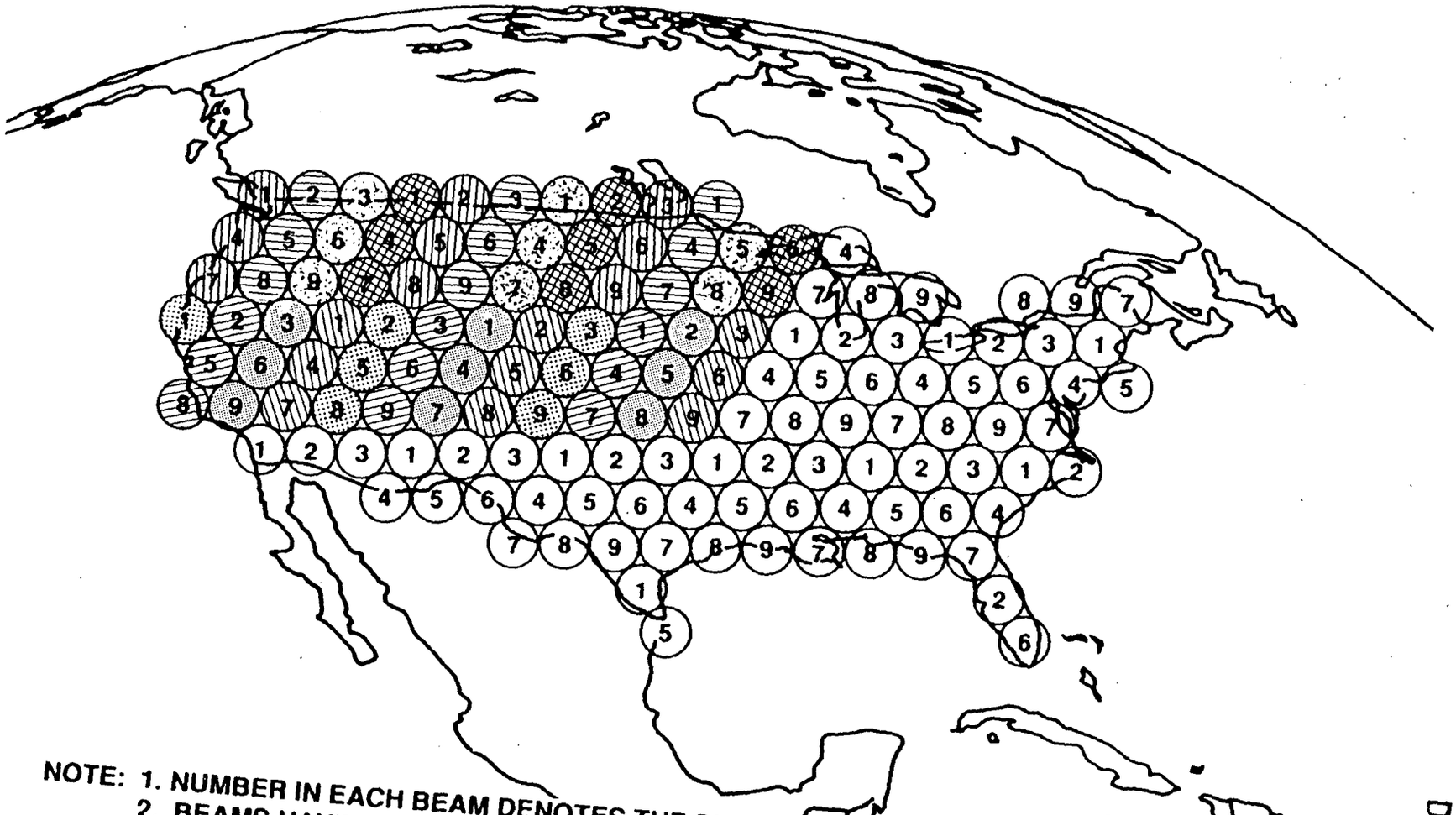

NOTE: 1. NUMBER IN EACH BEAM DENOTES THE SUBBAND ASSIGNMENT FOR THAT BEAM.
2. BEAMS HAVING THE SAME SHADED PATTERN BELONG TO THE SAME GROUP AND ARE CONTROLLED BY THE SAME INTERBEAM POWER MANAGEMENT UNIT. THIS FIGURE GIVES THE ARCHITECTURE FOR ONLY 8 GROUPS OF BEAMS, OUT OF A TOTAL OF 16 GROUPS.

Figure 1.9. An Illustration of Beam/Frequency Architecture for the 9-Beam Interbeam Power Management

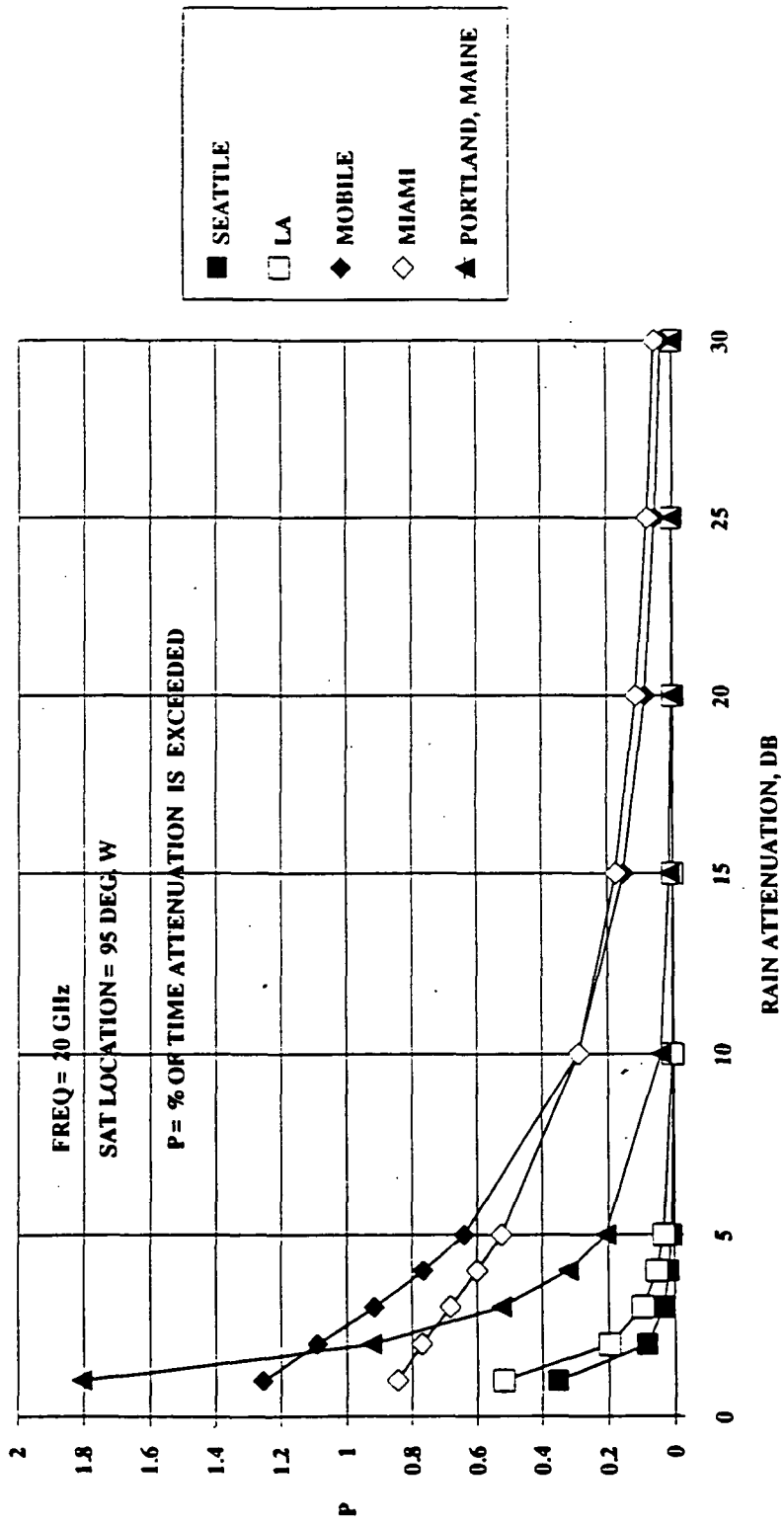

Figure 1.10. Rain Attenuation at 20 GHz for Selected Locations

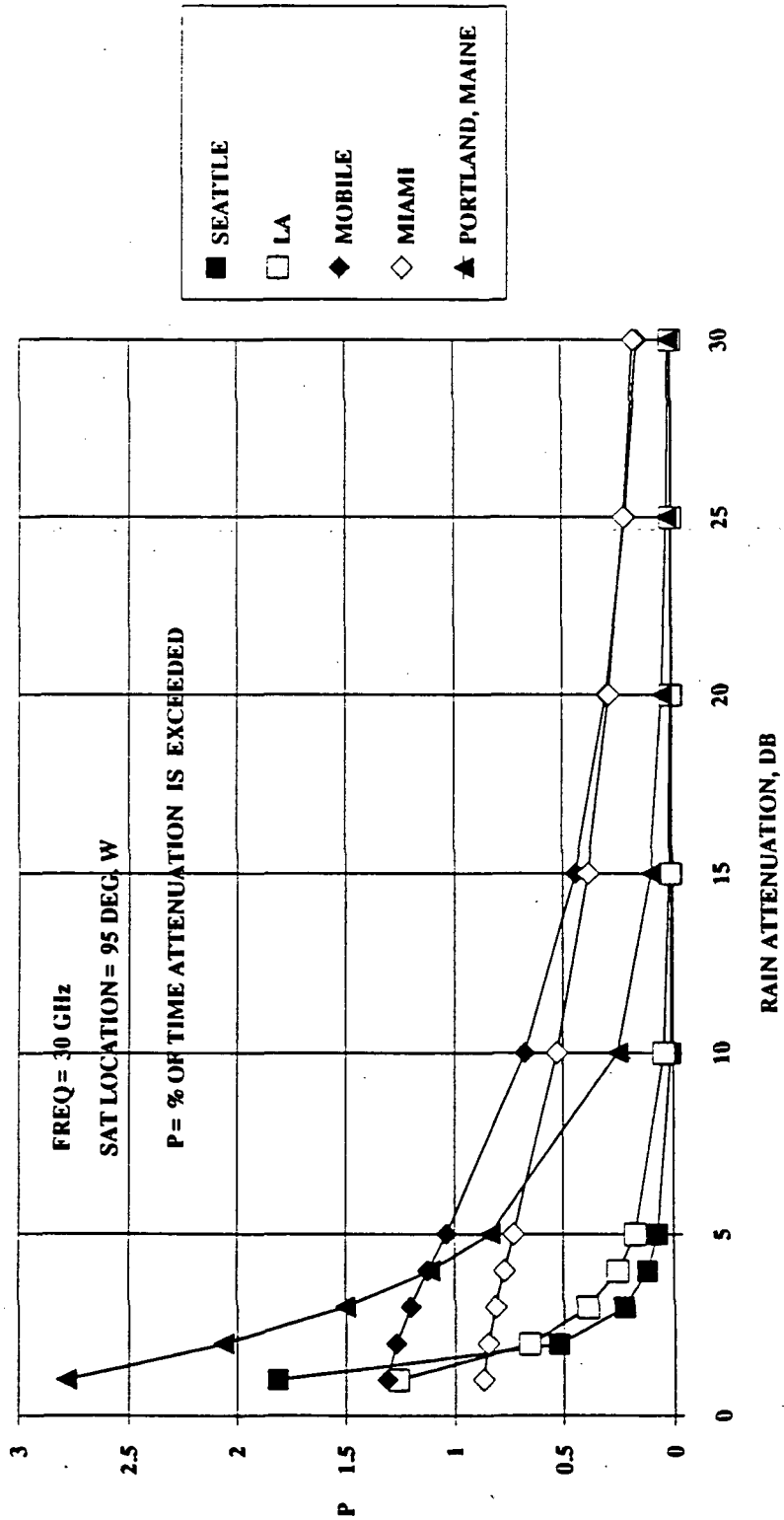

Figure 1.11. Rain Attenuation at 30 GHz for Selected Locations

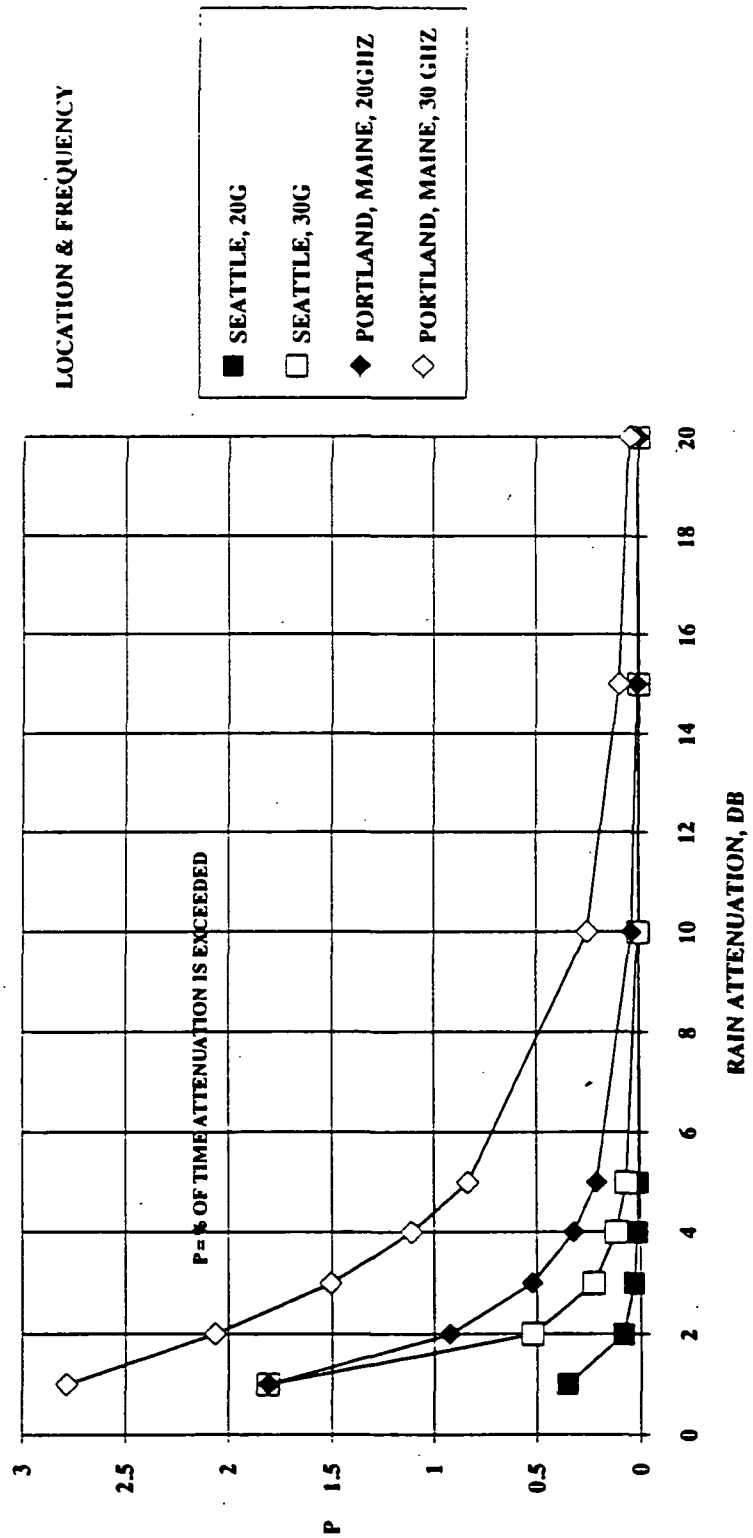

Figure 1.12. Percentage of Time vs. Rain Attenuation at 20 and 30 GHz for Selected Locations (Seattle, and Portland, Maine)

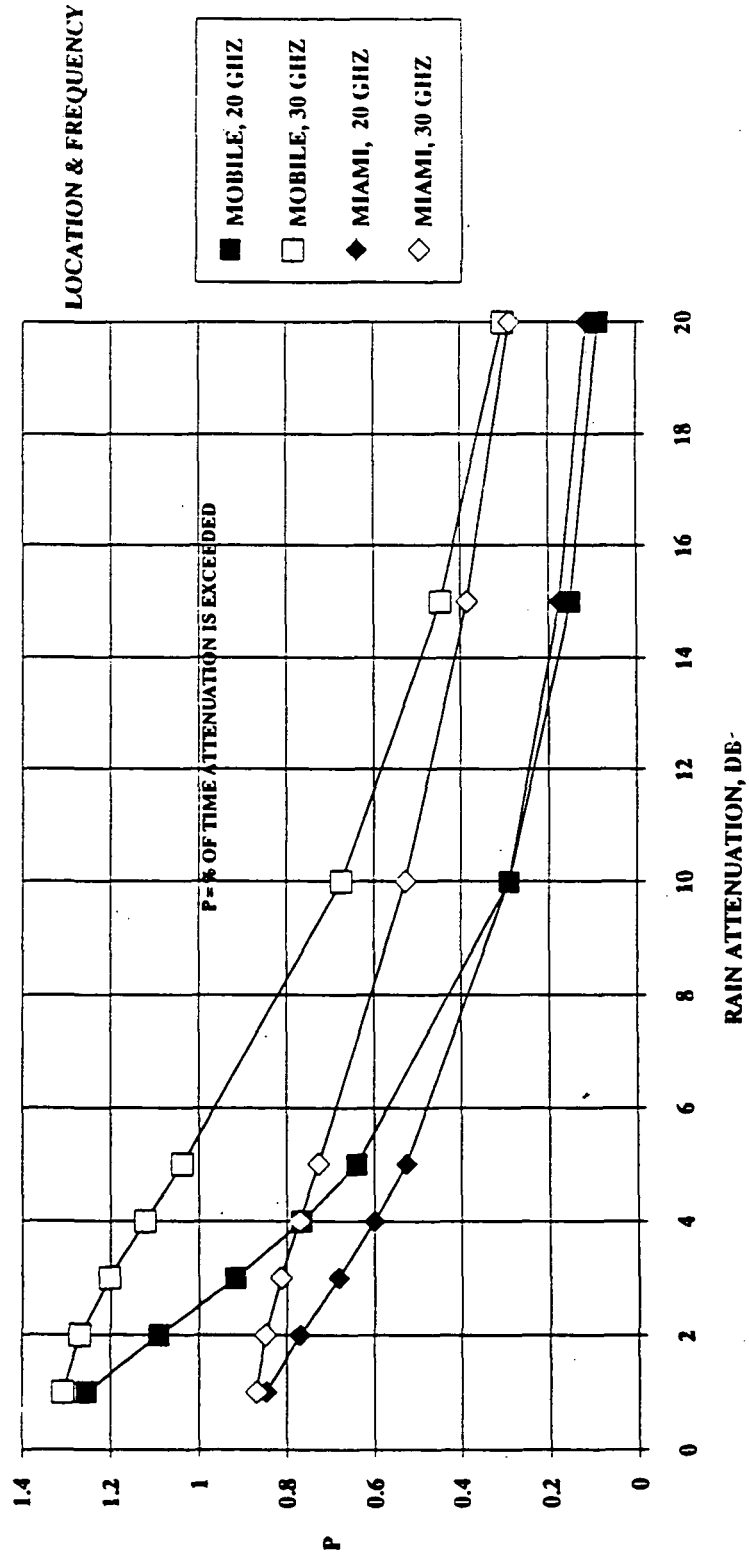

Figure 1.13. Percentage of Time vs. Rain Attenuation at 20 and 30 GHz for Selected Locations (Mobile and Miami)

Table 1.1. Relative Capacities and Bandwidth Requirements for CDMA and FDMA [7]

ACCESS SCHEMES	LINK Eb/N0 dB	CODING (CONVOLUTIONAL)	CAPACITY (#CHANNELS) RETURN	FORWARD	BANDWIDTH (MHz) UP-LINK	DN-LINK	TOTAL	SAT RF POWER SPLIT(TOT/F/R)
FDMA (RET)/ TDMA (FWD)	3	R=1/2, K=7	8072	8216	111.8	110.3	222.1	410/390/20 W
"	2.3	R=1/3, K=7	9483	9653	183.4	181	364.4	410/390/20 W
CDMA (RET)/ TDMA (FWD)	2.3	R=1/3, K=7	10143	8452	65.1	183	248.1	410/335/75 W
"	1.5 (R)/ 2.3 (F)	SUP. ORTH.(K=10)/ R=1/3, K=7	10142	9331	69.1	180	249.1	410/375/35 W
FDMA (RET)/ TDMA (FWD)	3	R=1/2, K=7	10493	10433	142.3	143	285.3	520/494/26 W
"	2.3	R=1/3, K=7	12328	12258	233.6	234.6	468.2	520/494/26 W
CDMA (RET)/ TDMA (FWD)	2.3	R=1/3, K=7	12171	10565	78.6	206.4	285	520/425/95 W
"	1.5	R=1/3, K=9	13894	13523	99.8	258.2	358	520/470/50 W
"	"	"	19069	11411	85.1	225	310.1	520/390/130 W
"	1.5 (R)/ 2.3 (F)	S. ORTH.(K=11)/ R=1/3, K=7	17851	11411	101.8	356.3	458.1	520/460/60 W

Note: For a 10:1 data-to-voice traffic ratio, a 1.4 s average message delay, 2% voice blocking probability, 90 s/call/user/hr, 1000 bits/data message, one channel can servean average of 100 users

Table 1.2

Rain Attenuation, SNR Degradation, and Compensation Techniques

	FREQ (GHZ)	ATTEN-UATION (DB)	OVERALL SNR DEGRADATION (DB)	COMPENSATION TECHNIQUES[1]
FORWARD:				
UPLINK	30	2.5	0	UPLINK POWER CONTROL
DOWNLINK	20	1.0	1.5	WITHIN NORMAL LINK MARGIN
RETURN:				
UPLINK	30	2.5	2.5	WITHIN NORMAL LINK MARGIN
DOWNLINK	20	1.0	<0.1	NEGLIGIBLE EFFECTS ON THE OVERALL SNR

(1) To achieve 98% link availability for BPTs.

Table 1.3. Return Link Budget for BPTs (4.8 kbps Voice, Clear Sky, 20-Degree Elevation, 1.0E-3 BER, R=1/2, and K=7)

		USER TO SAT					SAT TO SUPPLIER				
	PDF	DESIGN	FAV TOL	ADV TOL	MEAN	VAR (X.01)	DESIGN	FAV TOL	ADV TOL	MEAN	VAR (X.01)
TRANSMITTER PARAMETERS	---										
1)XMIT POWER,DBW	TRI	-7.80	.3	.3	-7.80	1.50	-15.00	.30	.30	-15.00	1.50
2)XMIT CIRCUIT LOSS,DB	REC	-.50	.1	.4	-.65	2.08	-.50	.10	.40	-.65	2.08
3)ANTENNA GAIN,DBI	TRI	22.80	.5	.5	22.80	4.17	26.90	.50	.50	26.90	4.17
4)EIRP,DBW ((1)+(2)+(3))		14.50			14.35		11.40			11.25	
5)POINTING LOSS,DB	TRI	-1.55	.68	.88	-1.62	10.20	.00	.00	.00	.00	.00
PATH PARAMETERS											
6)SPACE LOSS,DB		-214.03			-214.03		-210.51			-210.51	
(FREQUENCY,GHZ/GHZ =		30.00					20				)
(RANG= 40000 KM)											
7a)ATMOSPHERIC ATTN, DB	TRI	-.70	.50	.50	-.70	4.17	-.90	.40	.40	-.90	2.67
7b)RAIN ATTN, DB	TRI	.00	.00	.00	.00	.00	.00	.00	.00	.00	.00
8)E.O.B.LOSS,DB	TRI	-4.00	1	1	-4.00	4.17	-3.00	.50	.50	-3.00	4.17
9)MULTIPATH LOSS,DB	GAU	.00	0	0	.00	.00	.00	.00	.00	.00	.00
10)SHADOWING LOSS,DB	DEL	.00	0	0	.00		.00	.00	.00	.00	
RECEIVER PARAMETERS											
11)POLARIZATION LOSS,DB	TRI	-.50	0	0	-.50	.67	-.50	.20	.20	-.50	.67
12)ANTENNA GAIN,DBI	TRI	52.50	1	1	52.50	16.67	57.50	1.00	1.00	57.50	16.67
13)POINTING LOSS,DB	TRI	-1.23	0	0	-1.23	.00	-.09	.02	.02	-.09	.01
14)RECEIVED SIGNAL POWER,DBW		-155.01			-155.23		-146.10			-146.25	
(SUM OF LINES 4 - 13)											
15)SYSTEM TEMPERATURE,DBK	GAU	29.07	.30	.61			27.15	.62	.95		
(CIRCUIT LOSS,DB =		-1.50	0	0			-1.00	.10	.40		)
(RCVR N.F. ,DB =		3.00	0	0			3.00	.20	.20		)
(EXTERNAL ANT TEMP,K =		280.00	0	0			81	20	18		)
(INTERNAL ANT TEMP,K =		.00	0	0			.00	0	0		
(RAIN INDUCED TEMP,K =		.00	0	0			.00	0	0		
16)RECEIVED NO,DBW/HZ	GAU	-199.53	.30	.61	-199.38	2.30	-201.45	.62	.95	-201.28	6.78
((15)-228.6 DBW/HZ)											
(BANDWIDTH,KHZ =		20.00					20.00				)
CHANNEL PERFORMANCE											
17)RCVD C/NO,DB-HZ ((14)-(16))		44.52			44.15		55.34			55.03	
18)EFFECTIVE C/NO,DB-HZ		44.50			44.13		55.16			54.86	
(OVERALL C/I,DB =	GAU	26.00	1	1	26.00	11	26.00	1.00	1.00	26.00	11.11)
(INTERBEAM ISOLATION =		26.00	1.00	1.00			99.00	1.00	1.00	99.00	)
(INTERSAT. ISOLATION =		99.00	.50	.50			99.00	.50	.50	99.00	)
(INTERMOD ISOLATION =	TRI	99.00	1.00	1.00			26.00	1.00	1.00	26.00	)
(TURNAROUND C/NO =	GAU						44.50			44.13	57.03)
(NO(UP)/NO(REQUIRED) =		.75		.25			.75				)
19) END-TO-END C/NO, DB-HZ							43.91			43.78	
20) MODEM/RADIO LOSS, DB=	TRI	.00			.00		-1.00	.30	.30	-1.00	1.50)
21)REQUIRED C/NO,DB-HZ		41.06			41.06		39.81			39.81	
(REQUIRED EB/NO,DB							3.00				)
		---			---	---	---			---	---
22)PERFORMANCE MARGIN,DB		3.44			3.07	.76	3.09			2.97	1.04
((19)+(20)-(21))						(1 SIG)					(1 SIG)

Table 1.4. Forward Link Budget for BPTs (4.8 kbps Equivalent Voice/Data Channels, Clear Sky, 20-Degree Elevation, 1.0E-5 BER, R=1/2, and K=7)

		SUPPLIER TO SAT.					SAT TO USER				
	PDF	DESIGN	FAV TOL	ADV TOL	MEAN	VAR (X.01)	DESIGN	FAV TOL	ADV TOL	MEAN	VAR (X.01)
TRANSMITTER PARAMETERS	---										
1)XMIT POWER,DBW	TRI	-3.00	.30	.30	-3.00	1.50	-6.80	.30	.30	-6.80	1.50
2)XMIT CIRCUIT LOSS,DB	REC	-1.00	.10	.40	-1.15	2.08	-1.50	.10	.40	-1.65	2.08
3)ANTENNA GAIN,DBI	TRI	57.50	1.00	1.00	57.50	16.67	52.50	1.00	1.00	52.50	16.67
4)EIRP,DBW ((1)+(2)+(3))		53.50			53.35		44.20			44.05	
5)POINTING LOSS,DB	TRI	-.09	.02	.02	-.09	.01	-1.23	.05	.05	-1.23	.04
PATH PARAMETERS											
6)SPACE LOSS,DB		-214.03			-214.03		-210.51			-210.51	
(FREQUENCY,GHZ/GHZ =		30.00					20				)
(RANG= 40000 KM)·											
7a)ATMOSPHERIC ATTN, DB	TRI	-.70	.50	.50	-.70	4.17	-.90	.40	.40	-.90	2.67
7b)RAIN ATTN, DB	TRI	.00	.00	.00	.00	.00	.00	.00	.00	.00	.00
8)E.O.B.LOSS,DB	TRI	-3.00	.50	.50	-3.00	4.17	-4.00	.50	.50	-4.00	4.17
9)MULTIPATH LOSS,DB	GAU	.00	.00	.00	.00	.00	.00	.00	.00	.00	.00
10)SHADOWING LOSS,DB	DEL	.00	.00	.00	.00		.00	.00	.00	.00	
RECEIVER PARAMETERS											
11)POLARIZATION LOSS,DB	TRI	-.50	.20	.20	-.50	.67	-.50	.20	.20	-.50	.67
12)ANTENNA GAIN,DBI	TRI	26.90	.50	.50	26.90	4.17	19.30	.50	.50	19.30	4.17
13)POINTING LOSS,DB	TRI	.00	.00	.00	.00	.00	-.70	.29	.40	-.74	2.00
14)RECEIVED SIGNAL POWER,DBW		-137.92			-138.07		-154.34			-154.53	
(SUM OF LINES 4 - 13)											
15)SYSTEM TEMPERATURE,DBK	GAU	28.06	.30	.61			28.23	.60	.86		
(CIRCUIT LOSS,DB =		-.50	.10	.40			-.50	.10	.40		)
(RCVR N.F. ,DB =		3.00	.20	.20			3.50	.20	.20		)
(EXTERNAL ANT TEMP,K =		280.00	0	0			107	20	18		)
(INTERNAL ANT TEMP,K =		.00	0	0			119.60	18	19		
(RAIN INDUCED TEMP,K =		.00	0	0			.00	0	0		
16)RECEIVED NO,DBW/HZ	GAU	-200.54	.30	.61	-200.39	2.32	-200.37	.60	.86	-200.24	5.91
((15)-228.6 DBW/HZ)											
(BANDWIDTH,KHZ =		20.00					20.00				)
CHANNEL PERFORMANCE											
17)RCVD C/NO,DB-HZ ((14)-(16))		62.62			62.32		46.03			45.71	
18)EFFECTIVE C/NO,DB-HZ		62.24			61.96		45.98			45.67	
(OVERALL C/I,DB =	GAU						22.99	1.00	1.00	22.99	11.11)
(INTERBEAM ISOLATION =							26.00	1.00	1.00	26.00	)
(INTERSAT. ISOLATION =							99.00	.50	.50	99.00	)
(INTERMOD ISOLATION =	TRI	30.00	1.00	1.00	30.00	16.67	26.00	1.00	1.00	26.00	)
(TURNAROUND C/NO =	GAU						62.24			61.96	52.41)
(NO(UP)/NO(REQUIRED) =		.10					.10				)
19) END-TO-END C/NO, DB-HZ							45.83			45.57	
20) MODEM/RADIO LOSS, DB=	TRI	.00			.00		-1.50	.30	.30	-1.50	1.50)
21)REQUIRED C/NO,DB-HZ		51.31			51.31		41.31			41.31	
(REQUIRED EB/NO,DB							4.50				)
22)PERFORMANCE MARGIN,DB		10.93			10.65	.72	3.02			2.76	1.02
((19)+(20)-(21))						(1 SIG)					(1 SIG)

Table 1.5

Salient Features of the Baseline System Design

OPERATING FREQUENCY	
UPLINK	30 GHZ
DOWNLINK	20 GHZ
COVERAGE CONCEPT	
SAT/SUPPLIERS	CONUS BEAM
SAT/USERS	142 SPOTBEAMS
MULTIPLE ACCESS	
SUPPLIERS	TDMA
USERS	FDMA
GENERIC SERVICES	VOICE AND DATA
DATA RATES	
FORWARD (NORMAL)	100 KBPS (BPT) 300 KBPS (EPT)
RETURN (NORMAL)	4.8 KBPS (BPT)
RAIN COMPENSATION	
FORWARD	UPLINK POWER CONTROL & VARIABLE DATA RATE
RETURN:BPTs	VARIABLE DATA RATE
RETURN:EPTs	UPLINK POWER CONTROL & VARIABLE DATA RATE
LINK AVAILABILITY	98% FOR BPTs @ 4.8 KBPS >98% FOR EPTs
INTERBEAM POWER MANAGEMENT	9-BEAM POWER MANAGEMENT
FREQUENCY REUSE CAPABILITY	16 TIMES (FOR SPOTBEAMS)
SYSTEM CAPACITY*	
RAW DUPLEX CHANNELS	2800 (100% DUTY CYCLE), OR
DUPLEX VOICE CHANNELS	7500 (VOX=35%)

NOTE:
* System capacity is given in terms of the number of equivalent channels at 4.8 kbps each assuming that all user terminals are BPTs.

Table 1.6

Summary of the Satellite Design

SPOTBEAM	
ANTENNA SIZE (TRANSMIT)	3 M
(RECEIVE)	2 M
NUMBER OF SPOTBEAMS	142
ANTENNA GAIN	52.5 DBI
ANTENNA BEAMWIDTH	0.35 DEG
SYSTEM G/T	23.4 DB/K
AVERAGE EIRP/BEAM	58.7 DBW
CONUS BEAM	
ANTENNA GAIN	27.0 DB
ANTENNA BEAMWIDTH	7.7 DEG
SYSTEM G/T	- 1.2 DB/K
EIRP	46.1 DBW
SATELLITE MASS (GTO)	6500 LB
SATELLITE POWER (EOL)	4.0 kW

Table 1.7

Design Requirements for the BPT

ANTENNA GAIN @20 GHZ	19.3 DBI
ANTENNA GAIN @30 GHZ	22.8 DBI
ANTENNA TRACKING/COVERAGE CAPABILITY	
AZIMUTH	360.0 DEG
ELEVATION	15-60 DEG
RECEIVE G/T	-9.0 DB/K
TRANSMIT POWER	0.17 W
NORMAL DATA RATE	
RECEIVE	100 KBPS
TRANSMIT	4.8 KBPS
OTHER REQUIREMENTS	
SIZE	HANDHELD
MODEM	VARIABLE RATE

APPENDIX A

IMPACTS OF NONUNIFORM USER DISTRIBUTION ON SATELLITE CAPACITY

Miles K. Sue

1.0 INTRODUCTION

User distribution is not uniform throughout CONUS. This presents a challenge to the design of a CONUS coverage system. Fixed multiple beams with frequency reuse is a technology that has often been suggested for CONUS-coverage satellite systems providing services such as mobile and personal communications. For simplicity, most satellites are designed to provide a fixed but equal eirp for each spotbeam, i.e., the same HPA output power for all beams. In other words, these satellites are designed for a uniform user distribution. When the distribution is nonuniform, saturation may occur in some beams while other beams may have unused capacity, consequently reducing the system's effective capacity. This problem is more acute for systems with narrow spotbeams. For systems with relatively large beams, this problem is less severe due to the averaging effects. The problem of nonuniform user distribution was addressed in [11] using a simplified triangular probability density function (pdf) to model the user distribution. The results of that study are summarized here.

2.0 ANALYSIS

There are two adverse effects. The first is a reduction of system capacity. The second is that users in some beams may be denied services. This happens when the number of users in a beam exceeds the designed capacity for that beam. The system designer is forced to trade capacity utility for service quality, as illustrated in Figure A.1. This figure shows the effects of nonuniform user density (number of users per beam) on the effective capacity (or satellite utility) for a system designed for a uniform distribution. The vertical axis gives the potential system utility normalized to the utility for a uniform distribution as a function of two parameters: Alpha and Beta. These parameters characterize the user distribution and the transponder design. Alpha relates the user density to the transponder design. Specifically, it gives the fraction of beams in which the number of users exceeds the design value. Beta is a user distribution parameter; it is a measure of the spread between the most probable user density and the maximum density. It takes on values between 0 and 1. When Beta is 1, it implies that the probable value equals the maximum value. As indicated by Figure A.1, the reduction is significant for small values of Beta.

Figure A.2 is similar to Figure A.1, showing the relative capacity (or satellite utility) as a function of the variance of user density. As expected, a larger variance will result in a lower capacity.

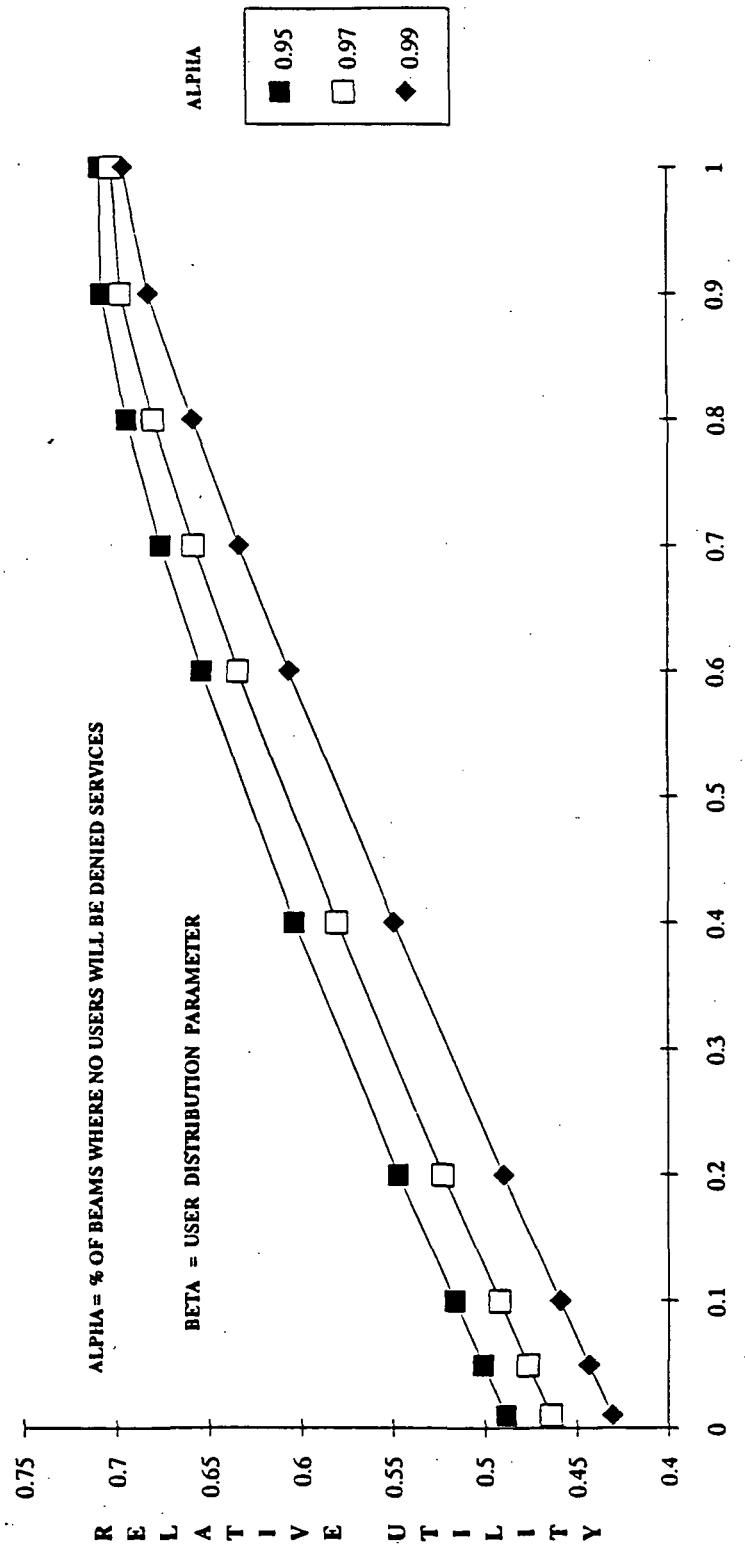

Figure A.1. Relative Satellite Capacity (Utility) vs. User Distribution

43

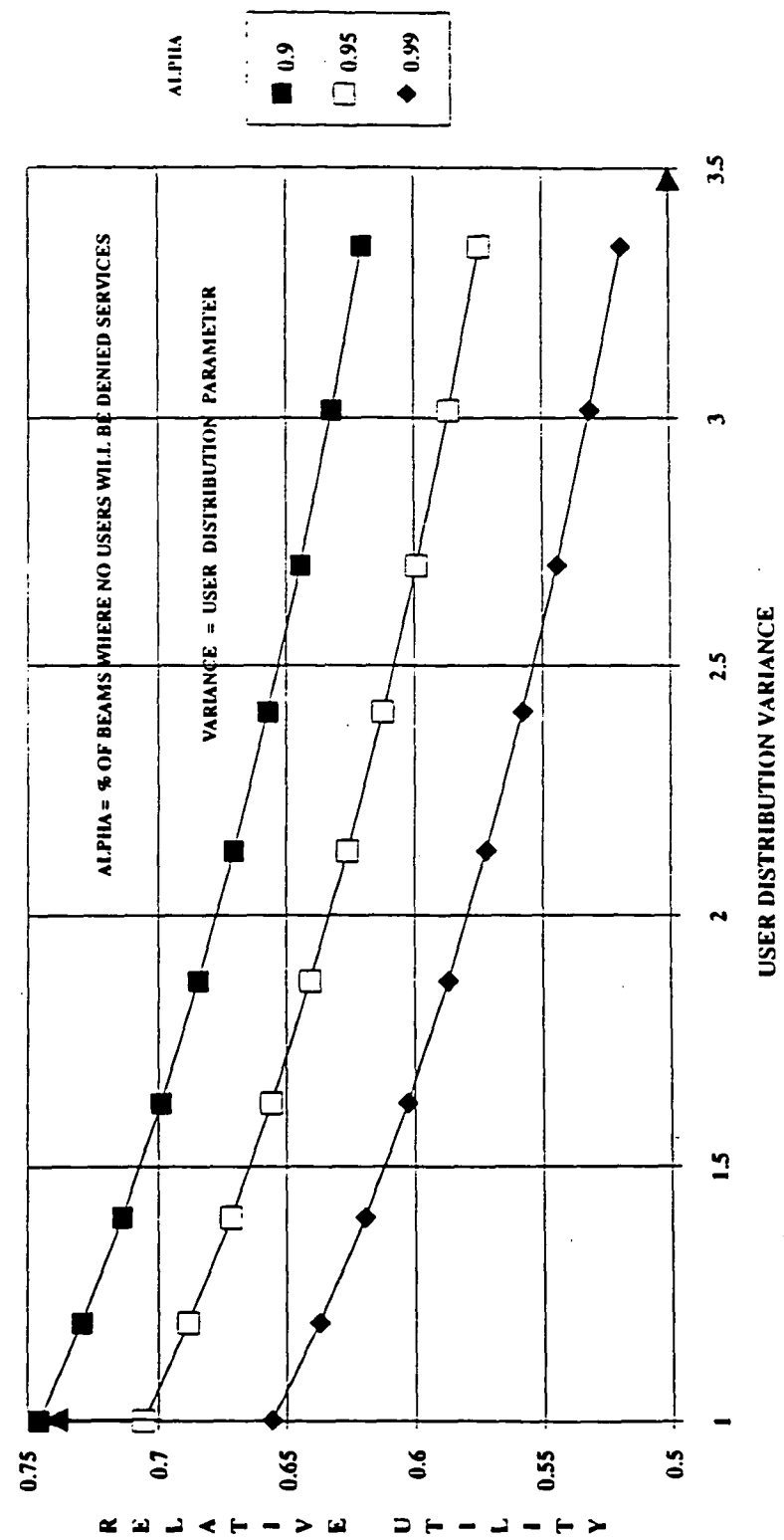

Figure A.2. Relative Satellite Capacity (Utility) vs. Variance of User Density

APPENDIX B

USER TERMINAL RADIATION LEVEL ESTIMATES

(Derived from Dessouky and Jamnejad [12])

1.0 INTRODUCTION

The current design requires the user terminal to have a 0.17-W transmitter and a transmit antenna with about 23-dBi gain. The resulting eirp is 14.5 dBW. While these values are preliminary and subject to future revision, it is necessary to estimate the radiated power flux density in order to insure that safety standards will be complied with.

2.0 CURRENT SAFETY STANDARD

The current ANSI standard for frequency above 1.5 GHz is 5 mW per square centimeter averaged over a 6-minute period. This standard includes a safety factor of 10 or more. At 30 GHz, the eye, particularly the cornea, is most susceptible to radiation damage due to the lack of blood circulation which drains the deposited heat. Independent experiments recently conducted by the USAF School of Aerospace Medicine using cat's eyes have suggested that incident densities up to 100 mW/cm^2 did not cause any harm [9]. Although this kind of study may eventually result in a relaxation of the acceptable radiation level, the PASS design goal is to meet the current safety standard.

3.0 RADIATION LEVELS VS. ANTENNA SIZE AND TRANSMIT POWER

To estimate the radiation density, a plot has been created and shown in Figure B.1, obtained from Chapter 5. This plot gives the normalized radiation density as a function of the normalized distance from the antenna for selected antenna gain, along with an upper bound of peak radiation level. The radiation density is normalized to the radiated RF power (in watts) and the square of the operating frequency (in GHz). The distance from the antenna is given in terms of the axial distance in wavelengths. To obtain the actual radiation density (mW/square cm), the normalized value is multiplied by the square of the operating frequency (GHz), and by the radiated RF power (watts). For example, the peak radiation level for a 25-dBi antenna at 30 GHz occurs 8 wavelengths (8 cm) from the antenna. The peak density is equal to 153xP, where P (watts) is the radiated power. If P is .2 watts, the peak radiation density is 30.6 mW. Chapter 5 contains a more detailed discussion of the antenna radiation level.

The estimates above give only the radiation density. Other factors, including exposure time and transmitter duty cycle, should be considered in order to determine whether the user terminal radiation level complies with established safety standards.

4.0 ESTIMATED RADIATION LEVEL FOR PASS USER TERMINALS

The current user terminal is designed to have a 23-dBi transmit antenna, 0.17-W transmitter power, and correspondingly, 14.5-dBW eirp. Using the design values and assuming a typical voice traffic scenario (i.e., a 90-second call with 35% duty cycle), the peak radiation density produced by the user terminal under these conditions is estimated to be 3.6 mW averaged over a 6-minute period, which complies with the current safety standard. The peak radiation density occurs at a point on the antenna boresight about 6 cm from the antenna aperture. The radiation density drops off rapidly as the distance from the aperture increases. The peak radiation density can be further reduced by employing a larger user antenna. If we increase the antenna gain, for example, from 23 to 25 dBi and maintain the same eirp, the resulting peak radiation level, which occurs at about 8 cm from the antenna aperture, would be reduced to about 1 mW/cm^2, averaged over a 6-minute interval.

In summary, by carefully choosing the design parameters and operating scenarios, PASS user terminals can meet the current safety standard.

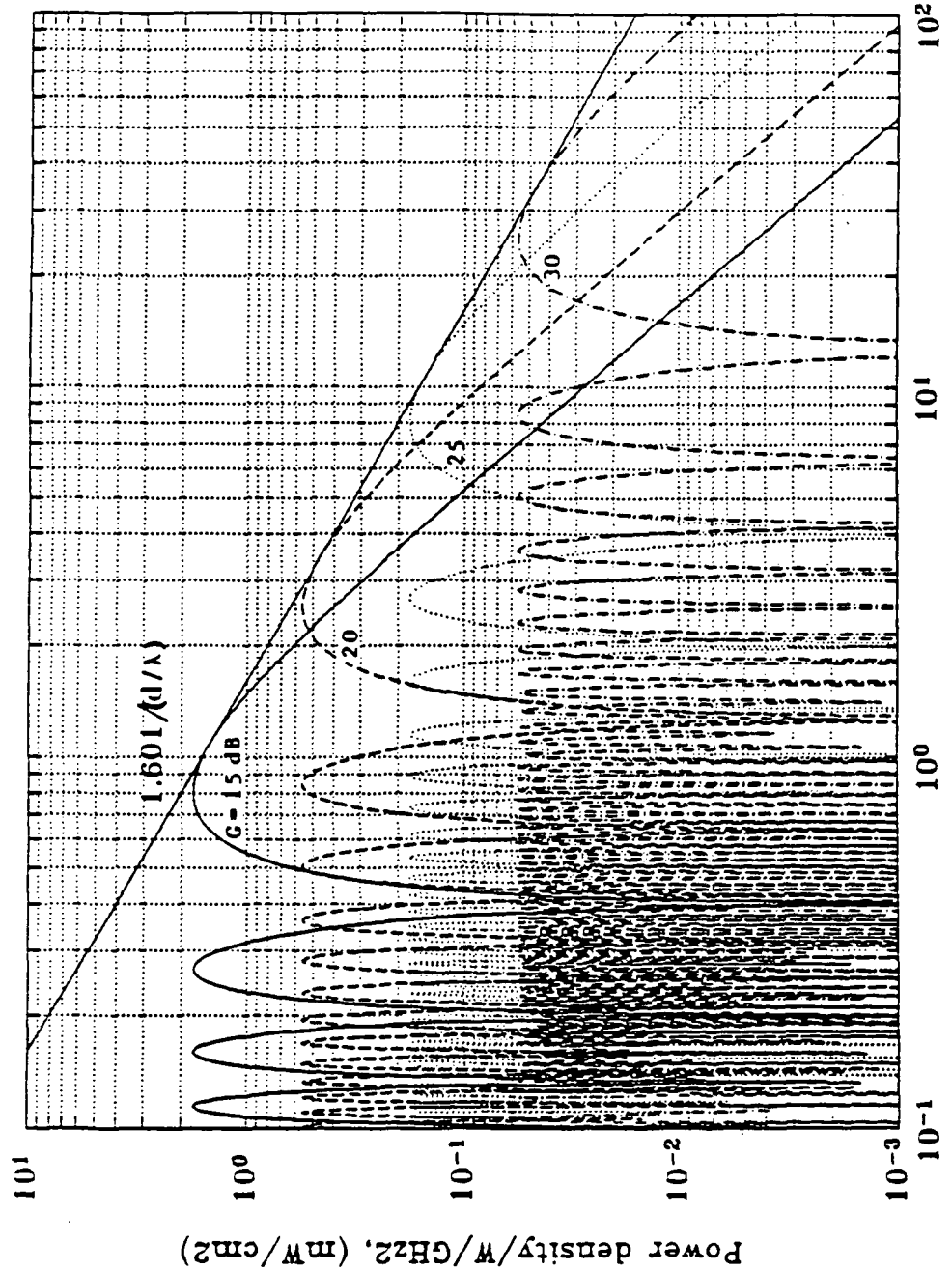

Figure B.1. Power Density vs. Axial Distance for Uniformly Illuminated Aperture Antenna (Obtained from Chapter 5)

APPENDIX C

PASS RAIN ATTENUATION COMPENSATION TECHNIQUES AND AN ASSESSMENT OF SERVICE AVAILABILITY

Miles K. Sue

1.0 INTRODUCTION

PASS is a satellite-based communications system, currently designed to operate in the 20/30 GHz bands. These bands are chosen because of the ample available bandwidth and the potential for developing small terminals, both of which are key to the success of PASS. These bands, unfortunately, are sensitive to rain effects. This appendix discusses the rain compensation techniques proposed for small terminals and examines their impacts on link performance.

2.0 PASS RAIN COMPENSATION TECHNIQUES

As stated in Chapter 1, a combination of uplink power control and an adjustable data rate is employed in the current design to combat rain attenuation. Uplink power control is applicable to the uplinks from the suppliers who are equipped with large, fixed earth stations. When increased uplink power from the suppliers fails to fully compensate for rain degradation, the data rate will be reduced to close the link. Uplink power control will not be employed by the small personal terminals due to their limited power capability. Instead, only a variable data rate scheme will be used. During rain, the data rate will be reduced by a factor equal to multiples of 2.

3.0 DESIRED SERVICE AVAILABILITY AND ESTIMATED RAIN ATTENUATION

PASS's main objective is to provide personal communications. The design goal is to maintain 95% to 98% availability for the basic personal communications services, i.e., 4.8 kbps voice. This goal is based on a number of factors, including the nature of services, users' willingness to accept occasional outages or delays, the practicality of providing the required rain margin, the resulting system complexity, and costs.

The rain attenuation corresponding to 98% availability has been estimated to be 1.0 dB at 20 GHz and 2.5 dB at 30 GHz, based on five selected locations representing the four corners of CONUS and one southern location, as described in Chapter 1.

4.0 FORWARD LINK ANALYSIS

The forward link is downlink limited, i.e., the overall (end-to-end) C/N_o is essentially determined by the downlink C/N_o, as indicated by Table 1.4. The end-to-end clear-sky link margin is about 3.0 dB with 1-sigma variation of 1 dB.

In the forward direction, rain attenuation is more severe on the uplink than on the downlink. Fortunately, the uplink rain

attenuation (2.5 dB) can be fully compensated for by uplink power control. Hence, it will not affect the overall link performance.

Although the downlink rain attenuation is smaller, it has two adverse effects: it causes an increase in system noise temperature in addition to signal attenuation. For systems with a very low system noise temperature, the first effect can be more pronounced than the second and can result in significant performance degradation. The operating system noise temperature of the small PASS personal terminals is in the neighborhood of 650 k. The relatively high noise temperature makes these terminals insensitive to the rain-induced increase in sky noise temperature, as shown in Figure C.1. This figure shows the total signal-to-noise ratio (SNR) degradation as a function of rain attenuation for selected values of the receiving system noise temperature. The total SNR degradation includes the combined effects of signal attenuation and increased system noise temperature. As evident in Figure C.1, the total SNR degradation is caused mainly by signal attenuation for the typical PASS user terminals.

Two key parameters affect the service availability. The first is the clear-sky link variation due to all possible variations of link parameters with the exception of rain attenuation, e.g., transmit power, antenna pointing error, thermal noise, etc. The clear-sky link variation in units of dB, x, can be modeled as a random variable having a gaussian probability density function (pdf) with mean μ_x and variance σ_x^2. The second parameter is the rain attenuation, y, which has the well-known log-normal pdf. Ignoring the effects caused by the increase in system noise temperature, the total link attenuation due to the combined effects of x and y is given by

$$z = \begin{cases} x & \text{no rain} \\ x+y & \text{during rain} \end{cases} \qquad \text{Eq. (1)}$$

The pdf of x, $p_x(x)$, is given by

$$p_x = \frac{1}{\sqrt{2\pi}\,\sigma_x} \exp\left(-(x-\mu_x)^2 / 2\,\sigma_x^2\right) \qquad \text{Eq. (2)}$$

The pdf of y which can be derived from its log-normal pdf is given by

$$p_y(y) = \frac{1}{\sqrt{2\pi}\,\sigma_y\, y} \exp\left(-(\ln(y) - \mu_{\ln(y)})^2 / 2\,\sigma^2_{\ln(y)}\right) \quad \text{Eq. (3)}$$

where $\mu_{\ln(y)}$ is the mean of ln(y), which happens to equal the natural logarithm of the median of y, and $\sigma^2_{\ln(y)}$ is the variance of ln(y).

Assuming that x and y are independent, the conditional pdf of z during rain is then given by

$$p_z(z|rain) = p_x(x) * p_y(y) \quad \text{Eq. (4)}$$

where * denotes convolution. In the absence of rain, the conditional pdf of z is identical to that of x. The total probability of z is obtained by averaging the two conditional probabilities with and without rain,

$$p_z(z) = (1-p_o)\, p_x(x) + p_o\, p_z(z|rain) \quad \text{Eq. (5)}$$

where P_o is the probability that rain occurs at any point along the propagation path. The link availability for a given link margin can then be obtained by integrating $p_z(z)$.

The above analysis has been applied to estimate the service availability for three locations: Mobile, Miami, and Portland (Maine). The first step is to determine the rain attenuation statistics and the clear-sky link variation statistics. The rain attenuation statistics have been computed using Manning's rain model and by assuming that the satellite is located at 95 degrees west longitude. The statistics for the clear sky link variation have been computed using a spread-sheet link design program by specifying the favorable and adverse tolerances and the associated pdf for each link variable. The statistics for the clear-sky link variation can be obtained from the link budget table and are tabulated in Table C.1, along with the rain attenuation statistics.

Figure C.2 shows, as an example, the pdf of x, the pdf of y, the conditional pdf of z during rain, the total pdf of z, and their relationships for Portland, Maine. The link availability can be obtained from Figure C.3, which gives the percentage of time that the total attenuation on the link exceeds a given link margin. As indicated, the 3.0-dB link margin would provide approximately 99% availability. It should be noted, however, that the effect of increased system noise temperature has not been included in Figure C.3. For the range of service availability targeted for basic

personal communications, increased system noise temperature will not result in more than 0.4-dB degradation based on the five locations examined. Allowing pessimistically 0.5 dB to account for the effect of increased system noise temperature, the resulting link availability would be approximately 98%.

5.0 RETURN LINK ANALYSIS

The return link is from the user to the supplier, via the satellite. A clear sky link budget is shown in Table 1.3, with a clear-sky link margin of 3.0 dB and σ_x equal to 1.0 dB. The return link is different from the forward link in that it is basically uplink limited instead of downlink limited. Rain attenuation on the downlink, which is less than 1.0 dB approximately 98% of the time, would have negligible impacts (less than 0.1 dB) on overall link performance.

Service availability for the return link is thus mainly determined by uplink rain attenuation and variations in link parameters. Ignoring the contributions of downlink rain attenuation, service availability for the return link has been estimated using Eqs. (1)-(5) and results are shown in Figure C.4. The rain attenuation and link variation statistics are tabulated in Table C.2. Figure C.4 shows that the 3-dB link margin would be adequate 98% of the time.

6.0 HIGHER AVAILABILITY FOR CRITICAL SERVICES

The foregoing analyses have determined the availability of basic personal communications services at the nominal data rate of 4.8 kbps. There are services offered by PASS, such as emergency communications, that require a higher availability. The variable data rate scheme is designed to satisfy these needs. By reducing the data rate from 4.8 kbps to 2.4 kbps, the link availability can be increased to about 99%, as indicated by Figures C.3 and C.4. A further reduction below 2.4 kbps would result in an even higher service availability, although the improvement becomes increasingly negligible.

7.0 CONCLUSIONS

Service availability for PASS has been estimated to be 98% at 4.8 kbps and 99% at 2.4 kbps based on the three locations examined. While an expanded study that includes more locations would be needed to fully establish PASS service reliability, the analysis of the three selected locations, comprising areas with heavy rain as well as areas with low elevation angles, has provided a quick assessment of PASS's rain compensation strategy and the resulting service quality. Results indicate that the impacts of rain attenuation for PASS-like systems are moderate and can be mitigated without relying on complicated on-board baseband processing technologies.

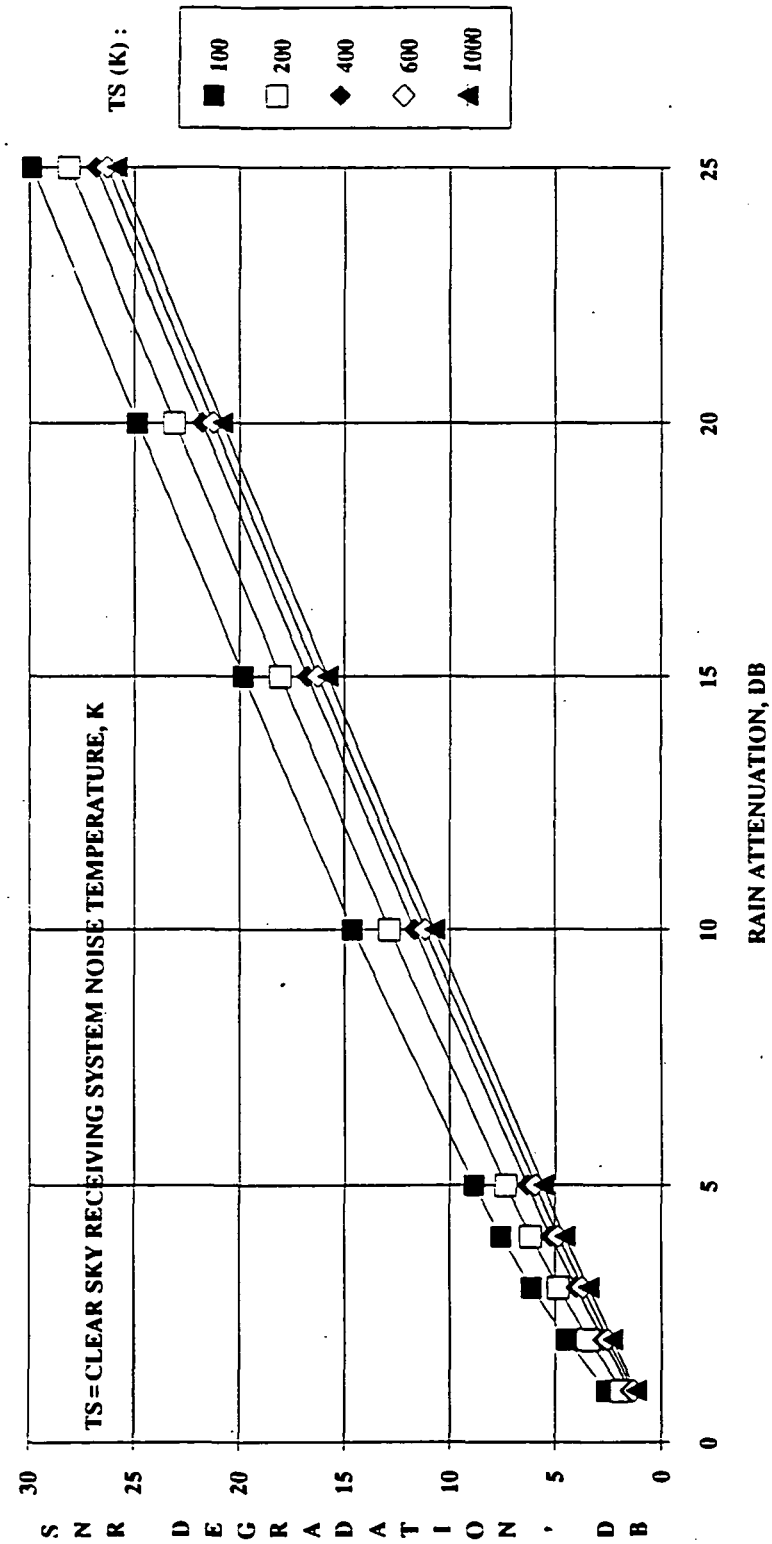

Figure C.1. Total SNR Degradation vs. Rain Attenuation with Clear-Sky System Noise Temperature as a Parameter

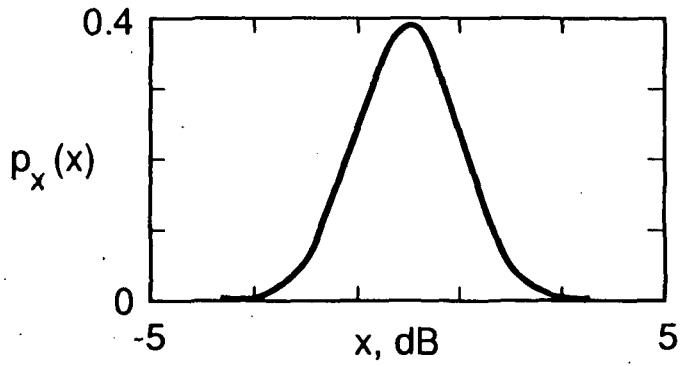

a. pdf of the Clear-Sky Link Variations, x.

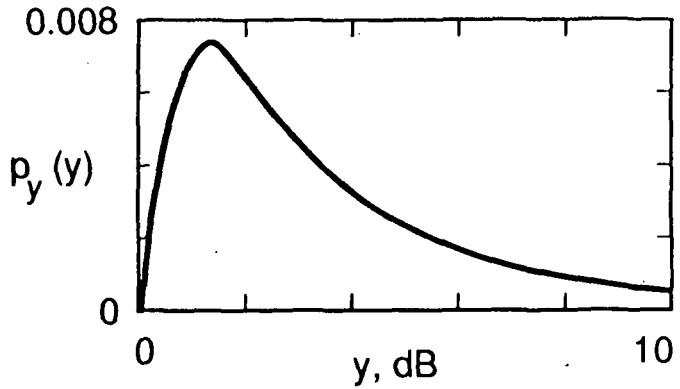

b. pdf of Rain Attenuation, y.

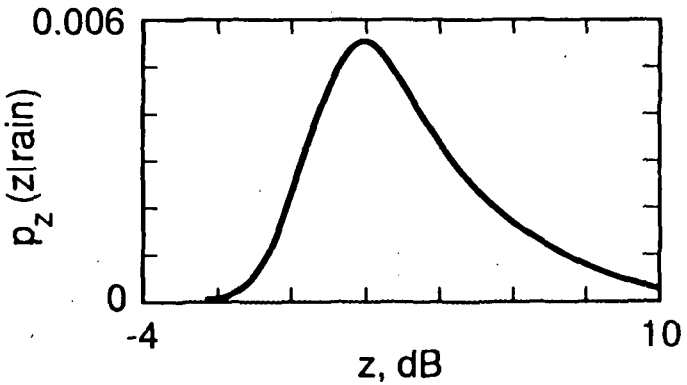

c. pdf of the Total Link Attenuation, z, Conditioned on Rain:
$p_z(z|rain) = p_x(x) * p_y(y)$

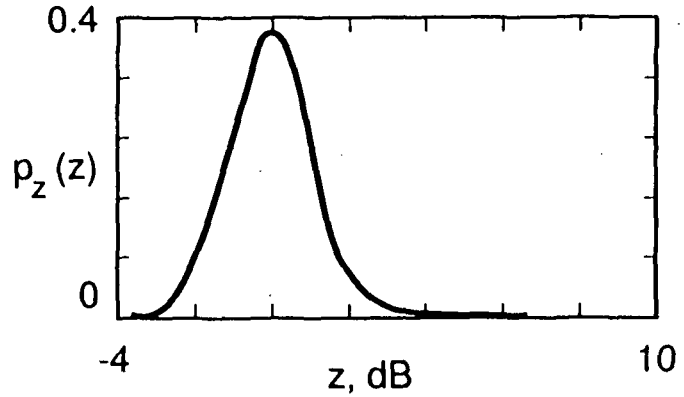

d. Total pdf of z, Averaged Over Rain and no Rain Cases: $p_z(z) = (1-P_o)\ p_x(x) + P_o\ p_z(z|rain)$; P_o = Probability of Attenuation

Figure C.2. An Illustration of $p_x(x)$, $p_y(y)$, $p_z(z)$, and Their Relationships

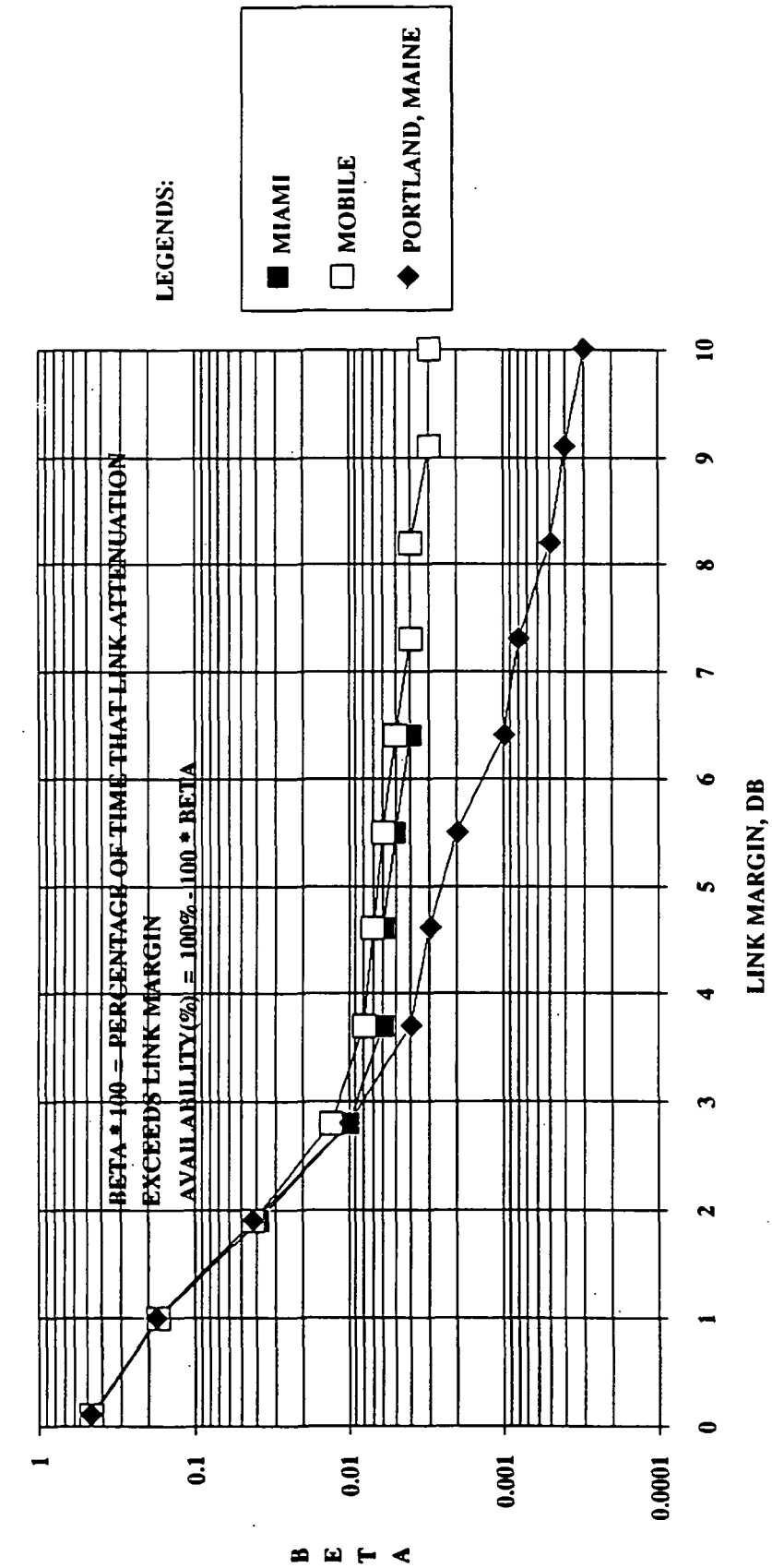

Figure C.3. Percentage of Time That the Total Link Attenuation Exceeds the Link Margin for the Forward Link

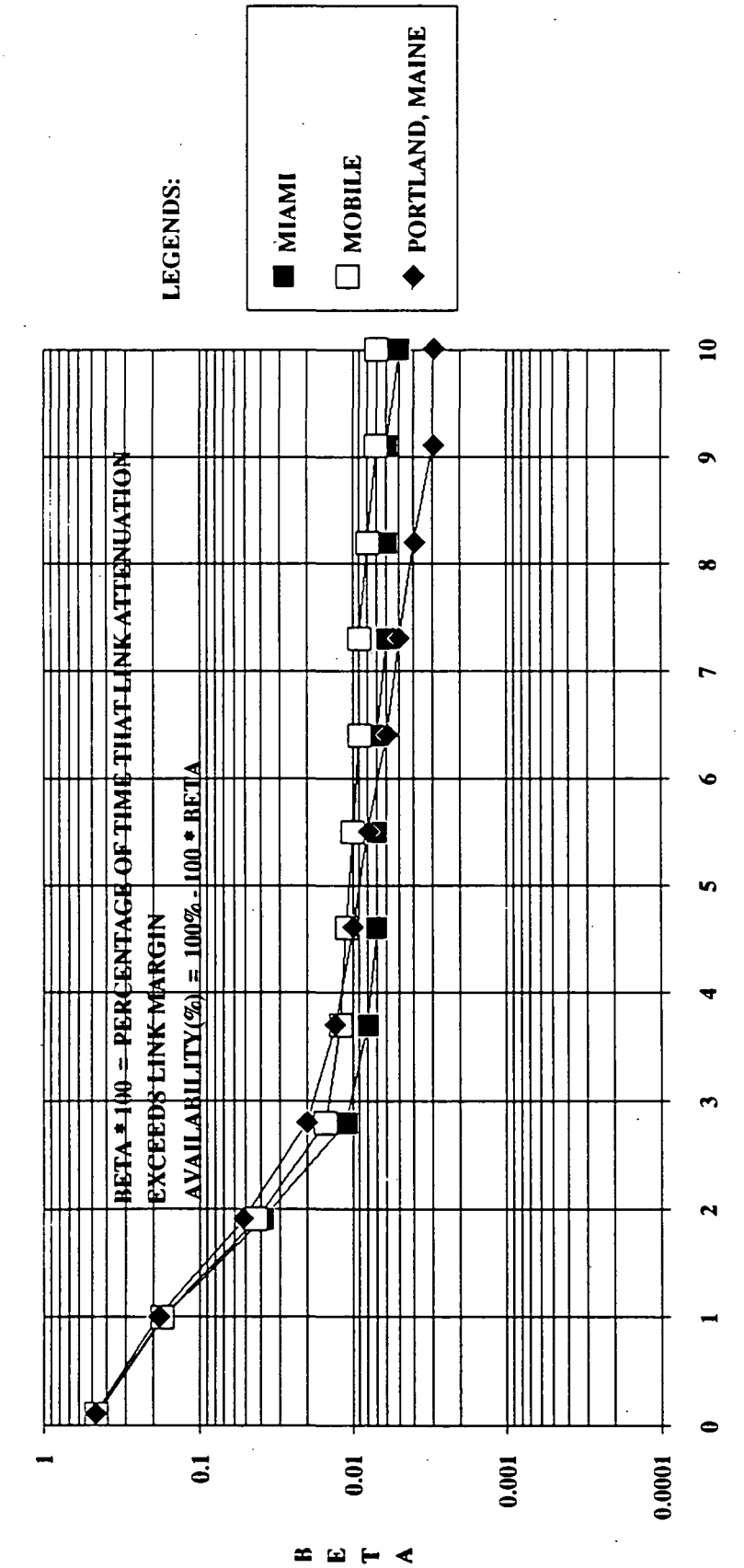

Figure C.4. Percentage of Time That the Total Link Attenuation Exceeds the Link Margin for the Return Link

54

Table C.1.

Key Parameter Values for the Forward Link

KEY PARAMETERS	MIAMI, FLORIDA	MOBILE, ALABAMA	PORTLAND, MAINE
$\mu_{ln(y)}$, dB	12.9	10.3	2.8
σ_y, dB	0.98	0.89	0.89
P_o, %	0.9	1.3	3.2
μ_x, dB	0.0	0.0	0.0
σ_x, dB	1.0	1.0	1.0

Table C.2.

Key Parameter Values for the Return Link

KEY PARAMETERS	MIAMI, FLORIDA	MOBILE, ALABAMA	PORTLAND, MAINE
$\mu_{ln(y)}$, dB	6.5	4.8	1.2
σ_y, dB	1.0	0.9	1.0
P_o, %	0.9	1.3	3.2
μ_x, dB	0.0	0.0	0.0
σ_x, dB	1.0	1.0	1.0

REFERENCES

[1] "Telecommunications 2000," NTIA, 1989.

[2] Signatron, Inc., "20/30 GHz FSS Feasibility Study, Final Report," prepared by Signatron Inc., under contract to Jet Propulsion Laboratory (JPL), JPL Contract No. 957641, February 1987.

[3] M. K. Sue, A. Vaisnys, and W. Rafferty, "A 20/30 GHz Personal Access Satellite System Study," presented at the 38th IEEE Vehicular Technology Conference VTC-88, Philadelphia, June 15-17, 1988.

[4] P. Estabrook, J. Huang, W. Rafferty, and M. Sue, "A 20/30 GHz Personal Access Satellite System Design," International Conference on Communications, Boston, Massachusetts, June 11-14, 1989.

[5] M. K. Sue, editor, "Personal Satellite System Concept Study," JPL Report D-5990, February, 1989.

[6] M. Motamedi and M. K. Sue, "A CDMA Architecture for a Ka-Band Personal Access Satellite System," Proceedings of the 13th AIAA International Communications Satellite Systems Conference, Los Angeles, CA, March 1990.

[7] K. Dessouky and M. Motamedi, "Multiple Access Capacity Trade-Offs for a Ka-band Personal Access Satellite System," to be presented at the International Mobile Satellite Conference, Ottawa, Ontario, Canada, June 18-20, 1990.

[8] M. K. Sue, K. Dessouky, B. K. Levitt, and W. Rafferty, "A Satellite Based Personal Communications System for the 21st Century," to be presented at the International Mobile Satellite Conference, Ottawa, Ontario, Canada, June 18-20, 1990.

[9] USAF report on radiation experiments at 30 and 90 GHz using cat's eyes, to be released in 1990 by USAF School of Aerospace Medicine.

[10] R. M. Mannings, "A Unified Statistical Rain Attenuation Model for Communication Link Fade Predictions and Optimal Stochastic Fade Control Design Using A Location Dependent Rain Statistics Data Base," International Journal of Satellite Communications, Volume 8, P11-30, 1990.

[11] M. K. Sue, "An Aeronautical Mobile Satellite System Study, Part II, Technical Report," JPL Publication D-4457, September 1, 1987.

[12] "Radiation Levels of the Ka-band Mobile Terminal," K. Dessouky and V. Jamnejad, JPL IOM 3392-90-016, dated February 21, 1990.

56

CHAPTER 2

MULTIPLE ACCESS TRADE STUDY

Masoud Motamedi

2.0 INTRODUCTION

The Personal Access Satellite System (PASS) strawman design, as described in the PASS Concept Study Report[1], (hereafter referred to as the Strawman Design) utilizes a hybrid Time Division Multiple Access (TDMA)/ Frequency Division Multiple Access (FDMA) implementation. TDMA is used for the forward direction (from Suppliers to Users), and FDMA for the return direction (from Users to Suppliers). In the forward direction each transponder has a narrow band pilot channel plus two relatively high rate data and voice channels. In the return direction, access to the system by users is provided using narrow band Single Channel Per Carrier (SCPC), frequency division, Demand Assigned Multiple Access (DAMA). The channel assignment is done by a Network Management Center (NMC).

An alternative architecture is proposed that will require minimal real time coordination and yet provide a fast access method by employing random access Code Division Multiple Access (CDMA). This chapter addresses the CDMA system issues such as (1) connecting suppliers and users, both of whom may be located anywhere in the CONUS, when the user terminals are constrained in size and weight; and (2) providing efficient traffic routing under highly variable traffic requirements. It is assumed that bandwidth efficiency is not of paramount importance.

CDMA or Spread Spectrum Multiple Access (SSMA) communication is a method in which a group of carriers operate at the same nominal center frequency but are separable from each other by the low cross correlation of the spreading codes used[2]. Interference and multipath rejection capability, ease of selective addressing and message screening, low density power spectra for signal hiding and security, and high-resolution ranging are among the benefits of spread spectrum communications.

The problem of allowing multiple users to simultaneously access a channel without causing an undue amount of degradation in the performance of any individual user is a classical one in communications. Multiple access is the process

by which a large number of stations interconnect their links. The two most common techniques, FDMA and TDMA, attempt to solve the problem by separating the signals in frequency and time, respectively. In CDMA architectures, stations use spread-spectrum transmissions with low cross correlating codes to share a channel with minimal interference. Each of these techniques has certain drawbacks associated with it.

For example, in FDMA, anytime the channel through which the signals are transmitted is nonlinear, intermodulation products will be generated. In TDMA, the intermodulation problem does not exist, but accurate synchronization of all users becomes important in system design. Furthermore, if interference such as jamming or multipath is present, large degradations in system performance can result in both FDMA and TDMA systems[3].

For such reasons, CDMA has become a competitive multiple access scheme in certain situations. Multiple access can be achieved by spread spectrum code division using direct pseudonoise sequences, frequency hopping, or combinations of these techniques. A primary necessity of such systems is the requirement for sets of spreading signals which have the two properties that 1) each signal can easily be distinguished from a time-shifted version of itself, and 2) each signal can easily be distinguished from every other signal in the set[4]. One of the major benefits of CDMA is the lack of central frequency and timing control. A CDMA system is usually operated in an asynchronous manner so that network timing problems do not exist. There is a penalty for this flexibility, of course, and that is a smaller capacity due to the imperfect orthogonality of the spreading sequences of the various users. The inter-modulation problem does not go away with CDMA, but the capability of rejecting external interference is invariably the crucial factor in deciding to implement a CDMA system.

In FDMA each uplink RF carrier occupies its own frequency channel. Guard bands between adjacent frequency channels allow for imperfect filters and oscillators. Receiving earth stations select a desired carrier by RF and IF filtering. No clocking control exists between channels. Other than remaining "on frequency," there is no coordination between accessing stations once a channel is assigned. FDMA requires stable sources for up- and down-conversions.

In CDMA all users operate at the same nominal frequency and simultaneously use the entire repeater bandwidth. The im-

portant feature of CDMA is that unlike FDMA and TDMA, minimal dynamic (freq. and time) coordination is needed between the various transmitters in the system. In addition, CDMA techniques can provide substantial levels of antijam capability to combat deliberate or unintentional interference, and have a low probability of intercept to reduce the probability of reception by unauthorized users. Furthermore, CDMA allows a graceful degradation of performance as the number of simultaneous users increases. Conversely, when the system is underused, the extra capacity allowed for code noise is automatically realized as increased link margin.

Tables 2-1 and 2-2 summarize the advantages and disadvantages of using CDMA and FDMA respectively. The choice of a multiple access method depends on the application. For the purposes of this report Demand Access (DA) and Random Access (RA) are considered as viable methods for PASS. In general, when most of the users in a communications system do not transmit continuously, the channel need not be allocated permanently. Therefore it could be very advantageous to either dynamically assign the different channels according to the traffic requirements imposed on the system (DA) or allow random communications (RA). Systems requiring DA normally lead to utilization of FDMA whereas RA is more suited to CDMA. Some of the characteristics of systems employing RA or DA are shown in Table 2-3.

The complete CDMA architecture consisting of block diagrams of the user terminal, the supplier station, the Network Clock and Monitor Center (NCMC) and the satellite is provided along with the access methods and frequency/time plans. The complexity of developing the CDMA system is compared to the complexity of the DAMA system. The inherent advantages and disadvantages of the two architectures are noted and their respective throughput performance is discussed.

2.1 SPREAD SPECTRUM SYSTEM

The envisioned system using the properties of spread spectrum communications would give the users and suppliers of a personal communications system near complete freedom of access. Equipped with a user terminal, a subscriber could randomly access a host of voice and data services, similar to the ones described in the strawman design. The system contains a space segment, user equipment, and a ground segment that includes a NCMC and a number of supplier stations.

TABLE 2-1. ADVANTAGES AND DISADVANTAGES OF CDMA

ADVANTAGES	DISADVANTAGES
. MULTIPATH REJECTION . MINIMUM REAL TIME COORDINATION . LOW PROBABILITY OF INTERCEPT . GRACEFUL DEGRADATION IN PERFORMANCE AS NUMBER OF USERS INCREASE . REDUCED SPECTRAL DENSITY . PRECISE RANGE MEASUREMENT . CODE DIVERSITY & POLARIZATION DIVERSITY COMBINED, ENABLE ORBIT REUSE WITH OMNI ANTENNA . INCREASED CODING W/O INCREASED BANDWIDTH	. NEED OF SPREADING SEQUENCES WITH GOOD CORRELATION PROPERTIES . NEAR-FAR PROBLEM: UPLINK POWER CONTROL IS REQUIRED

TABLE 2-2. ADVANTAGES AND DISADVANTAGES OF FDMA

ADVANTAGES	DISADVANTAGES
. EACH UPLINK OCCUPIES OWN FREQUENCY CHANNEL . NO CENTRAL TIMING COORDINATION	. GUARD BANDS REQUIRED . NETWORK MONITORING AND CONTROL . REQUIRE STABLE FREQ. SOURCE . EXTENSIVE NMC SOFTWARE REQUIREMENT . NO VOICE ACTIVITY FACTOR BENEFIT IN A BANDWIDTH LIMITED SITUATION

TABLE 2-3. ADVANTAGES OF ACCESS METHODS

DEMAND ACCESS	RANDOM ACCESS
. VOLUMES, ORIGINS, AND DESTINATIONS HIGHLY VARIABLE . FULL CONTROL REQUIRED . TWO CHANNELS FULLY OCCUPIED FOR ONE CONVERSATION	. SHORT BURSTS OCCURRING AT RANDOM TIMES (USE ACTIVITY FACTOR IMPROVEMENT) . LIMITED SYSTEM CONTROL . SOME TRANSMISSIONS LOSS ACCEPTABLE (REPEATS ARE NECESSARY)

The communications link in the forward and return links follow the same format as the PASS strawman design, namely:

(a) Signals transmitted by the suppliers will be received by the satellite through the CONUS beam, filtered, routed to one of the spotbeams according to their destination, frequency converted, and subsequently transmitted to the intended user using the multibeam antenna.

(b) Signals originating from the user will be received via one of the spotbeams, filtered, frequency translated according to the channeling plan, and transmitted to the suppliers via the CONUS beam.

2.1.1 System Architecture

As previously mentioned, the satellite employs both CONUS and spotbeam antennas. The system has been designed for maximum flexibility, minimum coordination, and ease of operation. In this section a baseline architecture is provided to describe the operation of a CDMA system. In developing this architecture, it is assumed that bandwidth is available and that simplicity of operation is the most important factor.

2.1.2 Multiple Access Scheme

The multiple access property of spread spectrum communication is used in developing a scheme that would allow random access to users and suppliers. Taking advantage of spreading by nearly orthogonal codes, the transmissions in a given link can share the full allocated bandwidth in spreading their respective data. In the uplink of the user terminal this capability is provided by allowing all users transmissions to be at the same nominal frequency in a given spotbeam. Similarly, in the downlink to the user terminals all of the supplier transmissions are centered at a nominal frequency. Access to the system in the forward direction (from suppliers to users) is provided using a hybrid TDM/CDMA scheme, and in the return direction (from users to suppliers) using Random Access Code Division Multiple Access (RACDMA).

In the downlink to the user, the spotbeam signals share the full assigned bandwidth in relaying the suppliers spread signals to all the users. Each supplier can use any of a number of PN sequences that are preassigned to it by the organizers of the system, in spreading its data. As shown in

Fig. 2-1, the supplier forms its own TDM channel by packetizing the data or voice addressed to different users and sending it via a spotbeam. The data rate used is a multiple of the return rate, thus a number of users can be addressed simultaneously, however in order to communicate to multiple users in a spotbeam at the same instant in time, a second spreading sequence must be employed. It should be noted that this flexibility comes at the price of developing a method of informing the selected user of the change in its inbound spreading code. Furthermore, the number of simultaneous transmissions from a supplier should be set by the organizers of the system in order to limit the code noise in the channel.

In the return direction RACDMA is utilized in order to allow simultaneous communications by hundreds of users in a given spotbeam. The transmissions from a user terminal are via random bursts that are spread using pre-assigned supplier PN sequences, i.e. all of the users communicating with a supplier use the same PN code as their spreading sequence. A user terminal can spread its data using a code that is preassigned to it by the supplier or receive instructions to utilize one of many user resident codes. The proper selection of codes with low cross correlation and autocorrelation is essential.

The multiple access property of spread spectrum communication is also employed in developing a pilot reference for the full system. The pilots generated at the NCMC are transmitted and relayed to the spotbeams exactly in the same fashion as the supplier transmissions to the users.

2.1.3 Frequency Plan and Channelization

The frequency plan is driven by the simplicity requirement of the system architecture and multiple access scheme. For the baseline design, the available uplink and downlink spectra are divided into two parts for the CONUS beams and the spotbeams. In both the uplink and downlink spotbeams, frequency reuse is employed in order to reduce spectrum requirement. Thus, as depicted in Fig. 2-2, in the forward and return links of the CONUS beams, the allocated bandwidths are divided to N subbands where N is the number of spotbeams utilized (for the current design N=142 beams). In the downlink the N subbands are frequency converted to one of nine center frequencies and are transmitted via the N spotbeams. In the return direction the exact reverse process occurs whereby all the users transmit at the center frequencies of the spotbeams that they are in and N downlink

subbands are used to relay these signals. This channelization will require [2*N*Forward Chip Rate] of bandwidth for the CONUS uplink and [2*N*Return Chip Rate] for its downlink; using opposite polarization, the bandwidth requirement is lowered by a factor of two.

Contrary to the CONUS beams using such a wide bandwidth (assuming high chip rates), the spotbeams will only require 9*2*Forward Chip Rate in the downlink and 9*2*Return Chip Rate in the uplink.

Overall bandwidth requirements for the uplink and downlink are:

Up: (N*Forward Chip Rate)+(18* Return Chip Rate) Eq. 2-1

Down: (N* Return Chip Rate)+(18*Forward Chip Rate) Eq. 2-2.

2.1.4 System Operation

2.1.4.1 SATELLITE TRANSPONDER

The satellite transponder, as shown in Fig. 2-3, can be regarded as a bent pipe that achieves signal routing to spotbeams by frequency translation. The signal from a spotbeam is frequency shifted per the frequency plan shown in Fig. 2-2 and sent with the signals of the other spotbeams to the CONUS transmitter for transmission to all of the suppliers and the NCMC. The forward direction of the satellite transponder is basically the reverse of the return link where all of the incoming frequencies are down-converted to one of nine downlink frequencies and are sent to the corresponding spotbeams. One oscillator is used as the reference for both the uplink and downlink conversions so that the automatic frequency control, performed by the NCMC, on the pilot is simplified.

2.1.4.2 USER TERMINAL

A block diagram of the user terminal is shown in Figure 2-4a. The received RF signal is down converted and is filtered by a channel filter with a bandwidth equal to twice the chip rate. After being level controlled by an Automatic Gain Controller (AGC), the signal is divided and provided to three elements that operate as follows (refer to Fig. 2-4b for the flow diagram of the receiver operation):

1. An acquisition unit or better known as the "correlator" performs the rough code acquisition. The unit

initially searches for the pilot chip sequence in all nine frequency subbands in order to initialize carrier and chip recovery. Upon completion of this function and indication of lock from the "carrier and chip recovery" unit, it starts the search for transmissions from a supplier station. The performance of this element is a function of the frequency offset therefore a sweep controller is required.

2. A carrier and chip recovery that locks to the incoming pilot and thereby corrects the Voltage Controlled Oscillator (VCO) frequency for proper up and down conversion. Note that the unit also controls a sweep control circuitry which performs the function of searching the range of frequency uncertainty. Once the recovery unit has correctly locked to the pilot, it sends the "LOCK" signal to the acquisition unit to initiate the search for an acquisition sequence from a supplier. Furthermore, the unit provides the chip clock and functions as the local reference to all other parts of the terminal thus locking the full terminal to the stabilized oscillator at the NCMC.

3. A data correlator channel that processes the input signal to produce a full-amplitude despread signal for data demodulation. Due to the recovery of carrier and chip clocks of the reference pilot, there is no need for any elaborate demodulation scheme at this point.

In the transmit portion the following functions can be performed by the user:

- Insert messages to be sent to the supplier
- Start a voice conversation or data
- Select a code for his reply, and
- Initiate an emergency message.

The user terminal will form the sequence of data words that make up the transmitted burst. This burst consists of:

a. A synchronization sequence that allows the supplier to detect the presence of the burst, identify the spreading code that is being used, and establish coarse timing,

b. A header, that includes the user's address and a small amount of control information; and

64

c. Message bits possibly followed by redundant bits for error detection/correction.

This serial binary sequence is modulo-2 added to the PN sequence corresponding to the receiving supplier and is then supplied to the modulator. Figure 2-4a gives an example of the format of a voice conversation.

2.1.4.3 Ground Stations

Network Clock & Monitor Center

The NCMC as shown in Fig. 2-5 consists of a pilot generating circuit, a pilot recovery unit, and a billing station.

The pilot generator or the network reference clock modulates a PN code on N carriers and transmits them to the satellite. The pilot generator is locked to a very accurate clock and is constantly updated by the control line from the pilot recovery unit. The recovery unit tracks the return pilot from the satellite so that the drifts in the satellite Local Oscillator (LO) are compensated.

The billing station will need the capability of recognizing the start and stop times of all communication both in forward and return directions. Since this information is available at supplier stations, one could envision a central billing that gets its information from all of the supplier stations rather than receiving all of the communication. An on-line billing station such as the one shown in Fig. 2-5 requires the same receiving circuitry of the suppliers and numerous receivers similar to the one used in a user terminal.

Supplier Stations

The supplier stations in the CDMA baseline design have full control in communicating with their users. Each supplier has a spreading code assigned to it by the system coordinator. Using this code a supplier can simultaneously communicate to users scattered over CONUS without any coordination with the NCMC or any other supplier. Figure 2-6 shows the block diagram of a supplier station. As seen in the figure, the forward portion of a supplier station consist of M processor, spreader, and frequency shift chains, where M is a function of the number of users and the number of beams. Each processor time division multiplexes the data to users in a beam prior to sending it to a spreader. The frequency reference for the synthesizer and the up converter used is

locked to the pilot received from the satellite. LO_1 to LO_M may be set by the Processor for any of N different frequencies corresponding to the destination beams.

In the return portion, the station must monitor the downlink transmissions, lock its reference to the pilot, and detect, acquire and track all incoming transmissions addressed to it. Due to the asynchronous nature of the system, all of the N beams have to be monitored simultaneously leading to requirements for a down converter and N frequency translators that feed N acquisition units. The output of the acquisition units feed a controller that can select any of the available demodulator-decoder chains. Once synchronization is obtained, the data portion of the transmissions must be demodulated and decoded. The responses from users will be spread by the same PN code thus all the filters and PN code generators used at a supplier station are identical. Figure 2-6 also shows the option of having multiple incoming codes by adding the appropriate acquisition units. It should be noted that there are only a few codes that a supplier may use and these can be generated by or stored in the user terminals. Furthermore, it is possible for a supplier to command a user terminal to use a second spreading sequence by communicating to the user on the first code and requesting a change of code. This process is also followed when a second supplier needs to talk to a user that is not assigned to it. In the second case the change of code (to the code of the second supplier) command is sent by the first supplier after receiving a request to transmit by the second supplier.

The key parts of a supplier station are the acquisition (ACQ) units that monitor the RF spectrum coming from each spotbeam. The ACQs utilize devices that are matched to the first part of the chip sequences that spread the user's replies. These devices will serve the dual purpose of detecting the presence of return signals, and identifying the code being used by that user. Because of possible frequency uncertainty on the incoming burst transmissions, multiple filters may have to be used in parallel.

2.1.5 PERFORMANCE CONSIDERATIONS

In developing a criterion for the performance of a multiple access system, the number of users supported is of the most importance. The number of users is a function of the traffic model used. Market survey is required before a realistic model is developed thus for the purposes of this report,

instead of basing the study on an arbitrary traffic model, the maximum number of simultaneous channels is considered.

The PASS FDMA design requires 142 spotbeams to cover CONUS, and provides an equivalent of two thousand 4.8 Kbps channels (9.6 Mbps) in each of the forward and return directions. Therefore the same total data rate and number of channels are used as the required capacity in the case of CDMA. Taking from the strawman design case a 1 dB modem implementation loss, and a 3 dB margin, and taking an E_b/N_o of 4.5 dB as the required level in providing a 10^{-5} bit error rate using K=7, rate 1/2 convolutional coding and Viterbi decoding, then the total required E_b/N_o at the input to the receivers is 8.5 dB.

Weber, Huth, and Batson in a paper titled "Performance Consideration of Code Division Multiple-Access Systems"[5] discuss the number of users that can be accommodated in a direct-sequence spread spectrum multiple access system. As opposed to the operation of acquisition and tracking, they consider only communication performance and use the probability of bit error as the performance measure. For a randomly accessed CDMA system consisting of a number of users transmitting at equal powers, the above mentioned paper gives the means of calculating the degradation in bit error rate as a function of the number of simultaneous users for both coded and uncoded data to be:

$$DF = \frac{1}{1-(n-1)(R_b/R_c)(E_b/N_o)} \qquad \text{Eq. 2-3}$$

where DF is the Degradation Factor, n is the number of simultaneous users accessing the channel, R_b is the bit rate, and R_c is the spread rate or chip rate.

In the forward direction of the CDMA system there are 142 frequency subbands each including transmissions to a particular spotbeam. On the average each subband should be capable of handling 67.6 Kbps (9.6 Mbps/142) of data or equivalently four 19.2 Kbps channels. Substituting in Eq. 2-3,

$$DF = \frac{1}{1-(4-1)(19200/R_c)(E_b/N_o)}$$

gives the degradation in bit error as a function of R_c and E_b/N_o. Figure 2-7 shows the total one-direction bandwidth (assuming same chip rate for forward and return directions) and the degradation in BER performance as a function of the chip rate and the required E_b/N_o. As seen from the plots, the degradation and its slope approach zero as chip rate

increases. In order to avoid near-far problems inherent to a non-power controlled CDMA system, the operating point should be selected at a high chip rate (>10 Mcps) and thus a high bandwidth requirement. For PASS, assuming power control is applied, a chip rate of 2.88 Mcps is selected. This leads to a degradation of ≈0.7 dB with a bandwidth requirement of 460 MHz. Figure 2-8 gives the degradation as a function of the number of simultaneous supplier channels for the 2.88 Mcps operating point. Note that if an extra 0.3 dB of degradation is allowed, the capacity will increase by 50%. In order to provide the extra margin, the E_b/N_o should remain the same and either the front end or the coding gain has to improve.

In the return direction, the link is to support two thousand 4.8 Kbps channels transmitted via the spotbeams. These channels affect the performance of the receivers at every supplier station. Taking the 2000 as the total number of simultaneous users and without including the increased capacity due to the voice activity factor, each beam will have to support an average of 14 users at an E_b/N_o of 8.5 dB at any instant of time. Plots of degradation as a function of chip rate for E_b/N_os of 8.5, 9, and 10 dB are shown in Fig. 2-9. Assuming the same chip rates are to be used in both forward and return directions, the plot of 8.5 dB gives a degradation of 0.8 dB. Figure 2-10 depicts the effect of increasing the number of simultaneous transmissions on the link performance, namely a 25% increase in capacity for a 0.2 dB extra degradation in code noise.

In order to increase the margin to compensate for the degradation due to code noise, a more effective coding scheme without any increase in the required bandwidth, or on-board processing could be considered. Figure 2-11 depicts the amount of extra margin required as a function of the uplink and downlink bandwidths. These plots can be used in determining a suitable operating point based on the complexity of the coding algorithm used.

2.1.6 CHALLENGES

The key feature of a spread spectrum system is the pseudo-noise (PN) transmission that allows for CDMA. Acquisition and synchronization to the PN are the problems in employing CDMA. Rapid acquisition implies short sequences, while longer sequences with ever-increasing time-bandwidth products are required to decrease cross correlation of multiple user systems. In any spread spectrum system, the purpose of the acquisition subsystem is to establish coarse (i.e., to

within one chip duration) time alignment of the transmitted PN sequence and a locally generated replica of it. There are several available techniques for establishing coarse synchronization.

The acquisition subsystem can be thought of as a correlator that is matched to the incoming code. A matched filter can either operate at IF or can be a digital device that operates on data decisions. Due to discrete sampling, the digital devices have slightly inferior performance as compared to analog devices, however they provide the flexibility of automatic changing of the spreading code and chip rate.

The candidate technologies for implementing matched filters are charged couple devices (CCDs), digital correlators, and surface acoustic wave (SAW) filters. CCDs perform many of the same functions as SAW devices except in a different range of bandwidth. Most practical CCDs are limited to a bandwidth of 10 MHz whereas SAW filters can be much wider. For matched filter applications in systems requiring high chip rates and fixed matching codes SAWs are recommended (programmable SAWs are available but not widely used). CCD is a clocked device that samples the signal appearing at its input. Because in neither the user terminals nor the supplier stations a synchronous chip-rate clock is available in the receiver prior to pilot acquisition, it is necessary to sample the input signal at some multiple of the chip rate or use a SAW matched filter.

In a user terminal, the acquisition unit is initially searching for a continuously running pilot. Thus a serial search of the incoming PN sequence, using discrete integrated circuits, can be performed. This requires a longer acquisition time than using a SAW matched filter, however it can be developed very simply and cost effectively by using VLSI technologies. For the supplier station it is recommended that SAW filters be used. It should be noted that SAW filters will require temperature compensation in order to stay at their nominal center frequency. The development of acquisition methods, providing high processing gain at negative signal-to-noise ratios in the presence of wide frequency shifts, is the only challenge of using CDMA beyond those listed in the strawman design.

2.1.7 BASELINE ADVANTAGES AND DISADVANTAGES

The CDMA system will provide random and unrestricted access to suppliers by the users and to the users by suppliers. The task of the network management center has been minimized

to a pilot generating and correcting center by decentralizing its functions to the supplier stations. Two thousand simultaneous channels are provided as the baseline capacity, however in a full-duplex two-way voice conversation the typical duty cycle for each side of the channel is less than 50%. Accordingly using a voice activity factor of 40% the number of channels increases to approximately 5000 voice-only channels. Figure 2-12 is a good example of the tradeoff between simultaneous data and voice channels.

These advantages come with a large bandwidth requirement, and 0.7 dB extra coding gain in each link. As was calculated in the previous section, the bandwidth required for the uplink and downlink of the CONUS beam is very high. In order to alleviate this shortcoming, some possible alternatives are discussed shortly.

As a result of a simplified network management center the problem of unauthorized use is one that enters into any spread spectrum system design. Although it is not easy to restrict the use of a wideband transponder, it is possible to monitor it at all times. In the case of a bent pipe transponder one could envision monitoring the average levels of the uplinks and downlinks and comparing them with samples of the total traffic as reported by the supplier stations. Based on the statistics and user distribution model, it is possible to detect the presence of unauthorized users. Of course one should keep in mind that the cost of building a supplier station from scratch is an expensive way of getting channel capacity. Fortunately, if one of the alternatives of the next section is implemented, this problem automatically disappears.

2.1.7.1 Bandwidth Efficient Alternatives

There are several methods that can be explored for use in PASS. Two possible solutions are:

Onboard Multi-carrier Spreading

The high bandwidth requirement is due to the one subband per spotbeam allocation as received or transmitted by the CONUS beams. The excess bandwidth in the forward direction can be minimized by utilizing a satellite switched TDMA format. This is accomplished by assigning a narrowband portion of the available spectrum to each supplier in order to allow a high rate TDM channel to transmit all of the spotbeam data to the satellite. Upon demodulation of the data, at the satellite, the transponder can encode, spread and transmit

the data through appropriate spotbeams. It is possible to implement a number of code generators onboard the satellite and assign different codes to suppliers.

In the return direction due to the high number of users and codes being utilized, onboard processing is much more complicated. It may be possible to implement the reverse process, however, an in depth tradeoff study between bandwidth efficiency and satellite complexity is required.

Note that if this alternative is implemented, the spread pilots will be generated onboard the satellite, thus simplifying the design of the NCMC. Furthermore, the hardware requirement of the supplier station is drastically reduced by transferring some of the hardware to the satellite.

Onboard Spreading and Despreading

The second option is related to the first one. The difference is that the full bandwidth available for the uplink and the downlink of the CONUS beam is assigned to a spread channel. A supplier station spreads the signal using a PN code preassigned for a spotbeam (N codes will be used). The satellite transponder will in this case consist of N receiver chains that acquire and demodulate the signals and based on the supplier ID respread the data for transmission by the spotbeam.

The onboard processing in the return direction consists of acquisition and demodulation of simultaneous signals originating from users all around CONUS. The transmissions from user terminals will all start with a known acquisition sequence followed by a destination address. The spread sequence would be used to do the initial detection of an incoming signal. The destination address would then be used to send the signal to the appropriate supplier. The receivers onboard the satellite continuously search for the PN acquisition code and upon detection of one start a demodulator/decoder chain similar to the one presented for the supplier station. The recovered signal is then respread and transmitted via the CONUS beam in conjunction with all other signals. This method would require a single code acquisition chain along with multiple demodulator chains.

As compared to the previous option, this alternative solution is more favorable because all communication is spread over the same bandwidth instead of dividing it among different suppliers. Furthermore onboard processing increases the available link margin in both forward and return directions.

However, the design of the return link of the transponder is not trivial.

2.2 FDMA SYSTEM

As previously mentioned, the PASS strawman design calls for TDMA channels in the forward direction and DA/FDMA in the return direction. Figure 2-13 describes the strawman frequency plan in which the NMC transmits the pilot for all of the spotbeams. Each beam has at least a TDM high rate channel (HRC) and a low rate channel (LRC) on which all suppliers can communicate to their respective users. These channels along with the pilot form a frequency segment per spotbeam, i.e, N frequency segments are transmitted to the satellite via the CONUS beam. In the downlink of the forward direction frequency reuse is employed in converting the N uplink segments to nine frequency subbands for transmissions by the spotbeams.

In the return direction once again frequency reuse is used in transmitting a number of HRCs and LRCs via spotbeams to the suppliers. The downlink in this case consists of N distinct frequency segments.

In order for a user (or a supplier) to gain access to a channel, it sends a request to the NMC in order to be assigned either a frequency slot (or a time). Upon reception of the channel assignment, the user terminal automatically will tune its synthesizer to the appropriate frequency. Meanwhile the supplier will synchronize its TDM clock to the appropriate interval. Note that because of the single channel per carrier (SCPC) nature of the transmissions from the user, wide guard bands may have to be included in the frequency plan to avoid interference if Doppler shifts are present.

Figures 2-14 to 2-17 show the block diagrams of the transponder, a user terminal, the NMC, and a supplier station respectively.

2.3 COMPARISON

The strawman design and the CDMA option are functionally the same, however from an operational point of view and system complexity there are pronounced differences.

The satellite transponder follows a bent-pipe architecture with frequency shifting in accordance with the frequency plan. Except for the bandwidth of filters and the change in

local oscillators, the transponder is very similar to the one described in the CDMA baseline design.

The user terminal is different in the sense that the initial search is for one of nine narrowband pilot frequencies rather than spread ones. The user terminal's phase locked loop (PLL) in conjunction with the sweep controller searches and locks to the pilot. Upon locking to the pilot, the synthesizer sets the appropriate up conversion and down conversion frequencies. The shaded blocks in Fig. 2-15 give an indication of the areas of difference between this design and the CDMA one. Due to the large number of channels, the synthesizer required for the FDMA design may be very complicated.

The most pronounced difference between the two systems shows up in the design of the NMC. The NMC is the central controller of the PASS strawman design. The role of this portion of the system is to listen for requests from suppliers and users, assign channels, and wait for the end of conversations. Furthermore, it includes pilot generation and recovery along with the billing functions. The NMC of the FDMA architecture is by far the most complicated portion of the ground segment. The CDMA architecture simplifies the design of the NMC by allowing random access in both forward and return directions, however the option exists for a supplier to control the users communications by virtue of start and stop commands. This function can be beneficial for system peak hours where control is required. Note that this option is distributed among all suppliers therefore an elaborate network management center will not be required.

From a hardware point of view, the supplier station depicted in the strawman design is less complicated than the CDMA one. Due to the demand access nature of the architecture, there are far less on-line receiver chains required to support the users. Upon receiving authorization from the NMC, the request channel can set a transmit chain and a receive chain to the assigned frequency and commence communication with its user. In conclusion, the difference in the hardware is due to the real time assignment of frequency compared to the preassigned codes of the suppliers.

Considering both the ground and space segments, the design complexity of the CDMA and FDMA systems are comparable. Although the bandwidth requirement driven by the use of CDMA is approximately ten times that of FDMA, it is anticipated that with the advent of more powerful error correcting codes and higher output satellite power systems, the number of

users per unit bandwidth will increase beyond that of FDMA[6]. This is because the transmitted bandwidth of the FDMA channel is proportional to the amount of coding that is applied to the data, hence, for a given channel bandwidth the more coding that is applied, the lower the number of user channels that can be accommodated. In the case of CDMA the data is spread over the total bandwidth of the channel, thus the increase in coding bits required by the more powerful error correcting codes does not decrease the available user bandwidth and furthermore could conceivably allow for an increase in the number of users due to increased channel coding and satellite power system performance.

The following table summarizes these differences:

Table 2-4 DESIGN COMPARISON

	CDMA BASELINE	PASS STRAWMAN
Hardware Complexity:		
- Transponder	Simple	Simple
- User Terminal	Moderate	Moderate
- NMC	Simple	Complex
- Supplier	Complex	Moderate
Operation:	Simple	Moderate
Bandwidth: (Using Dual Polarization)	460 MHz Uplink 460 MHz Downlink	27 MHz Uplink 27 MHz Downlink
Capacity:	2000 4.8 Kbps DATA 5000 VOICE w/ VAF of 0.4	2000 4.8 Kbps Chs.
Margin:	≈2.3 dB Each Link	≈3 dB Each Link
Coding:	No effect on BW	Effects BW

2.4 CONCLUSION

The design of a CDMA architecture for the Personal Access Satellite System has been presented. Employing the properties of spread spectrum communication, the architecture

calls for unrestricted access to suppliers by users and vice versa. As compared to the FDMA strawman design, the CDMA baseline provides a more flexible access method, comparable hardware complexity, and the possibility of more voice channels (by virtue of the voice activity factor) at the expense of 0.7 dB degradation in each link and a ten time increase in the bandwidth required. The degradation can be compensated for by some additional error-correction-coding without increasing the overall bandwidth. Alternative methods are required in order to decrease the bandwidth requirement.

The random access spread spectrum architecture provides an alternate method for implementing the PASS concept. It is believed that unrestricted access, without capacity and time consuming channel assignment, are required for a personal satellite system at the turn of the century.

REFERENCES

[1] M. K. Sue, ed., "Personal Access Satellite System Concept Study," JPL D-5990, Jet Propulsion Laboratory, February 1989.

[2] J. K. Holmes, Coherent Spread Spectrum Systems. New York: John Wiley, 1982.

[3] K. Feher, Digital Communications: Satellite/Earth Station Engineering. Englewood Cliffs, NJ: Prentice-Hall, 1981.

[4] D. V. Sarwate and M. B. Pursley, "Crosscorrelation properties of pseudorandom and related sequences," Proc. IEEE, vol. 68, pp. 593-619, May 1980.

[5] C. L. Weber, G. K. Huth, and B. H. Batson, "Performance Consideration of Code Division Multiple-Access Systems," IEEE Transactions on Vehicular Technology, vol. VT-30, No. 1, pp. 3-10, February 1981.

[6] K. Dessouky, and Masoud Motamedi, "FDMA and CDMA PASS Design Tradeoffs, Comparison of Results, and Conclusions," JPL Interoffice Memorandum No. 3392-90-001, January 1990.

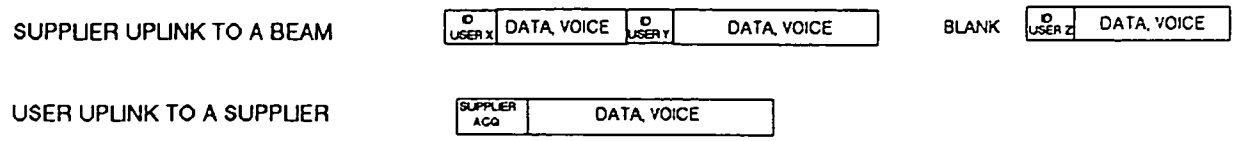

Figure 2-1 SAMPLE TIME PLAN

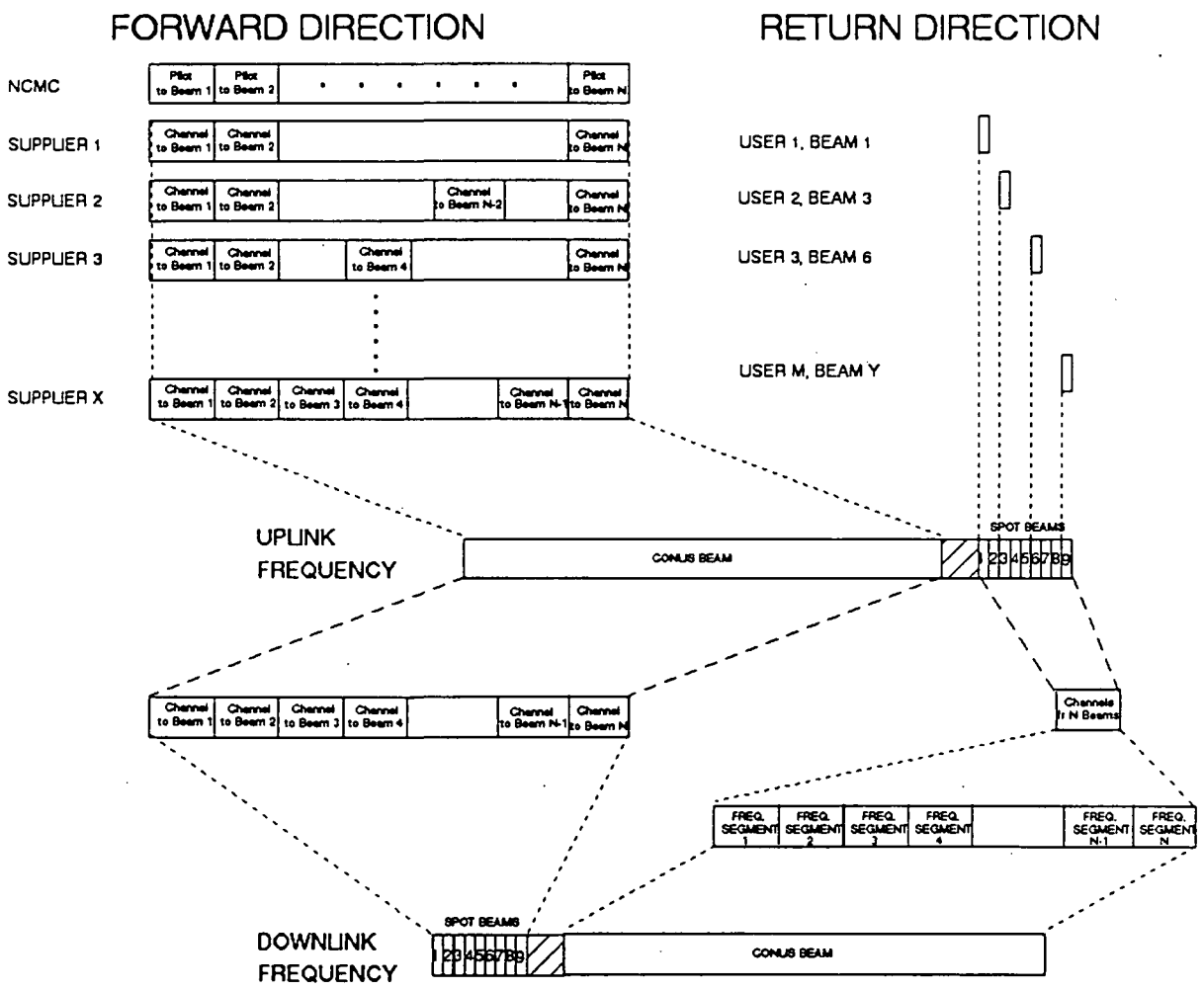

Figure 2-2 BASELINE FREQUENCY PLAN

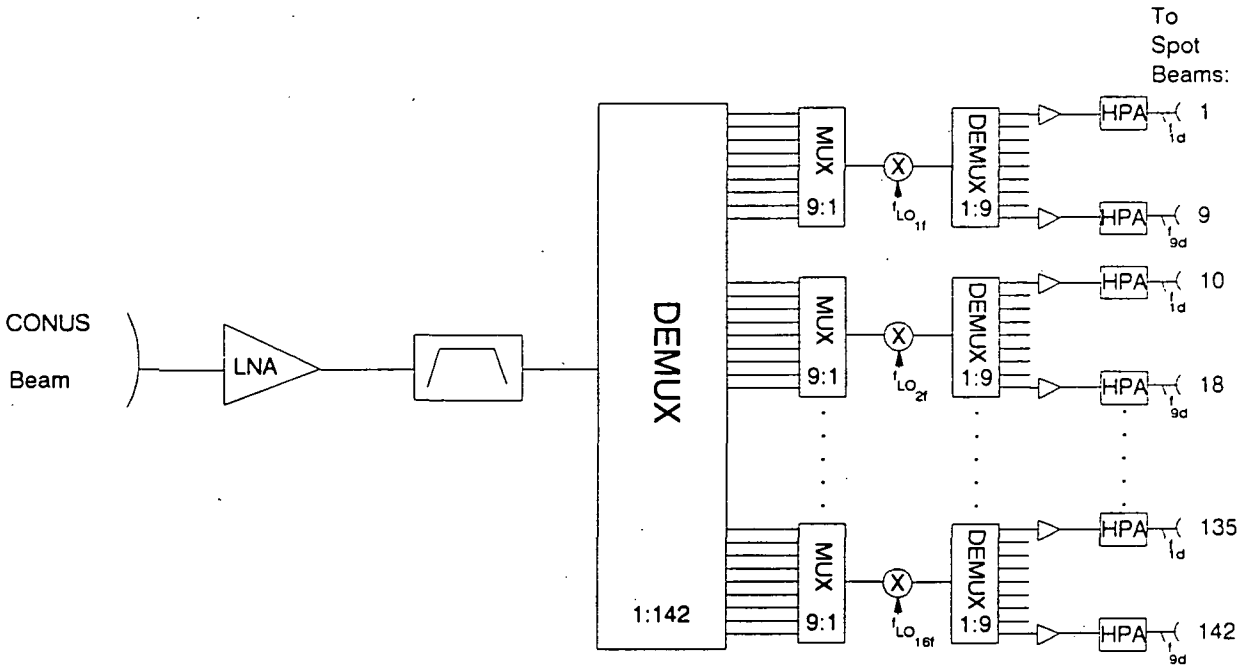

(a) FORWARD LINK

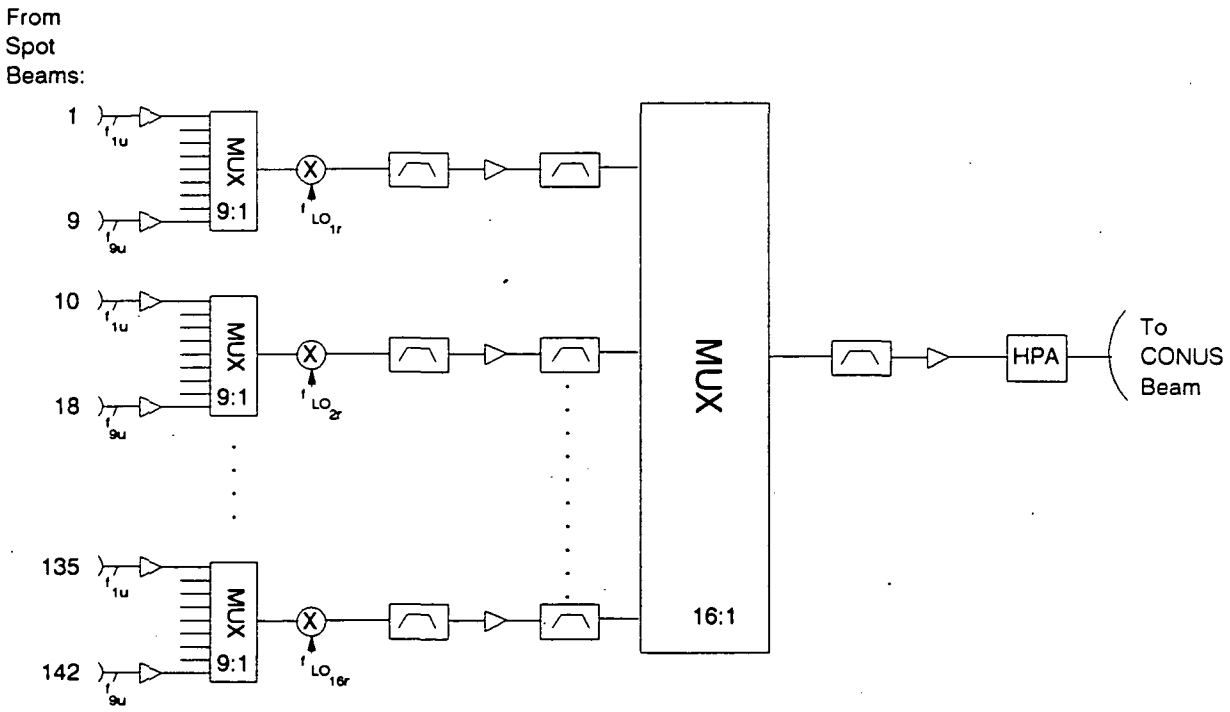

(b) RETURN LINK

Figure 2-3 CDMA SATELLITE TRANSPONDER

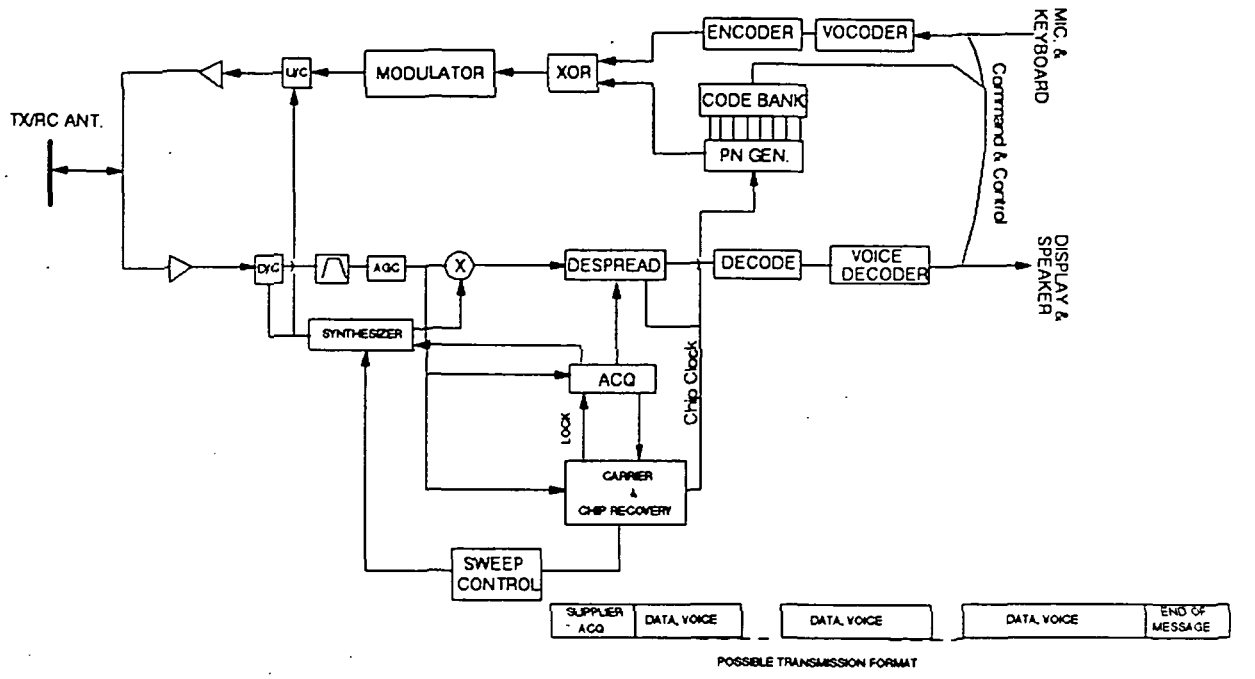

Figure 2-4a CDMA USER TERMINAL

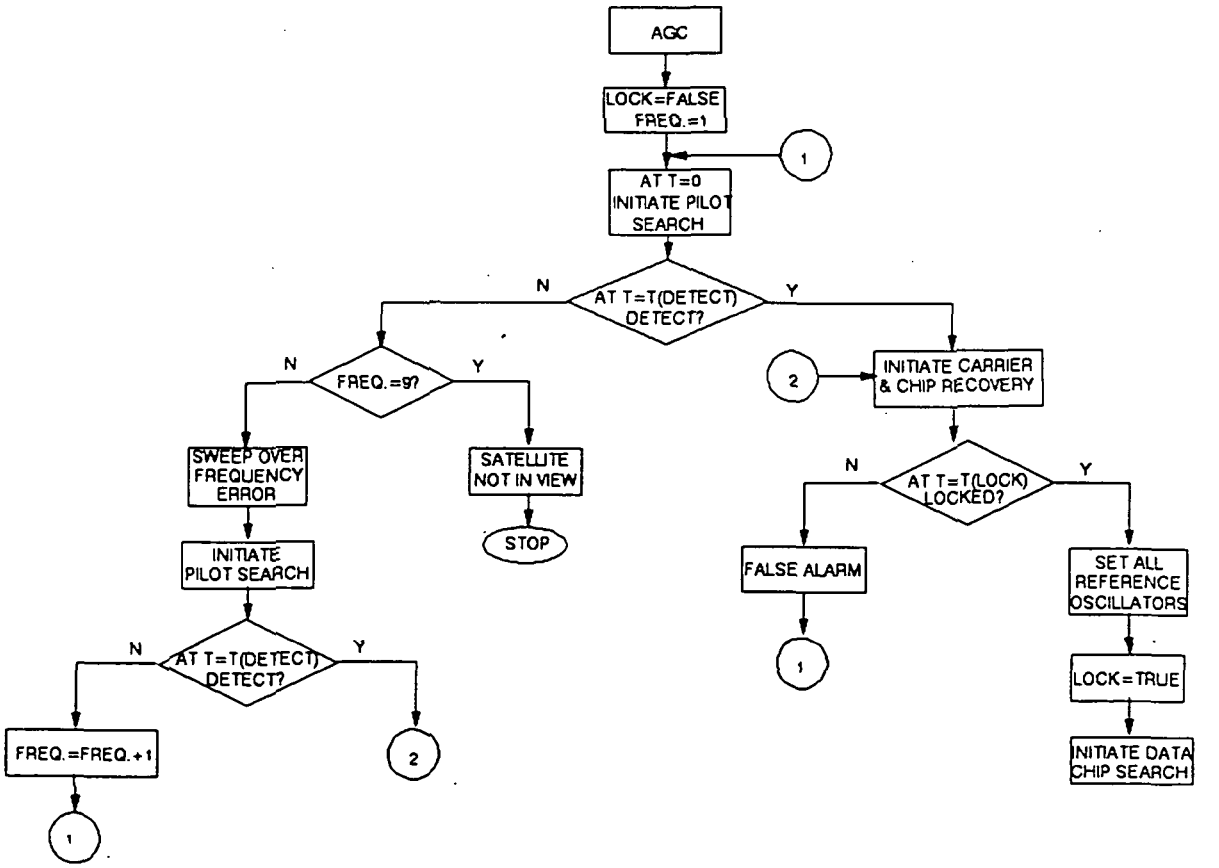

Figure 2-4b ACQUISITION FLOW DIAGRAM

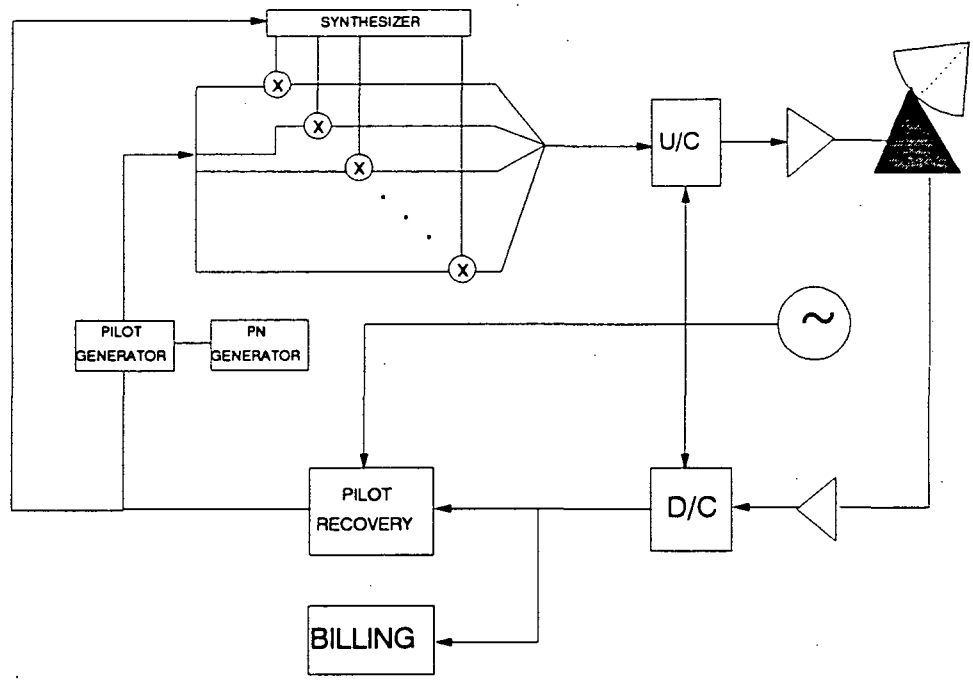

Figure 2-5 NCMC BLOCK DIAGRAM (CDMA)

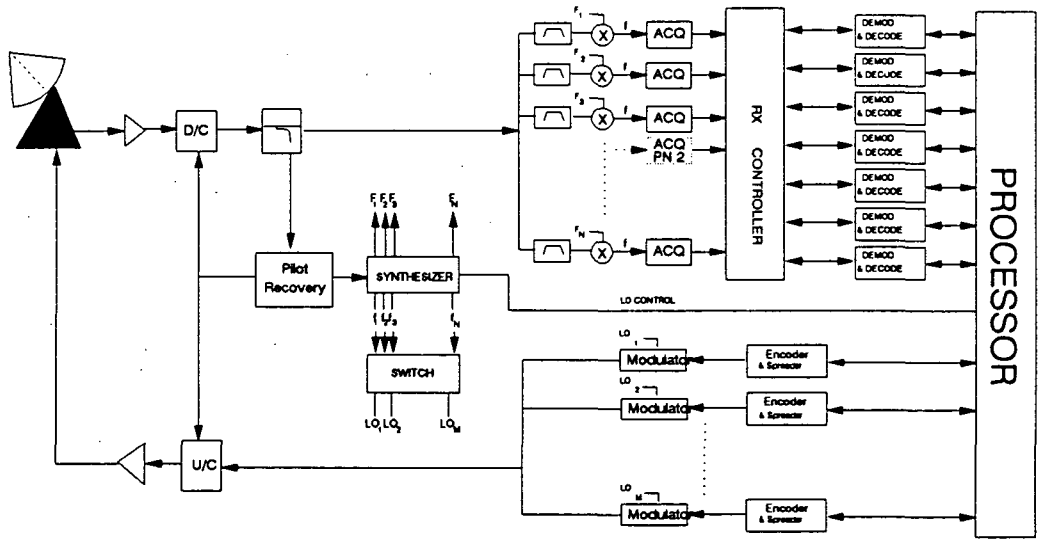

Figure 2-6 CDMA SUPPLIER STATION

FIGURE 2-7 DEGRADATION AS A FUNCTION OF CHIP RATE FOR THE FORWARD LINK (FOUR SIMULTANEOUS SUPPLIERS, 19.2 KBPS EACH)

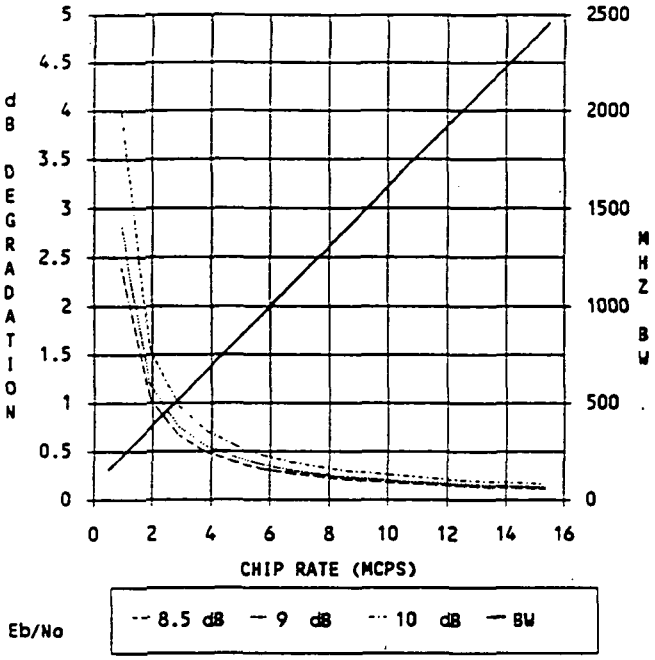

FIGURE 2-8 DEGRADATION AS A FUNCTION OF SIMULTANEOUS SUPPLIERS, Eb/No=8.5 dB

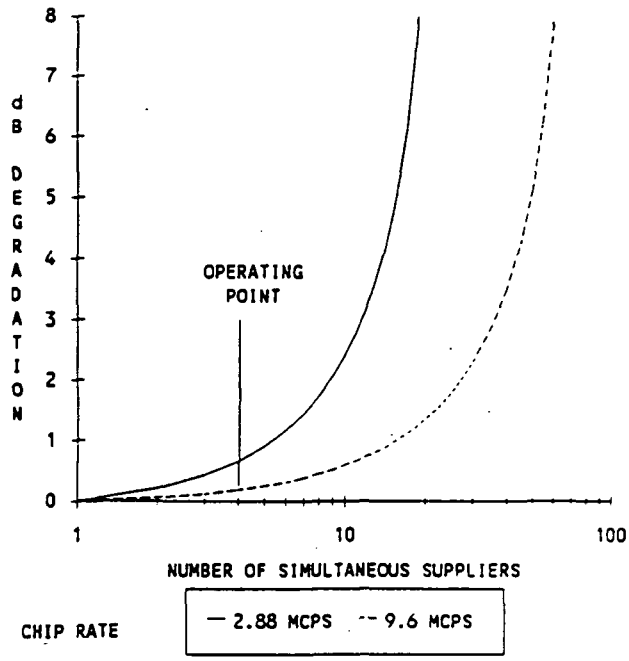

FIGURE 2-9 DEGRADATION AS A FUNCTION OF CHIP RATE FOR THE RETURN LINK (FOURTEEN SIMULTANEOUS USERS, 4.8 KBPS EACH)

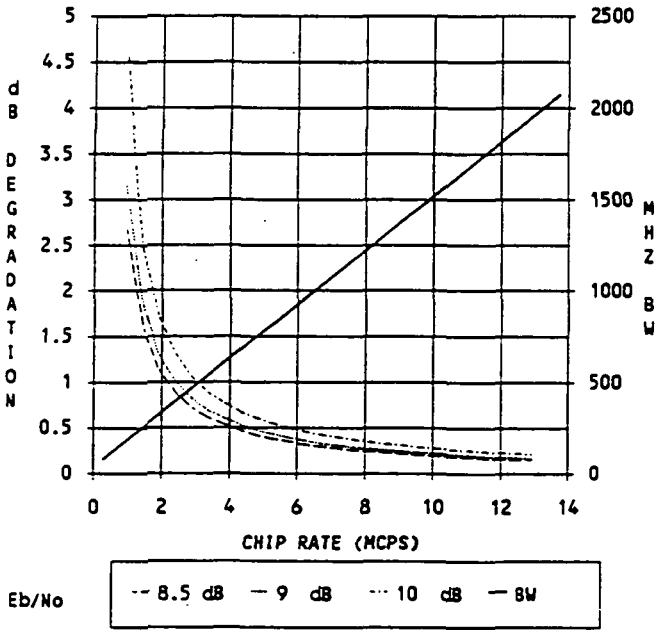

FIGURE 2-10 DEGRADATION AS A FUNCTION OF SIMULTANEOUS USERS, Eb/No=8.5 dB

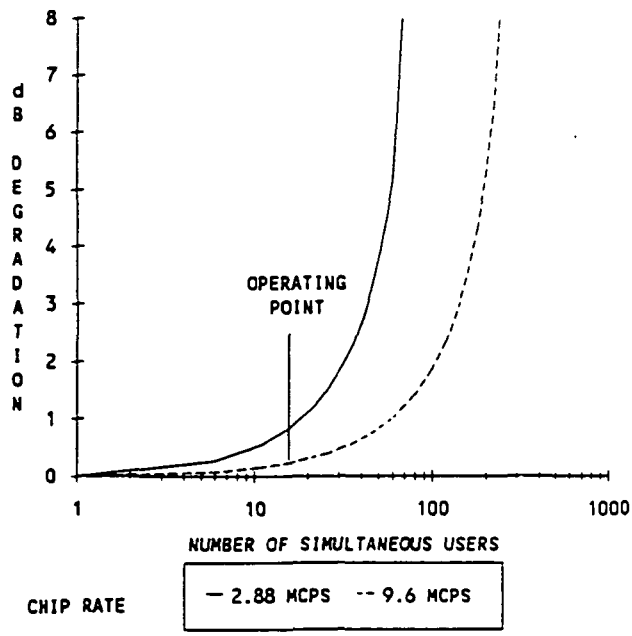

FIGURE 2-11 DEGRADATION AS A FUNCTION OF TOTAL BANDWIDTH, FOURTEEN 4.8 KBPS USERS & FOUR 19.2 KBPS SUPPLIERS PER BEAM, Eb/No = 8.5 dB

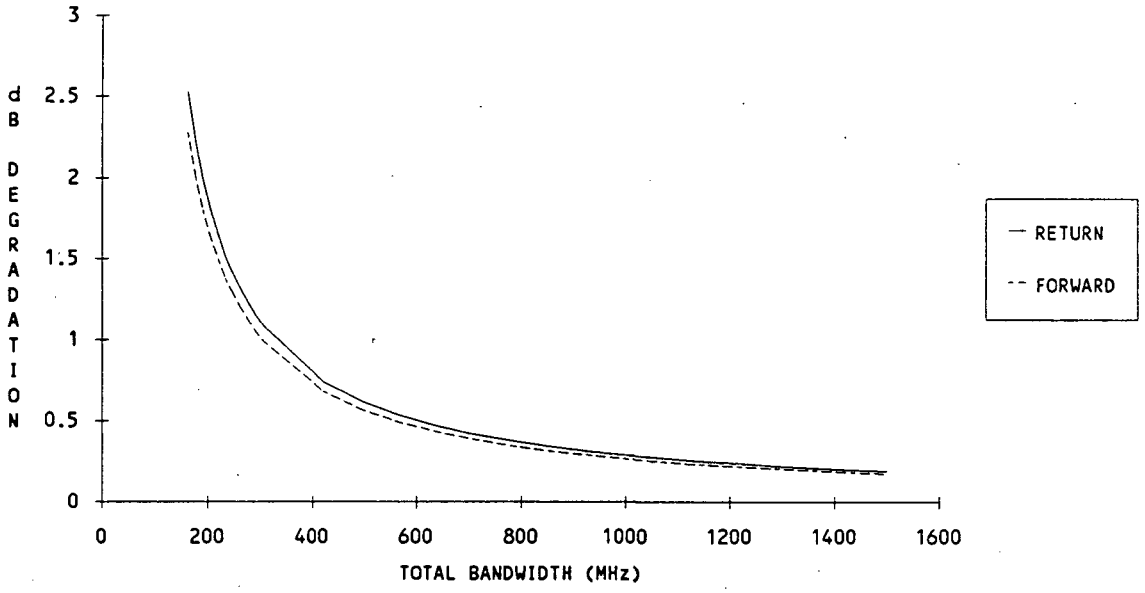

FIGURE 2-12 TRADEOFF BETWEEN VOICE CHANNELS & DATA CHANNELS, VOICE ACTIVITY FACTOR = 0.40

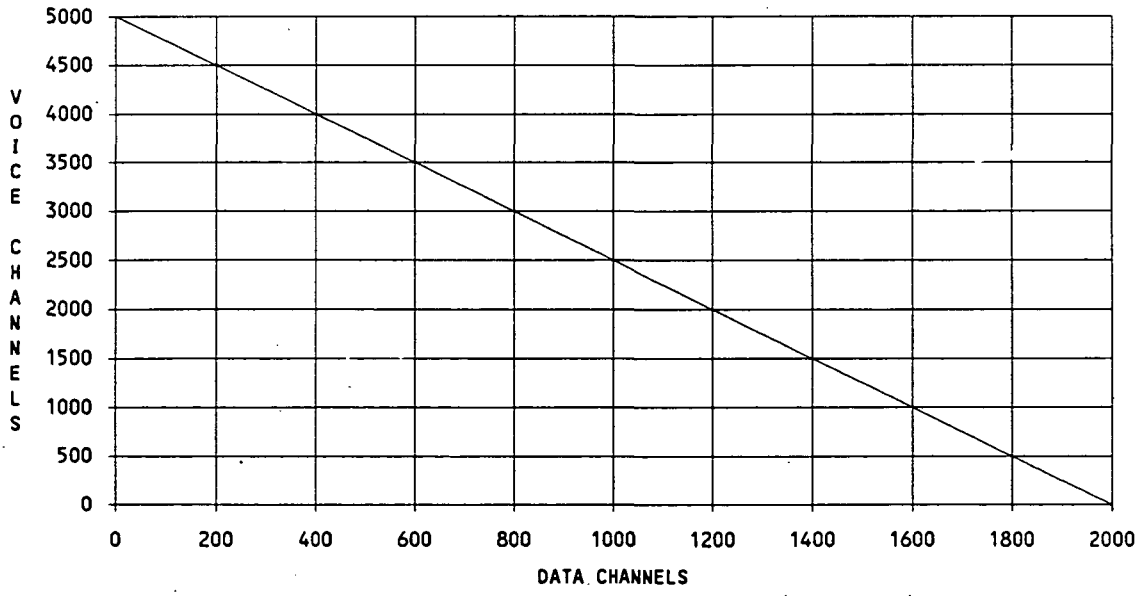

83

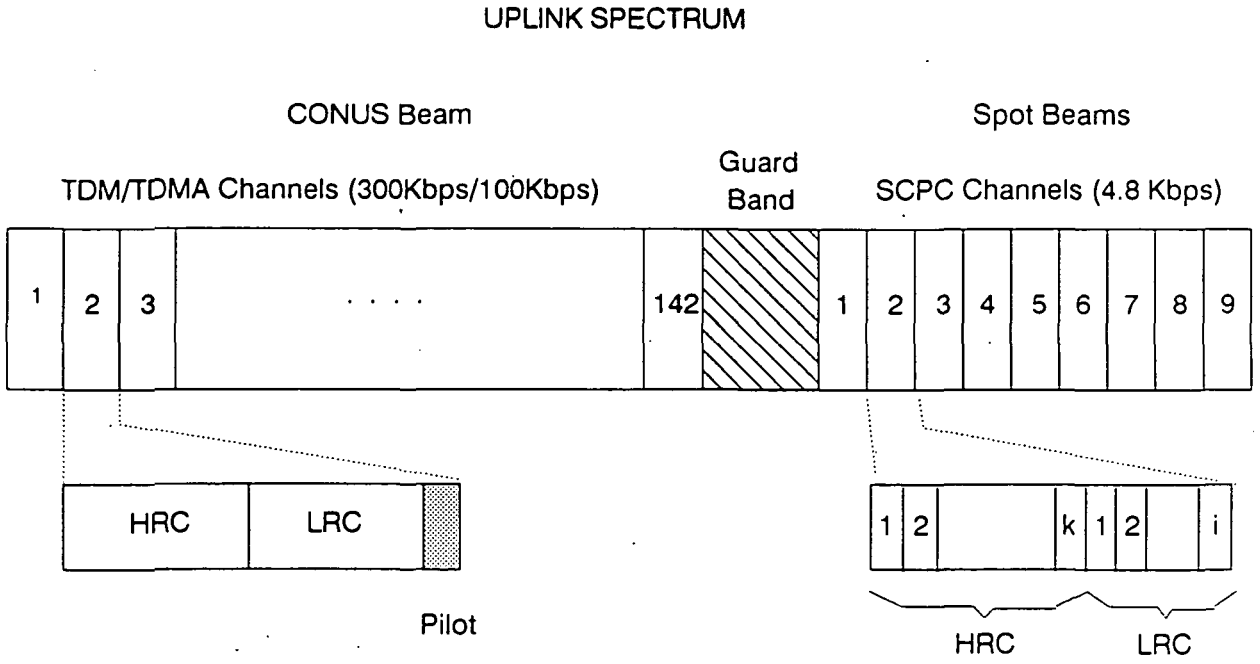

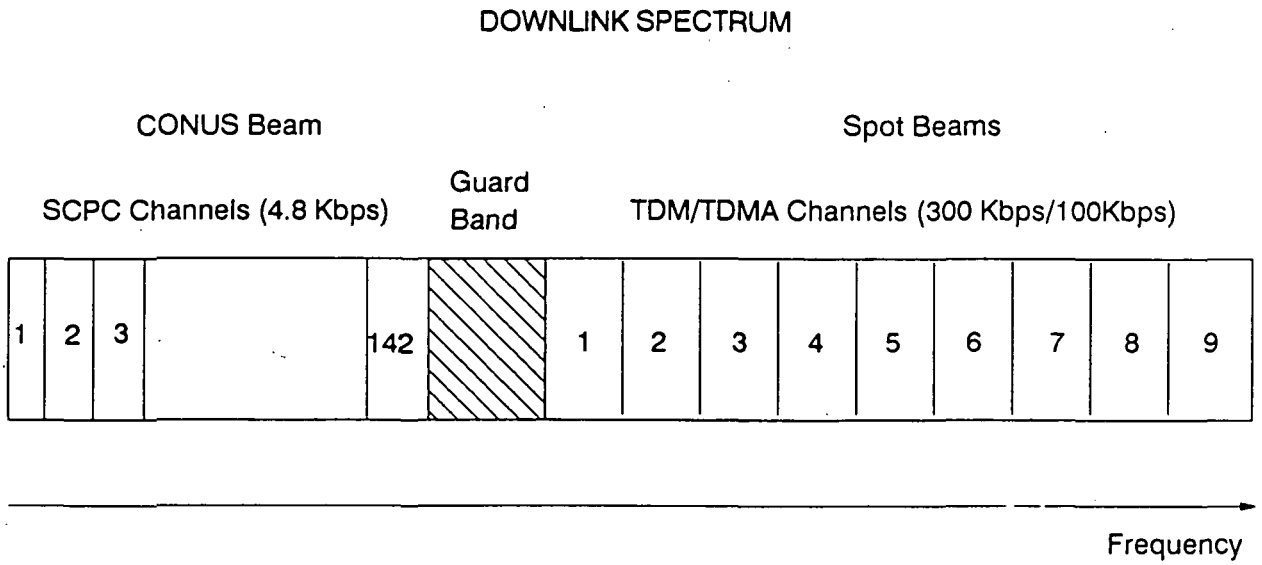

CONUS Beam:

142 uplink frequency bands for 142 fixed beams. Each Beam is addresses by a specific frequency, i.e. uplink band j is for the j th beam.

Spot Beams:

User in the 142 fixed beams use 9 uplink channels to transmit their SCPC uplink signals to the suppliers.

Figure 2-13 FDMA FREQUENCY PLAN

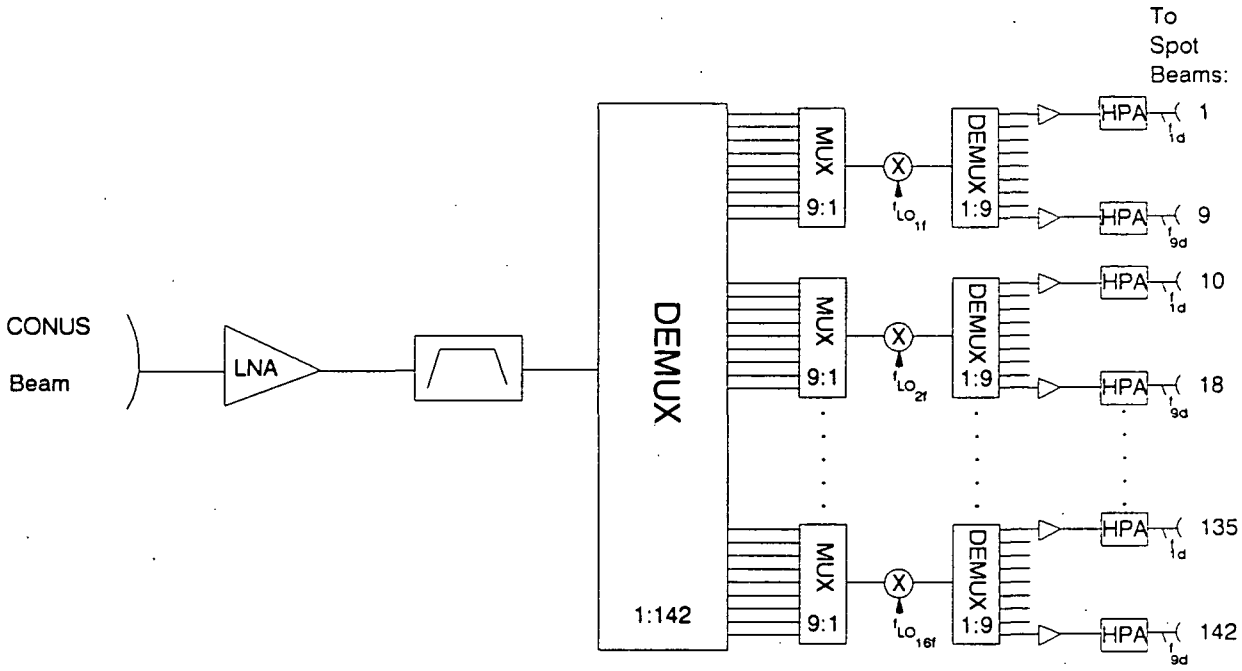

(a) FORWARD LINK

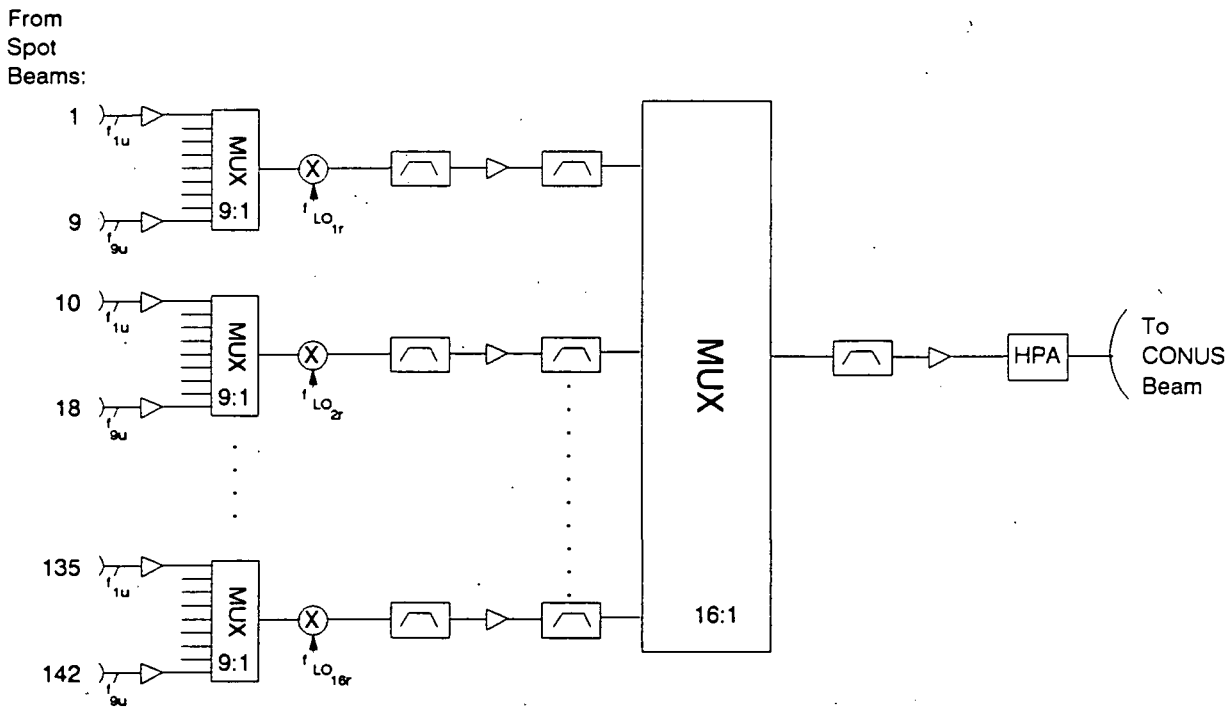

(b) RETURN LINK

Figure 2-14 FDMA SATELLITE TRANSPONDER

84

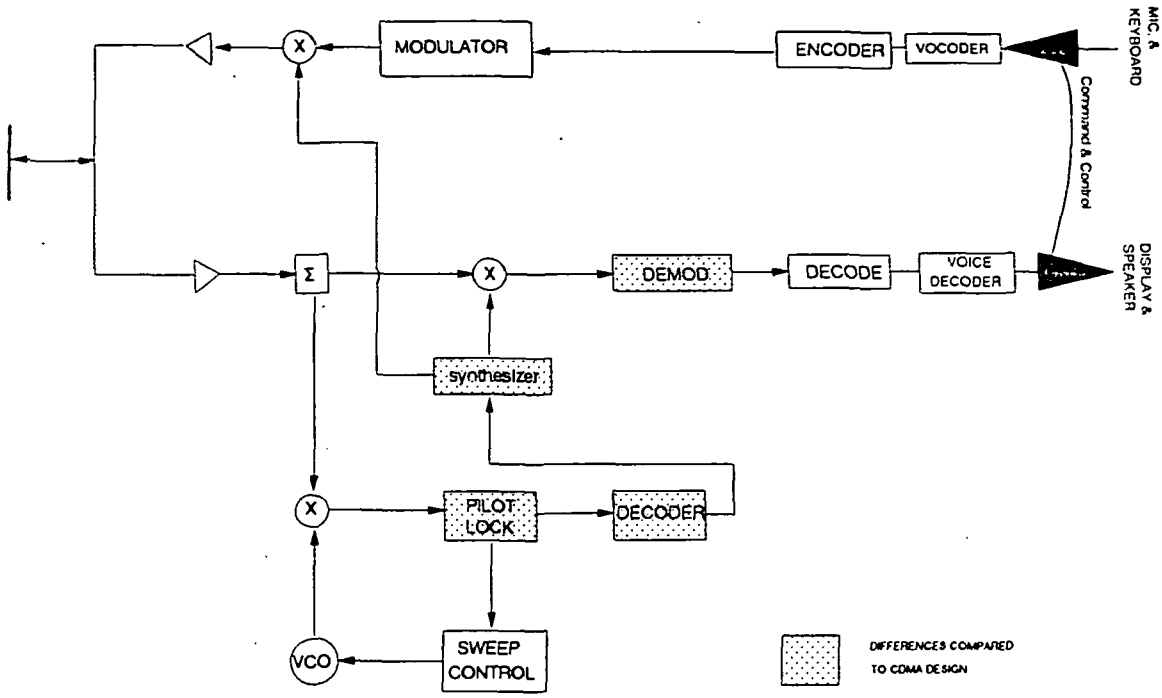

Figure 2-15 FDMA USER TERMINAL

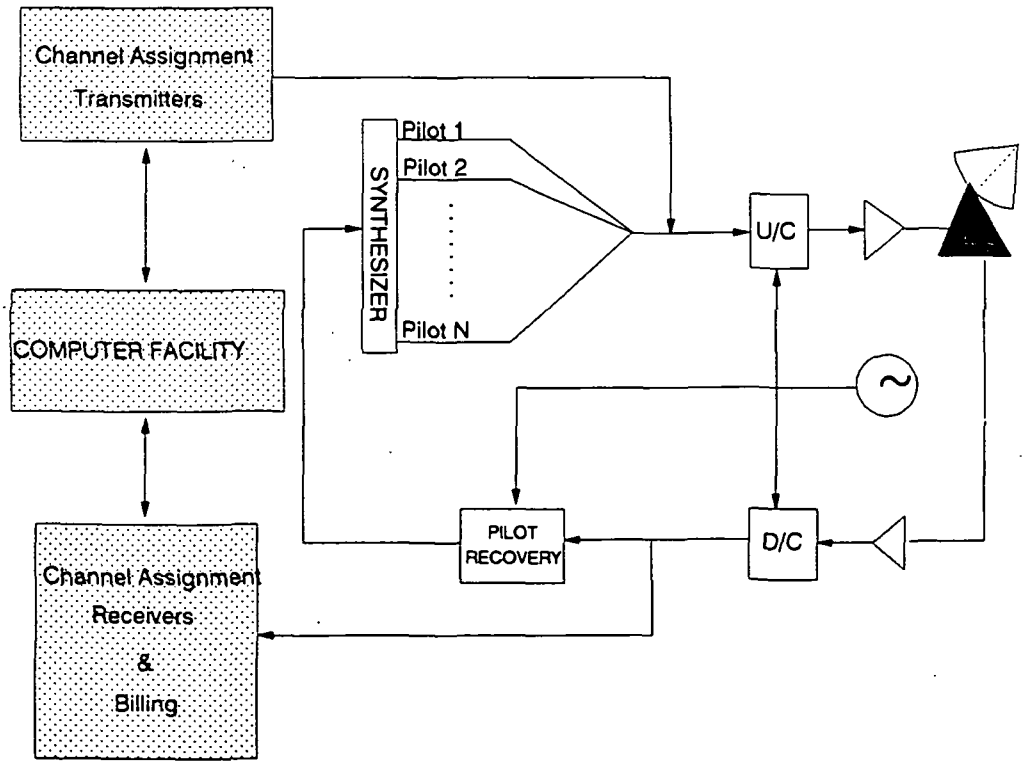

Figure 2-16 FDMA- NMC BLOCK DIAGRAM

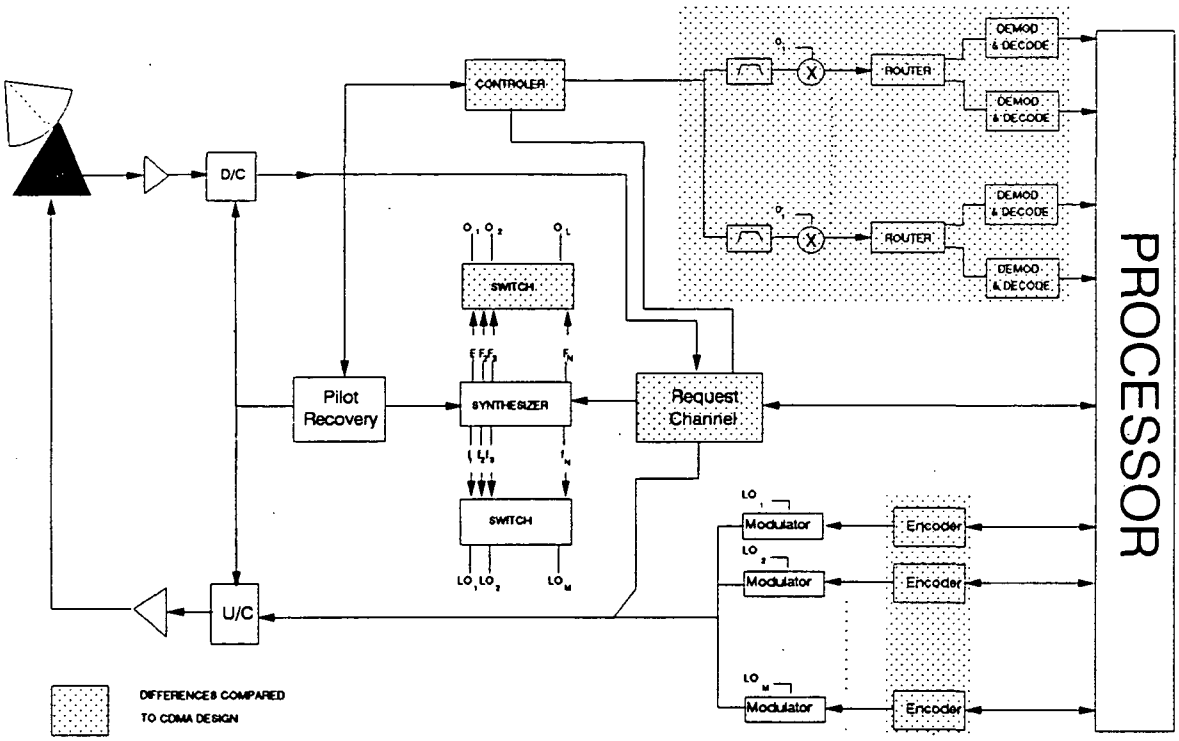

Figure 2-17 FDMA- SUPPLIER STATION

56

Chapter 3
Antenna Beam Coverage Concepts

Dr. Polly Estabrook and Masoud Motamedi

3.1 Introduction

The strawman PASS design calls for the use of a CONUS beam for transmission between the supplier and the satellite and for fixed beams for transmission between the basic personal terminal (BPT) and the satellite. The satellite uses a 3m main reflector for transmission at 20 GHz and a 2m main reflector for reception at 30 GHz. The beamwidth of the reflector is 0.35°. To cover CONUS 142 fixed beams are needed. A sample fixed beam coverage plan for CONUS is shown in Figure 3.1. In the strawman design, suppliers transmit to the users on a 100 Kbps TDMA carrier for the low rate channel and on a 300 Kbps TDMA carrier for the high rate channel. The uplink frequency of this TDMA carrier is chosen according to the coverage area - or beam location - in which the user is located. Users with Basic Personal Terminals (BPTs) transmit a SCPC signal at 4.8 Kbps in the frequency band assigned to their coverage area. The time and duration of supplier transmissions are determined by the network management center (NMC) as are the specific transmit frequencies for the users [1].

The decision to employ spot beams to link users to the satellite was motivated by several factors. Major differences in beam characteristics are listed in Table 3.1; the entries are based on various satellite descriptions [2,3,4,5]. The use of spot beams, whether fixed, switched or scanning, allows users to operate with satellites having higher $EIRP$ and G/T than possible with CONUS beams. Operation with small terminals is therefore possible. Spot beams also allow spectral reuse through assignment of the same frequency to geographically separated beams. Connecting users via spot beams rather than with a CONUS beam brings about two problems: difficulty in providing a broadcast channel and the necessity for the satellite transponder to be designed specifically to connect users in various spot beams. The importance of the latter is reduced in the strawman design by the use of CONUS and spot beams, the drawback then being that user to user communication requires a two hop satellite link. For PASS, the advantages of spot beam use – primarily the ability to work with small terminals – outweigh the disadvantages and motivate their use over designs employing only

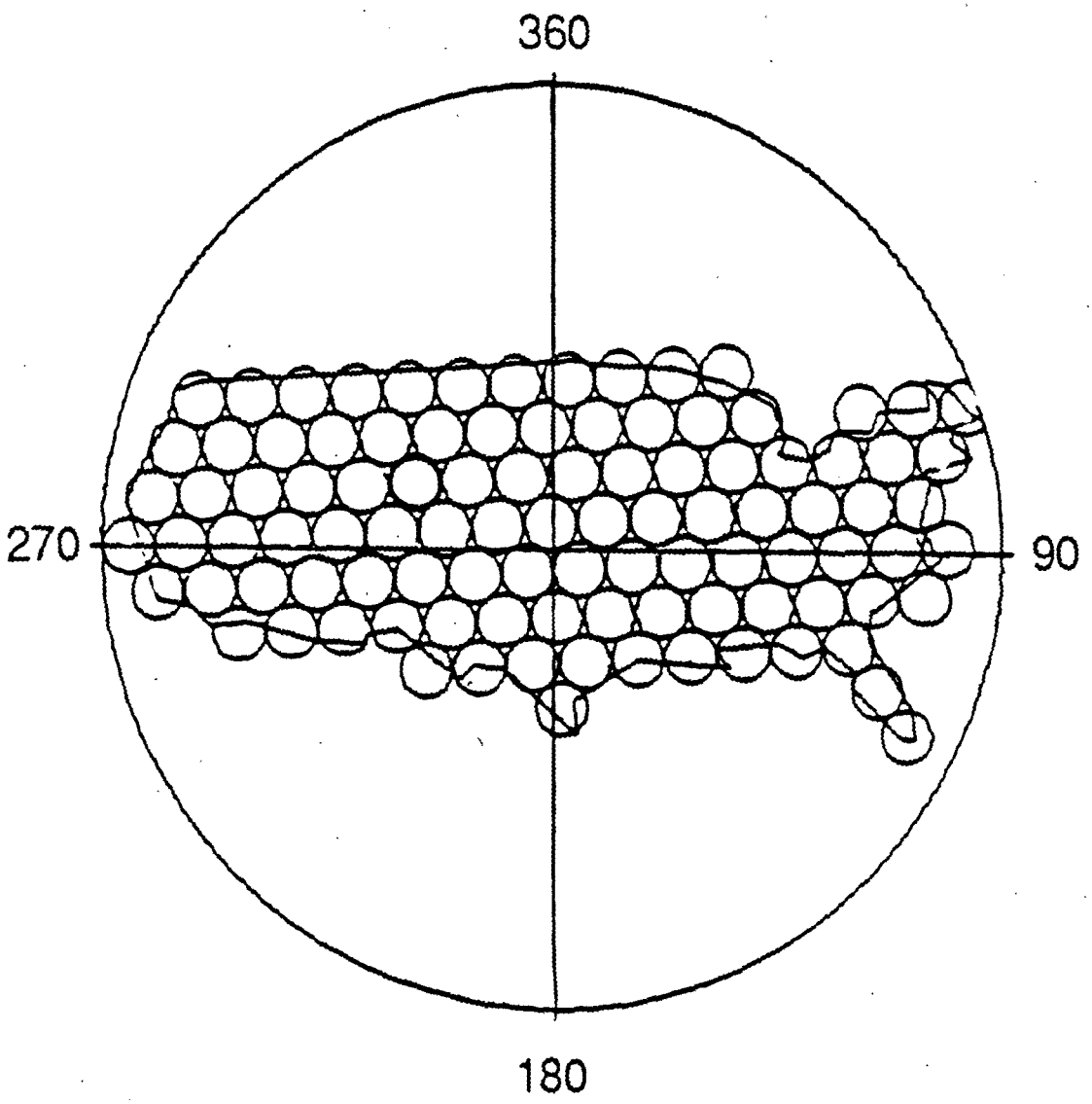

Figure 3.1: Fixed beam CONUS coverage (from [1]).

CONUS beams.

There are several types of spot beams under consideration for the PASS system besides fixed beams. The beam pattern of a CONUS coverage switched beam is shown in Figure 3.2: that of a scanning beam is illustrated in Figure 3.3. Here a switched beam refers to one in which the signal from the satellite is connected alternatively to various feed horns, each of which create a beam focused on a different geographical region. In Figure 3.2 the coverage pattern of four switched beams is identified. Each beam is shown as illuminating five areas, all identified by the same fill pattern. For example, the hatched beam is shown as capable of illuminating either an area on the West Coast, or one of three Mid-Western locations or an area on the East Coast. In the satellite transponder the output signals (in the forward direction, these signals are on a TDMA carrier; in the return direction, they are SCPC carriers) bound for any of these five areas are connected to a switch which alternatively connects to one of five possible antenna feeds (see Section 3.2.2). Scanning beams are here taken to mean beams whose footprints are moved between contiguous regions in the beam's coverage area. In Figure 3.3 CONUS coverage is achieved by dividing the US into 16 North-South sections. Other types of spot beams can be considered for PASS such as the hopping beam configuration used by ACTS [2]. For the purposes of this chapter, switched beams and scanning beams are considered to share similar characteristics.

Table 3.2 lists the advantages and disadvantages of switched/scanning beams relative to fixed beams. The advantages of fixed beams are that less centralized control over the network is necessary to coordinate communication between supplier and user and that they possess greater capacity for frequency reuse. The main advantage of switched/scanning beams is their ability to match the satellite's capacity to variable traffic needs.

The difference in the ability of these two beam types to effectively match current traffic requirements to satellite capacity can be understood as follows. Because the envisaged spot beams, whether fixed, switched, or scanning, handle traffic from a small area (about 135 mile diameter for a 0.35° beamwidth), the number of users or traffic demands within a beam will be fluctuate rapidly depending on the time of day, the season, etc. In addition the traffic requirements will vary greatly from beam to beam. Although the bandwidth given to each fixed beam and the size of satellite power amplifier associated with it can be pre-set prior to satellite launch according to the expected traffic per beam, this static solution can not efficiently match the satellite power and bandwidth to the traffic. Some techniques for distributing satellite power according to traffic variations when fixed beams are used are discussed in Chapter 5.

In contrast, scanning or switched beams have the advantage that they transmit and collect data from several coverage areas. Thus the time distribution of the traffic is averaged over several coverage areas. Futhermore switched/scanning beams are capable of picking up or delivering traffic to each of their coverage areas within one TDMA frame. The beam's dwell time is dynamically adjusted to match the traffic needs of a particular coverage area. In this way the time-varying distribution of the traffic can be smoothed. This results in a better match of the satellite's capacity to network traffic, or a reduced probability of users in one beam being queued up to use the satellite while other beams have no traffic. Although

Table 3.1: Comparison of CONUS and Spot Beam Characteristics

	CONUS Beam	Spot Beam
System:		
Broadcast Channel	Yes	Possible; but may require satellite processing and switching
Potential for small E/S	Limited	Yes
Match satellite capacity to traffic requirements	Good (depending on access tech.)	Some (depending on spot beam type)
Frequency Reuse	No	Yes
Transponder Complexity:	Simple	Complexity depends on comm. link: 1. Somewhat complex if unsymmetric link † 2. More complex if spectral reuse used (eg. PASS strawman design) 3. Very complex if interbeam connection is required (i.e. certain advanced satellite designs)
Satellite Antenna Complexity:	Simple	Complex BFN required
User Terminal Complexity:	Low May require higher gain ant. & higher EIRPs	Higher

† An unsymmetrical link is used to mean one where the CONUS beam used to RX/TX from hub and spot beams used to TX/RX to the user terminals.

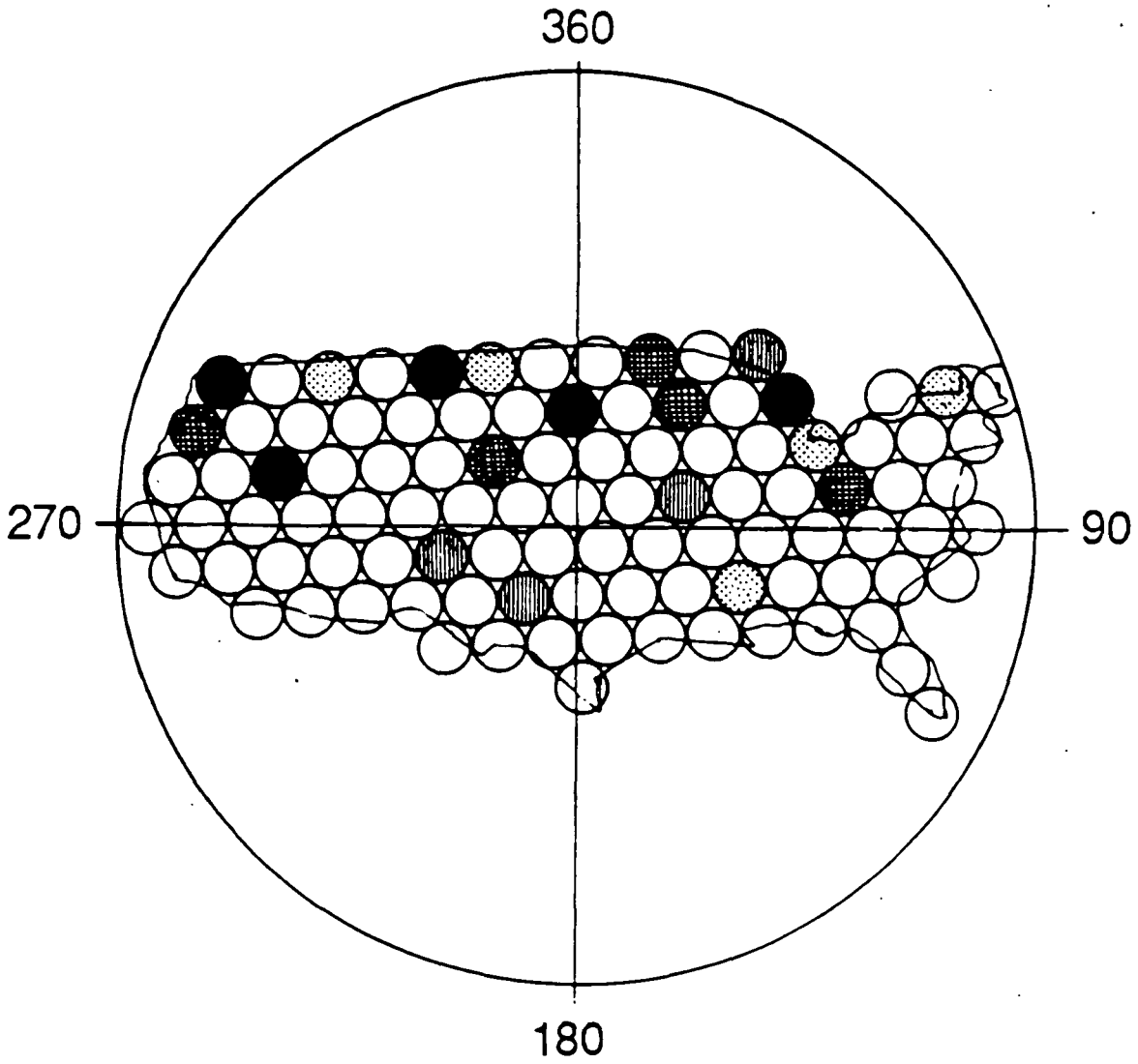

Figure 3.2: Switched beam CONUS coverage.

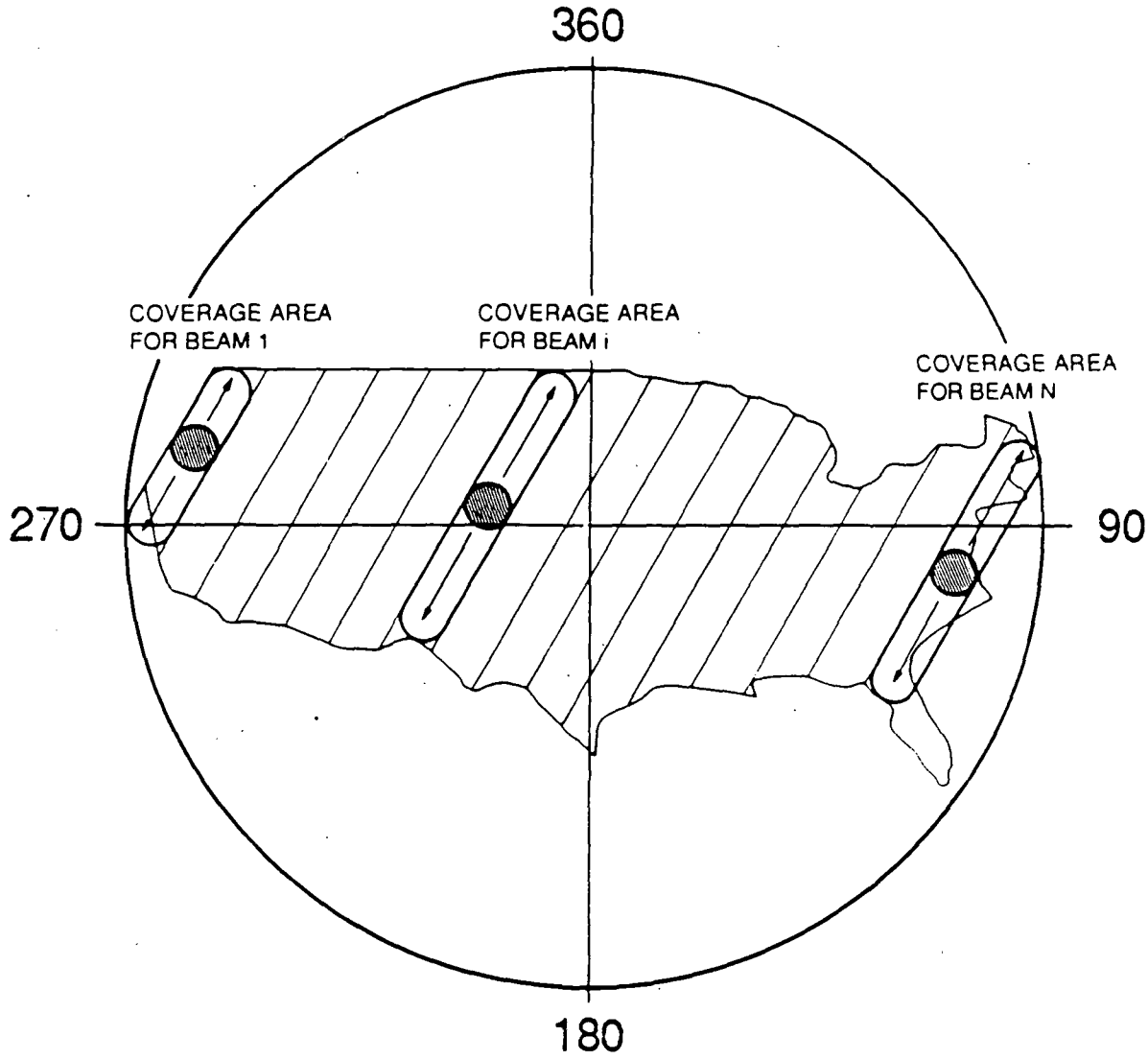

Figure 3.3: Scanning beam CONUS coverage.

93

Table 3.2: Pro's and Con's of Switched/Scanning Beams Relative to Fixed Beams

Advantages	Disadvantages
System Design:	
Better traffic match achieved by dynamically varying dwell time	Non-continuous coverage of CONUS Higher link data rate required Higher level of control over network req'd to synchronize transmissions.
Possible component and weight reduction in transponder	Reduced frequency reuse capability Increase in signal delay (Tradeoff between voice delay and supplier overhead for choice of scan rate)
User Communication:	
	Burst modem with variable duration due to variable dwell time Special acquisition equipment
Multibeam Antenna Design:	
Possible simplification of beam forming network	Increase in insertion loss between HPA and feed

this plan does not simplify bandwidth or power allocation between switched/scanning beams it does reduce the need for these measures. Beam dwell time is calculated by the NMC and dispersed by the NMC to the satellite and user terminals.

Operation with switched/scanning beams instead of fixed beams changes the system in other ways as well. First, users are not guaranteed a constant connection with the satellite, e.g. they will not receive the satellite beacon all of the time, nor can they request a channel at any time. Although this may be transparent to the user, their receiver must be able to transmit and receive in prescribed time windows and for variable lengths of time, must be instructed on how to find these times. Second, users must possess burst modems with variable burst duration times to work with beams having variable dwell times. In addition the data rate of the burst modems must be higher than that needed when fixed beams are used. Assuming that the beam accesses a particular coverage area once every T_{period} sec and that it remains in contact for, on the average, $T_{duration}$ sec, then the user data rate with the switched or scanning beam, R_s, must be increased by a factor inversely proportional to the coverage duty cycle:

$$R_s = R_f \cdot \frac{T_{period}}{T_{duration}} \tag{3.1}$$

where R_f is the 4.8 Kbps data rate used with fixed beams. The number of scan sites/beam, N_P, is therefore

$$N_P = \frac{T_{period}}{T_{duration}}. \tag{3.2}$$

These differences effect system design and performance. They result in greater delay for voice transmission. They require higher data rates on both the forward and return links to be supported. They necessitate changes in user terminal hardware so that frequency and time synchronization with the satellite can be maintained.

This chapter examines the consequences of using switched/scanning in lieu of fixed beams in the PASS design and attempts to evaluate the advantages and disadvantages listed in Table 3.2. Two uses of switched/scanning beams are examined. The first scenario calls for replacing the fixed beams used for communication between the user terminals and the satellite with switched/scanning beams, i.e. on the user terminal uplinks and downlinks. The second scenario utilizes switched/scanning beams for the downlink from the satellite to the user terminal and fixed beams for the uplink from the user terminal to the satellite. It is referred to as the hybrid beam concept. Using switched/scanning beams on both the user terminal's uplinks and downlinks will maximize the system advantages brought by the use of these beams at the price of system complexity. The hybrid beam concept seeks to reduce the system complexity and variety of requirements on the user terminal by using fixed beams for the satellite uplink.

To illustrate the implications of switched beams use on PASS system design, operation at two beam scan rates is explored. Scan rate is defined as $1/T_{period}$. For both switched beam examples, each beam is taken to access 10 coverage areas. The low scan rate, corresponding

74

to T_{period} of 2 sec and $T_{duration}$ of 200 msec, was chosen to minimize the supplier overhead per transmission and to illustrate the case where complete spatial acquisition can be performed during one access time. The fast scan rate, corresponding to T_{period} of 20 msec and $T_{duration}$ of 2 msec, was set so as to minimize voice signal delay.

The use of switched/scanning beams on the user terminal uplinks and downlink is examined in Section 3.2. The implications of the hybrid beam concept are studied in Section 3.2.6.

An important issue, relevant to both beam scenarios, is the pilot acquisition and the implications of rapid acquisition on pilot power and user terminal local oscillator stability. This is detailed in Section 3.3. Conclusions are presented in Section 3.4.

3.2 Switched/Scanning Beams for User Terminal Uplinks and Downlinks

First the system performance obtained with these beam types is investigated, then the ensuing transponder complexity is discussed, and finally the user terminal and supplier station complexity is detailed. Performance advantages and disadvantages with both multibeam antenna approaches are tabulated and summarized in Section 3.2.5. The hybrid beam scenario is discussed in Section 3.2.6.

3.2.1 System Performance

In this section the system performance is quantized by various parameters and the communication link between user terminal and supplier station is reexamined to determine which components must be changed for operation with switched/scanning beams. The parameters used to quantize performance are: the spectrum requirement, the tradeoff of voice delay vs. supplier overhead per transmission, and the efficiencies of the fixed and switched beams.

Spectrum Requirement

The spectrum required for the forward and return links resulting from the strawman design are shown in Figure 3.4 (the high rate channels between suppliers and enhanced personal terminals are denoted by HRC; the low rate channels between suppliers and basic personal terminals are labelled by LRC). A possible frequency plan for the switched/scanning beam scenario (that corresponding to the transponder design discussed in Section 3.2.2) is shown in Figure 3.5. In this figure, N_P is taken to be 10, the number of switched/scanning beams is then 14. Five frequency bands are estimated as necessary for these 14 beams, assuming frequency reuse.

Defining frequency reuse as in the PASS Concept Study [1], Table 3.3 lists the overall frequency reuse factor for switched/scanning beams when the number of beam positions per beam, N_P, is varied from 1 (equivalent to a fixed beam) to 15. The number of output frequencies required to address the 142 coverage areas, N_{F_s}, cannot be determined exactly without knowledge of the coverage areas addressed by each switched beam. In fact the value

C-2

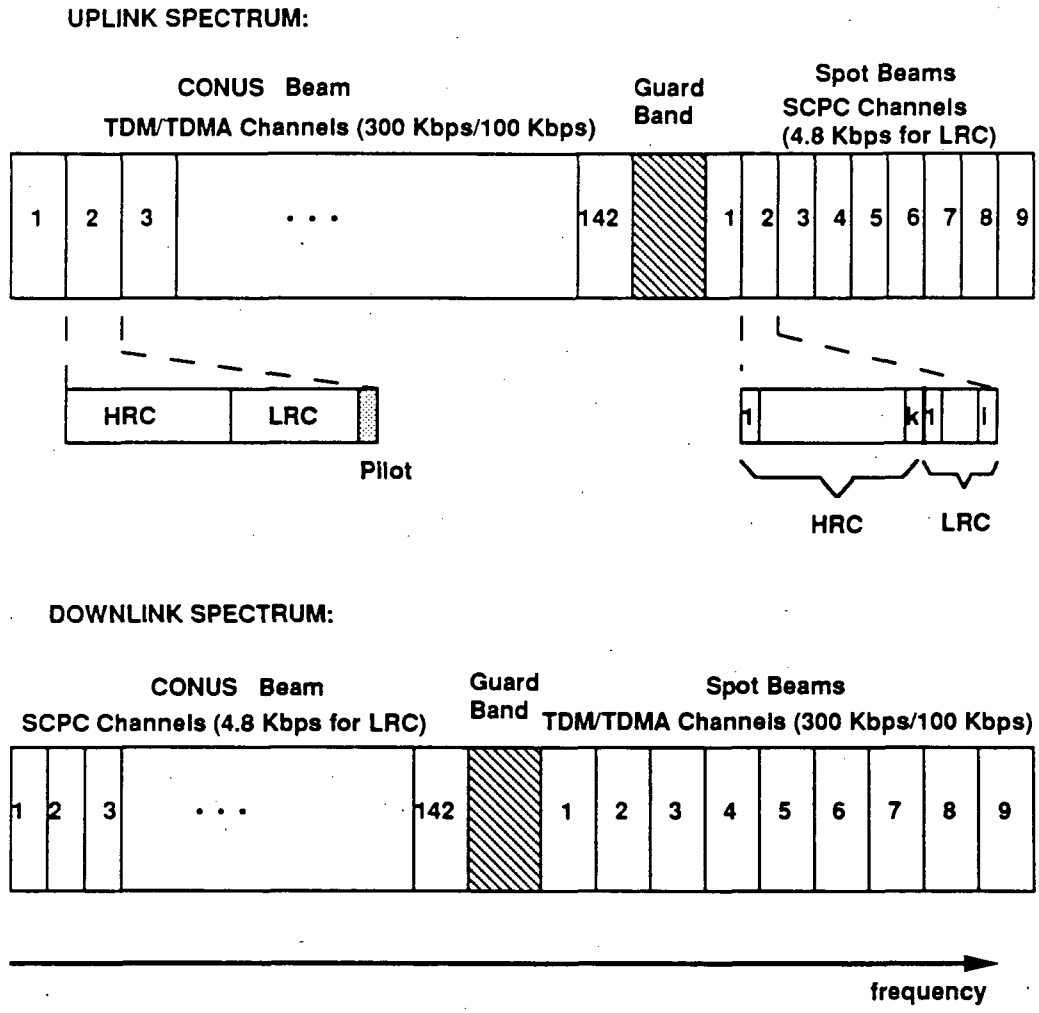

CONUS Beam:

142 uplink frequency bands for 142 fixed beams. Each beam is addressed by a specific frequency, ie. uplink band j is for j th Beam.

Spot Beams:

Users in the 142 fixed beams use 9 uplink channels to transmit their SCPC uplink signals to the suppliers.

Figure 3.4: Frequency plan for the fixed beam coverage concept.

96

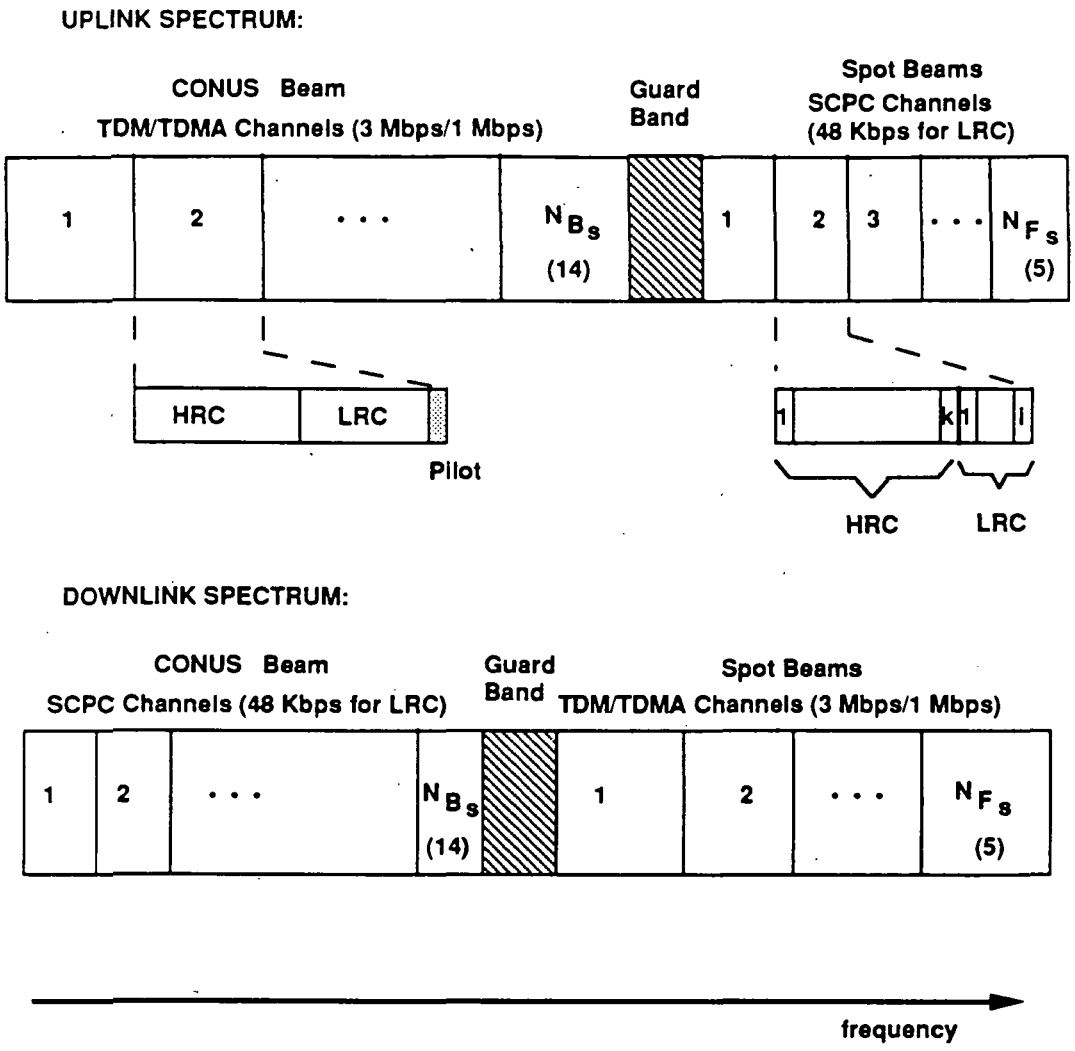

CONUS Beam:

N_{Bs} uplink frequency bands for N_{Bs} switched beams. Each beam is addressed by a specific frequency, i.e. band j is for the jth switched beam.

Switched/scanning Beam:

Users in the N_{Bs} switched beams use N_{Fs} uplink channels to transmit their SCPC uplink signals to the suppliers.

Figure 3.5: Frequency plan for the switched/scanning beam coverage concept ($N_P = 10$).

of N_{F_s} for a given N_P is probably not the same for switched and scanning beams because it may be possible to reuse these spot beam frequencies more often with scanning beams. The values for N_{F_s} listed in the table are best-case estimates. From Table 3.3 it is seen that the overall frequency reuse factor drops from 1.88 achieved with the fixed beam scenario to 1.43 with the switched/scanning beams when N_P is 15.

Table 3.3: Overall Frequency Reuse as the number of beam positions per beam, N_P, is varied.

N_P	Number of Switched/ Scanning Beams N_{B_s}	Number of Output Frequencies N_{F_s}	Net Equiv. Frequency Reuse
1	142	9	$\frac{284}{151} = 1.88$
5	28	6	$\frac{56}{34} = 1.65$
8	18	5	$\frac{36}{23} = 1.57$
10	14	5	$\frac{28}{19} = 1.47$
15	10	4	$\frac{20}{14} = 1.43$

Another way to gauge the spectral requirement of the switched/scanning beam scenario relative to the fixed beam design can be accomplished by assuming values for certain parameters and calculating the required bandwidth. From Figure 3.4 the uplink and downlink bandwidths can be written as:

$$BW_{up_f} = 142 \cdot \Delta f_{TDMA} + N_{F_f} \cdot \Delta f_{SCPC} \tag{3.3}$$

$$BW_{down_f} = 142 \cdot \Delta f_{SCPC} + N_{F_f} \cdot \Delta f_{TDMA} \tag{3.4}$$

where Δf_{TDMA} is the bandwidth of the two TDMA carriers (HRC and LRC) and the pilot in each beam, Δf_{SCPC} is the bandwidth allocated to all the SCPC channels in each beam, and N_{F_f} is the number of frequency bands necessary to address the 142 fixed beams. In the strawman design N_{F_f} is 9. The assumption here is that all beams are accorded the same bandwidth.

When a switched/scanning beam is used the bandwidth requirements can be written by replacing the 142 fixed beams by $(142/N_P)$ switched beams. The bandwidth requirements become:

98

$$BW_{up_{s/s}} = N_{B_s} \cdot \Delta f'_{TDMA} + N_{F_s} \cdot \Delta f'_{SCPC} \tag{3.5}$$

$$BW_{down_{s/s}} = N_{B_s} \cdot \Delta f'_{SCPC} + N_{F_s} \cdot \Delta f'_{TDMA} \tag{3.6}$$

where $\Delta f'_{TDMA}$ is the bandwidth of the two TDMA carriers (HRC and LRC) per beam, and, N_{B_s} is the number of switched/scanning beams, equal to $\frac{142}{N_P}$. Values for N_{B_s} and N_{F_s} for a given N_P can be found from Table 3.3. $\Delta f'_{TDMA}$ and $\Delta f'_{SCPC}$ for the switched/scanning beams have N_P higher data rates than their fixed beam counterparts. They can be written as:

$$\Delta f'_{TDMA} = N_P \cdot \Delta f_{TDMA}, \tag{3.7}$$

and

$$\Delta f'_{SCPC} = N_P \cdot \Delta f_{SCPC}. \tag{3.8}$$

Substituting Eqns. 3.7 and 3.8 into Eqns. 3.5 and 3.6, we find:

$$BW_{up_{s/s}} = 142 \cdot \Delta f_{TDMA} + N_{F_s} \cdot N_P \cdot \Delta f_{SCPC} \tag{3.9}$$

$$BW_{down_{s/s}} = 142 \cdot \Delta f_{SCPC} + N_{F_s} \cdot N_P \cdot \Delta f_{TDMA}. \tag{3.10}$$

The ratio of total bandwidth required for both uplink and downlink in the switched/scanning beam scenario to that required in the fixed beam case is then expressed as:

$$BW_{total}{}_{\text{s/s–fixed}} = \frac{142 + N_{F_s} \cdot N_P}{142 + N_{F_f}}. \tag{3.11}$$

Eq. 3.11 shows that the bandwidth expansion factor in the switched/scanning beam scenario is not a function of Δf_{TDMA} or Δf_{SCPC}. $BW_{total}{}_{\text{s/s–fixed}}$ varies from 1.14 for $N_P = 5$ to 1.34 for $N_P = 15$.

It is also of interest to compare the bandwidth expansion factors for uplink and downlink beams separately. To do so, values for Δf_{TDMA} and Δf_{SCPC} must be assumed. Let us then consider the simple case where there are no HRCs in either forward or return link. We also consider the bandwidth required by the pilot to be far less than that of the low rate TDMA channel. The null-to-null bandwidth requirements for the coherent BPSK modulation with $r = 1/2$, $K = 7$ convolutional coding assumed in the strawman design can then be written as:

$$\Delta f_{TDMA} \simeq 4 * 96\text{Kbps} \simeq 400\text{KHz} \tag{3.12}$$

and

$$\Delta f_{SCPC} \simeq i \cdot 4.8\text{Kbps} \simeq i \cdot 19.2\text{KHz} \tag{3.13}$$

where i is the maximum number of SCPC 4.8 Kbps channels allotted to each beam. Note that all areas covered by the same switched or scanning beam utilize the same SCPC band (see Figure 3.5).

To calculate the switched beam bandwidth requirement for comparison with the bandwidth required in the fixed beam scenario, the signal bandwidth given by Eqns. 3.12 and 3.13 is taken to represent both the signal bandwidth plus pilot bandwidth, for the TDMA case, and the signal bandwidth plus guard band for the SCPC case. Bandwidth requirements are calculated by substituting Eqns. 3.12 and 3.13 into Eqns. 3.9 and 3.10 and assuming two values of i, the maximum number of SCPC channels per beam. The results are listed in Table 3.4. The first case, $i = 14$, corresponds to the present strawman design. As discussed in Appendix A, the system is power limited by the satellite to 2000 duplex channels at 4.8 Kbps. If these channels are distributed evenly among the 142 spot beams then there would be ≈ 14 channels/beam. The second case, $i = 100$, is given for comparison. It represents operation with a more powerful satellite or with a more power efficient modulation technique.

From Eqns. 3.9 and 3.10 and Table 3.4 it can be seen that the uplink bandwidth is determined principally by the TDMA signal and that the relative bandwidth required by the SCPC signals becomes important for large i or large N_P. The downlink signal bandwidth is principally determined by the SCPC channels requirement, thus the effect of the TDMA channels is more obvious for lower values of i.

Tradeoff of Voice Delay and Supplier Overhead/Transmission

Operation with both fixed and switched beams permits the supplier to tradeoff the desire to achieve low transmission delay against the need to maintain a low number of overhead bits per transmission. However in the switched/scanning beam scenario the period of the beam sets the tradeoff, whereas in the fixed beam case it can be set at the operator's discretion. This tradeoff is particularly important for voice signals where delay must be minimized.

In the fixed beam case, a supplier with voice traffic for user A in Beam j can either place each vocoder packet as it is output from the vocoder in the outbound TDMA frame with the user's address or the supplier can store up several packets and transmit them in one TDMA frame with one address message. The former case minimizes voice delay time and the latter minimizes overhead per message. To calculate the minimum delay and overhead in the switched/scanning beam case, performance with two values for beam period is considered.

Voice Delay The voice delay calculation is based on the MSAT-X vocoder performance. This 5 Kbps vocoder produces a 100 bit frame every 20 msec, creating therefore 50 frames per sec. The communication system for the forward link, from supplier to user, is depicted in Figure 3.6. If the signal delay in a component is significant it is listed above the component. These delay values are worst case estimates, but should be accurate enough to permit valid beam comparisons. The return link signal delay is equivalent to the forward link delay as it is determined by the delay in the codex, the encoder/decoder, the burst modem wait period, the uplink and downlink propagation paths, and the satellite. The transceiver components

Table 3.4: Bandwidth Requirements for the Switched/Scanning Beam Scenario

N_P	BW_{up}	BW Expansion Ratio	BW_{down} Ratio	BW Expansion
	$i = 14$			
1	59.22 MHz	1	41.77 MHz	1
5	64.86 MHz	1.10	50.17 MHz	1.20
8	67.55 MHz	1.14	54.17 MHz	1.30
10	70.24 MHz	1.19	58.17 MHz	1.39
15	72.93 MHz	1.23	62.17 MHz	1.49
	$i = 100$			
1	74.08 MHz	1	276.24 MHz	1
5	114.40 MHz	1.54	284.64 MHz	1.03
8	133.60 MHz	1.80	288.64 MHz	1.04
10	152.80 MHz	2.06	292.64 MHz	1.06
15	172.00 MHz	2.32	296.64 MHz	1.07

Note: The assumptions made for these calculations are (1) no HRCs on either the forward or return link; (2) equal sized TDMA carriers and SCPC bandwidths per beam; (3) low rate TDMA carrier and pilot bandwidth is 400 KHz; (4) SCPC channel and guard band bandwidth is 19.2 KHz.

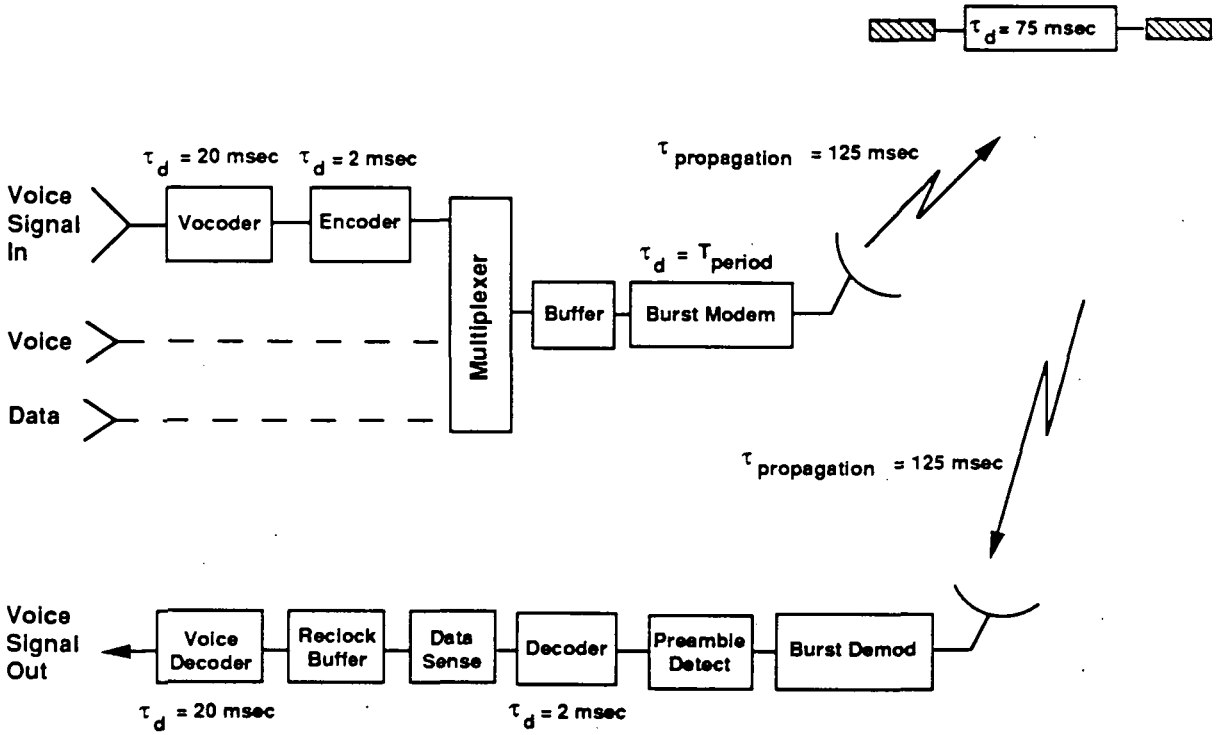

Figure 3.6: Communication system components and associated delay used for voice delay calculation.

at the user terminal and supplier terminal differ from those shown in Fig. 3.6.

In the fixed beam situation, one voice packet is sent every 20 msec, similar to the case when the switched/scanning beam is operated in the fast scan mode. The one way voice delay (supplier → user) is then 369 msec according to Fig. 3.6 (with no wait time for the burst modem). The round trip voice delay (supplier → user → supplier) is then ~ 0.74 sec. If a switched/scanning beam is used, vocoder packets are stored in the burst modulator prior to transmission once every T_{period} sec (100 vocoder packets are queued up in the slow scan mode, 1 packet in the fast scan mode). Thus the round trip transmission takes:

$$\tau_{\text{rd trip}} = 2\left(T_{period} + T_{satellite} + \sum_{\text{all delays}} \tau_d + 2\tau_{\text{propagation}}\right). \qquad (3.14)$$

For the fast scan rate (T_{period} = 20 msec, $T_{duration}$ = 2 msec) $\tau_{\text{rd trip}}$ = 0.78 sec; for the slow scan rate (T_{period} = 2 sec) $\tau_{\text{rd trip}}$ = 4.74 sec. The fast scan rate produces a voice delay that is nearly identical to the fixed beam delay as the scan rate has been chosen to match the vocoder output rate. The difference in fixed and fast scan delay is due mostly to the use of burst modems, which add a delay of 20 msec to the round trip scan delay. Table 3.5

Table 3.5: Round Trip Voice Delay for Various Switched Beam Periods

T_{period}	Rnd Trip Delay (user to supplier to user)
Fixed Beam	0.74 sec
20 msec	0.78 sec
500 msec	1.74 sec
1.0 sec	2.74 sec
1.5 sec	3.74 sec
2.0 sec	4.74 sec

gives the round trip delay, from supplier to user to supplier for the fixed beam and for the switched/scanning beam with various beam periods.

Information Throughput – Supplier Overhead per Transmission Supplier overhead per transmission for different spot beams can be roughly estimated by assuming a TDMA frame structure and taking the offered traffic to be of voice origin. A generic TDMA frame is shown in Figure 3.7. Obviously the greater the data transmitted from supplier to user in one TDMA frame the lower the transmission overhead. Usage of a switched/scanning beam with a slow scan rate results in more data transmitted per preamble bit worth of overhead and therefore results in a lower overhead/transmission. Using voice packets as the message unit, the overhead/transmission can be estimated as T_{period} is increased.

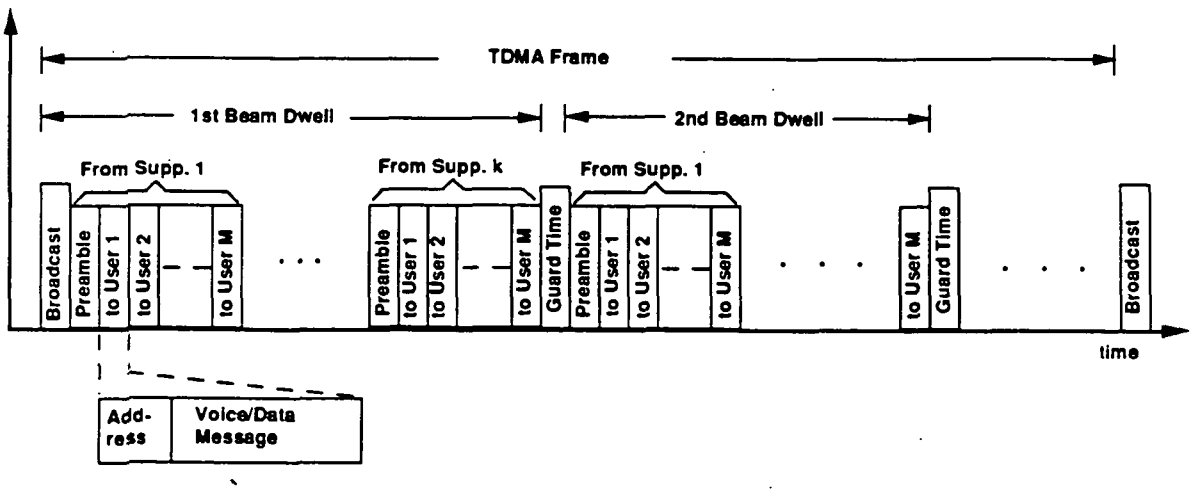

Figure 3.7: Generic TDMA frame format used for overhead calculation.

Let

P_P denote the preamble bit packet,
P_A denote the address bit packet,
and, P_V denote the 100 bit vocoder packet length,

then the supplier overhead/transmission can be written as follows:

$$\text{Overhead/transmission}_{\text{ jth supplier}} = \frac{N_j \cdot P_A + P_P}{N_j \cdot M \cdot P_V}$$

where N_j is the number of users addressed by the jth supplier and M is the number of vocoder packets per transmission,

$$M = \frac{T_{period}}{T_{vocoder}};$$

$T_{vocoder}$ being the time between subsequent vocoder packets, i.e. 20 msec.

This expression can be simplified by assuming that the 100 bit vocoder packet length is long enough to accomodate a preamble or an address, i.e. $P_A \leq P_V$ and $P_P \leq P_V$. Then the supplier overhead/transmission can be written as:

$$\begin{aligned}\text{Overhead/transmission}_{\text{ jth supplier}} &= \frac{N_j \cdot P_V + P_V}{N_j \cdot M \cdot P_V} \\ &= \frac{N_j + 1}{N_j \cdot M}.\end{aligned}$$

When one supplier communicates with several (>10) users, the above equation can be reduced simply to

$$\begin{aligned}\text{Overhead/transmission}_{\text{ jth supplier}} &\approx \frac{1}{M} \\ &= \frac{T_{vocoder}}{T_{period}}.\end{aligned}$$

The above equation is plotted in Figure 3.8 for the MSAT-X vocoder frame rate of 20 msec. For the slow and fast scan beams assumed here, the supplier overhead/transmission is found to be

$$\text{Overhead/transmission}_{\text{ jth supplier}} = \begin{cases} \frac{N_j \cdot P_V + P_V}{N_j \cdot 100 \cdot P_V} \rightarrow \frac{1}{100} & \text{Slow scan} \\ \frac{N_j \cdot P_V + P_V}{N_j \cdot P_V} \rightarrow 1 & \text{Fast scan.} \end{cases}$$

The overhead/transmission for the jth supplier can be estimated for the fixed beam by assuming again that all N_j users being addressed are sent signals of voice origin. Since each supplier transmits to the BPT's at a rate of 100 Kbps, a maximum of 20 voice signals can

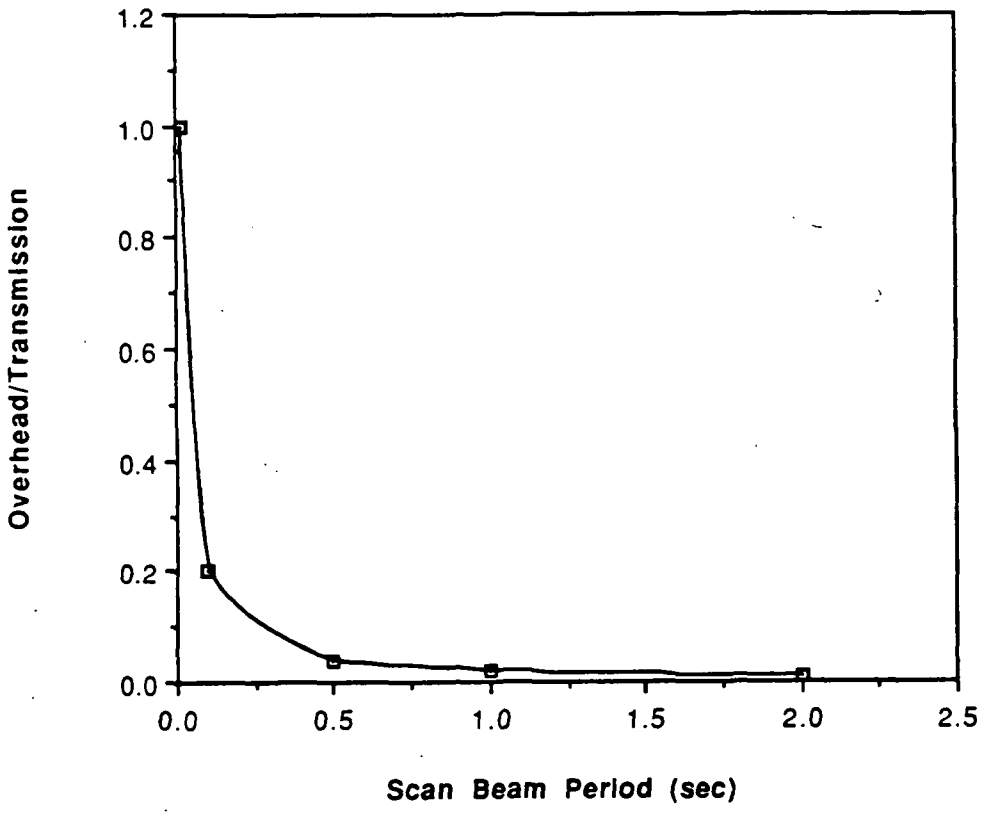

Figure 3.8: Overhead/transmission vs. scan beam period.

be sent in one TDMA frame (for a 5 Kbps vocoder). If this traffic requirement is assumed, then only one vocoder packet can be sent to each BPT in a TDMA frame, hence $M = 1$ and $N_j = 20$. The overhead/transmission can then be estimated to be ≈ 1, or one overhead packet required for every vocoder packet. If not all users addressed by that supplier are voice users then the supplier can choose between sending more than one vocoder packet per TDMA frame, thus lowering the overhead/transmission at the expense of an increase in voice delay, or sending one vocoder packet/TDMA frame, thereby operating with a high overhead/transmission but with the minimum voice delay of 0.74 sec.

Fixed and Switched Beam Efficiencies

As discussed in the introduction, fixed beams have the disadvantage that the satellite capacity can not be easily reconfigured so as to match the traffic requirements. Thus, in general, fixed satellite power and bandwidth are allocated to each beam irrespective of the number of users. Although methods for sharing the high power amplifier's power between beams do exist, switched/scanning beams still remain more efficient at matching traffic requirement with satellite capacity due to their variable dwell time. This is particularly true if the traffic possesses large geographical and temporal variations.

No precise calculation of the relative efficiencies between beam types has been performed. However a rough value for fixed beam efficiency is thought to be 50%; the switched/scanning beam is thought to be about 95% efficient. The high efficiency of the latter reflects the fact that the probability that none of the users in the N_P coverage areas need to use the beam is low. A more accurate means of gauging the relative beam type efficiencies is necessary. For this chapter, they have been taken to be:

$$\eta_{Traffic} = \begin{cases} 1.0 & \text{Switched Beam with non-adaptive power,} \\ 0.5 & \text{Fixed Beam with non-adaptive power.} \end{cases}$$

A disadvantage arising from the use of switched beams is the need for guard time between transmissions from each coverage area to allow for the switching time of the beam. This reduces the efficiency of the TDMA and the SCPC signals. For ACTS, the ferrite switches in the beam forming network are specified to have a switching time of less than 75 μsec in order to allow the beam to hop to many locations within the 1ms TDMA frame period [2]. Assuming the total wasted transmission time could take 5% to 20% of the transmission time, the time usage efficiencies of the two beam types can be written as,

$$\eta_{TXtime} = \begin{cases} 0.75 - 0.90 & \text{Switched Beam} \\ 1.0 & \text{Fixed Beam.} \end{cases}$$

The overall efficiencies of switched and fixed beams can now be compared.

$$\eta_{overall} = \eta_{Traffic} \cdot \eta_{TXtime}$$

$$\eta_{overall} = \begin{cases} 0.75 - 0.90 & \text{Switched Beam} \\ 0.5 & \text{Fixed Beam.} \end{cases}$$

As the switched beam's scan rate increases, the guard time required between transmissions occupies a greater fraction of the total transmission time. The beam's efficiency drops. Therefore the 90% beam efficiency is associated with the slow scan beam and the 75% estimate is associated with the fast scan. Under these assumptions the efficiency of a switched beam is higher than that of a fixed beam.

Link Calculation

The communication links detailed in the strawman design must be reanalyzed to evaluate which components may be changed in order to support the N_P higher data rate required by the use of switched/scanning beams. The uplink and downlink C/N_0 values for the forward and return link in the strawman design are given in Table 3.6. It can be seen that the overall C/N_0 is determined principally by the link between the BPT and the satellite.

Table 3.6: C/N_0 Values for Strawman Design

	Forward Link Supp. → User	Return Link User → Supp.
C/No_{up}	69.9 dB/K	46.9 dB/K
C/No_{down}	58.8 dB/K	50.3 dB/K
$C/No_{overall}$	57.4 dB/K	44.2 dB/K
$C/No_{required}$	54.5 dB/K	41.3 dB/K

Forward Link The higher data rate on the forward link can be accommodated by increasing the transmit power from the supplier stations slightly and by increasing the transmit power per TDMA channel on the downlink from its current 4W per low rate TDMA data channel. Using a switched/scanning beam with N_P coverage areas per beam means that (1) the outgoing bit rate will be increased by N_P and (2) the number of outgoing TDMA channels will be reduced by N_P. This occurs because the data from N_P fixed beams is being handled by one switched/scanning beam. If, for example, N_P is 10, then the 100 kbps bit rate of the TDMA channel carrying information for the basic personal terminals (the low rate channel) will be increased to 1 Mbps. As before, there will be one low rate TDMA channel (now 1Mbps) per beam, however now the 142 fixed beams will be replaced by 14 switched/scanning beams. If we allow the power of the TDMA beam to increase to compensate for the 10 times higher data rate, then the satellite transmit power per low data rate TDMA carrier will increase

from its current 4W to 40W. The availability of 40W solid state high power amplifiers (SS-HPA) is poor as typical SS-HPAs at 30 GHz provide 1-5 Watts. Hence travelling wave tube amplifiers (TWTA) would have to be used. The latter weigh more and have a greater volume but their efficiency is greater than that of solid state amplifiers. This one positive side effect is important because the channel capacity is limited by the DC power generation capability of the satellite in the strawman PASS design (see Appendix A).

Return Link To accomodate the higher data rate on the return link from BPT to satellite, the most possible changes in the communication components are to 1) increase BPT transmit power from current 0.3 W/channel; or 2) increase the satellite receive antenna gain (current antenna has 2m diameter). The BPT's power can easily be upgraded from 0.3 W/channel and still be accomplished with SS-HPA's. The penalty then will be increased radiation from the BPT antenna. Increasing the satellite's antenna size increases transponder complexity dramatically as discussed in Appendix B and should be avoided if possible.

3.2.2 Transponder Complexity

Connectivity between fixed and CONUS beams is achieved in the strawman design by the transponder as depicted in Figure 3.9. 142 4W HPA's are required to produce the 142 antenna feed signals. The 9:1 multiplexers and demultiplexers and the 16 different local oscillators and mixers are required to obtain the frequency reuse factor of 9 on the downlink.

A possible transponder design is depicted in Figure 3.10 for a switched/scanning beam design. A CONUS beam is still used to link the suppliers and the satellite; the switched or scanning beams are used to link the BPT's and the satellite. If each beam is taken to have 10 scan sectors, then the 142 fixed beams can be replaced by $\approx$ 14 switched beams. The number of output frequency bands needed for the 14 switched beams, N_{F_s}, is taken to be 5. Although the transponder design may seem more complex at first glance, a significant number of expensive or heavy components have been eliminated: the number of HPA's required drops from 142 to 14 and the number of local oscillators required is reduced from 16 to 3.

However, in the forward link, the signal from each of the HPA's are passed to a switch that connects the signal to one of the N_P feeds for that switched beam. One of the possible disadvantages of switched beams is the increased insertion loss in the signal path presented by this switch. Because a fixed switched beam design is considered here, the number of feeds and gain modules associated with each feed is not reduced through the use of switched beams. However if a hopping beam scenario is employed, such as that used by ACTS, it would be possible that the beam forming network would also be simplified.

3.2.3 User Terminal Complexity

When a scanning beam is used, the user terminal will differ from that in the strawman design in that it must transmit a burst signal and receive a burst TDMA signal. The terminal must

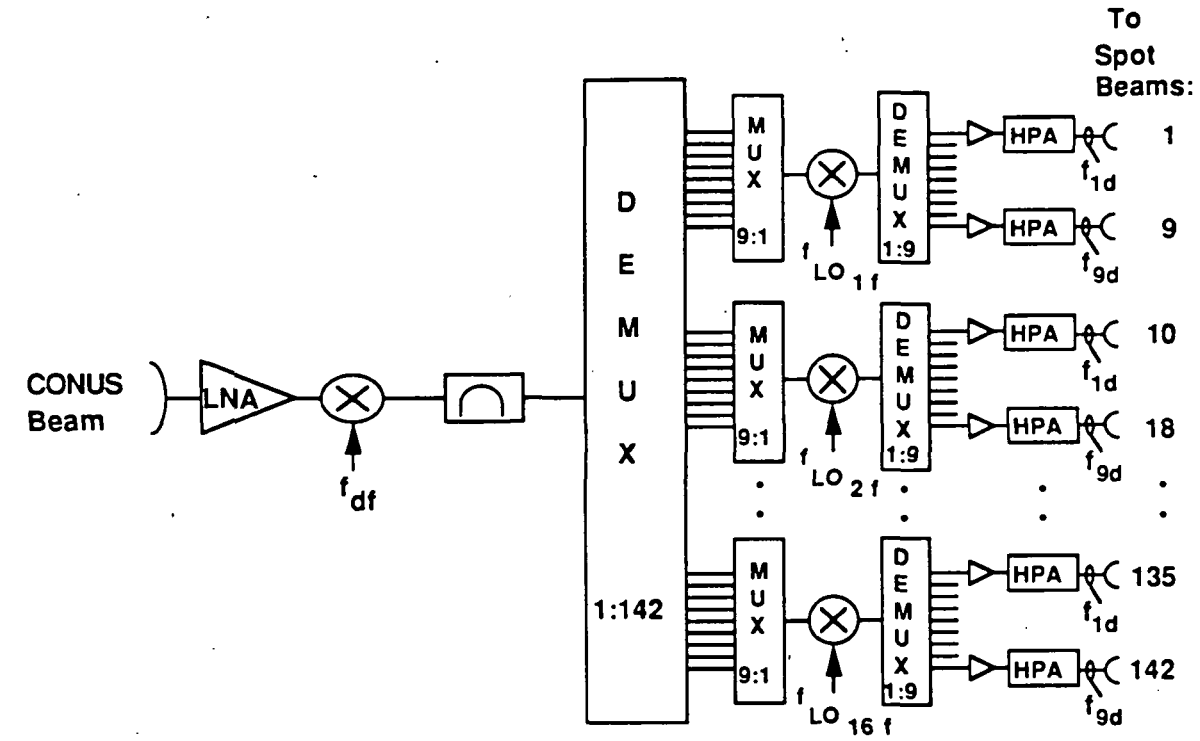

(a) forward link

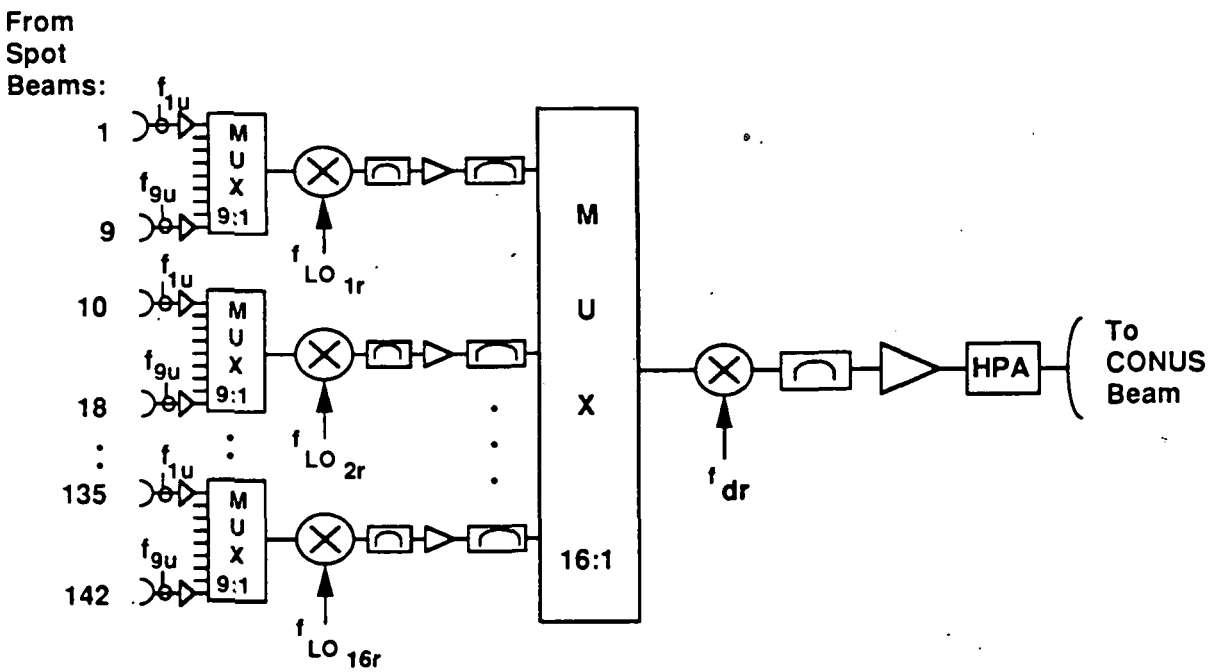

(b) return link

Figure 3.9: Strawman transponder design for CONUS and fixed beams.

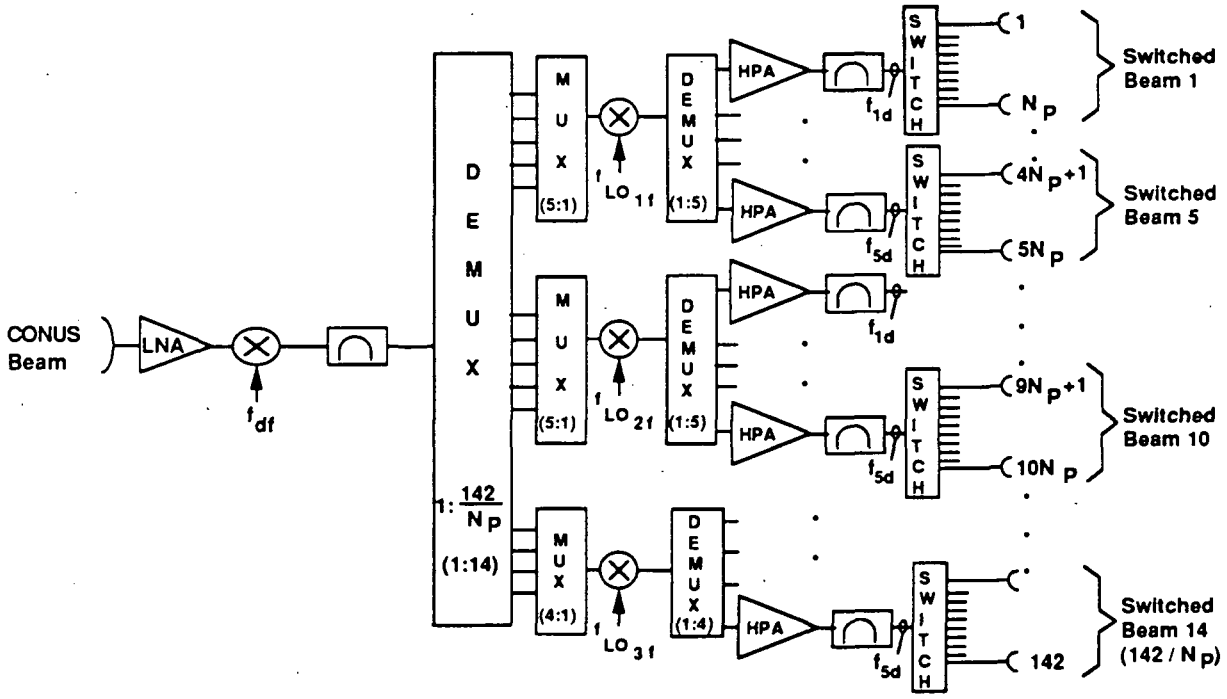

(a) forward link ($N_p = 10$)

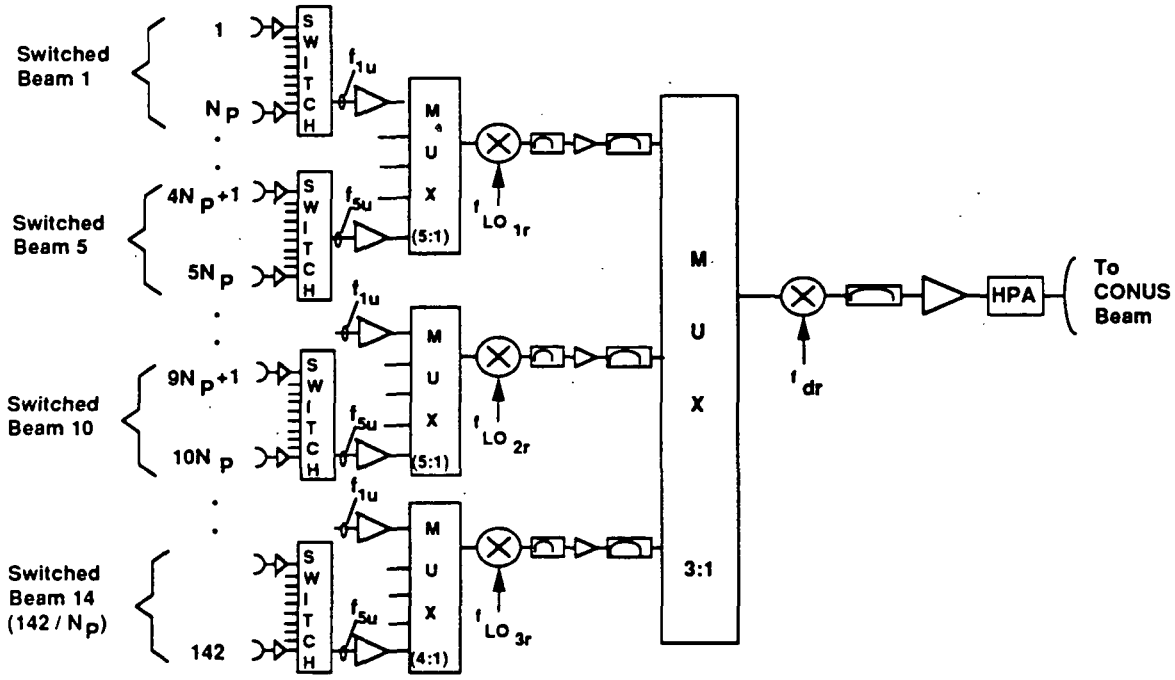

(b) return link ($N_p = 10$)

Figure 3.10: Possible transponder design for CONUS and scanning beams.

possess a receiver that can acquire and process the incoming signal quickly. The operation of the receiver is done in two stages. The first phase is the initial acquisition of the pilot whereby a spatial and frequency acquisition are performed. In the second phase time and frequency synchronization with the incoming scanning or switched beam is maintained and the data is demodulated. The first phase is discussed in detail in Section 3.3. The second phase is discussed below.

The pilot frequency must be within the bandwidth of the acquisition loop when the switched beam returns to a given coverage area. Acquisition time depends on input C/N_0, loop BW and frequency deviation since last lock. The short term stability for two types of crystal oscillators is given in Table 3.7 and is plotted in Fig. 3.11 for various switched/scanning beam periods at 20 GHz and 30 GHz. The data in Table 3.7 is taken from the Vectron catalog [6]. From this figure, the maximum deviation between satellite passes of a 20 GHz local oscillator in the BPT can be seen to be 400 Hz or 600 Hz for the 30 GHz transmit signal assuming the satellite antennas use the slow beam rate corresponding to $T_{period} = 2$ sec.

Two methods can be used to compensate for transmit signal frequency offset at 30 GHz:

1. Use $f_{REFERENCE}$ from last satellite pass. At most the 30 GHz signal will be off by 30 - 600 Hz. The $f_{REFERENCE}$ from the last satellite pass is locked to the received pilot at 20 GHz.

2. Acquire pilot and receive preamble before transmit - i.e. stagger RX and TX beams. Then the TX signal will be locked to the NMC generated pilot and thus precisely on frequency.

Frequency deviation for the TX and RX signals should be designed to be well within the loop bandwidth at the BPT and the supplier. Using a VCXO these frequency offsets seem to be within allowable loop bandwidths. As shown in Table 3.7 higher stabilities are achievable using TC-VCXO's or OC-VCXO's although at a higher cost.

3.2.4 Supplier Station Complexity

In the strawman design, the supplier stations receive continuous signals from each user. In the switched/scanning beam scenario currently envisaged, users covered by the same beam would share the uplink SCPC channel, thus f_1 might be used by User 1 in Coverage Area 1 of Beam 1, by User 5 in Coverage Area 2 of Beam 1, ..., and finally by User m in the N_Pth coverage area of this beam. The supplier (and the NMC) station then have to rapidly acquire the bursty transmissions from various users with slightly different carrier frequencies. The use of switched/scanning beams with variable dwell times requires supplier stations to have for burst demodulators. Variable data rate modems are required in the strawman design to compensate for rain fade. Currently variable rate burst modems are used for high speed computer communications (19.2 Kbps modems). They should not be difficult to develop for this application.

Table 3.7: Stability and Price of Voltage Controlled Crystal Oscillator Sources

	Short Term Stability	Long Term Stability	Prices Quant. 1-2	Prices Quant. 10,000
OC-VCXO	$1 \cdot 10^{-10}$ Hz/sec	$1 \cdot 10^{-7}$ Hz/sec	\$ 600 - 700	\$ 100 - 150
TC-VCXO	$5 \cdot 10^{-9}$ Hz/sec	$3.2 \cdot 10^{-6}$ Hz/sec	\$ 500 - 550	\$ 50 - 100
TC-VCXO	$5 \cdot 10^{-9}$ Hz/sec	$1 \cdot 10^{-6}$ Hz/sec	\$ 450 - 500	\$ 40 - 80
VCXO	$1 \cdot 10^{-8}$ Hz/sec	$1 \cdot 10^{-5}$ Hz/sec	\$ 200 - 300	\$ 10 - 12

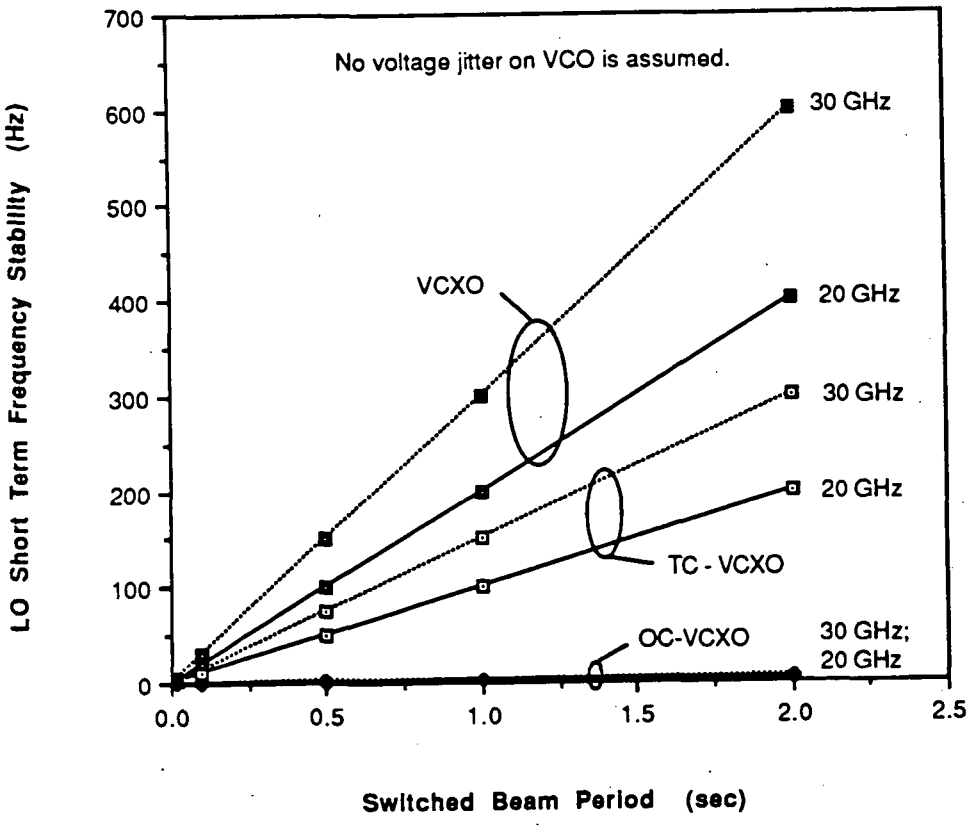

Figure 3.11: LO short term frequency stability vs. switched beam period.

3.2.5 Relative Advantages and Disadvantages

The implications of replacing the 142 fixed beams (of 0.35° beamwidth) with a reduced number of switched/scanning beams have been examined. Conclusions are summarized in Tables 3.8 and 3.9 where the characteristics of slow and fast scan switched beams are compared with those of the current fixed beam PASS design. System operation can be characterized by several parameters, beam efficiency or match of satellite capacity with traffic needs, spectrum requirements, voice signal delay, supplier overhead/transmission, and required burst data rate that must be supported by the communication link. From the user's point of view, rapid acquisition of the beam at the onset of the communication link is of importance, and to a lesser degree the time required for spatial beam location is of interest.

Table 3.8: Switched and Fixed Beam Characteristics from the System Point-of-View

	Slow Scan	Fast Scan	Fixed Beam
T_{period}	2 sec	20 msec	
$T_{duration}$	200 msec	2 msec	
N_P	10 cov. areas/beam	10 cov. areas/beam	1 cov. area/beam
Beam Efficiency w.r.t. Traffic Variations	90 %	75 %	50 %
Req'd Burst Data Rate			
From BPT	50 Kbps	50 Kbps	5 Kbps
From Supplier	1 Mbps	1 Mbps	100 Kbps
Net Equiv. Frequency Reuse	1.5	1.5	1.9
Normalized Overall BW Requirements	≈ 1.3	≈ 1.3	1.0
Min. Conversation Delay	4.74 sec	0.78 sec	0.74 sec
Supplier Overhead per Transmission	Low	High	High
NMC Overhead to Broadcast Beam Dwell Time	High	High	Nonexistent

Table 3.9: Switched and Fixed Beam Characteristics from the User Point-of-View

	Slow Scan	Fast Scan	Fixed Beam
T_{period}	2 sec	20 msec	
$T_{duration}$	200 msec	2 msec	
N_P	10 cov. areas/beam	10 cov. areas/beam	1 cov. area/beam
Frequency Stability between Sat. Passes			
RX at 20 GHz	4 - 400 Hz	0.04 - 4 Hz	N/A
TX at 30 GHz	6 - 600 Hz	0.06 - 6 Hz	N/A
Need to restart acquisition loop	Low	Low	N/A
Spatial Acquisition	All 108 essays performed in one satellite pass	At 1 essay per satellite pass: 2.16 sec	216 msec

Switched/scanning beams have been found to allow a better match between traffic requirements with large geographic and temporal variations and satellite capacity. Their use reduces the number of local oscillators and high power amplifiers required on-board the satellite and hence may reduce payload weight and size. No additional equipment is thought to be necessary in the user and supplier terminals to acquire the non-continuous satellite signal. Reacquisition of the satellite pilot can be accomplished without reentering into the receiver's acquisition mode as the pilot will be within the loop's tracking bandwidth.

The cost of using switched/scanning beams lies in the four areas. First, higher EIRP user terminals will be necessary to support the higher burst data rates. This can be achieved by increasing the size of the HPA in the user terminals at the cost of higher radiated power from the terminals. Second, burst modems will be needed at the user terminals and supplier stations instead of non-burst modems. Third, the NMC will have more functions to perform and more precise control of the network will be necessary. Four, spectral efficiency, accomplished in the strawman design through frequency reuse, will be slightly reduced by the use of switched/scanning beams, the total required bandwidth (uplink and downlink) being 1.2 to 1.4 times that required with fixed beams.

Optimum beam scan rate is determined by tradeoffs in various parameters. As the beam scan rate decreases (its period and duration over one coverage area increases) the following occur: the round trip delay incurred by signal of voice origin increases; information throughput at the supplier station increases; and, the need to restart signal acquisition process at user terminal between satellite beam accesses increases. Operation with a slow

scan beam, such as exemplified in Tables 3.8 and 3.9, is most likely impossible due to its poor delay performance: 4.7 sec for voice communications. Scan rates closer to that typified by the fast scan beam will have to be used.

Enhanced match of satellite capacity usage and the possibility of reduced transponder complexity make consideration of switched/scanning beams of interest for PASS although their system price is high. To reduce this price, a satellite design employing multibeam antennas with switched/scanning beams on the downlink to the user terminals and with fixed beams on the uplink from the user terminals will be examined next.

3.2.6 Hybrid Beam Concept

Another possibility for the design of the satellite is to use multibeam antennas with switched/scanning beams on the downlink to the user terminals and with fixed beams on the uplink from the user terminals. This hybrid design would eliminate the need to transmit from the user terminals with the higher EIRP necessary to support the higher burst rate from the terminals. In addition no burst modems would be required at the user terminal - although burst demodulators would still be necessary. However the advantages of using a fully switched/scanned beam system, ie. the enhanced match of satellite capacity to user traffic and the possibility of reduced transponder complexity, would then not be fully realized.

3.3 Pilot Acquisition and Detection Time

The detection of a pilot from a satellite that employes scanning or switching beams is very similar to the detection of bursty radar signals in presence of clutter. In order for a user terminal using a scanning antenna to lock to the incoming TDMA type pilot, it has to scan in azimuth and elevation until it detects the incoming energy, to synchronize to the scanning beam scan rate, and then perform a fine tuning both in frequency and phase. A fast detection mechanism must be used if the time duration of a beam in a given geographic area is to be minimized.

A great amount of effort has been expended over the past twenty years on the subject of the properties, configurations, performance, and implementation of signal detectors and many reports and papers are available which delineate basic detector topology and optimum configurations and methods for performance analysis [7,8,9]. The results produced lay the necessary foundation and provide bounding criteria for detectability as a function the principal parameters. Several possible ways are available in performing the frequency search; eg. swept IF, wide-open, or multi-channel configurations. The swept-IF receiver mixes the incoming signal with an oscillator signal whose frequency varies as periodic sawtooth. A relatively narrow-band IF filter which follows looks at successively different portions of frequency uncertainty. The wide-open receiver employs an IF filter which is sufficiently wide to accommodate the entire frequency uncertainty and thus, no actual sweep is performed. The multi-channel receiver employs parallel sweep in which a bank of IF filters simultaneously "looks" at different portions of the frequency uncertainty. All publications report that if

certain requirements are fulfilled, the wide-open receiver has the fastest detection time and is the easiest to implement. For this study it is assumed that a wide-open receiver with an envelope detection scheme using an accurate threshold is employed; data from the references cited above is applied to evaluate the performance of the proposed PASS architecture.

3.3.1 Detection Mechanism

The detection of a pilot from a switching beam by a scanning user beam can be looked at as a three dimensional problem where the receiver has to search in the space, frequency, and time domains until a predetermined energy level is detected. The block diagram of such a receiver is shown in Figure 3.12. The receiver's task is to detect the presence of a TDMA pilot by moving the antenna beam, either mechanically or physically, to different locations in azimuth and elevation. At each location (or direction) a frequency search in a set of predetermined bandwidths is performed. Once the detection is obtained a fine tracking loop is activated to synchronize the receiver with the scanning rate of the satellite antenna and lock to frequency and phase of the pilot. Figure 3.13 shows a simplified flow diagram of this process.

Spatial Search

A user terminal, without any prior history of its position, when turned on has to initiate a search in both azimuth and elevation. In order to detect the pilot, the user antenna has to move to a maximum of M directions where:

$$M = \frac{360^\circ}{W_{azimuth}} \cdot \frac{90^\circ}{W_{elev}} \tag{3.15}$$

and $W_{azimuth}$, W_{elev} are the beamwidths of the user antenna in azimuth and elevation, respectively. The antenna beam moves to one azimuth-elevation cell at a time and stays there until the frequency search is completed thus requiring a maximum of $M-1$ direction changes for a maximum possible switch time of:

$$T_{switch} = (M-1)T_{dir} \tag{3.16}$$

where T_{dir} (sec) is the antenna direction switch time.[1]

Frequency Search

Assuming a constant carrier pilot is employed, for a system such as PASS that employs frequency reuse techniques, the frequency search consists of observing N different frequency regions each having a bandwidth equal to the frequency uncertainty at the input of the matched filter.

[1] In deriving the equations in this report, it is assumed that the satellite is in direct view of the user antenna.

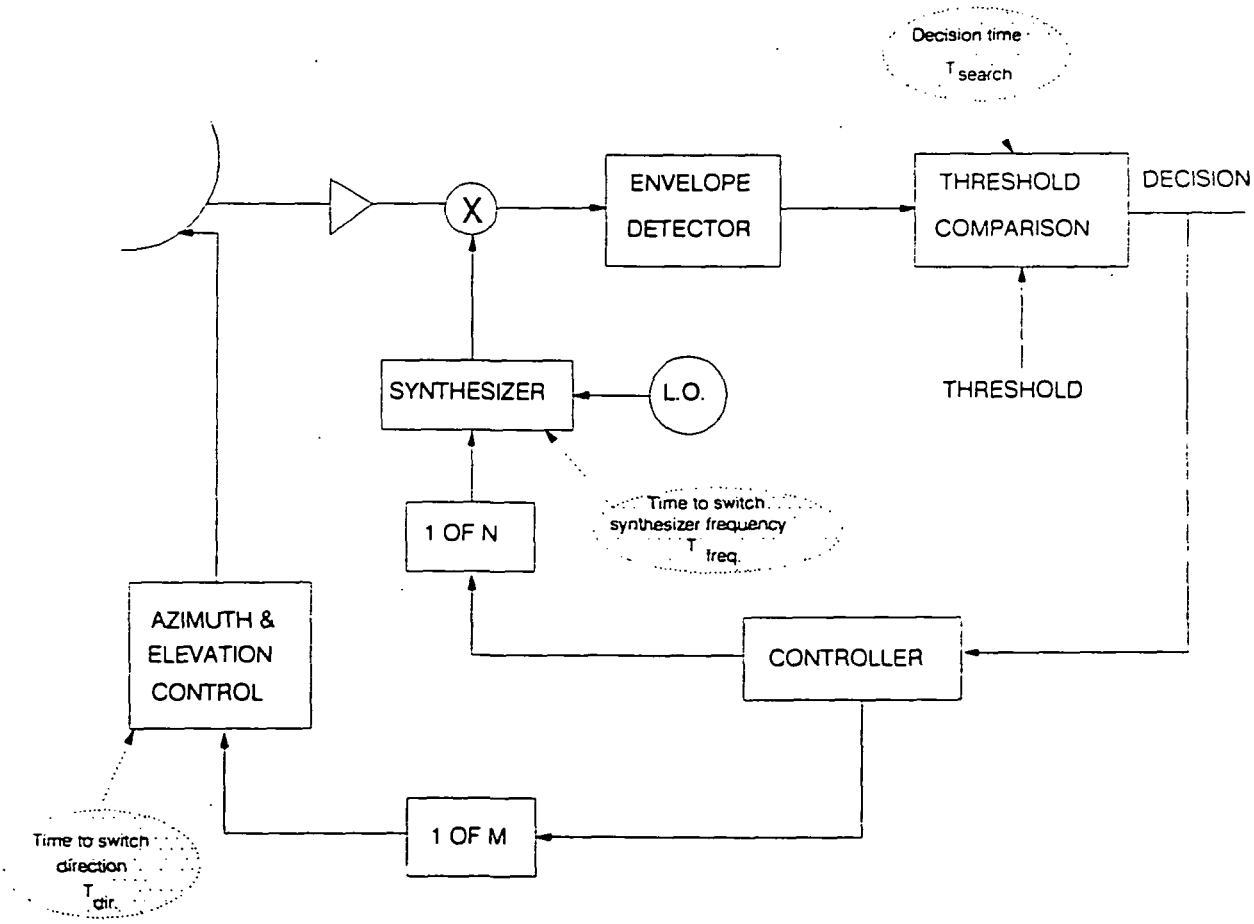

Figure 3.12: Receiver block diagram.

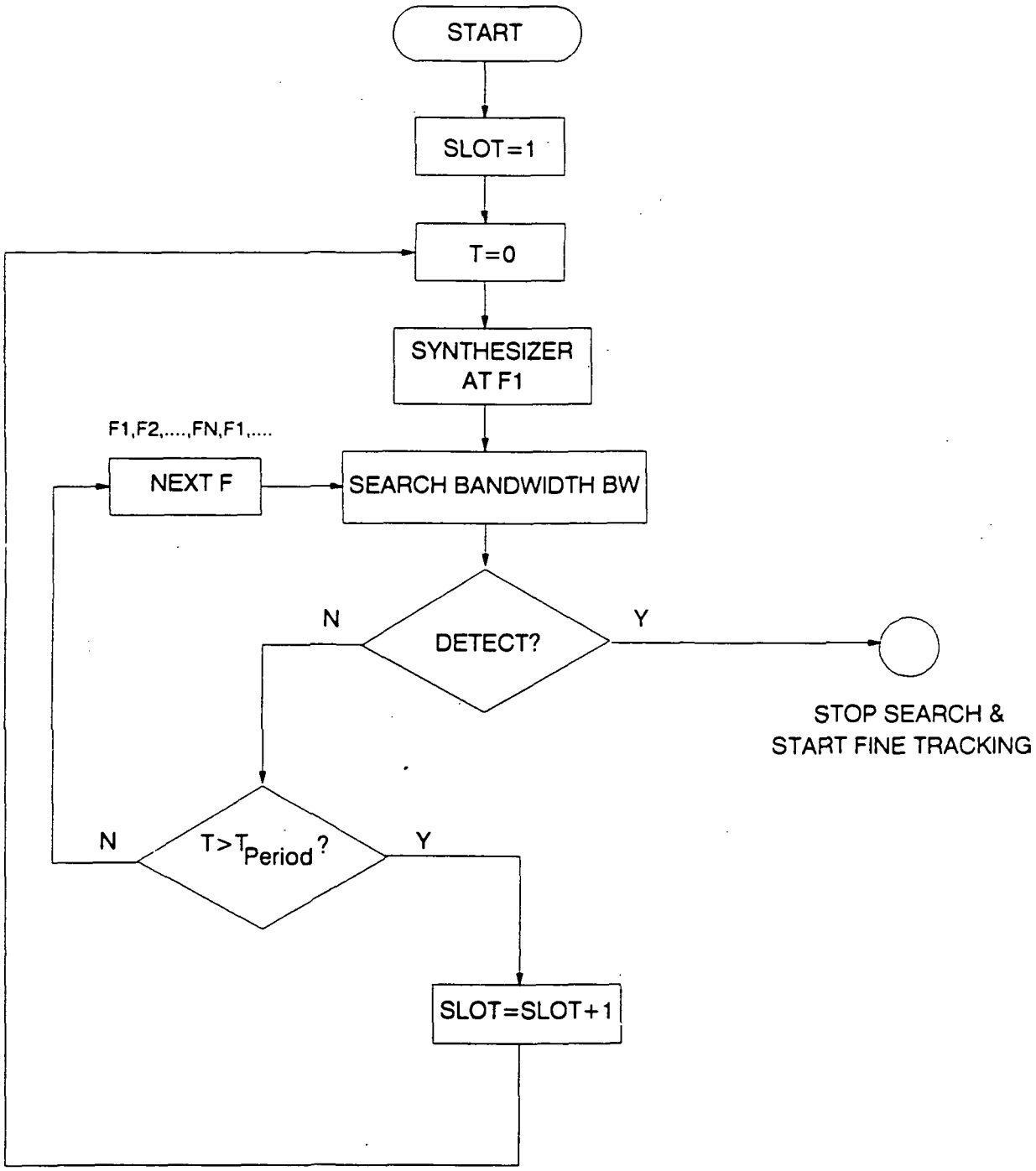

Figure 3.13: Detection flow diagram.

The frequency uncertainty is due to downconversion error (δf) and possibly some Doppler shift (δF). At each spatial cell N frequency regions, each being a maximum of $\pm(\delta f + \delta F)$ off from the expected value, have to be searched. The total search bandwidth at each frequency is:

$$BW_{IF} = 2(\delta f_{max} + \delta F_{max}). \tag{3.17}$$

The receiver's downconversion error is a function of the local oscillator drift and the center frequency of the incoming pilot, that is:

$$\delta f_{max} = F_{down} \cdot \text{Oscillator long term accuracy} \tag{3.18}$$

where F_{down} is the down link frequency from the satellite hereafter assumed to be 20 GHz. The Doppler shift for stationary applications consists of only the satellite Doppler which is ideally compensated for by the NMC so that only residual Doppler shift is present at the input of the receiver, thus,

$$\delta F \approx 0.$$

To ensure proper detection a small detection bandwidth is required and thus instead of sweeping the full bandwidth of the N pilots, it is assumed that the synthesizer frequency is switched to one pilot frequency at a time leading to a maximum synthesizer switch time of:

$$T_{synth} = (N-1)T_{freq} \tag{3.19}$$

where T_{freq} is the synthesizer frequency switch time.

At each frequency region an integration of the energy in a bandwidth $2\delta f_{max}$ is done by the matched filter for a period of time T_{search} that depends on the nominal link conditions. The output of the matched filter is envelope detected and is then compared to a predetermined threshold that ideally ensures the detection of the pilot. This scheme, because of its preset threshold will occasionally detect noise pulses that are sometimes as high as the actual signal thus causing what is known as a false alarm. Numerous studies have shown the tradeoffs between probability of detection (P_d) and false alarm rate (FAR) as a function of the channel C/N_0. The results of [7] will be applied in Section 3.3.2 in conjunction with the parameters of the PASS strawman design.

When the user terminal antenna is pointed towards the satellite, there must be a reasonably high probability that the receiver will detect the pilot. This is difficult as the pilot and the user terminal receiver are initially asynchronous and because, as viewed from the user terminal, the pilot occupies only a brief interval. Thus the probability of detection must be very close to unity and that false alarms must occur infrequently. Given that frequency reuse techniques are used, and assuming that an envelope detection scheme with an accurate threshold is employed, the initial detection time (T) of the receiver depends on δf, δF, N, P_d, FAR, T_{freq}, T_{search}, and C/N_0 of the link. These parameters will be applied in Section 3.3.2.

Time Search

Time search is not a function of the detector characteristics, however it sets the system requirements that have to be met in order to ensure that both spatial and frequency searches conclude with a true detection. These requirements are on the selection of the satellite scan period (T_{period}), and duration ($T_{duration}$) of the beam at a given location.

For proper spatial acquisition to occur, assuming that the time to switch a synthesizer is less than the time to switch to a new spatial cell, the minimum $T_{duration}$ should be selected such that:

$$T_{duration} = T_{synth} + (N+1)T_{search} \tag{3.20}$$

that is the scanning beam should be pointed to a given geographic region at least long enough for the receiver to search all N frequency regions. The second term in the right side of the equation is the total search time of all of the $N+1$ bandwidths where the extra search time is to compensate for possible race conditions. Furthermore, it should be ensured that the total time the user antenna is oriented in one of M directions (T_{dd}) meets the following requirement:

$$T_{dd} \geq T_{period}, \tag{3.21}$$

thus resulting in a maximum detection time of:

$$\begin{aligned} T_{detect} &= MT_{period} + T_{switch} \\ &= MN_P T_{duration} + T_{switch}. \end{aligned} \tag{3.22}$$

where N_P is the scan factor defined as the ratio of the scan period of the satellite beam to its $T_{duration}$. It is obvious from Equations 3.20 to 3.22 that the scanning rate of the satellite beams is a function of the search time of the user receiver. The overall search time T_{search} is basically a function of the link condition C/N_0 and the expected P_d.

3.3.2 Numerical Example

In order to minimize T_{search}, it is vital that the probability of detecting energy in the detection bandwidth be very high and that the number of false alarms be very low. For a given bandwidth, a specific S/N is required to meet the desired probability of detection and false alarm rate. The probability that the signal will be detected, P_d, is given by Skolnik to be [7]:

$$P_d = \frac{1}{2}\left(1 - \text{erf}\left[\frac{v_T - A}{\sqrt{2\Psi_0}}\right]\right) + \left(\frac{\exp\left[\frac{-(v_T-A)^2}{2\Psi_0}\right]}{2\sqrt{2\pi}\frac{A}{\sqrt{\Psi_0}}}\right)\left(1 - \frac{v_T - A}{4A} + \frac{1 + \frac{(v_T-A)^2}{\Psi_0}}{\frac{8A^2}{\Psi_0}} - \cdots\right) \tag{3.23}$$

where the error function, erf, is defined as:

Table 3.10: Bandwidth vs. Oscillator Long Term Drift

Oscillator Long Term Drift	Bandwidth BW_{IF}
± 1 PPM	40000 Hz
± 0.1 PPM	4000 Hz
± 0.01 PPM	400 Hz
± 0.001 PPM	40 Hz

$$\mathrm{erf}Z = \frac{2}{\sqrt{\pi}} \int_0^Z e^{-u^2} du,$$

v_T is the detector threshold voltage, A is the signal amplitude, and Ψ_0 is the mean-square value of the noise voltage. He furthermore shows that the probability of false alarms, P_{FA}, is:

$$P_{FA} = \exp\left(-\frac{v_T^2}{2\Psi_0}\right) = \frac{1}{TBFA \cdot BW_{IF}}$$

and

$$\frac{A}{\Psi^{\frac{1}{2}}} = \left(\frac{2S}{N}\right)^{\frac{1}{2}}$$

where $TBFA$ is the average Time Between False Alarms. The results of the above equations are plotted in Figs. 3.14 and 3.15. Fig. 3.14 plots the required signal-to-noise ratio as a function of the probability of false alarm for a number of detection probabilities, namely 90%, 95% and 99%. As is evident from the plots, for a given P_d, higher P_{FA} result in lower requirements for S/N. The time between false alarms is plotted as a function of the false alarm rate in Fig. 3.15 for four oscillator stabilities. The relationship between oscillator stability and IF bandwidth is given by Eqns. 3.17 and 3.18; this trade-off is quantified in Table 3.10. For a given TBFA, Fig. 3.15 shows that the higher the accuracy of the oscillator the higher P_{FA}, and, thus the lower the required S/N. For example, in order to get a P_d of 99% at a $TBFA$ of 1 minute, a SNR of 14.8, 14.4, 13.8, and 13 dB is required for an oscillator accuracy of 1, 0.1, 0.01, and 0.001 PPM, respectively.

The signal-to-noise ratio at the input of the detector is given as a function of C/N_0 and BW_{IF}:

$$\frac{S}{N} = \frac{C}{N_0} - 10\log(BW_{IF})$$

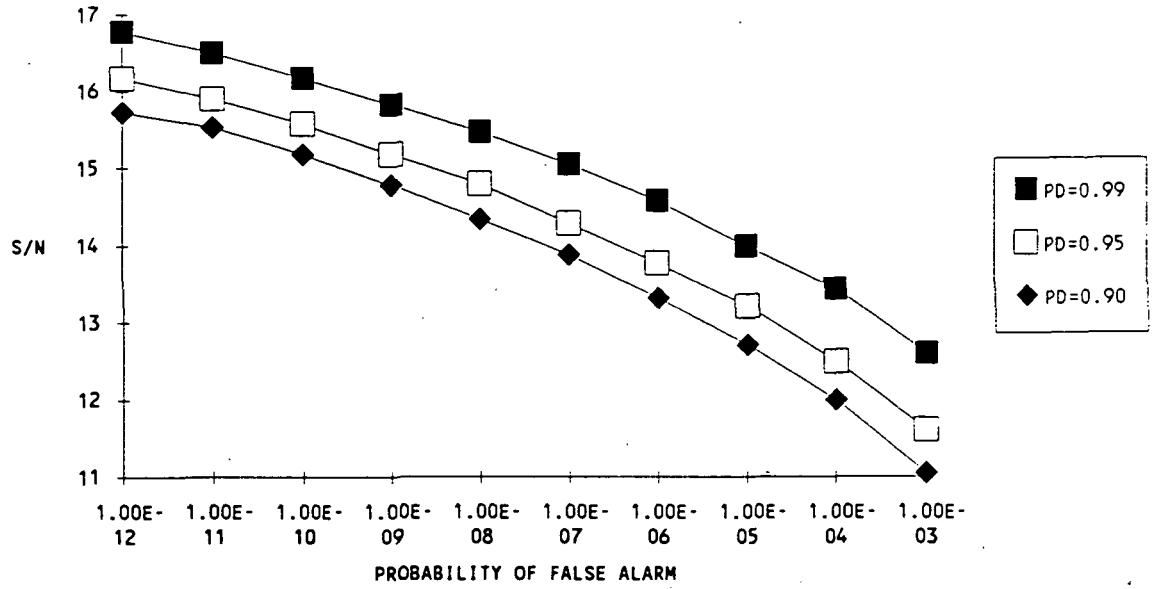

Figure 3.14: Required signal-to-noise ratio vs. probability of false alarm as a function of detection probability.

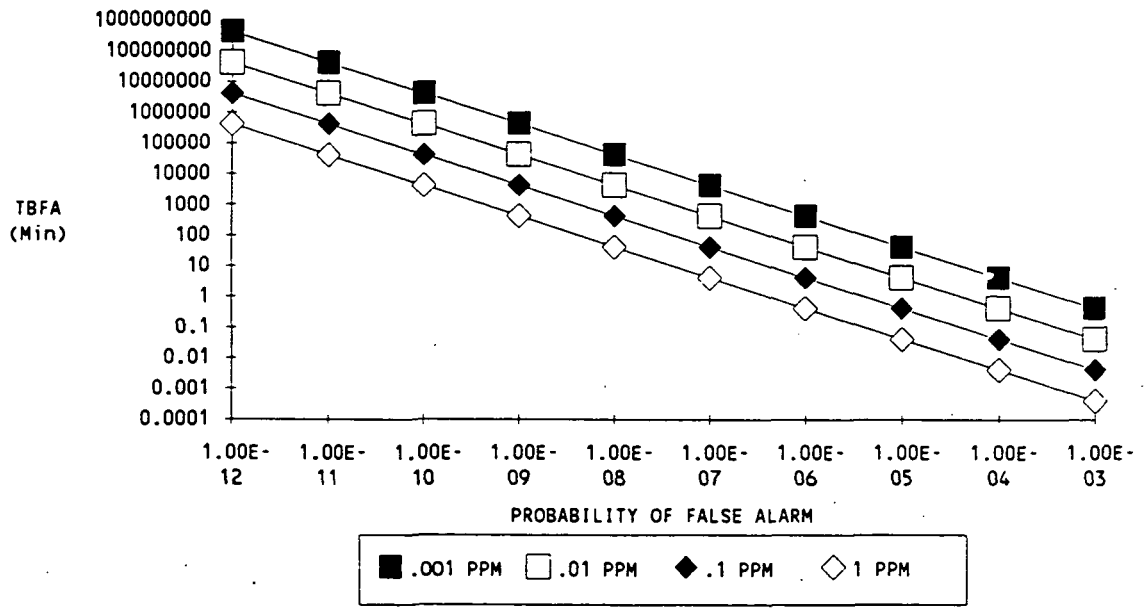

Figure 3.15: Mean time between false alarms vs. probability of false alarm as a function of oscillator accuracy.

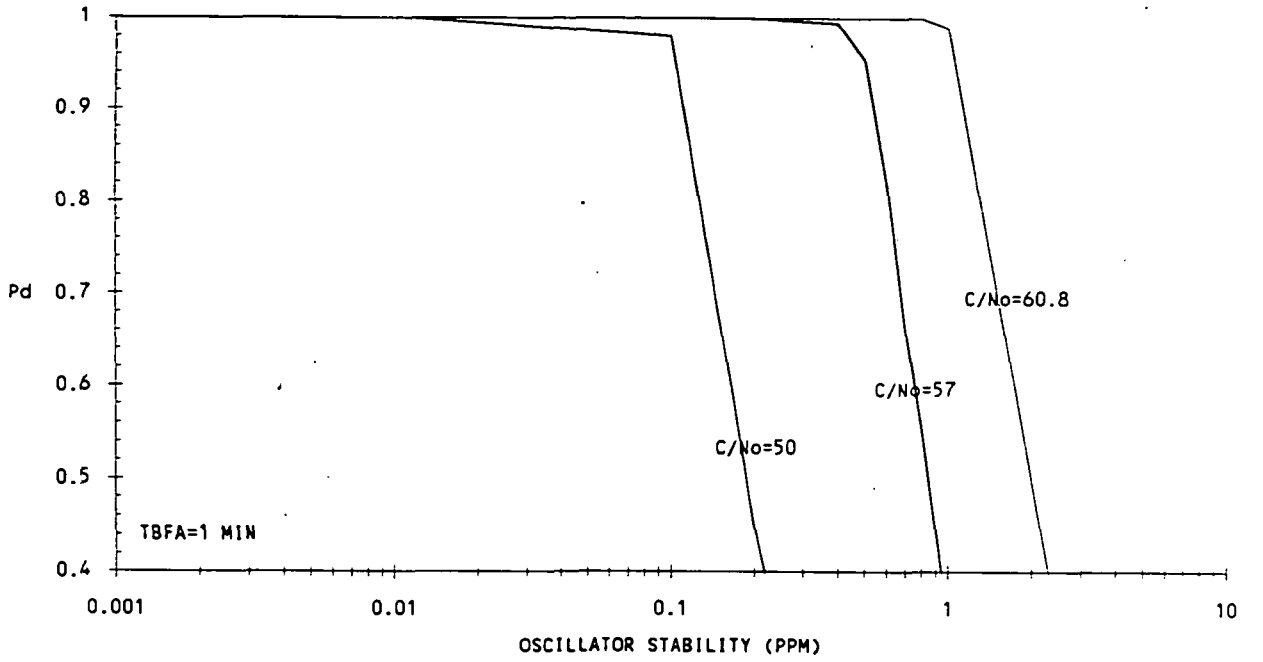

Figure 3.16: Probability of detection as a function of oscillator stability for different C/N_0 values.

For a TBFA of 1 minute, the probability of detection as a function of oscillator drift for C/N_0 of 50, 57 and 60.8 dB-Hz is plotted in Fig. 3.16. Note that a probability of detection of 99% corresponds to an oscillator stability of 0.02, 0.32, and 1 ppm for C/N_0 of 50, 57, and 60.8 dB-Hz, respectively.

The PASS strawman design supports a C/N_0 of 57 dB-Hz at the input to the user terminal receiver for the low rate 100 Kbps TDMA carrier and calls for a pilot channel whose C/N_O is much less than that of the TDMA carrier. A scanning beam covering N_P regions will require the forward link data rate to increase N_P times. The higher data rate will necessitate an increase of $10\log(N_P)$ in the effective radiated power of the satellite. Assuming N_P is 10, the received C/N_0 will increase to 67 dB-Hz for the same class of satellite as the strawman design. Table 3.11 gives the pilot power as a percentage of the LRC TDMA carrier power for various oscillator stabilities for a $TBFA$ of 1 minute and a P_d of 0.99. The data for the table is taken from Fig. 3.16. For $N_P = 10$, assuming that the pilot power should be no more than 10% of the power in the low data rate channel, an oscillator stability of better than 0.32 ppm is needed to perform the initial acquisition.

Once the required C/N_0 has been set, the minimum switched/scanning beam duration time, i.e. that required for the receiver to search all N pilots, can be determined from Eq. 3.20 for the operational system values listed in Table 3.12. Given that there are 9 pilots bands which the receiver must search at a given spatial direction, and assuming that the synthesizer frequency switch time, T_{freq}, is 10 μsec, T_{synth} can be found from Eq. 3.19 to be:

Table 3.11: Required Pilot Power at the Satellite for Pilot Acquisition

Oscillator Stability (ppm)	Required Pilot C/N_0 (dB-Hz)	Pilot Power as a % of the low rate TDMA channel power)
1.00	60.8	24
0.32	57.0	10
0.10	50.4	2
0.01	39.8	0.2

$$T_{synth} = (9-1)\ 10 \cdot 10^{-6} = 80\ \mu\text{sec.} \tag{3.24}$$

If only a short time is allowed for observation, determination, and processing of a given bandwidth, then T_{search} can be assumed to be 1msec. T_{search} depends on the signal-to-noise of the pilot. Assuming 9 pilots ($N = 9$) and ten scan regions per beam ($N_P = 10$), $T_{duration}$ can be calculated from Eq. 3.20 to be:

$$T_{duration} = 80\ \mu\text{sec} + (9+1) \cdot 1\ \text{msec} = 10.08\ \text{msec.} \tag{3.25}$$

Under the operational assumptions shown in Table 3.12, the minimum beam dwell time over a particular area must then be 10.08 msec in order for the receiver to search for the 9 possible pilots at a given spatial location. This minimum beam duration time has been computed assuming an oscillator with long term stability of 0.32 ppm is used and that the pilot C/N_0 is 57 dB-Hz. From Table 3.7, a VCXO could be used at a cost of \$10 - \$12 in 1000 unit quantities. Operation with more stable oscillators or with higher pilot C/N_O's will reduce the minimum beam duration time at the expense of using a higher cost LO or more satellite power.

In order to find the time required to search all spatial locations M for the presence of the satellite pilot, T_{detect}, the number of spatial locations and the time for the antenna to move from direction to direction, T_{dir}, must be given. The former can be calculated from Eq. 3.15 given $W_{azimuth}$ and W_{elev} and the latter can be found from Eq. 3.16 given T_{dir}. Values for $W_{azimuth}$, W_{elev}, and T_{dir} are given in Table 3.12 and used to find:

$$T_{switch} = (100-1)\ 20 \cdot 10^{-6} = 1.98\ \text{msec.} \tag{3.26}$$

Using Eqs. 3.22, 3.25 and 3.26, T_{detect} is found to be:

$$T_{detect} = 100 \cdot 10 \cdot 10.08 + 1.98 = 1082\ \text{msec} = 1.082\ \text{sec.}$$

These results are meant to identify the dependency of $T_{duration}$ and T_{detect} on oscillator stability and pilot C/N_O. Under the conditions stated above, an oscillator with 0.32 ppm

Table 3.12: Operational Values

PARAMETER	Assumed value
F_{down}	20 GHz
Oscillator Long Term Drift	1, 0.1, 0.01, 0.001 ppm
δF (Doppler Compensation by the NMC)	0
N	9
P_d	99%
$TBFA$	1 min
N_P	10
T_{freq}	10 μsecs ‡
T_{search}	1 msec
$W_{azimuth}$	18°
W_{elev}	18°
T_{dir}	20 μsecs †

† Estimated value for the switch time of phase shifter.
‡ Derived from current low cost synthesizer specification.

long term stability can be used to detect the pilot if its C/N_O is 57 dB-Hz; alternatively an oscillator with 1 ppm long term stability can be used if the pilot C/N_O is 60.8 dB-Hz. However these results, based on the data provided in Table 3.11, assume a perfect receiver and no margin has been left for errors. In practice there will be other factors that will influence these results and careful consideration should be made to ensure perfect detection. Some of these factors are presented in the next section.

3.3.3 Practical Considerations

Threshold Setting

Many wideband detectors have been built to operate in different frequency bands, and have been used extensively for different applications. As a result, the technology needed for this type of detector is fairly well in hand. From a functional standpoint, the most difficult problem is that of setting and maintaining the receiver threshold value. Proper setting of this value is essential to meeting the specified P_d and P_{fa}. If the threshold is too low, an excessive false alarm rate is obtained while, if it is too high, detection of the actual signal may be missed. Even if the threshold is set properly initially, time, temperature, and voltage variations, and other dynamic conditions, will affect the overall detector such that the initial setting will become incorrect. Further, the receiver effective noise temperature will change as the receiving antenna is subject to varying background temperature due to changing angles and fields of view. For example, a 1 dB change in the threshold can result in three orders of magnitude change in false alarm probability. Thus, some precise, automatic, periodically updating method of threshold termination is needed. Devices that accomplish this purpose are called $CFAR$ (CONSTANT-FALSE-ALARM-RATE).

$CFAR$ complexity varies based on the application. A $CFAR$ may be obtained by observing the noise in the vicinity of the pilot and adjusting the threshold in accordance with the measured background. Figure 3.17 illustrates the cell-averaging $CFAR$ which utilizes a tapped delay-line to sample the bandwidths in either side of the bandwidth of interest i.e. the frequency bandwidths of Section 3.3.1 can be used as the sample points. (For a detailed description of this method please see Chapter 10 of [7].) For the purposes of this study it should be noted that a loss of about 1 dB in performance will be added to the required SNR.

There are several other methods for achieving $CFAR$ at the output of the low-pass filter. These methods are complex and all result in some loss of performance. It is obvious that some method is required to be able to perform this detection, however for a hand held terminal, requiring ease of implementation and low cost components, this may be formidable.

Voice Delay

In the switched beam scenario the period of the beam sets the voice delay and it is extremely important to minimize this delay. From Eq. 3.20 it is clear that the minimum delay is a function of the overall detection time of the user terminal. Table 3.5 plots the round trip

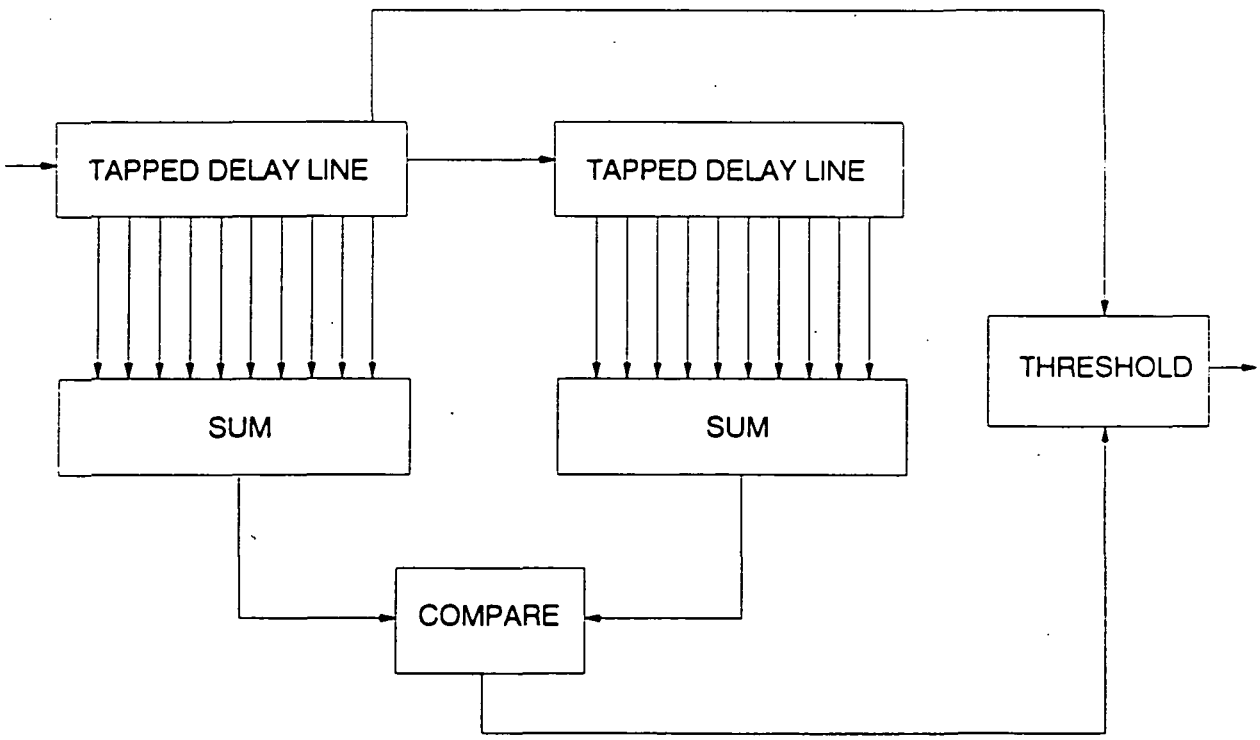

Figure 3.17: Cell averaging $CFAR$.

voice delay for the switched beam vs. T_{period} for various values of N_P. Applying the results of the example, namely,

$$T_{period} = 10T_{duration} = 100.8\text{msecs},$$

to Eq. 3.14, the minimum roundtrip delay achievable is 0.274 sec, which is a minimal impact as compared to the fixed beam case. However, this number increases exponentially with the decrease in pilot transmit power.

3.3.4 System Impact

The equations determining pilot acquistion have been presented. The interrelationship between pilot C/N_O, P_d, $TBFA$, and user terminal oscillator stability has been quantified. Examples of the tradeoff between long term oscillator stability and pilot C/N_O in determining the minimum beam duration time required – or time necessary for the receiver to check all possible pilot bands when the user antenna is pointed in a given direction – have been given for the specific case where P_d is 0.99 and $TBFA$ is 1 minute. Oscillators with stabilities of 0.32 ppm and 1 ppm can be used with pilot C/N_O's of 57 dB-Hz and 60.8 dB-Hz to achieve a $T_{duration}$ of 10 msec, assuming a P_d of 0.99 and a $TBFA$ of 1 minute. Lower beam duration times can be arrived at if oscillators with higher stabilities, and higher costs, or higher power pilots are utilized. The pilot powers listed above represent 10% and 24% of the power of the TDMA low rate channels, respectively. This is the minimum acceptable power for these oscillator stabilities. However detection in fading environment will require even greater power. Furthermore, there are manufacturing and aging tolerances that need to be considered. If one allows a 3 dB margin to compensate for all of the possible errors i.e. noise fluctuations, threshold settings, aging tolerances, etc., then an overall increase of 7 dB of power will be required to acquire the pilot. This will either put a big burden on the satellite or decrease the capacity of the system. The 7 dB power increase can be minimized by permitting longer integration time in the pilot acquistion circuit. However this will increase $T_{duration}$ and hence lead to a greater round trip voice delay.

3.4 Conclusion

The PASS strawman design calls for the use of a CONUS beam for transmission between the supplier and the satellite and for fixed spot beams for transmission between the basic personal terminal (BPT) and the satellite. 142 such beams, of 0.35° beamwidth, are necessary to cover CONUS. This chapter explores the consequences of replacing these 142 fixed beams by a number of switched or scanning beams, each of which would address N_P coverage areas. Several advantages are gained through the use of satellite switched/scanning spot beams instead of fixed spot beams. They lie primarily in improved system operation and enhanced ease of satellite hardware and implementation. First, the use of switched beams on-board the satellite provides a method to efficiently match satellite capacity with traffic

needs particularly if the traffic is non-uniformly distributed in time and geographical location. Second, the transponder design may be simplified and component weight reduced. Third, replacing the 142 fixed beams by $142/N_P$ switched, or scanning, beams may simplify the overall beam forming network design on-board the satellite.

Several drawbacks arise through the use of switched beams. As continuous communication with each coverage area is no longer possible as with fixed spot beams, communication to and from the switched/scanning beams must occur at higher data rates if the average data rate achieved with fixed beams is to be sustained. Thus the communication links must be modified to support these higher data rates and a higher level of control over the system will be necessary to maximize system throughput. The network management center will also have more tasks to perform. In addition to those duties required in the strawman design – notifying users of their start-of-transmission times, transmission duration, and frequency assignment – it will have to distribute to suppliers and users information about the beam's dwell time over their coverage area to insure the correct orchestration of all transmissions and calculate an efficient switch plan for the satellite switched beam (i.e. the duration and sequence of the switch's states). User communication will be effected in two ways: (1) all users must possess variable data rate burst modems to accommodate the variable beam dwell time, and, (2) fast acquisition mechanisms may be necessary in order to rapidly lock onto the satellite beacon at the onset of every connection period with the satellite. Furthermore the use of switched beams instead of fixed beams will reduce frequency reuse capability slightly.

To illustrate the implications of switched beams use on PASS system design, operation at two beam scan rates is explored. Beam scan rate denotes the frequency with which the beam accesses the same coverage area. Scan rate is defined in terms of the period of the beam and is equal to $1/T_{period}$. Each beam is taken to dwell over each coverage area for, on the average, $T_{duration}$ and has the capability of addressing N_P coverage areas ($N_P = T_{period}/T_{duration}$). For both switched beam examples, each beam is assumed capable of accessing 10 coverage areas. The low scan rate, corresponding to T_{period} of 2 sec and $T_{duration}$ of 200 msec, was chosen to minimize the supplier overhead per transmission and to illustrate the case where complete spatial acquisition can be performed during one access time. The fast scan rate, corresponding to T_{period} of 20 msec and $T_{duration}$ of 2 msec, was set so as to minimize voice signal delay.

The requirement of a fast acquisition mechanism was explored. It was shown that the user terminal oscillator stability sets the lower limit of the receiver's front-end C/N_0. Table 3.11 shows the required pilot C/N_0 in dB-Hz and in terms of the low data rate channel C/N_0 as a function of the oscillator long-term stability. The data obtained indicates that, under perfect conditions, i.e. no noise fluctuations, optimum detector setting, etc., an oscillator stability of 0.32 ppm is necessary to keep the pilot channel power at 10% of the data channel level. Including some margin for these tolerances would require a better oscillator and hence a more expensive user terminal. Given that the right combination of oscillator stability and C/N_0 is selected then, for a ten area scanning beam ($N_P = 10$), the voice delay achievable is close to that of the strawman design, however this number increases exponentially as the received pilot power decreases.

Conclusions are summarized in Tables 3.8 and 3.9 where the characteristics of slow and fast scan switched beams are compared against those of the strawman fixed beam PASS design. System operation can be characterized by several parameters, beam efficiency or match of satellite capacity with traffic needs, spectrum requirements, voice signal delay, supplier overhead/transmission, and required burst data rate that must be supported by the communication link. From the user's point of view, rapid acquisition of the beam at the onset of the communication link is of importance, and to a lesser degree the time required for spatial beam location is of interest.

Optimum beam scan rate is determined by tradeoffs in various parameters. As the beam scan rate decreases (its period and duration over one coverage area increases) the following occur: the round trip delay incurred by signal of voice origin increases; information throughput at the supplier station increases; and, the need to restart signal acquisition process at user terminal between satellite beam accesses increases. Operation with a slow scan beam, such as examplified in Tables 3.8 and 3.9, is probably not practical due to its poor delay performance: 4.7 sec for voice communications. Scan rates closer to that typified by the fast scan beam will have to be used.

Switched/scanning beams have been found to allow a better match between traffic requirements with large geographic and temporal variations and satellite capacity. Their use reduces the number of local oscillators and high power amplifiers required on-board the satellite. No additional equipment is thought to be necessary in the user and supplier terminals to acquire the non-continuous satellite signal. Reacquisition of the satellite pilot can be accomplished without reentering into the receiver's acquisition mode as the pilot will be within the loop's tracking bandwidth.

The cost of using switched/scanning beams can be divided into four categories. First, higher EIRP user terminals and satellites will be necessary to support the higher burst data rates. The former can be achieved by increasing the size of the HPA in the user terminals at the price of increased radiated flux. The latter can be accomplished by using TWTs in place of solid state high power amplifiers at the cost of greater weight and volume. Second, burst modems will be needed at the user terminals and supplier stations instead of non-burst modems. Acquisition of the pilot when the user terminals are pointed in one spatial direction in $\simeq 10$ msec implies that oscillator stabilities of better than 0.32 ppm with a pilot C/N_O of 57 dB-Hz, or 10% of the low rate TDMA channel power, or of better than 1 ppm with a pilot C/N_O of 60.8 dB-Hz, or 24% of the data channel power, is necessary to achieve a P_d of 0.99 with a $TBFA$ of 1 minute. Third, the NMC will have the additional function of dynamically varying the beam duration time depending on the user traffic, thus a more precise control of the network will be necessary. The overhead in the forward link will increase as the NMC will have to distribute the variable dwell time of the beam for each pass to all the users within that beam. Four, this system will not be able to service mobile terminals as they would not be able to continuously track the satellite during motion of the mobile. Spatial and frequency acquisition would have to be performed prior to the reception or transmission of any data and would thus require very slow scan beams with the ensuing long signal delay times. Lastly, spectral efficiency, accomplished in the strawman design through frequency

reuse, will be slightly reduced by the use of switched/scanning beams, the total required bandwidth (uplink and downlink) being 1.2 to 1.4 times that required with fixed beams. The use of a hybrid system, employing switched/scanning beams on the downlink to the user terminal and fixed beams on the uplink from the user terminal would alleviate some of these problems but also reduce the incentive to use switched/scanning beams.

If the use of these beams are further explored two topics deserve deeper analysis: the evaluation of a more precise range for beam efficiency, this being the main advantage for switched/scanning beam use; and a quantitative study of the acquisition scheme employed to assess their operation with spread spectrum multiple access techniques.

Appendix A

Channel Capacity of the Strawman PASS Design

System capacity of the strawman design is limited to the equivalent of 2000 duplex voice channels. This is determined by the RF power in the satellite. The currently conceived PASS satellite should be capable of generating 2.5 KW of DC power from solar wings. It is expected that this will translate to greater than 400 W of RF power. Currently the link from satellite to users requires 4W per 100 Kbps TDMA channel or 0.19W per 4.8 Kbps portion of the channel. Thus 2000 4.8Kbps channels would utilize 384 Watts. The link from satellite to suppliers calls for a maximum of 0.01W per SCPC channel; 2000 channels would then require 20 Watts. The strawman bandwidth requirements for communications to the BPT's can be taken from Table 3.4. The uplink bandwidth required is $\approx$ 60 MHz, the downlink bandwidth would be 42 MHz, assuming no high rate TDMA carriers are used, that the bandwidth required for the low rate TDMA carrier and the pilot is 400 KHz, and that the bandwidth required for a 4.8Kbps SCPC carrier with guard band is 19.2 KHz.

Appendix B

Beam Concept Impact on Satellite Antenna

The use of switched beams with N_P coverage areas/beam will require that the users transmit at a higher data rate, R_s, if the average data rate from the users is to remain constant:

$$R_s = N_P \cdot R_f$$

where R_f is the data rate supported by the fixed beam design. Consequently the link must be modified to support an N_P higher data rate. Here we consider the return link from BPT to supplier. In the preliminary PASS design, the C/N_0 of this link is set by the uplink from the BPT.

B.1 Return Link Assumptions

The communications link must be modified to support the higher data rate. If we want to use a solid state HPA at the BPT, then we cannot assume that running the HPA in burst mode will increase either the available output power or the HPA's efficiency as would be the case with a TWT [1]. If we stipulate that the transmit power and the antenna size of the BPT must remain constant so that the flux density emitted from the BPT is not increased, then we can vary only the G/T of the satellite to accomodate the higher data rate. If we further assume that no improvements can be made in the satellite system temperature, then we are left making up the required link change of N_P by increasing the antenna gain by a factor of N_P.

[1] This is based on a discussion with Dick Reis of Varian's Electron Device and Systems Group.

B.2 Antenna Size and Beam Number for CONUS Coverage

Denoting the fixed satellite antenna gain by G_f, its diameter by d_f, and its 1/2 power beamwidth by ϕ_{b_f} and the new switched satellite antenna gain by G_s, its diameter by d_s, and its 1/2 power beamwidth by ϕ_{b_s}, we wish to calculate the impact that increasing the satellite antenna gain from G_f to G_s will have on the number of beams coverage areas required to cover CONUS and thereby calculate the number of switched beams necessary given our initial assumption of N_p coverage areas/switched beam.

The following equations give the relationship between antenna gain, G, 1/2 power beamwidth, ϕ_b, beam coverage area, A_{beam}, and number of beam covering areas in CONUS, N_{cov}:

$$\begin{aligned} G &= \rho_a \cdot \frac{4\pi}{\lambda^2} \cdot Area \\ &= \rho_a \cdot \pi^2 \cdot \left(\frac{d}{\lambda}\right)^2 \end{aligned}$$

$$\begin{aligned} \phi_b &= \frac{\lambda}{d\sqrt{\rho_a}} \\ &\propto \frac{1}{\sqrt{G}} \end{aligned}$$

$$\begin{aligned} A_{beam} &= \pi\left(\frac{h sin 2\phi_b}{2}\right)^2 \\ &\simeq \pi h^2 {\phi_b}^2 \end{aligned}$$

The number of coverage areas required for CONUS is,

$$\begin{aligned} N_{cov} &= \frac{A_{CONUS}}{A_{beam}} \\ &\propto \frac{1}{{\phi_b}^2} \\ &\propto G. \end{aligned}$$

Let N_{B_f} be the number of fixed beams required for the initial case of fixed beam CONUS coverage and let N_{B_s} be the commensurate number of switched beams with N_p areas/beam necessary to cover CONUS. Then for the fixed beam case,

$$N_{B_f} = N_{cov};$$

whereas for the switched beam case,

$$N_{B_s} = \frac{N_{cov}}{N_p}.$$

If we force the satellite antenna to increase in size to make up the required power in the link, the following will occur:

$$\begin{aligned} R_s &= N_p \cdot R_f \\ G_s &= N_p \cdot G_f \\ d_s &= \sqrt{N_p} \cdot d_f \\ \phi_{b_s} &= \frac{1}{\sqrt{N_p}} \cdot \phi_{b_f} \\ N_{cov_s} &= N_p \cdot N_{cov} \end{aligned}$$

Increasing the satellite antenna's gain by N_p translates into increasing the number of coverage areas in CONUS by N_p which means that the number of switched beams that will be necessary to cover CONUS is:

$$\begin{aligned} N_{B_s} &= \frac{N_{cov_s}}{N_p} \\ &= N_{B_f} \end{aligned}$$

B.3 Example

Let the fixed beam scenario be as follows:

$$\begin{aligned} R_f &= 5 \text{ Kbps} \\ G_f &= 52.5 \text{ dBi} \\ d_f &= 3 \text{ meters} \\ \phi_{b_f} &= 0.35° \\ N_{B_f} &= 142 \text{ beams.} \end{aligned}$$

If a scanning beam is used with $N_p = 10$, or 10 coverage areas/beam, then

$$\begin{aligned} R_s &= 50 \text{ Kbps} \\ G_s &= 62.5 \text{ dBi} \\ d_s &= 9.5 \text{ meters} \\ \phi_{b_s} &= 0.11° \\ N_{B_s} &= 142 \text{ beams} \\ &\quad \text{with 10 areas/beam.} \end{aligned}$$

The satellite's antenna is far larger than in the fixed beam case and the beam forming network is far more complex, 142 beams with 10 areas/beam.

Of course, the conclusions would be different if the BPT HPA and antenna gain were permitted to increase.

B.4 Discussion

If instead of covering CONUS with N_{B_f} fixed beams we try to cover CONUS with N_{B_s} switched beams, where each switched beam must alternate between N_p areas, we find that the transmit and receive data rates at the BPT must increase by N_p to keep the average data rate/user constant.

Here we consider the impact of the higher transmit data rate on the BPT, i.e. on the PASS return link. We assume that the transmit power and the antenna size at the BPT are not permitted to increase to support the N_P times higher data rate. Only the size of the satellite receive antenna may grow to support the higher data rate. We then arrive at the conclusion that $N_{B_s} = N_{B_f}$.

For the preliminary PASS design, assuming each switched/scanning beam scans 10 areas, this means that the 142 fixed beams required to cover CONUS will be replaced by 142 switched/scanning beams each of which covers 10 areas. CONUS will then be covered by 1420 areas and serviced by 142 beams. The complexity of the beam forming network for the switched/scanning beam scenario is far higher than that of the fixed beam scenario.

Bibliography

[1] Miles K. Sue, editor. *Personal Access Satellite System Concept Study.* Jet Propulsion Laboratory, JPL D-5990 Edition, Feb. 1989.

[2] F. M. Naderi and S. J. Campanella. NASA's Advanced Communications Technology Satellite (ACTS): An Overview of the Satellite, the Network, and the Underlying Technologies. In *AIAA 12th International Communications Satellite Systems Conference*, pages 204 – 224, March 13-17 1988.

[3] G. Morelli and T. Matitti. The Italsat Satellite Program. In *AIAA 12th International Communications Satellite Systems Conference*, pages 112 – 121, March 13-17 1988.

[4] F. T. Assal, A. I. Zaghloul, and R. M. Sorbello. Multiple Spot-Beam Systems for Satellite Communications. In *AIAA 12th International Communications Satellite Systems Conference*, pages 322 – 331, March 13-17 1988.

[5] S. Joseph Campanella, Benjamin A. Pontano, and Harvey Chalmers. Future Switching Satellites. In *AIAA 12th International Communications Satellite Systems Conference*, pages 264 – 273, March 13-17 1988.

[6] Vectron Laboratories, Inc. *Vectron Catalog*, 1987.

[7] M. I. Skolnik. *Introduction to Radar Systems.* McGraw-Hill Book Co., New York, 1980.

[8] S. J. Erst. *Receiving Systems Design.* Artech House, Inc., Massachussetts, 1984.

[9] A. R. Martin and R. F. Cobb. A Guide to Acquisition Receiver Selection and Performance. *Microwave Journal*, 1968.

Chapter 4
Impact of Non-Geostationary Orbits on PASS

Dr. Polly Estabrook and Masoud Motamedi

4.1 Introduction

This chapter examines the use of satellites in non-geostationary orbits (NGO) for PASS. This work was undertaken in an effort to investigate alternative system designs to enhance the user capacity and/or reduce the system complexity. The system impact on parameters such as uplink and downlink carrier-to-noise ratios, roundtrip signal delay, Doppler shift, and reduction in satellite antenna size, is quantized for satellites in five circular non-geostationary orbits whose altitudes range from over 20,000 km to under 1,000 km and two elliptical orbits, the Molniya and the ACE orbits. The number of satellites necessary for continuous CONUS coverage and the number of satellite switchovers per day has been determined for the satellites in orbits from 20,000 km to 5,000 km. These higher altitude orbits have been selected for initial study as continental U.S. coverage from one satellite is then possible. Orbits inclinations from the equatorial plane by 0°, 45°, and 90° have been considered. The increased system complexity brought about by the use of satellites at such altitudes appears to outweigh the system advantages for the application considered in this chapter.

Use of satellites in non-geostationary orbits is motivated by the possibility of gaining the following system advantages: (1) the reduction of EIRP and G/T requirements on the user terminals, thus permitting smaller antenna apertures and smaller terminals, or, equivalently, an increased link margin; (2) lower signal delays through the satellite; (3) reduced satellite antenna size, both for the CONUS and the multiple beam antennas; (4) support of a global communication system, this being especially valid for non-equatorial orbits; and (5) the possibility of using several satellites to operate from higher Earth look angles thus reducing the fade margin and blockage requirements for mobile vehicles applications [1]. Lastly the use of NGO satellites permits the consideration of a greater range of launch vehicles which may permit lower launch costs due to the use of simpler launch vehicles or the launch of

several satellites per vehicle.

While NGOs offer a number of attractive features, there are other factors that must be considered: (1) several satellites will be necessary to provide continuous coverage to any area, hence, control algorithms to handle traffic switchover between satellites must be developed; (2) tracking antennas on Earth will be needed, certainly at the Network Management Center (NMC) and the supplier stations and possibly for the user terminals (although it may be possible to use azimuthally omnidirectional antennas for the latter in some applications [1]); (3) large Doppler shifts will require compensation mechanisms or the design of modulation techniques insensitive to frequency offsets; and (4) variations in link characteristics will occur as the satellite passes from directly overhead to its maximum slant angle. In addition, the design of the satellite will need to cope with radiation effects on the solar panels and electronics due to increased radiation exposure from the Van Allen radiation belt as well as support the more complex antenna pointing mechanisms necessary for non-geostationary operation. Finally, although the use of NGO satellites may alleviate crowding in the geostationary orbit, questions of possible interference between geostationary and NGO satellites must be resolved (see [2] for details).

To date, satellites in non-geostationary circular orbits have been proposed to provide a global mobile communications link at L-band [3]; elliptical orbits have been proposed to offer primary coverage in Europe for mobile users at L-band [1], to offer global coverage for personal and mobile users at Ku band [4], and, to offload traffic from GEO satellites at peak traffic hours for fixed users in the U.S. at C- and Ku-bands [2,5].

This chapter discusses the use of satellites in circular and elliptical orbits; the height of the circular orbits is varied from those at which all of CONUS is visible from the satellite to those at which only parts of CONUS are visible at any one time. All of CONUS is visible with satellites in the two elliptical orbits considered. CONUS coverage from the satellite enables one satellite to relay signals between geographically separated earth stations within CONUS at any one time and thus bypasses the need for intersatellite links (ISL). The three circular orbits from which CONUS coverage is possible have altitudes of 20,182 km, 10,353 km and 5,143 km. For these three orbits, system parameters are found for satellites whose inclination angles from the equatorial plane is 0°, 45°, and 90°. Similar system parameters are calculated for the two elliptical orbits. In addition the number of satellites required to provide continuous CONUS coverage is calculated for these three higher altitude circular orbits and the two elliptical orbits. System parameters only are given for the two circular orbits at 1,247 km and 879 km that will require ISL to link terminals on either side of CONUS.

The choice of orbit altitudes is explained in Section 4.2. The impact on the uplink and downlink PASS signals is explored in Section 4.3. The calculation of the coverage time provided by satellites in specific locations of a given orbit is delineated in Section 4.4. From this data, the number of satellites required for continuous CONUS coverage is calculated. In Section 4.5 the relative advantages and disadvantages of the use of non-geostationary satellites at these three altitudes are discussed as they relate to the PASS application. Conclusions are presented in Section 4.6.

The material in this chapter has been reported on in [6,7].

4.2 Orbit Parameters

Five circular orbits and two elliptical orbits have been chosen for characterization. The heights of the circular orbits vary from that required for geostationary orbit to those easily achievable with a small launch vehicle, such as PEGASUS. Their altitudes therefore span from 20,182 km to 879 km. Two elliptical orbits have been analyzed: the Apogee at Constant time-of-day Equatorial orbit (ACE) studied by Price et al. [2,5]; and the Molniya orbit. Their altitudes vary from 15,100 km to 1030 km for the ACE orbit and from 37,771 km to 426 km for the Molniya orbit.

4.2.1 Circular Orbit Characteristics

The heights of the circular orbits have been selected in order to simplify the subsequent calculation of the number of satellites required to provide 24 hr coverage over any chosen area. Satellites heights whose periods are integrally related to the length of one sidereal day, τ_E, are considered.[1]

In order to calculate the altitudes of the satellites meeting this constraint, the relationship between satellite period and height must be used. The following equations give the linear velocity of the satellite, v_s, its angular velocity, ω_s, and its period, τ_s, in terms of the gravitational constant, G, the mass of the Earth, M, the radius of the Earth, r_E, and the height of the satellite above the Earth, h:

$$v_s = \sqrt{\frac{G * M}{r_E + h}}, \tag{4.1}$$

$$\omega_s = \frac{v_s}{r_E + h}, \tag{4.2}$$

$$\tau_s = \frac{2\pi}{\omega_s}, \tag{4.3}$$

where

$$G = 6.67 * 10^{-8} \text{ cm}^3/\text{gm sec}^2, \tag{4.4}$$

$$M = 5.976 * 10^{27} \text{ gm}, \tag{4.5}$$

and

$$r_E = 6379.5 \text{ km}.$$

Eqns. 4.1, 4.2, and 4.3 can be used to express h in terms of τ_s :

[1] τ_E is 23 hrs, 56 min, and 4 sec or 86164 sec.

Table 4.1: Orbital Parameters for Several Circular Orbits

Altitude	Period	k:n	v_s	τ_d
35,784 km	86164 sec	1:1	11069 km/hr	239 msec
20,182 km	43082 sec	2:1	13946 km/hr	135 msec
10,353 km	21541 sec	4:1	17571 km/hr	69 msec
5,143 km	12309 sec	7:1	21174 km/hr	34 msec
1,247 km	6628 sec	13:1	26027 km/hr	8 msec
879 km	6154 sec	14:1	26678 km/hr	6 msec

$$h = \left(\frac{\tau_s^{\frac{2}{3}} (GM)^{\frac{1}{3}}}{(2\pi)^{\frac{2}{3}}} \right) - r_E \tag{4.6}$$

where we allow τ_s to take on only the following values: $\tau_s = \frac{n}{k} \tau_E$ where n and k are integers.

To explore the characteristics of non-geostationary orbits at a variety of altitudes, $n = 1$ and k values of 2, 4, 7, 13, and 14 are selected to produce satellite altitudes varying from 20,182 km to 879 km. Satellites can be referred to by the number of times the satellite orbits the Earth in one sidereal day, i.e. their k:n index. Satellite heights, periods, and velocities for the k values listed above are given in Table 4.1. Once the satellite height is chosen, then the distance between a point on Earth, viewing the satellite at an elevation angle of ϕ_l, and the satellite can be determined. This distance is known as the slant path z; it is shown in Fig. 4.1. The slant path can be calculated according to:

$$z = \sqrt{(r_E \sin \phi_l)^2 + 2 r_E h + h^2} - r_E \sin \phi_l. \tag{4.7}$$

The roundtrip signal delay can be computed from:

$$\tau_d = \frac{d}{c} \tag{4.8}$$

where c is the speed of light, $3 \cdot 10^5$ km/sec and d is the distance from transmitting user to satellite to the receiving station. This distance can vary from $2h$, when the satellite is directly over the transmitter and receiver, to $2z$, when both transmitter and receiver see the satellite at its maximum slant path. τ_d is shown in Table 4.1 for $d = 2h$.

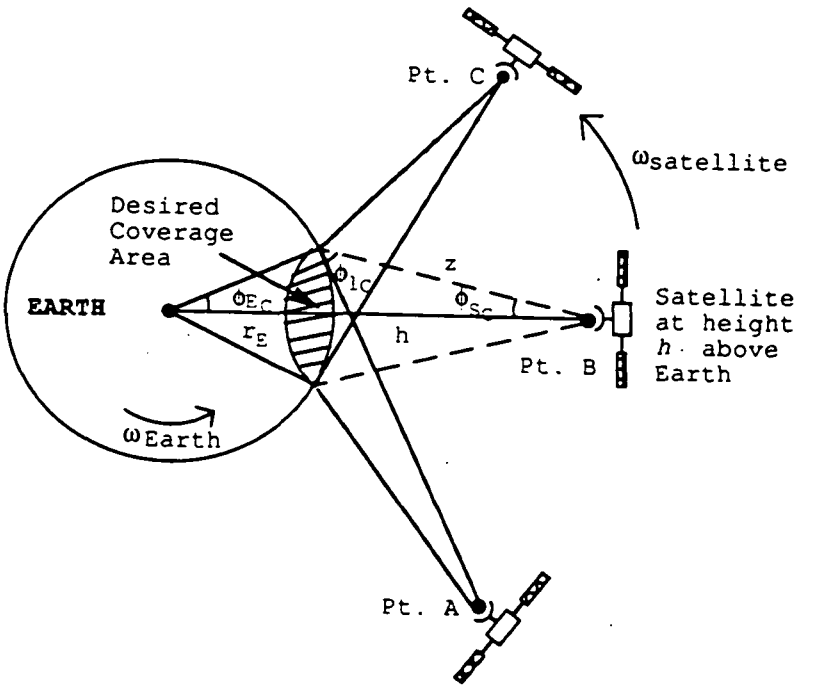

Figure 4.1: Satellite and earth station geometry for satellites in circular orbits.

4.2.2 Elliptical Orbit Characteristics

The ACE orbit is an elliptical equatorial orbit with five revolutions per day. It is sun-synchronous and highly eccentric (eccentricity = 0.49). The satellite is at the same point in its arc at the same time each day. The selected orbit has its apogee and perigee at altitudes of 15,100 km and 1,030 km, respectively. The Molniya orbit is a highly elliptical orbit at an inclination of 63.4°. With a perigee of 426 km and an apogee of 37,771 km, the satellite spends most of its orbital period ascending to its apogee. The maximum coverage period for CONUS is attained when its apogee is placed over the center of CONUS.

The following equations relate the period of the satellite's elliptical orbit around the Earth and the satellite velocity to the orbit's geometry:

$$\tau_s = \frac{2\pi a^{\frac{3}{2}}}{\sqrt{G * M}} \tag{4.9}$$

where G and M are defined in eqns. 4.4 and 4.5, respectively, and a is the major semiaxis of the ellipse. a is equal to one half of the sum of apogee and perigee;

$$v_s = \left[2G * M \left(\frac{1}{r_E + h} - \frac{1}{2a}\right)\right]^{\frac{1}{2}} \tag{4.10}$$

where r_E and h are defined above. Table 4.2 gives the period, velocity and roundtrip signal delay when satellites in the ACE and Molniya orbits are at their apogee.

Table 4.2: Characteristics of the ACE and Molniya Orbits

Orbit	Altitude	Period	v_s	τ_d
ACE	15,100 km	4.8 hrs	11152 km/hr	252 msec
Molniya	39,771 km	12 hrs	5590 km/hr	100 msec

4.3 Link Characteristics

4.3.1 Doppler Shift

The Doppler shift of the signal is proportional to the velocity vector of the satellite relative to the Earth's motion. Specifically it is proportional to the component of this relative velocity vector which lies in the direction of the receiving earth station, $v_{rel_{in}}$. The Doppler shift, $f_{Doppler}$, can be written as:

$$f_{Doppler} = \pm \left(\frac{v_{rel_{in}}}{c} f_c \right) \tag{4.11}$$

where c is the speed of light and f_c is the signal frequency. To determine the Doppler shift, $v_{rel_{in}}$ must be found from the angular velocity of the satellite, the inclination angle of the satellite's orbit with respect to the Equator, and the angle between the satellite and the user terminal on Earth.

When ϕ_l and Ψ are both zero, the Doppler shift can be calculated from the familiar expression:

$$f_{Doppler} = (\omega_E - \omega_s)\, r_E \frac{f_c}{c}.$$

For orbits with $\Psi = 0$ the maximum Doppler shift occurs when $\phi_l = 0$. These Doppler shifts are given in Table 4.3 at the PASS system uplink frequency of 30 GHz and at the downlink frequency of 20 GHz for a geostationary satellite and for the five circular orbits under consideration.

In order to determine the Doppler shift for satellites in circular orbits with non-zero inclination angles and for satellites in elliptical orbits, the relative velocity between the receiving earth station and the satellite must be found in terms of the satellite velocity vector, the velocity vector of that point on Earth, and the vector between the satellite and the receiving earth station. The following gives a synopsis of the necessary analysis to derive $v_{rel_{in}}$.

The velocities and locations of a satellite and an earth station can each be decomposed in terms of their three orthogonal components in the geocentric equatorial coordinate system. The origin of this coordinate system is the center of the Earth, its x-axis points towards the

143

Table 4.3: Maximum Doppler Shifts for Circular Orbits with $\Psi = 0$ and $\Psi = 45°$.

Altitude	$\Psi = 0$		$\Psi = 45°$	
	30 GHz	20 GHz	30 GHz	20 GHz
35,784 km (GEO)	0.0 KHz	0.0 KHz	0.0 KHz	0.0 KHz
20,182 km	46.5 KHz	31.0 KHz	131 KHz	87 KHz
10,353 km	139.6 KHz	93.0 KHz	216 KHz	144 KHz
5,143 km	279.1 KHz	186.1 KHz	344 KHz	229 KHz
1,247 km	558.2 KHz	372.2 KHz	493 KHz	329 KHz
879 km	604.8 KHz	403.2 KHz	510 KHz	340 KHz

Sun and the z-axis coincides with the Earth's axis of rotation. The velocity vector, $\vec{v_E}$, of an earth station at location $\vec{P_E}$ is:

$$\begin{aligned} \vec{v_E} &= r_E\ [\sin(\omega t) + \cos(\omega t + \beta)]\ \cos\theta_l\ \hat{i} \\ &\quad + r_E\ [\cos(\omega t) - \cos(\omega t + \beta)]\ \cos\theta_l\ \hat{j} \\ &\quad + 0\ \hat{k} \end{aligned} \tag{4.12}$$

where ωt denotes the angular distance moved in period t (ω being the angular velocity of the Earth), β is the angle from the x-axis at $t = 0$, and θ_l is the latitude of the earth station. The position ($\vec{P_s}$) and the velocity ($\vec{v_s}$) of a satellite can be written similarly. They are omitted from the text due to length of their expressions but can be found in [8].

The relative velocity between the earth station and the earth station and the satellite can be written as:

$$\vec{v_{rel}} = \vec{v_s} - \vec{v_E}. \tag{4.13}$$

The vector between the earth station and the satellite is known as P_{ES}. The component of $\vec{v_{rel}}$ along the unit vector in the direction of $\vec{P_{ES}}$ sets the Doppler velocity, i.e.

$$v_{rel_{in}} = \frac{\vec{v_s} \cdot \vec{P_{ES}}}{|\vec{P_{ES}}|} - \frac{\vec{v_E} \cdot \vec{P_{ES}}}{|\vec{P_{ES}}|}. \tag{4.14}$$

The Doppler shift of the carrier frequency, f_c, can be obtained by finding the velocity and position vectors of the satellite and the earth station. The Doppler shift is zero when

both $\vec{v_s}$ and $\vec{v_E}$ are perpendicular to $\vec{P_{ES}}$. For both the ACE and the Molniya orbits, this occurs when the satellite is at its apogee for those earth stations at the same longitude as the satellite. Alternatively, the Doppler shift will be maximized for earth stations directly under the satellite as the satellite ascending to its apogee or descending from it. The maximum Doppler shift at 30 GHz is approximately 300 KHz and 600 KHz for satellites in the ACE and Molniya orbits, respectively. Maximum Doppler shifts for satellites in circular orbits with $\Psi = 45°$ are given in Table 4.3.

These large Doppler shifts require a compensation mechanism or a modulation scheme capable of tolerating wide deviations. Doppler compensation techniques would be straightforward if all the communications were done by a central station. The central station would use a set algorithm to change the pilot frequencies going to the user terminals and the downlink frequencies to the supplier stations. However in PASS, where users for a given supplier can be located in different beams, frequency tracking and compensation would put a big burden on the Network Management Center (NMC). The NMC would have to keep track of the position (beam number) of all the users and change the inbound and outbound frequencies accordingly. This would require large guardbands and a real time frequency caiculation for all of the active users and suppliers of the system. In Appendix A, it is shown that a real time frequency calculation for all of the active users and suppliers of the system is required. In any case, even after the frequency corrections, depending on the position of a user within a beam pattern, there will be a small residual Doppler that will need to be corrected at the receiver.

The method of using a frequency insensitive modulation scheme has been studied by Simon [9]. Although a less sensitive modulation technique has been devised, larger link margins will be necessary as the frequency offset increases.

4.3.2 Propagation Loss

The use of NGO satellites at lower than GEO heights will reduce the propagation loss, L_P, suffered by the uplink and downlink signals. L_P can be calculated according to:

$$L_P = \left(\frac{4\,\pi\,d}{\lambda_c}\right)^2 \tag{4.15}$$

where λ_c is the wavelength corresponding to the carrier frequency f_c and d can vary from h, the height of the satellite, to z, the slant path to the satellite. L_P is listed in Table 4.4 along with the change in propagation loss, ΔL_P, as the satellite orbit altitude is decreased from GEO to 879 km for satellites directly located over the user terminal ($d = h$). As the satellite moves with respect to its coverage area, the range and elevation angle from the user terminals and supplier stations to the satellite varies. The ensuing variation in propagation loss is discussed in Section 4.3.5.

The use of elliptical orbits leads to a changing path range between the satellite and the users. Pt. A in Fig. 4.2 depicts the moment at which all of CONUS is visible from the elliptically orbiting satellite. At this point the range from the earth station (at the

Table 4.4: Propagation Loss for Circular and Elliptical Orbits

Altitude d	Propagation Loss 30 GHz	ΔL_P†
Circular Orbits:		
35,784 km (GEO)	213.1 dB	0 dB
20,182 km	208.1 dB	5.0 dB
10,353 km	202.3 dB	10.8 dB
5,143 km	196.2 dB	16.8 dB
1,247 km	183.9 dB	29.2 dB
879 km	180.9 dB	32.2 dB
Elliptical Orbits:		
ACE		
15,100 km *	205.5 dB	7.6 dB
Turn-on/Turn-off ‡	192.5 dB	20.6 dB
Molniya		
39,771 km *	214 dB	-0.9 dB
Turn-on/Turn-off ‡	186 dB	27.1 dB

† $\Delta L_P = L_{P_{GEO}}(h) - L_{P_{NGO}}(h)$ where h is the distance from the earth station to the satellite when the satellite is overhead.

* 20° elevation, at apogee, for earth stations in the center of coverage.

‡ 20° elevation, at turn-on, for earth stations at the farthest edge of coverage.

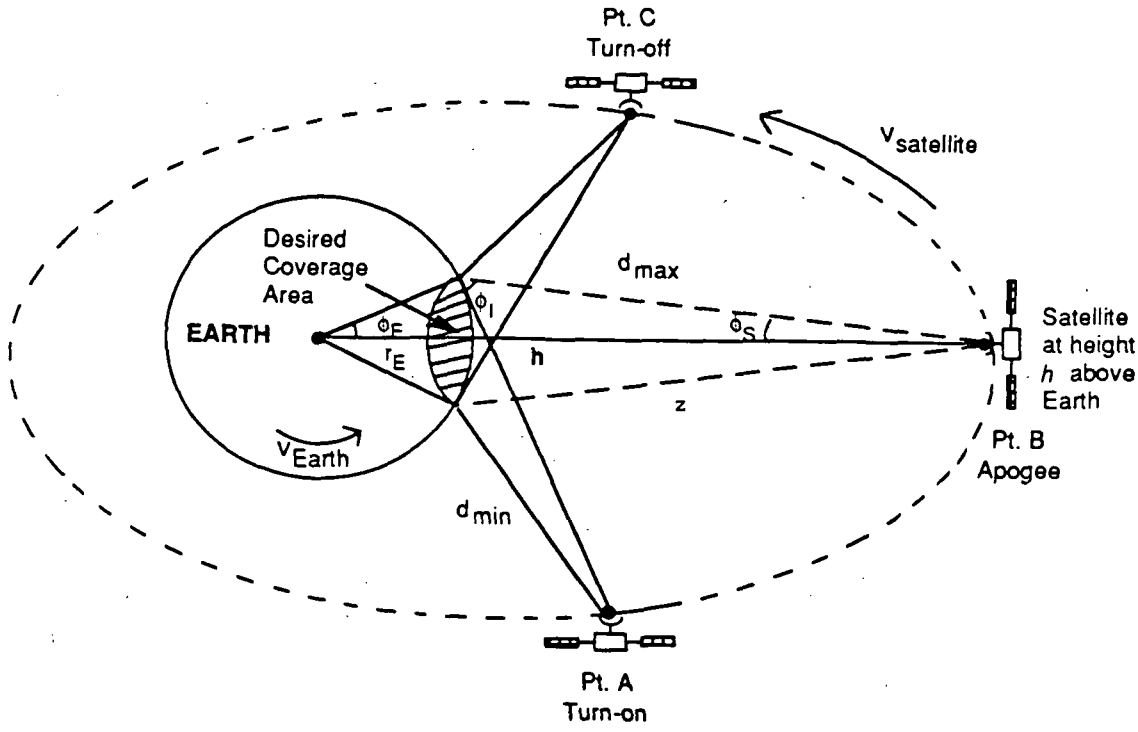

Figure 4.2: Satellite and earth station geometry for satellites in elliptical orbits.

closest edge of coverage) to the satellite, d_{min}, sets the minimum propagation loss. Pt. B depicts the satellite at its apogee; at this point the range from the earth station (at the farthest edge of coverage) to the satellite, d_{max}, sets the maximum propagation loss. Pt. C depicts the satellite at the last moment at which all of CONUS is visible. The propagation loss along with its variation compared to GEO is shown in Table 4.4. For the ACE orbit, the improvement in the path loss ranges from 7.6 dB to 20.6 dB. For the Molniya orbit, propagation loss increases relative to GEO by 0.9 dB at orbit apogee.

4.3.3 CONUS Coverage Antenna

The preliminary PASS system design utilizes two CONUS beam antennas on the satellite for all communication between the supplier and the satellite. The size of the receive antenna is 0.1m and that of the transmit antenna is 0.15m; both have a gain of 26.9 dBi. In order to determine the effect of operating with NGO satellites, the gain of a CONUS covering antenna is calculated for satellites at various heights h. The satellite is assumed to have a tracking antenna which is trained on CONUS whenever the latter is visible. This scheme is illustrated in Fig. 4.1. As the satellite moves from Pt. A through Pt. B to Pt. C, the antenna tracks CONUS. Antenna gain is calculated when the satellite is over the middle of

147

the U.S., i.e. Pt. B in Fig. 4.1.[2]

Antenna gain can be written as:

$$G_{ant} = \rho \frac{4\pi h^2}{2\pi h^2(1-\cos\phi_S)}, \tag{4.16}$$

where the numerator represents the surface area of a sphere of radius h and the denominator is the surface area into which the radiated power is directed and ρ is the aperture efficiency. The satellite then illuminates the area shown by the hatched lines in Fig. 4.1. For CONUS coverage, ϕ_S, ϕ_l, and ϕ_E in Fig. 4.1 are denoted by ϕ_{S_C}, ϕ_{l_C}, and ϕ_{E_C}, respectively. ϕ_{l_C} is then the minimum elevation angle required for CONUS coverage.

Using the relation $\frac{\sin\phi_s}{r_E} = \frac{\sin(90+\phi_l)}{r_E+h}$, ϕ_{S_C} can be expressed in terms of the minimum elevation angle on Earth to the satellite from:

$$\phi_{S_C} = 90^\circ - \cos^{-1}\left(\frac{r_E\cos\phi_{l_C}}{r_E+h}\right). \tag{4.17}$$

To find the minimum elevation angle necessary to see a satellite of height h from CONUS, six points on the perimeter of CONUS are defined. They are listed in Table 4.5. The elevation angle, ϕ_l, is calculated for each location by determining the angle between that location and the satellite. This angle, θ_{ES}, is shown in Fig. B.1 in Appendix B where the calculation of ϕ_l and θ_{ES} for any point and a satellite at any position is given.

Here we calculate the gain of a CONUS antenna specifically for the case of a satellite in an inclined orbit such that it passes over the center of the US, i.e. its latitude is 40° N and its longitude is 95° W. Satellites in the inclined orbits under consideration will have optimal CONUS coverage at this point. Satellites in equatorial orbits will, of course, never pass over a latitude of 40° N but will have optimal coverage when their longitude is 95° W; the gain of their CONUS antennas will at that point be slighly greater than that of their inclined orbit counterpart as the antenna beamwidth will be slightly narrower.

Once the elevation angles are calculated for each of the locations in Table 4.5, then ϕ_{l_C}, or the minimum value of ϕ_l, can be found. ϕ_{S_C} can then be calculated from Eq. 4.17 and the gain of a CONUS antenna can be found from Eq. 4.16.

ϕ_{l_C}, ϕ_{S_C} and CONUS antenna gain G_C (for $\rho = 0.5$) are given in Table 4.6; ϕ_{E_C} is not given as it does not vary with the satellite's height. The minimum CONUS elevation angle, ϕ_{l_C}, for a satellite at 35,784 km (equivalent to the height of a geostationary satellite) can be seen from Table 4.6 to be 64°.[3]

In Table 4.6 the 0-3 dB power beamwidth of the CONUS antenna, ϕ_{S_C}, increases from 3.8° to 60.7° and the gain of the CONUS antenna falls from 26.6 dB to 2.9 dB as the satellite

[2]Antenna gain for an equatorial orbit could be slightly larger as the beamwidth required to see CONUS from the Equator is less than that required when the satellite is directly over the center of CONUS.

[3]This angle should not be confused with the much lower 25° minimum earth station (E/S) elevation angle required to see a geostationary satellite located in the equatorial arc. A 25° or higher elevation angle is needed for the E/S within CONUS to see a satellite at 0° latitude, 95° longitude, and a height of 35,784 km.

Table 4.5: Cities Considered to Bound CONUS

City	Latitude	Longitude
Bay of Fundy, Maine	47.2°	-68.0°
Key Largo, Florida	25.0°	-80.5°
Brownsville, Texas	26.0°	-97.0°
San Diego, California	32.5°	-117.0°
Seattle, Washington	49.0°	-123.3°
Bottineau, North Dakota	49.0°	-100.0°
Center of USA	40.0°	-95.0°

Table 4.6: Satellite CONUS Antenna Characteristics

Altitude	CONUS Satellite Antenna			
	ϕ_{l_C}	ϕ_{s_C}	$G_{C\|_{\rho=0.5}}$	ΔG_C†
Circular Orbits:				
35,784 km	64°	3.8°	26.6 dB	0 dB
20,182 km	61°	6.7°	21.7 dB	-4.9 dB
10,353 km	55°	12.6°	16.2 dB	-10.4 dB
5,143 km	45°	23.0°	11.0 dB	-15.6 dB
1,247 km	13°	54.6°	3.8 dB	-22.8 dB
879 km	7°	60.7°	2.9 dB	-23.7 dB
Elliptical Orbits:				
15,100 km (ACE)	57°	9.3°	19.1 dB	-7.5 dB
39,771 km (Molniya)	65°	3.4°	27.5 dB	+0.6 dB

†$\Delta G_C = G_{C_{NGO}} - G_{C_{GEO}}$.

altitude h is decreased from 35,784 km to 879 km for the circular orbits. The 0-3 dB power beamwidth of the CONUS antenna increases from 3.8° for GEO to 6.7° for the ACE orbit and decreases slightly to 3.6° for the Molniya orbit. The change in CONUS antenna gain relative to a geostationary satellite, ΔG_C, is given in the table.

The CONUS antenna size reduction with decreasing gain can be found from the commonly known expression relating antenna gain to antenna area, A ($G_{ant} = \rho\, 4\pi/\lambda^2\, A$). The antenna diameter, d_{ant}, can be written as:

$$d_{ant} = \sqrt{\frac{G_{ant}}{\rho}} \cdot \frac{\lambda_c}{\pi}. \tag{4.18}$$

As the satellite altitude drops from 35,784 km (GEO orbit) to 20,182 km, the antenna diameter decreases 43% from 14.4cm to 8.2cm at 20 GHz. The reduction in antenna diameter relative to that required for GEO orbit at 20 GHz is 70%, 83%, 92.8%, and 93.5%, for NGO satellite altitudes of 10,353km (d_{ant} = 4.35cm), 5,143km (d_{ant} = 2.3cm), 1,247km (d_{ant} = 1.04cm), and 879km (d_{ant} = 0.94cm), respectively. When the ACE orbit is used the required CONUS antenna diameter is 6.1cm (58% reduction); when the Molniya orbit is utilized the required antenna diameter is slightly larger than that necessary for GEO, 16.0cm vs. 14.4cm (size increase of 11%).

4.3.4 Multibeam Antenna Gain

As currently envisaged, the PASS satellite uses two multibeam antennas (MBAs) for communication between the user terminals and the satellite. Each MBA has a beamwidth of 0.35° and uses an 142 beam feed network to cover CONUS. In the preliminary PASS design, the gain of both the transmit and receive MBAs is 52.5 dBi and their efficiencies are both taken to be 0.45, corresponding to a reflector diameter of 2m at 30GHz and 3m at 20GHz. As the satellite orbit height decreases, the spot beams must continue to cover the same area in CONUS. Therefore the required MBA beamwidth will increase from 0.35° and the gain of the MBA will decrease with decreasing satellite altitude.

The impact on antenna beamwidth and gain can be found by equating the GEO and NGO satellite multibeam antenna coverage areas, A_{cov}, given by the denominator of Eq. 4.16:

$$A_{covGEO} = 2\pi h_{GEO}^2\,(1 - \cos\phi_{S_{MBA_{GEO}}}) \tag{4.19}$$

and

$$A_{covNGO} = 2\pi h_{NGO}^2\,(1 - \cos\phi_{S_{MBA_{NGO}}}) \tag{4.20}$$

where $\phi_{S_{MBA_{GEO}}}$ is the half-angle subtended from the GEO satellite and $\phi_{S_{MBA_{NGO}}}$ is that subtended from the NGO satellite (refer to Fig. 4.1 for illustration). $\phi_{S_{MBA_{NGO}}}$ can be then found from Eq. 4.19 and 4.20 to be:

$$\phi_{S_{MBA_{NGO}}} = \cos^{-1}\left(1 - \left(\frac{h_{GEO}}{h_{NGO}}\right)^2 (1 - \cos\phi_{S_{MBA_{GEO}}})\right).$$

Table 4.7: Satellite Multibeam Antenna Characteristics

Altitude	G_{MBA} ($\rho = 0.45$)	ΔG_{MBA}†	d_{ant} (at 20GHz)	Size Change
For circular orbits:				
35,784 km	52.5 dBi	0 dB	3.0 m	0
20,182 km	47.5 dBi	-5.0 dB	1.7 m	43.6%
10,353 km	41.7 dBi	-10.8 dB	86.8 cm	71.1%
5,143 km	35.6 dBi	-16.8 dB	43.1 cm	85.6%
1,247 km	23.3 dBi	-29.2 dB	10.5 cm	96.5%
879 km	20.3 dBi	-32.2 dB	7.4 cm	97.5%
For elliptical orbits:				
15,100 km	45.0 dBi	-7.5 dB	1.3 m	57.7%
39,771 km	53.4 dBi	+0.9 dB	3.3 m	-11.1%

† $\Delta G_{MBA} = G_{MBA_{NGO}} - G_{MBA_{GEO}}$ (in dB).

The gain of the MBA on the NGO satellite can be found from Eq. 4.16, 4.19, 4.20 assuming that the aperture efficiencies of the NGO antenna and the GEO antenna are equivalent. Written in terms of the ratio of satellite heights, $G_{MBA_{NGO}}$ becomes:

$$G_{MBA_{NGO}} = \rho \frac{4\pi h_{NGO}^2}{A_{cov_{NGO}}} = \left(\frac{h_{NGO}}{h_{GEO}}\right)^2 G_{MBA_{GEO}}; \tag{4.21}$$

written in terms of the subtended coverage angles, $G_{MBA_{NGO}}$ becomes:

$$G_{MBA_{NGO}} = \left(\frac{1 - \cos\phi_{S_{GEO}}}{1 - \cos\phi_{S_{NGO}}}\right) G_{MBA_{GEO}}. \tag{4.22}$$

Antenna diameter for these MBAs can be calculated from Eq. 4.18. The ensuing size reduction when compared to GEO operation can then be found. Table 4.7 gives the gain of the MBA antenna and the gain penalty paid for the use of NGO satellites. The size of the MBA at 20 GHz and the size reduction benefit obtained by their use are also tabulated.

4.3.5 Impact on Link Equations

The PASS system is asymmetrical: the user terminal equipment, designed to be handheld and/or portable, is less powerful than the supplier station, a fixed E/S with a 4m antenna. In the communication link from the supplier to the user terminal, the downlink carrier-to-noise ratio sets the overall C/N. In the link from the user terminal to the supplier, the uplink C/N sets the overall C/N. Thus, in both cases the link between the user terminal and the satellite determines the overall quality of the link. In the subsequent discussion C/N_{up} refers to the uplink C/N from the user terminal to the satellite, and C/N_{down} refers to the downlink C/N

from the satellite to the user terminal. Both links utilize the satellite's MBAs. In addition $\Delta C/N_{up}$ refers to the change in C/N_{up} and $\Delta C/N_{down}$ refers to the change in C/N_{down} when the NGO satellite is used in place of the GEO satellite.

Degradation in either C/N_{up} or C/N_{down} will require more satellite power and lower satellite receiving temperature.[4] Use of better user equipment (higher gain antenna, higher transmit power, or lower receive temperature) is undesirable as it would increase the terminal's size and power consumption.

Eq. 4.23 gives the relationship between the carrier-to-noise ratio received at the satellite, $\frac{C}{No_{up}}$, the uplink propagation loss, and the satellite's receive MBA gain, G_{MBA_r}:

$$\frac{C}{No_{up}} = EIRP_E - L_{P_{up}} + G_{MBA_r} - T_{S_r} - L_{V_{up}} - k \quad \text{dB-Hz} \tag{4.23}$$

where $EIRP_E$ is the EIRP of the transmitting E/S, T_{S_r} is the satellite receiver noise temperature, k is Boltzmann's constant (-228.6 dBW/K-Hz), and, $L_{V_{up}}$ is the sum of several losses such as antenna pointing losses, clear sky atmospheric loss, and polarization losses. Eq. 4.24 gives the relationship between the carrier-to-noise ratio received at the E/S, $\frac{C}{No_{down}}$, the downlink propagation loss, $L_{P_{down}}$, and the satellite's transmit MBA gain, G_{MBA_t}:

$$\frac{C}{No_{down}} = P_{T_S} + G_{MBA_t} - L_{P_{down}} + \frac{G}{T}_E - L_{V_{down}} - k \ \text{dB-Hz} \tag{4.24}$$

where P_{T_S} is the satellite's transmit power and $\frac{G}{T}_E$ is the G/T of the receiving E/S and $L_{V_{down}}$ is the sum of miscellaneous downlink losses. These equations show that reductions in $L_{P_{up}}$ or $L_{P_{down}}$ from the use of NGO satellites rather than geostationary satellites (GEO) translate into improvements in the $\frac{C}{N}$ achievable while reductions in satellite antenna gain translate into degradation of $\frac{C}{N}$. The change in uplink C/N as a consequence of NGO satellites can be written as:

$$\Delta\frac{C}{N}_{up} = \left(G_{MBA_{r_{NGO}}} - G_{MBA_{r_{GEO}}}\right) + \left(L_{P_{up_{GEO}}} - L_{P_{up_{NGO}}}\right). \tag{4.25}$$

The change in downlink C/N can be written as:

$$\Delta\frac{C}{N}_{down} = \left(G_{MBA_{t_{NGO}}} - G_{MBA_{t_{GEO}}}\right) + \left(L_{P_{down_{GEO}}} - L_{P_{down_{NGO}}}\right). \tag{4.26}$$

To arrive at a worst case estimate of $\Delta C/N_{up}$ and $\Delta C/N_{down}$ when the NGO satellite is used, the improvement in propagation loss, ΔL_{P_2}, will be evaluated when both satellites are at their maximum slant path from the E/S given the minimum E/S elevation angle allowable. ΔL_{P_2} can be found from Eq. 4.15 where d is the slant path distance z. z is calculated from Eq. 4.7 for a particular ϕ_l. ΔL_{P_2} is then found to be:

$$\Delta L_{P_2} = \left(\frac{z_{GEO}}{z_{NGO}}\right)^2.$$

[4]Satellite antenna gain can not be changed as it is set by the antenna coverage area.

ΔL_{P_2} is, of course, frequency independent.

ΔL_{P_2} is in general less than ΔL_P listed in Table 4.4 as the latter tabulates the propagation loss improvement when both satellites are directly overhead. When the NGO satellite is directly overhead, ΔL_{P_2} is 0.76 dB higher than ΔL_P as the GEO satellite is still considered to be at its maximum slant path.

The change in MBA gain when the NGO satellite is used, ΔG_{MBA}, can be found from Eq. 4.21 or 4.22. It is equal to the ratio of the GEO to NGO satellite height when the satellite is overhead:

$$\Delta G_{MBA} = \frac{G_{MBA_{NGO}}}{G_{MBA_{GEO}}} = \left(\frac{h_{NGO}}{h_{GEO}}\right)^2 .$$

ΔG_{MBA} is given in Table 4.7. As both the change in propagation loss and in-antenna gain are independent of frequency, Eq. 4.25 and 4.26 can be written as:

$$\Delta\frac{C}{N} = \left(\frac{h_{NGO}}{h_{GEO}}\right)^2 \left(\frac{z_{GEO}}{z_{NGO}}\right)^2 . \tag{4.27}$$

$\Delta C/N$ is the change in link margin arising from the use of NGO satellites. It can be calculated from Eq. 4.27 taking z_{geo} to be the slant path for earth stations with elevation angles of 25° (z_{geo} = 39070 km). $\Delta C/N$ can also be found from:

$$\Delta C/N = \Delta G_{MBA} + \Delta L_{P_2}$$

where ΔG_{MBA} is given in Table 4.7 and ΔL_{P_2} is given in Table 4.8. $\Delta C/N$ is listed in Table 4.8 as z_{NGO} is varied from its maximum value (when the E/S elevation angle is at 10°) to its minimum value (when the satellite is directly overhead, i.e. $\phi_l = 90°$). $\Delta C/N$ will be negative, representing a degradation in C/N, whenever $z_{NGO} > h_{NGO}\,(\frac{z_{GEO}}{h_{GEO}})$. [5] $\Delta C/N$ will be positive, representing an improvement in C/N, when the satellite is directly over the E/S. $\Delta C/N$ will then be $(\frac{z_{GEO}}{h_{GEO}})^2$ or 0.76 dB. This is the maximum improvement in link margin that can be obtained from an NGO satellite assuming that both NGO and GEO satellites must illuminate the same region on Earth, that the antenna efficiencies, ρ, are equal, and, that identical space and ground segment components are used with both systems.

Table 4.8 also lists the slant path z and the propagation loss improvement ΔL_{P_2} as a function of E/S elevation angle ϕ_l. As the satellite moves accross the sky, the elevation angle required at the E/S varies from the minimum ϕ_l at which the system is operational, for example 10°, to 90° and back to 10°. For an NGO satellite at 20,182 km, $\Delta C/N$ varies from -0.99 dB to +0.76 dB and back to -0.99 dB. This variation in $\Delta C/N$ reflects the path loss difference as the satellite moves into and out-of-view from the user terminals and the supplier station. The variation will cause signal level changes that need to be compensated. In the PASS design where it is envisioned that a variable rate modem will be used to compensate for fades due to rain and snow, a new variable will have to be added to the algorithm. This variable, which is a function of time, will provide the means of distinguishing between a true fade and a change in the path loss.

[5] z_{GEO} is the slant path at $\phi_l = 25°$ or 39,070 km and h_{GEO} is 35,784 km. $\frac{z_{GEO}}{h_{GEO}}$ is then 1.09.

Table 4.8: Link Characteristics for Several Circular Orbits

ϕ_l	Slant Path z	Prop. Loss ΔL_{P_2}†	Link Margin $\Delta C/N$
Altitude = 35,784 km (GEO); MBA Gain = 52.5 dBi			
25°	39070 km	0 dB	
Altitude = 20,182 km; MBA Gain = 47.5 dBi			
10°	24700 km	3.98 dB	-0.99 dB
20°	23694 km	4.34 dB	-0.63 dB
30°	22791 km	4.68 dB	-0.29 dB
90°	20182 km	5.74 dB	+0.76 dB
Altitude = 10,353 km; MBA Gain = 41.7 dBi			
10°	14401 km	8.67 dB	-2.10 dB
20°	13440 km	9.27 dB	-1.50 dB
30°	12605 km	9.83 dB	-0.94 dB
90°	10353 km	11.54 dB	+0.76 dB
Altitude = 5,143 km; MBA Gain = 35.6 dBi			
10°	8551 km	13.20 dB	-3.65 dB
20°	7658 km	14.15 dB	-2.70 dB
30°	6922 km	15.03 dB	-1.82 dB
90°	5143 km	17.61 dB	+0.76 dB
Altitude = 1,247 km; MBA Gain = 23.3 dBi			
10°	3215 km	21.69 dB	-7.47 dB
20°	2532 km	23.77 dB	-5.39 dB
30°	2067 km	25.53 dB	-3.63 dB
90°	1247 km	29.92 dB	+0.76 dB
Altitude = 879 km; MBA Gain = 20.3 dBi			
10°	2528 km	23.78 dB	-8.41 dB
20°	1911 km	26.21 dB	-5.98 dB
30°	1518 km	28.21 dB	-3.98 dB
90°	879 km	32.96 dB	+0.76 dB

†$\Delta L_{P_2} = L_P(z)_{GEO} - L_P(z)_{NGO}$ where z is the maximum slant path for a given ϕ_l.

4.4 Number of Satellites Required for Continuous CONUS Coverage

4.4.1 Circular Orbit Results

In order to compute the number of satellites necessary to provide 24 hr coverage of a particular region, the start and stop times at which the satellite is visible from all points within that coverage area must be calculated. This coverage time, T_{cc}, depends on the minimum elevation angle, $\phi_{l_{min}}$, that the earth stations in the coverage area are permitted to operate with. T_{cc} is also a function of the initial angular position, θ_S, of the satellite in its orbit. Given a particular orbit, coverage area and $\phi_{l_{min}}$, T_{cc} and its corresponding start and stop times are calculated for satellite initial angular positions ranging from 0° to 360°. Then a reasonable set of satellite locations can be selected to maximize CONUS coverage. Continuous CONUS coverage generally requires the use of satellites in several orbit planes, all identically inclined from the equator. Satellites in each of these orbit planes are then chosen so that the start and stop times of each satellite overlap to provide 24 hr coverage of the coverage area in question. The number of satellites required for continuous area coverage is then computed from the number of satellites used in each of the identically inclined orbits. These steps are detailed below.

Calculation of the start and stop times for CONUS coverage for satellites in circular orbits at any inclination from the equator is performed with the aid of the program *eleangle.f*. In order to minimize computational time, only orbits whose period have an integer relationship to the Earth rotational period are considered, i.e. $T_{satellite} = n/k\ T_{earth}$ where n and k are integers. For the orbits described in Table 4.1, $n = 1$ and k is 2, 4, 7, 13 and 14. Satellites in these orbits will appear over the same spot on the Earth each day.

The program calculates the trajectory of the satellite as a function of time. Points on Earth are assumed to move relative to a Sun fixed coordinate system. This coordinate system has as its origin the center of the Earth; it is denoted in rectangular coordinates as x, y, and z where $z = 0$ specifies the equatorial plane of the Earth. Points on the surface of the Earth are specified by their longitude and latitude in the x, y, z coordinate system. As the surface of the Earth turns about this coordinate system, the longitudes of these points vary 360° from their Earth-prescribed values but their latitudes remain constant. Seven points within CONUS are chosen for the calculation: six cities on the perimeter of CONUS and one located roughly in the middle of the U.S.. The longitude and latitude of the points are shown in Table 4.5. The motion of any of these locations is described in Cartesian coordinates as:

$$\begin{aligned} x_{loc}(t) &= r_E \sin\phi \cos(\omega_E t + \theta), \\ y_{loc}(t) &= r_E \sin\phi \sin(\omega_E t + \theta), \\ z_{loc}(t) &= r_E \cos\phi, \end{aligned} \tag{4.28}$$

where the latitude and longitude of the terrestrial location are related to ϕ (ϕ = 90° - latitude) and θ (θ = longitude), respectively.

A second coordinate system, x', y', and z', is used to describe the motion of the satellite. Its x' - z' plane is inclined from the x' - z' plane by Ψ, the inclination angle of the satellite's orbit relative to the equatorial plane. The center of this coordinate system is also the center of the Earth; hence the centers of the two coordinate systems are co-located. In the x', y', and z' system, the satellite traces a circle whose radius is $h + r_E$:

$$\begin{aligned} x'_{sat}(t) &= (h + r_E)\ \cos(\omega_{sat} t + \theta_S), \\ y'_{sat}(t) &= (h + r_E)\ \sin(\omega_{sat} t + \theta_S), \\ z'_{sat}(t) &= 0, \end{aligned}$$

where h is the height of the satellite above the Earth, ω_{sat} is the angular velocity of the satellite and θ_S is the starting position of the satellite at $t = 0$. The satellite motion can be translated to the x, y, and z coordinate system according to:

$$\begin{aligned} x_{sat}(t) &= \cos\Psi\ x'_{sat}(t) - \sin\Psi\ z'_{sat}(t), \\ y_{sat}(t) &= y'_{sat}(t), \\ z_{sat}(t) &= -\sin\Psi\ x'_{sat}(t) + \cos\Psi\ z'_{sat}(t), \end{aligned}$$

or,

$$\begin{aligned} x_{sat}(t) &= (h + r_E)\ \cos\Psi\ \cos(\omega_{sat} t + \theta_S), \\ y_{sat}(t) &= (h + r_E)\ \sin(\omega_{sat} t + \theta_S), \\ z_{sat}(t) &= -(h + r_E)\ \sin\Psi\ \cos(\omega_{sat} t + \theta_S). \end{aligned} \tag{4.29}$$

The program finds the elevation angle, ϕ_l, from the seven points listed in Table 4.5 to the satellite for one satellite period according to Eq. B.4 in Appendix B. At the end of this period, the satellite's position relative to the points on CONUS is identical to that at the beginning of the calculation because of the integer relationship between Earth rotation period and satellite period.

The start and stop of each city's coverage period during one Earth day is determined by the times at which $\phi_l \geq \phi_{l_{min}}$. The start time for a CONUS coverage period is found by determining the time at which all seven points have elevation angles just greater than $\phi_{l_{min}}$ to the satellite. The end time is determined by the time interval before the elevation angle at one of the seven points falls below $\phi_{l_{min}}$.

Use of the program enables study of the number of satellites required vs. orbit height, orbit inclination angle, and minimum elevation angle. To illustrate the type of output it generates and to characterize the effect of inclination angle on the NGO satellite system, performance with satellites at an altitude of 20,182 km at three orbital inclination angles, $\Psi = 0°$, $45°$, and $90°$, will be detailed. The sequence of steps performed to calculate the number of satellites and their location necessary to provide continuous CONUS coverage is outlined in Figure 4.3.

1. For each orbit under consideration, find the orbit period τ_s, decide upon the appropriate time increment, e.g. $\frac{\tau_s}{100}$, and calculate time steps: $t(k) = (k-1)\ \frac{\tau_s}{100}$.

2. The latitude and longitude of each of the 7 points in CONUS listed in Table 4.5 is used along with $t(k)$ to find the motion of these points (relative to the center of the Earth) as a function of time: i.e. $x_{loc_1}(t(k))$, $y_{loc_1}(t(k))$, and $z_{loc_1}(t(k))$ are found using Eq. 4.28.

3. For a given initial satellite position, θ_S, find $x_{loc_1}(t(k))$, $y_{loc_1}(t(k))$, and $z_{loc_1}(t(k))$ from Eq. 4.29.

4. At each time increment $t(k)$ find the elevation angle between each location and the satellite i.e. $\phi_{loc_1}(t(k))$, $\phi_{loc_2}(t(k))$, $\cdots$, $\phi_{loc_7}(t(k))$ from Eq. B.4 in Appendix B

5. Do steps 2. - 4. for $t(k) = 0$ to τ_s.

6. Find the start and stop times $(T_{start}(1), T_{stop}(1))$ of each time window such that:

$$\begin{aligned} \phi_{loc_1}(t(k)) &\geq \phi_{l_{min}} \\ \phi_{loc_2}(t(k)) &\geq \phi_{l_{min}} \\ &\vdots \quad \vdots \\ \phi_{loc_1}(t(k)) &\geq \phi_{l_{min}}. \end{aligned}$$

   For satellites in inclined orbits, there may be more than 1 time window per day at which all of CONUS is visible. Denote the number of these time windows per day as i.

7. Perform steps 2. - 6. for satellites with initial angular positions in their orbit θ_S varying from 0° to 360°.

8. Plot $T_{start}(i)$ and $T_{stop}(i)$ for each of the i windows vs. the satellite initial angular position θ_S, e.g. see Fig. 4.5, 4.8, and 4.11.

9. From the above figure determine the set of optimum θ_S, $\left\{\theta_{S_{opt}}\right\}$, to get 24 hr CONUS coverage with the fewest satellites.

   If 24 hr coverage is not possible using satellites in this orbit plane only, then create another θ_S vs. T_{cc} pattern shifted in time to provide additional coverage. See Fig. 4.9 and 4.12 for examples.

Figure 4.3: Steps performed in the calculation of the number and the location of satellites required to provide continual CONUS coverage.

157

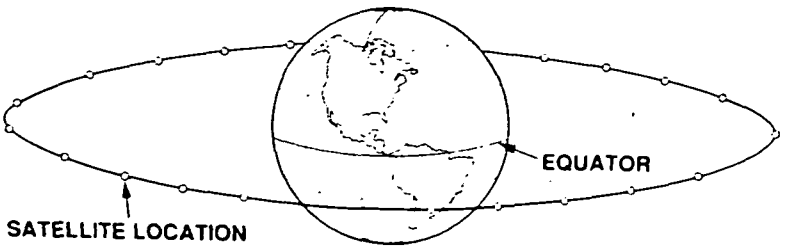

Figure 4.4: Satellite location for equatorial orbit.

Satellite orbit at 20,182 km, inclination angle at 0°

The first example concerns an equatorial circular orbit at 20,182 km (k:n = 2:1). The characteristics of this orbit are shown in Tables 4.1, 4.3 and 4.4. The program is run to find the complete coverage window for all seven cities assuming that at $t = 0$ the satellite at $\theta_s = 0°$ is at longitude = 0°. θ_S is varied in steps of 11.125°. The orbit and the satellites are shown in Fig. 4.4. The program results are given in Fig. 4.5. Note that each satellite, equally positioned around the orbital arc, sees CONUS once for the same amount of time during one Earth day.[6] The start and stop times of T_{cc} depend on the initial position of the satellite with respect to CONUS at $t = 0$. The program is run with $\Delta t = 95$ sec. Two values of $\phi_{l_{min}}$ are considered: $\phi_{l_{min}} = 10°$ and $\phi_{l_{min}} = 20°$. T_{cc} is 3:20 hrs for the former and 0:58 hrs for the latter. Because T_{cc} does not depend on satellite location in the orbital arc, the number of satellites, $N_{satellite}$, can easily be calculated according to:

$$N_{satellite} = \text{Integer}\left\{\frac{24 \text{ hrs}}{T_{cc} + T_{overlap}}\right\} \tag{4.30}$$

where $T_{overlap}$ is the amount of overlap desired between satellites and *Integer* is a function which rounds its argument up to produce an integer value. $N_{satellite}$ is then found to be:

$$N_{sat} = \begin{cases} 8 & \text{for } \phi_{l_{min}} = 10° \\ 25 & \text{for } \phi_{l_{min}} = 20° \end{cases} \tag{4.31}$$

Fig. 4.6 gives the angular location of the 8 satellites needed to provide CONUS coverage for $\phi_{l_{min}} = 10°$.

[6]The satellite sees CONUS once a day although it passes over the location where CONUS was twice in one day. In other words, let us assume that at $t = 0$ CONUS is visible to the satellite. This will be the case again at t = 23hrs 56min and 4sec. At $t \approx 12$ hrs, the satellite will pass over the point in the fixed coordinate system where CONUS was but CONUS will now have moved halfway around the globe and be invisible to the satellite.

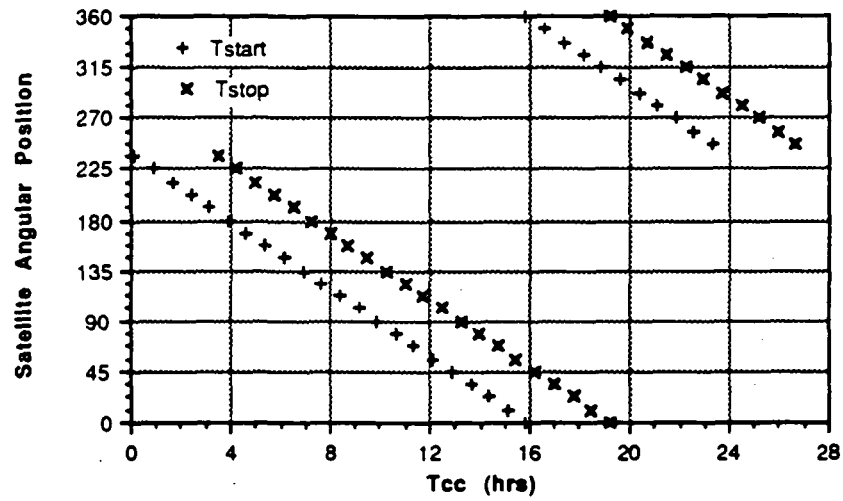

Figure 4.5: T_{cc} for each satellite 11.125° apart in an equatorial orbit at 20,182 km for $\phi_{l_{min}}$ = 10°.

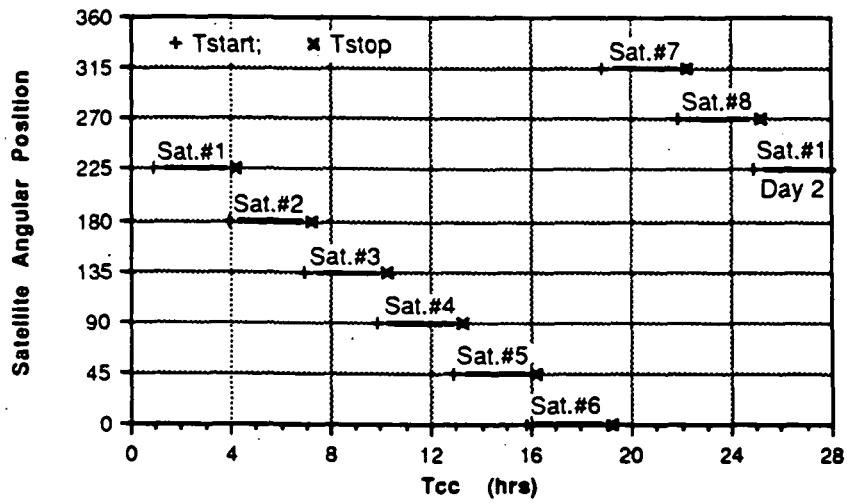

Figure 4.6: Location of the eight satellites necessary for complete CONUS coverage: equatorial orbit at an altitude of 20,182 km; $\phi_{l_{min}}$ = 10°.

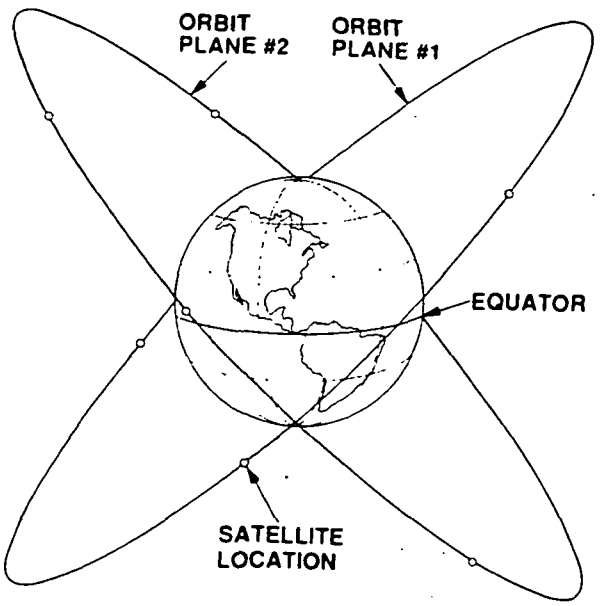

Figure 4.7: Satellite location for a circular orbit at an inclination angle of 45°.

Satellite orbit at 20,182 km, inclination angle at 45°

The performance of a circular 20,182 km orbit inclined from the equator by 45° is now found. Of course there are many such orbits that can be placed about the globe. Two are depicted in Fig. 4.7; they can be uniquely identified by their longitude at the equator at the time t = 0. The two depicted differ by 180°. The coverage times, T_{cc}, have been calculated for satellites spaced 11.125° apart in orbit #1; they are shown in Fig. 4.8. Again, the satellite sees CONUS only once every day, i.e. one coverage window per day. However, contrary to the equatorial orbit case, it is immediately apparent that T_{cc} depends on the satellite's angular position at $t = 0$. For θ_S from 135° to 225°, the satellite sees CONUS for very small time periods. This can be understood by examining Fig. 4.7: although satellites in this orbit will cross the longitudes corresponding to CONUS once per day and thus might be expected to be visible to CONUS, in fact some satellites will cross these longitudes when they are in the southern hemisphere and thus barely visible to CONUS. (No CONUS coverage is feasible for satellites at these angular positions when $\phi_{l_{min}} = 20°$.)

Examination of Fig. 4.8 shows that continuous CONUS coverage is not possible if satellites are placed only in this 45° orbit as no coverage is available from $t = 0$ hrs to $t = 0.5$ hrs and from $t \approx 16$ hrs to $t = 24$ hrs. If the T_{cc} coverage pattern can be shifted in time by 12 hrs, corresponding to angular difference in the 45° orbit of 180°, then continuous CONUS coverage can be achieved. The ensuing T_{cc} pattern is shown in Fig. 4.9. Orbits #1 and #2 differ only in their relative position to the Earth at $t = 0$. The relative position of CONUS and orbit #1 at $t = 0$ is identical to that of CONUS and orbit #2 12 hours later. To find the coverage pattern provided by satellites located in any 45° orbit, it is sufficient to calculate the T_{cc} obtained vs. θ_s for a specific 45° orbit and then shift the time axis of that pattern by t hours to arrive at the T_{cc} pattern of an orbit $t/24 \cdot 360°$ away.

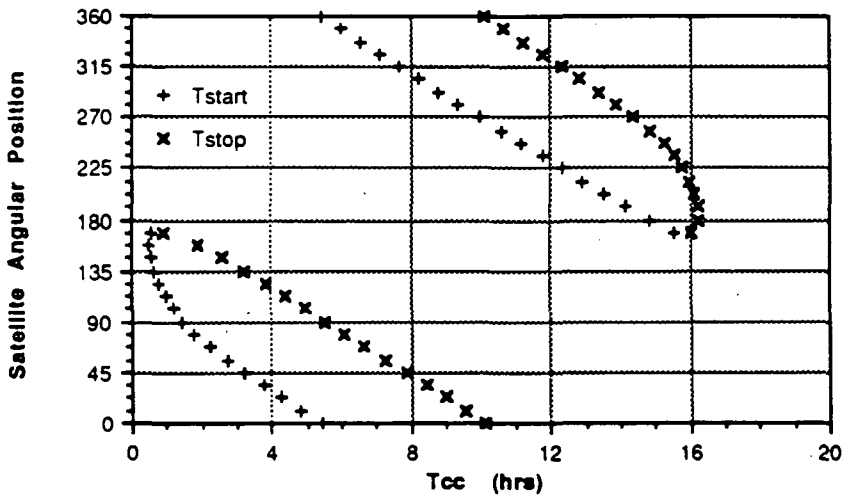

Figure 4.8: T_{cc} for each satellite 11.125° apart in a 20,182 km orbit inclined by 45° for $\phi_{e_{min}}$ = 10°.

Examination of Fig. 4.9 shows that 24 hr CONUS coverage can be achieved by choosing the appropriate initial angular positions for satellites in each of the 45° orbits. Because T_{cc} varies for each θ_S, the optimum satellite positions must be determined graphically. Choosing θ_S so as to maximize T_{cc}, three satellites can be placed at θ_S = 90°, 0°, and 270° in orbit #1 to provide greater than 12 hr coverage. Three satellites can be located at θ_S = 78.75°, 348.75°, and 270° in orbit #2 to provide the remaining 12 hrs of coverage. These six satellites are shown in Fig. 4.9. Thus six satellites are necessary with one coverage window per satellite per day. The number of coverage windows per day, N_{window}, is then six. N_{window} is a measure of the tradeoff complexity that will be necessary to handle the daily handoffs between satellites.

The average T_{cc}, $< T_{cc_{system}} >$, of these six satellites can be computed from the coverage time of each of these windows according to:

$$< T_{cc_{system}} >= \frac{\sum_{N_w=1}^{N_{windows}} T_{cc}}{N_{windows}} . \tag{4.32}$$

For this example, $< T_{cc_{system}} >$ is calculated to be 4hrs 26min. The overlap time between satellites can be found from:

$$\text{Overlap} = \frac{\sum_{N_w=1}^{N_{windows}} T_{cc} - 24\text{hrs}}{24\text{hrs}} . \tag{4.33}$$

In this case the overlap is computed to be 11%.

For $\phi_{l_{min}}$ of 20°, 8 satellites, 4 in each orbit, will suffice to provide continuous CONUS coverage with 16.8% overlap between satellites. $< T_{cc_{system}} >$ is 3hrs 30 min.

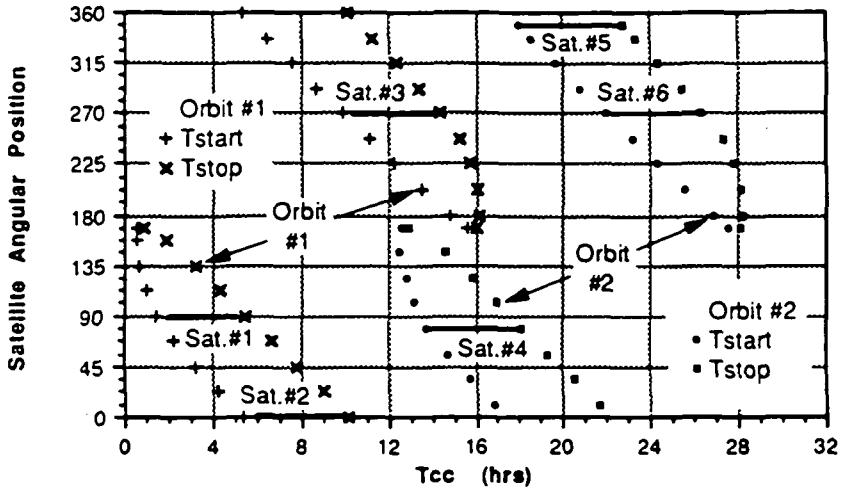

Figure 4.9: Satellite location in two 45° inclined 20,182 km orbits to provide continuous CONUS coverage assuming $\phi_{l_{min}} = 10°$.

Satellite orbit at 20,182 km, inclination angle at 90°

When satellite orbits at inclination angles of 90° are used, more satellites are necessary to achieve 24 hr coverage. Fig. 4.10 illustrates the case of two polar orbits separated by 97.5° – a minimum satellite geometry for $\phi_{l_{min}}$ is 10°. The coverage times for satellites in a 90° orbit are shown in Fig. 4.11 for $\phi_{l_{min}} = 10°$. For the majority of satellite angular positions, there are two coverage windows per day. However for θ_S from 56.25° to 45°, only one coverage window exists per day. In either case, the coverage period per window is very short. As with the 45° inclination angle orbits, it is necessary to place satellites in two orbits in order to provide continuous CONUS coverage. The optimum phase difference between these orbits must be determined by trial and error so as to select satellites in both orbits to provide 24 hr coverage. A possible solution to minimize the number of satellites required is given in Fig. 4.12. The two orbits differ by 6.5 hrs or 97.5°. Seven satellites, 4 in orbit #1 and 3 in orbit #2, are required. Satellites #1, #2, #3, and #5 are used twice each day. (The second coverage window of the satellite is drawn with a hatched pattern.) The number of coverage windows per day for continuous CONUS coverage, N_{window}, is then 11, meaning that a transceiver operating continuously would have to perform 11 satellite handoffs per day.

$< T_{cc_{system}} >$ can be calculated from Eq. 4.32 to be 2hrs 46min and the overlap can be found from Eq. 4.33 to be 26.7%.

For $\phi_{l_{min}} = 20°$, 3 satellite orbits are necessary; they are separated by 60°. $N_{satellite}$ is 9, N_{window} is 14, $< T_{cc_{system}} >$ is 2 hrs 9min, and there is 26% overlap between satellites.

The results for use of NGO satellites in a circular orbit at 20,182 km for orbit inclination angles of 0°, 45°, and 90° are shown in Table 4.9. Note that an inclination angle of 45° permits use of the smallest number of satellites and the fewest number of satellite handoffs

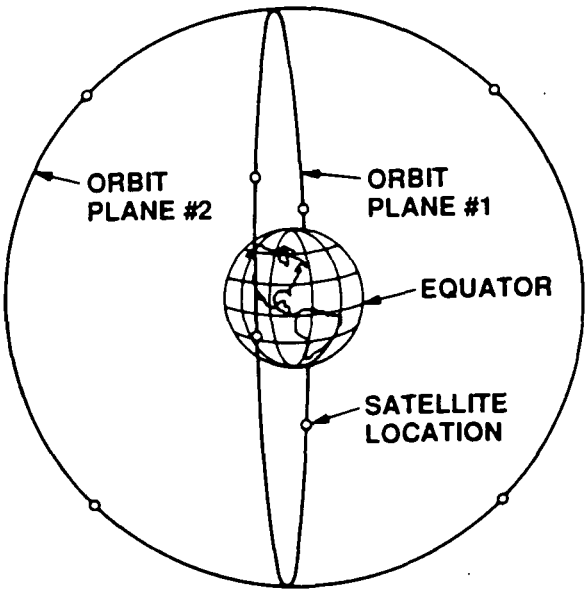

Figure 4.10: Satellite locations for two circular orbits at an inclination angle of 90°.

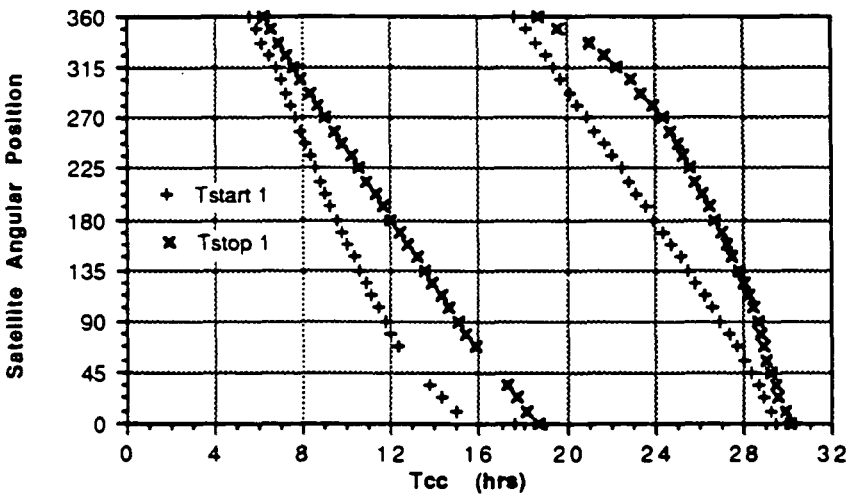

Figure 4.11: T_{cc} for each satellite 11.125° apart in a 20,182 km orbit inclined at 90° for $\phi_{l_{min}}$ = 10°.

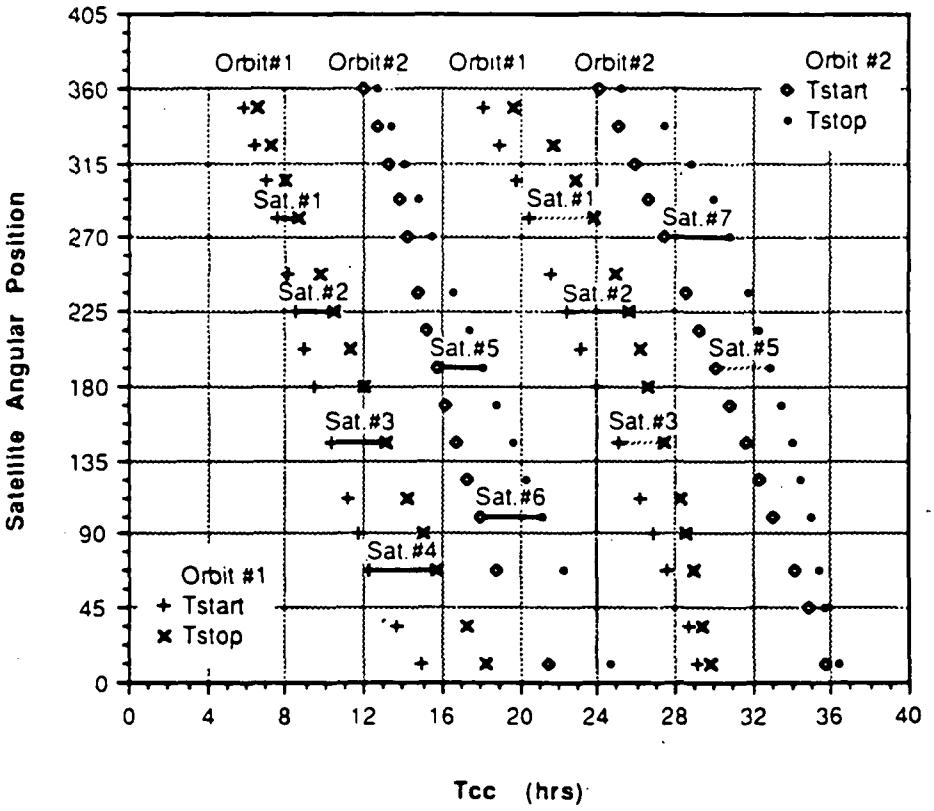

Figure 4.12: Satellite location in two 90° inclined 20,182 km orbits to provide continuous CONUS coverage assuming $\phi_{l_{min}} = 10°$.

Table 4.9: Satellite Orbit Parameters for Circular Orbits at a Height of 20,182 km for Various Inclination Angles, Ψ, and Min. Elevation Angle, $\phi_{l_{min}}$

	$\Psi = 0°$		$\Psi = 45°$		$\Psi = 90°$	
	$\phi_{l_{min}} = 10°$	$\phi_{l_{min}} = 20°$	$\phi_{l_{min}} = 10°$	$\phi_{l_{min}} = 20°$	$\phi_{l_{min}} = 10°$	$\phi_{l_{min}} = 20°$
$N_{satellite}$	8	25	6	8	7	9
Orbit Planes	1 plane	1 plane	2 planes	2 planes	2 planes	3 planes
$\Delta\theta_{orbit}$	N/A †	N/A	0°, 180°	0°, 180°	0°, 97.5°	0°, 60°, 120°
$N_{coverage}$	8	25	6	8	11	14
$< T_{cc_{system}} >$	3hrs 20min	59min	4hrs 26min	3hrs 30min	2hrs 46min	2hrs 9min
N_{window}	1	1	1	0, 1	1, 2	0, 2
Overlap	11.4%	2.5%	11.0%	16.8%	26.7%	26.0%

† Not Applicable.

per day.

Satellite orbit at 10,353 km, inclination angle at 0°, 45°, and 90°

The characteristics of NGO satellite systems operating at an altitude of 10,353 km are shown in Table 4.10 for orbit inclination angles of 0° and 45°. Orbit parameters are not shown for satellites in equatorial orbits when $\phi_{l_{min}}$ is 20° as it is not possible then for the satellite to see all of CONUS no matter what its initial angular position is. Although certain portions of the US are visible with elevation angles greater than 20°, at no time do all seven points chosen to represent the boundaries of CONUS have elevation angles greater than 20°. The overall effect of a reduction in satellite altitude by a factor of 2 is to reduce $< T_{cc_{system}} >$ by a factor of 3 to 4 so that, even though the number of satellites does not triple, the number of satellite handoffs per day does.

Satellite orbit at 5,143 km, inclination angle at 0°, 45°, and 90°

The characteristics of NGO satellite systems operating at an altitude of 5,143 km are shown in Table 4.11 for orbit inclination angles of 45° as satellites in equatorial orbits cannot provide CONUS coverage when $\phi_{l_{min}}$ is greater than 10°. The number of satellites required is now 26 for $\phi_{l_{min}} \leq 10°$ and 48 for $\phi_{l_{min}} \leq 20°$. $< T_{cc_{system}} >$ is 33 min and 23 min for $\phi_{l_{min}} \leq 10°$ and $\phi_{l_{min}} \leq 20°$, respectively. The number of satellite handoffs per day is 56 and 101 for $\phi_{l_{min}} \leq 10°$ and $\phi_{l_{min}} \leq 20°$, respectively.

Table 4.10: Satellite Orbit Parameters for Circular Orbits at a Height of 10,353 km for Various Inclination Angles, Ψ, and Min. Elevation Angle, $\phi_{l_{min}}$

	$\Psi = 0°$	$\Psi = 45°$	
	$\phi_{l_{min}} = 10°$	$\phi_{l_{min}} = 10°$	$\phi_{l_{min}} = 20°$
$N_{satellite}$	20	12	18
Orbit Planes	1 plane	2 planes	3 planes
$\Delta\theta_{orbit}$	N/A †	0°, 180°	0°, 120°, 240°
$N_{coverage}$	60	20	24
$< T_{cc_{system}} >$	25min	1hrs 28min	1hrs 7min
N_{window}	3	2	1, 2
Overlap	3.8%	22.1%	12.3%

† Not Applicable.

Table 4.11: Satellite Orbit Parameters for Circular Orbits at a Height of 5,143 km for an Inclination Angle, Ψ, of 45° and Two Minimum Elevation Angles, $\phi_{l_{min}}$

	$\Psi = 45°$	
	$\phi_{l_{min}} = 10°$	$\phi_{l_{min}} = 20°$
$N_{satellite}$	26	48
Orbit Planes	3 planes	3 planes
$\Delta\theta_{orbit}$	0°, 150°, 300°	0°, 132°, 264°
$N_{coverage}$	56	101
$< T_{cc_{system}} >$	33 min	23 min
N_{window}	3, 4	2, 3
Overlap	28.8%	60.8%

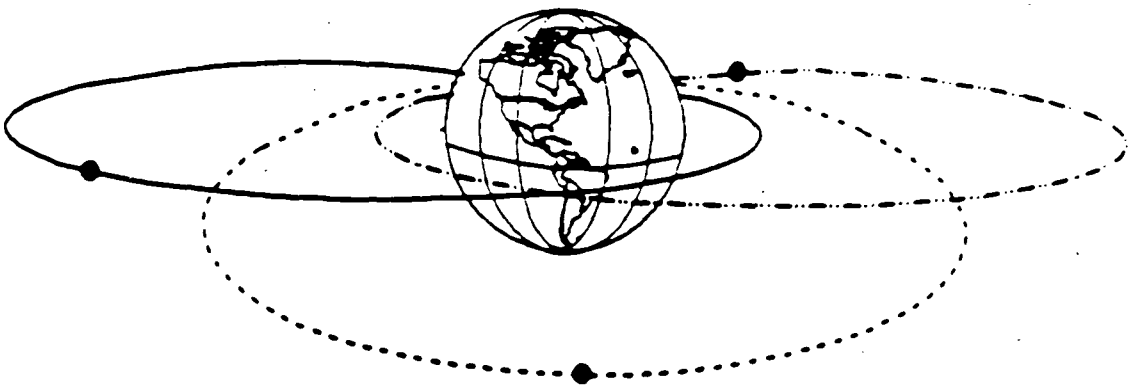

Figure 4.13: Satellite location for three satellites in three ACE orbits.

4.4.2 Elliptical Orbit Results

ACE orbit

Approximately eight satellites are required to provide continuous CONUS coverage from this orbit. The total coverage period and thus the number of satellites can be calculated from finding the turn-on and turn-off points of the satellite assuming that the satellite antennas have their boresights directed towards the center of CONUS during the coverage period. As depicted in Fig. 4.13 satellites in the ACE orbit can be phased in order to give a 24hr CONUS coverage. These satellites, with their orbit apogees at 0° latitude and -95° longitude, would turn their transponders on at the first point that $\phi_{l_{min}} = 20°$ and turn them off at the next $\phi_{l_{min}} = 20°$.

Molniya orbit

The satellites in the Molniya orbit are phased in the same fashion as the ACE satellites. Approximately three satellites, with their apogee at 37° latitude and -95° longitude, are required to provide continuous CONUS coverage from this orbit.

4.5 Advantages and Disadvantages of NGOs

The relative advantages and disadvantages to using NGO satellites for the PASS application can be measured in terms of the parameters mentioned in the introduction. This chapter has focused on determining some of them, for instance, the variation in propagation loss during the satellite's pass over CONUS, the impact on the signal uplink and downlink, the roundtrip signal delay, Doppler shift, reduction in the size of satellite antennas, number of satellite switchovers/day and the number of satellites required to cover CONUS continually. These parameters are given in Table 4.12 for the three NGO satellite altitudes at which

CONUS coverage from one satellite is possible and for the two elliptical orbits considered. An inclination angle of 45° is chosen to minimize the number of satellites although the use of non-equatorial orbits does lead to slightly higher maximum Doppler shifts and lower antenna gains.

In Table 4.12 ΔL_{P_1} represents the variation in propagation loss from the time when the satellite first becomes visible at $\phi_{l_{min}}$ to the time when the satellite is overhead, $\phi_{l_{min}} = 90°$. It is given by $L_P(z) - L_P(h)$ where z is the maximum slant path distance and h is the distance from the satellite to an E/S directly underneath it. It can be calculated from ΔL_{P_2} given in Table 4.8; for example $\Delta L_{P_1}(10°) = \Delta L_{P_2}(90°)$ - $\Delta L_{P_2}(10°)$. The link margin for the circular orbits is that shown in Table 4.8. For elliptical orbits it is calculated for earth stations within CONUS having the minimum elevation angle: for the Molniya orbit $\phi_{l_{min}}$ is 41°. N_{cov} and N_{sat} are taken from Tables 4.9, 4.10 and 4.11. The round trip delay is taken from Table 4.1 for the circular orbits and Table 4.2 for the elliptical orbits. Doppler shift is shown for circular orbits with $\Psi = 45°$; it is taken from Table 4.3. Doppler shift for the elliptical orbits is taken from Section 4.3.1. Satellite antenna size is given for the CONUS antenna ($\rho = 0.5$) and the MBA antenna ($\rho = 0.45$); these values are taken from Section 4.3.3 and Table 4.7.

As can be seen from Table 4.12, no improvement in the link is achieved with the NGO satellites in circular orbits as long as $\phi_{l_{min}}$ is 20° or less.[7] The gain in signal power brought about by the reduced propagation loss when NGO satellites are used is outweighed by the loss in satellite antenna gain. For the PASS design, the degradation in uplink C/N means that both suppliers and users will have to transmit higher EIRPs; the degradation in downlink C/N will require both suppliers and users to increase their receive G/T. This most certainly means that the size of the user antenna could not be reduced: directional antennas will still be necessary as in the preliminary design. Moreover the user and supplier antennas will require satellite tracking mechanisms for both circular or elliptical orbits. Both user and supplier transceivers will need to implement techniques to compensate for the Doppler shift of the signal which at 20 GHz and 30 GHz is substantial, up to 344 KHz for satellites in 45° inclined orbits at altitudes of 5,143 km. Lastly the variation in the link will necessitate some modification to the present rain fade control scheme wherein both users and suppliers utilize the signal strength of the pilot to determine the rain fade condition in their uplink and downlink.

A comparison of the orbits under consideration shows that the fewest number of satellites required for continual CONUS coverage is the Molniya orbit which requires only three. It also requires the smallest change in link margin when compared to the geostationary orbit. However this orbit has the highest maximum Doppler shift and possesses a wide range in path loss. The 20,182 km circular orbit has far less Doppler shift and negligible path loss change with less link margin degradation but requires 6 to 8 satellites depending on $\phi_{l_{min}}$. Lower orbits require greater numbers of satellites, have greater degradation in the link margin, possess higher variations in the path loss, and are characterized by higher Doppler shifts;

[7] Consideration of low elevation angles is necessary to maximize T_{cc} and hence minimize the number of satellite switchovers per day and the number of satellites necessary for continuous CONUS coverage.

Table 4.12: GEO and NGO Satellite Parameter Comparison

Elev. Angle $\phi_{l_{min}}$	Prop. Loss ΔL_{P_1}	Link Margin $\Delta C/N$	$N_{cov.}$	$N_{sat.}$	Roundtrip Delay (Overhead)	Doppler Shift(max) at 30 GHz	Satellite Antenna † at 20 GHz CONUS	MBA
Circular Orbits								
For 35,784 km (GEO) altitude satellite, $\Psi = 45°$:								
10°	0	0	1	1	239 msec	0 KHz	14.4cm	3.0m
For 20,182 km altitude satellites, $\Psi = 45°$:								
10°	1.8 dB	-0.99 dB	6	6	135 msec	131 KHz	8.2cm	1.7m
20°	1.4 dB	-0.63 dB	8	8			(43%)	(44%)
For 10,353 km altitude satellites, $\Psi = 45°$:								
10°	2.9 dB	-2.1 dB	20	12	69 msec	216 KHz	4.3cm	0.87m
20°	2.3 dB	-1.5 dB	24	18			(70%)	(71%)
For 5,143 km altitude satellites, $\Psi = 45°$:								
10°	4.4 dB	-3.6 dB	56	26	34 msec	344 KHz	2.3cm	0.43m
20°	3.5 dB	-2.7 dB	101	48			(83%)	(86%)
Elliptical Orbits								
For 15,100 km altitude (ACE) satellites, $\Psi = 0°$:								
20°	6 dB	-1.7 dB		8	252 msec	300 KHz	6.1cm	1.3m
							(58%)	(58%)
For 39,771 km altitude (Molniya) satellites, $\Psi = 63.4°$:								
41°‡	5 dB	-0.4 dB		3	100 msec	600 KHz	16.0cm	3.3m
							(-11%)	(-11%)

† Reduction in antenna size compared to GEO is given in parenthesis.

‡ The minimum elevation angle for earth stations within CONUS with the Molniya satellite is 41°.

however they have greater advantages in terms of signal delay and reduction in satellite antenna size.

Independent of the orbit, the benefits of using NGO satellites for this system are the reduced roundtrip signal delay and reduced satellite antenna size. The latter is of particular importance for the transmit and receive multibeam antennas where a size reduction of 16% to 79% is possible for satellite heights from 20,182 km to 5,143 km. This weight reduction in the communication payload may be offset by the more sophisticated antenna pointing mechanism required for the MBAs and by the larger solar cells, battery size, or electrical shielding which may be necessary to protect against the increased radiation found in these orbits. For satellite altitudes of 20,182 km and 10,353 km, the number of satellites and number of satellite switchovers per day are manageable.

Other advantages arising from the use of NGO satellites mentioned in the introduction, such as the possibility of global communications or improvements in the radio channel for mobile users, are not applicable to the PASS system as it is currently defined.

4.6 Conclusion

This chapter has studied the effects on the link characteristics of satellite in five circular non-geostationary orbits whose altitudes range from over 20,000 km to under 1,000 km and two elliptical orbits. The number of satellites necessary for continuous CONUS coverage and the number of satellite switchovers per day has been determined for the satellites in circular orbits from 20,000 km to 5,000 km as these altitudes allow CONUS to be covered by one satellite and for satellites in each of the elliptical orbits. Lower satellite altitudes require the use of more than one satellite and intersatellite links between satellites to provide CONUS coverage at any one time. The relative advantages and disadvantages of using NGO satellites for the PASS application are measured in terms of the following parameters: the impact on the signal uplink and downlink, the roundtrip signal delay, Doppler shift, reduction in the size of satellite antennas, number of satellite switchovers/day and the number of satellites required to cover CONUS continually.

The advantages of using satellites in circular orbits at altitudes ranging from 20,000 km to 5,000 km or in the ACE and Molniya elliptical orbits do not appear to outweigh the increased system complexity for the Personal Communication Satellite System application considered in this chapter. This is due, in large part, to this application's requirement to support real-time interactive voice between users located anywhere within CONUS. This requirement constrains the amount of time that the satellite can be used to be equal to the CONUS coverage time for high altitude satellites and sets the requirement for intersatellite links if lower altitude satellites are used. Greater system benefits might be realizable for this latter case. Such satellites would, however, require intersatellite links to maintain system interconnectivity. They will necessitate signal processing and routing functions on-board the satellite which may dramatically increase its cost and weight to values comparable to geostationary satellites.

Appendix A

Implication of Doppler Shift on the Complexity of the Channel Assignment Routine

To a stationary observer, the frequency of a moving transmitter varies with the transmitter's velocity. If a stationary transmitter's frequency is at f_T, the received frequency f_R is higher than f_T when the transmitter is moving toward the receiver and lower than f_T when the transmitter is moving away from the receiver. This change in frequency, or Doppler shift, is quite pronounced for low orbiting satellites and compensating for it requires intense frequency assignment and tracking.

For a non-geosynchronous satellite system linking supplier stations to users scattered around CONUS, direct supervision of the frequency assignment by a network management routine is required. The management routine has to ensure that no two signals in any link overlap, that is for any two signals centered at f_n and f_m in a given link,

$$|f_n - f_m| > BW, \tag{A.1}$$

where BW is the required data bandwidth.

For the PASS forward link, all the suppliers will have to compensate for the Doppler shift by tracking the incoming pilot from the satellite thus ensuring that the same nominal frequency is received by the satellite from all suppliers transmitting via a TDM/TDMA channel to a particular beam.

Denoting the signal destined to beam b by $F_{up}(b)$, onboard the satellite the signal is frequency shifted using a constant frquency $F_{for}(b)$ and is transmitted using beam b. This signal $F_{down}(b)$ received by user n, U_n, is in the form of:

$$F_{down}(b, U_n) = F_{up}(b) + F_{for}(b) + \text{Doppler}(U_n) \tag{A.2}$$

where Doppler(U_n) is the Doppler shift due to the motion of the satellite as observed by the n^{th} user. The Doppler shift varies from one user to the other as a function of their positions. Following the channel assignment of Eq. A.1 the network controller has to ensure that in an

area where frequency reuse is not implemented, for any beam number p and q ($p \neq q$), and and i and j ($i \neq j$),

$$|F_{down}(p, U_i) - F_{down}(q, U_j)| > BW_{forward}, \tag{A.3}$$

thus requiring wide guard bands or a constant changing of the TDMA channels center frequencies based on the location of the users in communication.

In the return direction where SCPC channels are assigned to users for transmission, the assignment procedure includes selection of an even greater number of center frequencies. In this link, assuming that Doppler correction is done on the inbound channel, means should be taken to correct the transmit frequency so that overlap at the satellite are avoided.. That is at the satellite for any k and l ($k \neq l$) in a region without frequency reuse:

$$|F_{user_k} - F_{user_l}| > BW_{return}. \tag{A.4}$$

Furthermore, the downlink from the satellite to the suppliers will require frequency correction based on the received pilot by the suppliers.

Appendix B

Calculation of the Elevation Angle from an Earth Station E to a Satellite at an Arbitrary Location, S.

For a satellite at a particular latitude, longitude and height, the elevation angle between a point on Earth and the satellite can be determined by taking the dot product between the vector from the center of the Earth to the point on the Earth, $\vec{E}$, and the vector from the point on Earth to the satellite, $\vec{ES}$:

$$\cos\theta_{ES} = \vec{E} \cdot \vec{ES}. \tag{B.1}$$

The vectors $\vec{E}$, $\vec{S}$, and $\vec{ES}$ and the angle θ_{ES} are shown in Figure B.1. $\vec{E}$, $\vec{S}$, and $\vec{ES}$ can be written in terms of the x, y, and z components of each vector as follows:

$$\begin{aligned} \vec{E} &= E_x\hat{i} + E_y\hat{j} + E_z\hat{k}, \\ \vec{S} &= S_x\hat{i} + S_y\hat{j} + S_z\hat{k}, \\ \vec{ES} &= ES_x\hat{i} + ES_y\hat{j} + ES_z\hat{k}. \end{aligned}$$

$\vec{ES}$ can also be expressed in terms of $\vec{E}$ and $\vec{S}$:

$$\vec{ES} = (S_x - E_x)\hat{i} + (S_y - E_y)\hat{j} + (S_z - E_z)\hat{k}. \tag{B.2}$$

The angle between $\vec{E}$ and $\vec{ES}$, θ_{ES}, can then be found from the definition of the dot product to be:

$$\theta_{ES} = \cos^{-1}\left(\frac{(E_x * (S_x - E_x)) + (E_y * (S_y - E_y)) + (E_z * (S_z - E_z))}{|E|\ |ES|}\right) \tag{B.3}$$

where $|E|$ and $|ES|$ represent the magnitude of $\vec{E}$ and $\vec{ES}$. The elevation angle from the point in CONUS to the satellite is then given by:

$$\phi_l = 90° - \theta_{ES}. \tag{B.4}$$

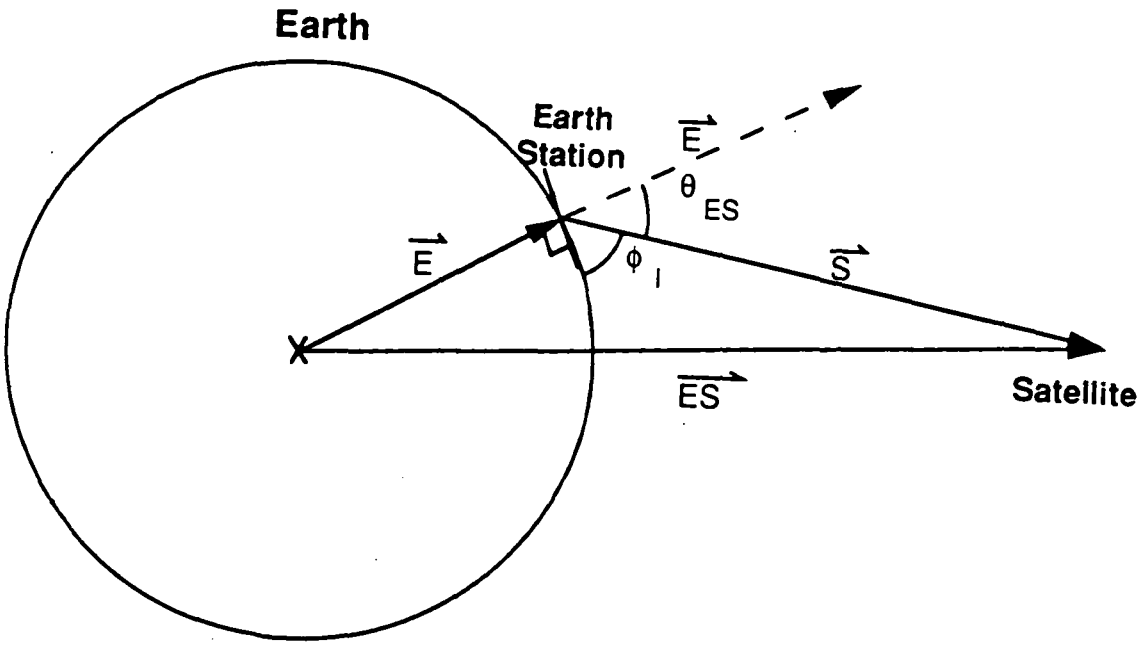

Figure B.1: Elevation angle geometry.

Bibliography

[1] Stuart, J.R., Norbury, J.A., and Barton, S.K., *Mobile Satellite Communications from Highly Inclined Elliptic Orbits,* AIAA 12th International Communications Satellite Systems Conference, March 13-17, 1988, Virginia, pg. 535 to 541.

[2] Price, Kent M., Doong, Wen, Nguyen, Tuan Q., Turner, Andrew E., and Weyandt, Charles, *Communications Satellites in Non-Geostationary Orbits,* AIAA 12th International Communications Satellite Systems Conference, March 13-17, 1988, Virginia, pg. 485 to 495.

[3] Richharia, M., Hansel, P.H., Bousquet, P.W., and O'Donnell, M., *A Feasibility Study of a Mobile Communication Network using a Constellation of Low Earth Orbit Satellites,* IEEE Global Telecommunications Conference, November 27-30, 1989, Texas, pg. 21.7.1 - 21.7.5.

[4] Nauck, J., Horn, P., and Göschel, W., - *LOOPUS - MOBILE - D - A New Mobile Communication Satellite System,* AIAA 13th International Communications Satellite Systems Conference, March 11-15, 1990, Los Angeles, California, pg. 886 to 899.

[5] Ford Aerospace, *The Use of Satellites in Non-Geostationary Orbits for Unloading Geostationary Communications Satellite Traffic Peaks, Volumes I and II,* NASA publication, CR-179-597.

[6] Estabrook, P. and Motamedi, M., *Use of Non-Geostationary Orbits for a Ka-Band Personal Access Satellite System,* AIAA 13th International Communications Satellite Systems Conference, March 11-15, 1990, Los Angeles, California, pg. 14 to 24.

[7] Motamedi, M. and Estabrook, P., *Use of Elliptical Orbits for a Ka-Band Personal Access Satellite System,* Second International Mobile Satellite Conference, June 17 - 20, 1990, Ottowa, Canada.

[8] *Orbital Flight Handbook Part 1 - Basic Techniques and Data*, NASA SP-33 Part 1, National Aero. and Space Admin., Washington, D.C., 1963, pg. III-24.

[9] Sue, M. (ed), *Personal Access Satellite System Concept Study*, JPL D-5990 (Internal Document), Jet Propulsion Laboratory, February 1989.

[10] Bousquet, M. and Maral, G., *Orbital Aspects and Useful Relations from Earth Satellite Geometry in the Frame of Future Mobile Satellite Systems,* AIAA 13th International Communications Satellite Systems Conference, March 11-15, 1990, Los Angeles, California, pg. 783 to 789.

[11] Pratt, Timothy and Bostian, Charles W., *Satellite Communications,* John Wiley & Sons, 1986.

CHAPTER 5: USER ANTENNAS

Dr. Vahraz Jamnejad
(with contributions from Paul Cramer)

5.0 INTRODUCTION

In the previous report on User Terminal Antennas (UTA's) for PASS (Chapter 6 of reference [1]), a variety of concepts were presented and discussed. Some of these concepts are presented in Figure 1 as reference. Two general categories of antennas were considered: Basic Terminal Antennas (BTA's), and Enhanced Terminal Antennas (ETA's). The ETA's employ relatively large and stationary (at least during operation) antennas, and are of more or less conventional designs. They will not be discussed here. The BTA's are more challenging and require further investigation in some detail. Specifically, there are some aspects of these antennas that need to be studied in further detail, in order to prove their feasibility and functionality in a technically as well as commercially viable system.

In this report we first tackle some issues that are of interest in the PASS antenna design in general. We discuss the effects of change in frequency on the size and gain requirements of the spacecraft as well as the ground antenna.

We then concentrate on the user antenna design considerations, specifically the basic terminal antennas (BTA's). We start with the fact that regardless of the specific design, the antenna has to operate at two relatively far apart frequencies, namely at 30 GHz transmit and 20 GHz receive frequencies. The challenges associated with this operation will be presented and some ways to resolve them will be presented. Then, trade-off study results will be given that provide limits on the gain, size, and complexity requirements of basic terminal antennas. Some design data and typical patterns will then be provided.

An issue that requires particular consideration is the significance of gain and figure of merit (G/T) in the transmit and receive modes of the antenna, respectively. This issue is particularly important in the light of experience gained during the mobile antenna experiments, where the increased noise temperature due to the antenna distribution network losses became a major cause of concern. This issue will be discussed at some length.

An important issue that requires particular attention is the radiation safety hazards associated with the operation of the basic personal antennas in Ka band frequencies at close range. The results of a preliminary investigation of this problem will be presented.

Finally, an outline of the critical technologies and development goals will then be presented, followed by an experimentation plan.

5.1 IMPACT OF FREQUENCY CHANGE ON USER AND SPACECRAFT ANTENNA GAIN AND SIZE

In this section we consider the effect of frequency change on gain and dimensions of the user terminal antennas of PASS. A summary of the relevant facts and figures is provided here, which is particularly useful for system designers.

The transmit antenna has a gain of

$$G_t = (4\pi / \lambda^2) A_t \tag{1}$$

in which λ is the wavelength and is related to frequency as

$$\lambda = C / f, \; C = 2.997925 \times 10^8 \text{ meters/second} \tag{2-a}$$

or

$$\lambda(\text{cm}) = 30 / f(\text{GHz}) \tag{2-b}$$

A_t in (1) is the effective aperture of the transmitting antenna in the direction of the receiving antenna. The isotopically radiated power at the receiving antenna location, EIRP, is given by

$$P_e = G_t P_t = (4\pi / \lambda^2) A_t P_t \tag{3}$$

in which P_t is the total power input to the transmitting antenna. The power density per unit areas (flux density), Φ, at a distance d, at the receiving antenna location is given by

$$\Phi = (P_e / 4\pi d^2) = (G_t / 4\pi d^2) P_t \tag{4}$$

The effective receiving aperture of the ground antenna in the direction of the incoming wave is defined as

$$A_r = (\lambda^2 / 4\pi) G_r \tag{5}$$

in which G_r is the gain of the receiving antenna in the direction of the incoming wave. The total received power, P_r, can therefore be written in one of the following equivalent forms:

$$P_r = A_r \Phi = \frac{A_t A_r}{d^2 \lambda^2} P_t = \frac{A_t A_r}{d^2 C^2} f^2 P_t \qquad (6\text{-a})$$

$$= \frac{G_t G_r}{(4\pi d/\lambda)^2} P_t = \frac{G_t G_r}{(4\pi d/C)^2} \frac{1}{f^2} P_t \qquad (6\text{-b})$$

$$= \frac{A_t G_r}{4\pi d^2} P_t \qquad (6\text{-c})$$

$$= \frac{G_t A_r}{4\pi d^2} P_t \qquad (6\text{-d})$$

The above equations are different versions of the well-known Friis transmission formula. In these formulas a polarization efficiency of 100% is assumed, i.e., the transmitter and receiver antenna field polarizations are perfectly matched. Otherwise a polarization efficiency factor must be included.

Although the second form (6-b) is usually used in link calculations in which the term $(4\pi d/\lambda)^2$ is referred to as the space loss, the other forms can sometimes be helpful in interpreting the relationships between transmit and receive antenna aperture size, gain, power, and frequency. For example, we can make the following observations.

Given a fixed distance between the transmitter and receiver, and a desired received power level,

i. from (6-a), for fixed transmit and receive antenna apertures, the required transmit power is inversely proportional to the square of frequency.

ii. from (6-b), for fixed transmit and receive antenna gains, the required transmit power is proportional to the square of frequency.

iii. from (6-c), for fixed transmitter aperture size and fixed receiver antenna gain, the required transmitter power is independent of frequency, while receiver antenna aperture size decreases with frequency increase.

iv. from (6-d), for fixed transmitter gain and fixed receiver aperture, the required transmit power remains independent of the frequency, while transmitter antenna aperture decreases with frequency increase.

Furthermore, it should be kept in mind that for a fixed gain the beamwidth remains constant, while for a fixed aperture size the beamwidth decreases with an increase in frequency. In general, the half-power (or 3-dB) beamwidth is approximately given as

$$BW^\circ \approx \frac{65}{D/\lambda} = \frac{65\ C}{D\ f}, \qquad (7)$$

for the aperture type antennas, in which D is the aperture dimension in the plane in which the beamwidth is considered.

The user terminal antenna in the PASS system is a medium gain antenna with a gain in the range of 15 to 25 dB, typically composed of an array of fixed gain radiating elements. These elements have fixed dimensions in terms of the wavelength (less than half a wavelength). Thus, for higher frequencies the actual size of the elements is reduced but their individual gain and beamwidth remain constant. Among these elements, dipoles, microstrip patches (circular or square) and crossed slots can be mentioned.

As frequency is increased, the gain of an array with a fixed number of such elements does not change. Instead, the overall size of the array is reduced. The inter-element separation of approximately half a wavelength is maintained in order to suppress the grating lobes. A higher gain is achieved by increasing the number of elements. Such an increase does not add significantly to the cost of a mechanically steered array. The cost increase can be substantial, however, for an electronically steered array where the number of relatively costly phase-shifters increases accordingly.

In either case, the increase in gain is accompanied by an increase in dividing network loss. This beamforming loss is, in general, proportional to the logarithm of the number of elements, while gain increases linearly with the number of elements; therefore, the overall effect is a net increase in gain.

5.2 BASIC PERSONAL TERMINAL ANTENNAS

5.2.1 IMPACT OF 20/30 GHZ FREQUENCY SEPARATION

Since there are no official frequency assignments for the PASS system at present, the question arises as to whether the use of the uplink (transmit) and downlink (receive) frequencies at around 30 and 20 GHz, respectively, may cause a problem in the design of the user antenna. We illustrate the problem with respect to a planar array antenna (with electronic steering in azimuth and elevation, or just mechanical steering in azimuth). No design problem exists if separate antennas are used for the two modes of operation. Employing two antennas, however, in addition to an increase in the total weight and size, could be much more expensive. A single antenna covering both frequencies is preferable. In this case, the transmit and receive antennas will use all or parts of the same aperture.

In general, two different types of user antennas can be considered: reflectors and arrays. The reflector antenna, due to its nonconformality and also due to the fact that it would require strictly mechanical steering, is less desirable from an operational point of view. However, in general, it has some strong points: it is broadband (in terms of frequency), has relatively low feed network loss, and is generally less expensive. Its bandwidth, of course, is determined by the feed. The feed, which can be either a horn or open waveguide, or a small array of elements such as microstrip patches, does not present any major problem in providing the necessary bandwidth.

The planar array of a number of radiating elements may be a more suitable antenna candidate. Although the array can also be steered strictly mechanically in both elevation and azimuth, it is more likely that in order to keep conformal, it will be electronically steered in both azimuth and elevation or at least in elevation with mechanical steering in azimuth. In either case two approaches are possible.

In one approach, broadband array elements can be used to provide operation across the total bandwidth from 20 to 30 GHz. This kind of frequency coverage is not really needed or required, since only a very small frequency band around each of the two frequencies is utilized in the system. Furthermore, such a broad bandwidth is hard to achieve using relatively simple planar elements.

However, this approach is relatively simple to implement, if the receive and transmit operating frequencies are very close to each other with only a few percent total bandwidth (e. g., 20/21.5 or 30/32 GHz). A 40/44 GHz system, with a bandwidth of less than 10 percent, would also fall in this category; namely, the same elements can be used to cover both frequencies.

A better approach is to use collocated elements such as dual stacked microstrip patches or other dual resonant radiating elements which cover very narrow frequency bands (on the order of 1 percent) centered at each of the two operating frequencies. This approach has the added advantage of providing an inherent isolation of up to 20 dB between the transmit and receive frequencies, thereby reducing the isolation requirements of the diplexers.

In another approach, the receive and transmit arrays can be separate but interleaved to occupy the same aperture. This approach has the advantage of relatively simple element design since elements in each array need to operate over a relatively small frequency band. Furthermore, a much better isolation than the collocated elements arrangement can be achieved. However, due to the increased spacing required between the elements of either array in at least one direction, electronic scanning in that direction will create high grating lobes, unless substrates with very high dielectric constant are used to reduce the element size and, hence, spacing. In general, the interleaved arrangement is most suited to a fully mechanically steered array or a hybrid mechanical/electronic scan array with mechanical scanning in the interleave direction.

In either approach, a major problem is the difference in inter-element separation at the two frequencies, in terms of wavelength, which could cause high grating lobes at the higher frequency, particularly for beams steered to low elevation angles. According to the array theory, if the array elements in a regular grid have a large inter-element spacing, grating lobes are produced which manifest themselves as large sidelobes which result in a loss of gain. This problem becomes even more significant for large scan angles. Specifically, the inter-element spacing should be less than or equal to

$$d = 0.5\ \lambda\ /(1 + \sin(\theta)),\ \text{for uniform rectangular grid,} \qquad (8\text{-a})$$

and

$$d = 0.577\ \lambda\ /(1 + \sin(\theta)),\ \text{for uniform triangular grid,} \qquad (8\text{-b})$$

in order to completely prevent the presence of grating lobes. The spacing must be definitely less than twice the above values so that the peak of the first grating lobe does not enter the picture. In Eqs. 8-a and 8-b, θ is the scan angle from zenith (or broadside of the array). For a broadside array (zero scan) the above limits reduce to 0.5 and 0.577 wavelength, respectively, and decrease as the scan angle is increased. Of course, the above values are based on the assumption of isotropic (uniform) element patterns. The natural taper of an actual element would reduce the grating lobe levels.

A representative case is illustrated in Figure 2. A linear array of six elements is considered. Two microstrip patches are stacked at each element position for 20 and 30 GHz performance. This array can be part of a complete planar array. We are, however, concerned with its performance in the plane of beam scanning in elevation.

Figure 3 shows the broadside and scanned patterns of the linear array of six elements with 0.6 cm inter-element spacing. This spacing translates into 0.4 wavelength at the 20 GHz (with 1.5 cm wavelength), and the corresponding spacing for the collocated elements at 30 GHz (with a wavelength of 1 cm) is 0.6 wavelength. This is quite acceptable for the broadside array. However, for the beam scanned to 70 degrees from zenith (to provide coverage at 20 degree elevation) this is far larger than the 0.258 wavelength limit obtained from Eq. 8-a and even larger than the absolute limit of twice that value, i.e., 0.516. In the plots, we have assumed that each element has a half-power beamwidth of 90° at 30 GHz and 135° at 20 GHz.

It may be noted that the higher taper of the narrower element beamwidth at higher frequency partially compensates for the higher array grating lobe at this frequency. As can be seen, the performance at 20 GHz is satisfactory for both the scanned and non-scanned cases. For the 30 GHz case, however, the grating lobe is even higher than the main lobe and not acceptable.

A better result is obtained if the inter-element spacing is reduced to 0.5 cm. In this case, the spacing is 0.33 λ at 20 GHz and 0.5 λ at 30 GHz. This provides a more acceptable performance as shown in Figure 4, although the backlobe for the 30 GHz scanned case is still relatively large. It can be further reduced by amplitude tapering of the array elements. Also, as the number of elements is increased, the grating lobe effect is further reduced as long as the spacing is less than twice the value given in Eqs. 8-a and 8-b.

Furthermore, by introducing non-uniformity in the array lattice and breaking the symmetry of the configuration, one can reduce or neutralize the grating lobes at the expense of complications in the mechanical design and fabrication.

It should be noted that a reduction of inter-element spacing to accommodate the higher frequency, causes the spacing at the lower frequency to be much less than half a wavelength, and since the element size is typically somewhat less than half a wavelength this may seem to create a problem. This problem, however, can be solved by dielectric loading of the element. Thus, by increasing the dielectric constant the element aperture can be reduced to fit the available spacing.

In any case, as long as the total array aperture is used for operation at both transmit and receive frequencies, the resultant array pattern will be narrower and have a higher gain at the higher frequency (30 GHz). If required, it is possible to employ only an inner subset of the array elements at the higher frequency, in order to achieve the same beamwidth and gain as the lower frequency.

In conclusion, it is feasible to obtain reasonable antenna array performance at 20/30 GHz by the use of, for example, dual-stacked microstrip patch elements providing coverage at both frequencies. A simpler design can be employed, however, if the frequency separation is less than 10 percent, for example at the 40/44 GHz range. The latter system will also result in much smaller antenna dimensions for the same gain requirement.

5.2.2 PARAMETRIC STUDIES: GAIN, SIZE, WEIGHT

As an aid in deciding the size, weight and gain of the user antenna, trade-off studies have been performed and will be graphically presented. The emphasis here is on a planar array with a number of identical elements on a uniform grid.

Assuming an inter-element separation of approximately 0.5 and 0.577 wavelength, for the square and hexagonal (equilateral triangular) grid arrays, respectively, the total number of required elements as a function of the array diameter is given by

$$N \approx \pi\,(D/\lambda)^2, \quad \text{for a circular array, square lattice,} \tag{9-a}$$

$$N \approx 4\,(D/\lambda)^2, \quad \text{for a square array, square lattice,} \tag{9-b}$$

and

$$N \approx 0.25 + (1.5\ D/\lambda)^2, \text{ for a hexagonal lattice} \tag{9-c}$$

The case of a circular array with a square grid is graphically shown in Figure 5.

The gain of the planar array with a beam scanned θ degrees from the zenith is approximately given as

$$G = \eta\ (4\ \pi\ A\ /\lambda^2)\ \cos(\theta) \tag{10}$$

Usually it is assumed that a planar array is more efficient than a reflector antenna system because there is no illumination and edge taper loss is involved. For a well optimized reflector design these two losses cause an efficiency factor of about 0.8 (1 dB). As we shall see, as the number of elements in an array increases, the feed distribution network loss can be substantially higher. The array efficiency, η, is composed of three parts:

$$\eta = \eta_{el}\ \eta_{taper}\ \eta_{bfn}, \tag{11}$$

in which η_{el} is the array element loss which is relatively low and in the range

$$\eta_{el} \approx 0.9 - 0.99 \text{ dB}, \tag{12-a}$$

and η_{taper} is array taper which may be introduced in order to reduce the sidelobe levels and may be in the range

$$\eta_{taper} \approx 0.8 - 1 \text{ dB}, \tag{12-b}$$

and finally η_{bfn} is the beam-forming network loss. This loss in general can be given as

$$\eta_{bfn} \approx 3.32 \log (N)\ L_{div} + L_{\phi}, \tag{12-c}$$

in which N is the number of array elements, L_{div} is the equivalent loss per two-way divider, and L_{ϕ} is the loss in the phase shifter. For an n-bit phase shifter the loss is n times the loss per single bit phase shifter. The divider loss is calculated based on the assumption of a binary tree divider network. At Ka band frequencies, loss per two-way divider can be in the following range:

$$L_{div} \approx 0.3 - 1 \text{ dB}.$$

Figure 6 shows the dividing network loss as a function of the number of array elements N based on the assumption of an optimistic figure of 0.3 dB per divider. It is seen that the loss in dB increases as a logarithmic function of the number of elements, and for a few hundred elements could reach a few dBs, much more than the illumination and spill-over loss in a reflector antenna.

The phase shifter loss at the Ka band frequencies can be even more significant. Digital phase shifters presently under development can have several dBs of loss per bit. Instead, one can use continuously variable ferrite phase shifters with relatively little loss (a few tenths of dB). Unfortunately, this type of phase shifter is bulky and does not easily lend itself to integrated circuit manufacturing techniques.

The beamforming network loss can be altogether avoided if one implements an active array antenna. In an active array, a TR (Transmit/Receive) module will be located behind each radiating element or a small subarray of such elements.

In this way, the loss in the beamforming network will not be a high power loss in the transmit mode, and also will not contribute significantly to the receiver noise temperature (see Section 5.2.3). Such an active array can be manufactured using MMIC (Microwave Monolithic Integrated Circuit) techniques. The cost and complexity associated with such a design is presently quite significant, but may be substantially reduced in the next few years.

Figure 7 shows the gain of a completely mechanically steered array. No phase shifter loss and no beam scan loss are present, since it is assumed that the array is mechanically steered in both azimuth and elevation. Figure 8 shows the gain of both the passive and active (without the network and phase shifter loss) phased arrays versus the number of elements. The curves are based on Equations 10, 11, and 12. Three bit phase shifters with a loss of 2 dB per single bit is assumed.

The issue of the weight of the array antenna is more complicated and requires more detailed designs before accurate numbers can be produced. However, based on prior experience and some rough estimates regarding the components, the weight is estimated in the range of 5 to 10 g/sq cm (0.07 to 0.14 lb/sq in.), with the lower figure closer to a phased array design while the higher is closer to a mechanically steered design.

5.2.3 GAIN AND FIGURE OF MERIT (G/T)

G/T is a figure of merit to measure the performance of a receiving system. For active array antennas, the array configuration (i.e., the order of the amplifiers and the dividing/combining layers) impacts the overall system G/T. A study has been performed and is documented in Appendix I.

5.2.4 DESIGN DATA FOR SELECTED ANTENNA CONCEPTS

In general, from beam pointing considerations, we identify five feasible types of design for PASS user antennas in order to provide the required CONUS coverage, i.e., 360 degrees in azimuth and 20 to 60 degrees in elevation:

i) Fully electronically steered planar array.

ii) Fully mechanically steered in both azimuth and elevation. The antenna in this case can be either a planar array or a reflector antenna.

iii) Hybrid mechanically/electronically steered planar array. In this case, the beam can be rotated mechanically in azimuth, while beam tilt in elevation can be provided by electronic scanning or switching.

iv) Mechanical steering in azimuth with a fixed broad beam in elevation.

v) Electronic scanning or switching in elevation with a full 360 degree coverage beam in azimuth direction.

In this section, we present some design data for a fully electronically steered antenna and a fully mechanically steered antenna. Only gain and pattern information will be provided.

For planar phased array design we consider a uniform equilateral triangular (i.e., hexagonal) grid which has the highest array packing efficiency, namely, it requires the smallest number of elements per given area (see Eqs. 9(a-c)). Two examples of hexagonal arrays are given in Figures 9(a-b). The total number of elements in such an array is given by

$$N = 3\,m^2 - 3\,m + 1,$$

in which m is the generating number of the hexagonal grid and is equal to the number of elements on each side of the hexagon. Figure 10 provides far-field patterns for the 91 - element array of Figure 9(a).

A rectangular array can be used in a fully mechanically steered array. Both azimuth and elevation steering are provided. Figure 11 shows a possible layout of the array configuration while Figure 12 shows its mechanical design layout and Figure 13 provides typical far-field patterns.

A reflector antenna can also be used for the mechanically steered case. However, reflectors are usually used for gain of 30 dB or higher. Typically, the dimensions of the

reflector must be larger than about 10 wavelengths. Otherwise, the performance of the antenna suffers both in terms of the increased sidelobes as well as lower gain.

5.2.5 CRITICAL TECHNOLOGIES AND DEVELOPMENT GOALS

The aim of user antenna development is the design and mass production of very small, light weight, and economical units with good performance across the frequency band of operation and over the entire geographical region of interest, namely CONUS. As has been revealed in the process of this study as well as in the experience gained in the MSAT-X project, there are a number of challenges that have to be overcome.

One group of challenges has to do with the optimization of the antenna pattern characteristics, such as gain, polarization performance, and sidelobes and backlobes, given the constraints of small size and portability. Another group of challenges is associated with the requirement, selection and specification of RF components and materials that are or will be of a mature technology in the near future at relatively low prices.

Amenability of the design to integration and ease of fabrication in a mass production environment also falls within this category. The procurement of small, reliable and low-cost mechanical moving parts such as motors, rate-sensors, etc., and the development of efficient techniques for acquisition and pointing in one or two dimensions constitute a third category of challenges.

We identify the following technologies as some of the more important ones in reaching the objectives of this program.

1) **Necessary software development:** There is already a vast base of antenna analysis, synthesis, and design software presently available at JPL. However, these tools need to be further refined, modified and optimized for the kind of antenna performance goals that are relevant to the PASS system.

   One objective is to provide a complete characterization of ground plane effects in the antenna pattern analysis. Also needed will be the development of fast and efficient pointing software for the acquisition and tracking of the satellite. This is particularly significant considering the ambulatory environment of the PASS user antenna, requiring fast and reliable tracking in azimuth and elevation.

2) **New element and array concepts:** Both mechanically as well as electronically steered planar array antennas are prime candidates for the user antenna. As has been discussed, a very large number of radiating elements may be required to achieve the relatively high gains required at 15 to 20 degrees elevation. New and innovative element designs with very broad beams or tilted beams with relatively high gains at low elevations can reduce the number of needed elements. New sub-array and

arraying concepts to reduce the number of required elements and reduce the side and back lobes are also needed.

3) **Low loss, reliable and inexpensive RF components:** In both electronically and mechanically steered array design at Ka band frequencies, design and development of low-loss power divider/combiners is important, since the overall loss depends on the number of elements and the loss per divider unit. Reducing the two-way divider/combiner loss to 0.1-0.3 dB levels will significantly enhance the PASS user antenna development.

Of more concern are the phase shifters needed in the electronically steered phased arrays. There are continuously variable ferrite phase shifters of relatively low loss (a few tenths of dB) with potential application to Ka band frequencies. These are, however, relatively bulky and do not easily lend themselves to MMIC design and fabrication techniques. Solid state digital phase shifters presently available or under development, on the other hand, show unacceptably high losses (a few dB per bit), although they are suitable for Monolithic Integrated designs.

Advances in either category are required in order to make a phased array approach economically and technically feasible. Solid state switching elements required for electronically switched beams are also in the category of components which need to be made at low cost with high reliability and low loss.

4) **Low cost and reliable T/R modules:** High circuit losses introduced by the dividers and phase shifters in the array beam forming networks can be overcome by the introduction of T/R (Transmit/Receive) modules at the element or sub-array level. Development of low cost and reliable T/R modules within the MMIC configuration is an essential part of making phased array antennas attractive for PASS and similar applications.

5) **Small, inexpensive, and reliable pointing hardware:** Due to the mobile or ambulatory nature of the user antenna, design and selection of appropriate satellite acquisition and tracking hardware (or pointing system hardware in general) are as important as the RF subsystem design.

For instance, the development of small or miniature motors, preferably with a flat or pancake design no more than a few inches in diameter, with sufficient torque (more than 15 to 20 oz.-in.), reliable long term performance and available at low cost (less than $100 in large quantities), is a major component of a successful design. So are the rotary joint, the support bearings, and particularly inexpensive rate sensors with accurate and reliable performance. Again, the emphasis here is on the miniaturization as well as low cost.

5.2.6 RECOMMENDATIONS

Based on a literature survey and study performed in the course of this work we make the following recommendations for the development of basic personal terminal antennas:

i) The most likely candidate for a personal terminal in the next five years is a mechanically steered antenna (with tilted aperture). The fully mechanically steered array with automatic azimuth rotation and elevation tilt capability is perhaps the most promising in terms of cost, complexity and reliability. Both planar passive arrays as well as reflector-type antennas can be employed in such a system. Transmit gains of 20 to 25 dB can be expected from these antennas, with a receive G/T of 8 to 10 dB an achievable goal.

ii) As the MMIC technology matures and low loss, relatively low cost phase shifters and solid state amplifiers with acceptable efficiency, power handling capability, and relatively low cost with high packaging efficiency become available, a tilted or planar array with mechanical rotation capability for azimuth acquisition and tracking, and electronic scanning in elevation, becomes a feasible option. In such a system only linear sub-arrays of the total array may require phasing and T/R module, and hence the complexity and required packaging efficiency is well below a full fledged phase array design.

iii) Finally, in about 5 to 10 years the maturity of MMIC technology may be such that the idea of a fully electronically steered planar array antenna with T/R modules at each radiating element, providing a very low loss and hence low noise and high gain antenna in a small package of the order of 10 cm in size with gains of the order of 25 dB or higher and a G/T of better than -5 dB, will achieve economic feasibility. This, however, presupposes an intensive effort on the part of NASA and private industry to actively pursue and continue research and prototyping in the K_a band and higher frequency regimes.

5.3 USER ANTENNA RADIATION SAFETY CONCERNS

An important consideration in the design of the user antenna for the Personal Access Satellite System is the safety hazards associated with the radiation at Ka band frequencies. This is because of the proximity of the antenna to the user (from a few inches to a few feet), relatively high gain of the antenna, and lack of sufficient information on the effects of radiation at 20/30 GHz frequencies. There exists an ANSI document outlining safety standards for human exposure to RF radiation [2] and many papers and documents studying various aspects of the subject (see, e.g., [3]). Appendix II presents a short study of this subject with useful information on the RF radiation hazards in general and with specific application to the PASS system. It also indicates the need for further investigation, perhaps by an outside agency (e.g., a university), for reaching a satisfactory conclusion.

Here we present a short summary of the main issues of concern and some plots that can be useful in relating the antenna input power and the radiation levels (RF field intensity) for various antenna gains and distance from the antenna to the user.

i) In many antenna applications the transmitting antenna is far from the system users. Therefore, the radiation effect on the user is either nonexistent or minimal. In any case the user is in the far field of the antenna. The plot in Figure 14 gives a definition of different regions of an antenna in terms of the antenna size, wavelength and distance from the antenna aperture. As can be seen in this figure, for antenna apertures of about 5 to 10 centimeters (5 to 10 wavelengths at the 30 GHz transmit frequency), a user at a distance of a few inches from the antenna would be in the mid to near field of the antenna.

Characterization of the field in the near-field region is usually more complicated than the far-field region. However, the main point of interest here is the fact that in this region the field has a substantial longitudinal component (in the propagation direction) in addition to the transverse components which are also present in the far field. Studies have shown [4] that, in general, the longitudinal field component does not have any noticeable adverse effect on biological tissue and only the transverse field components need to be considered. From this it can perhaps be concluded that for a far field and a near field of comparable strength, the former has more deleterious effects. This is an area that needs further study.

Furthermore, due to the proximity of antenna to the user, the user body becomes a scatterer of energy and distorts and redistributes the overall field pattern. This problem has not been dealt with in any substantial degree. A simple approximation is to assume the same field distribution with and without the presence of the nearby objects.

ii) The RF radiation effects can be divided into two general categories: the heat effects and the chemical/cellular effects. Most studies have shown that only heat effects (a rise in temperature in the body tissues) have significant adverse effects on the biological tissues. Most of the chemical effects are either insignificant and/or reversible.

iii) Two criteria have been developed for characterizing the radiation effects:

The first criterion is related to the exposure of the human body to a uniform field, namely whole body exposure. This is an average, and according to established standards, the maximum power density per unit of area of the human body should not exceed a specific level (e.g., 5 mW/cm^2 at 30 GHz). This is based on the assumption that the average Specific Absorption Rate (SAR), namely the time rate at which electromagnetic energy is coupled to the body, will not exceed 0.4 W/Kg averaged over the whole body and over a 6 minute period. Figures 15 and 16 provide generic curves for the power density of aperture antennas at various distances from the antenna and for different antenna aperture sizes.

The second criterion relates to the localized effects of the RF field. According to this criterion the spatial peak SAR should be below 8 W/Kg per any one gram of body tissue.

This is a more important consideration when the radiation source is close to the subject of exposure.

iv) Most of the theoretical as well as experimental investigations of the radiation effects, to date, have been performed at frequencies below X-band (8 GHz or less). Only recently there has been an interest specifically in the Ka band region of RF spectrum, although sufficient and conclusive results are not yet available.

Recent findings [5], however, tend to indicate that the problem may not be as critical as some may have suspected and that the radiating safety levels specific to the Ka-band frequency range do indeed fall within the already established standards.

At any rate, should the radiation levels at 30 GHz prove to be excessive, there are certain ameliorative measures that can be taken. Aside from the obvious solution of reducing the transmitted power level which, depending on the system link budget requirements may or may not be feasible, the following measures may prove appropriate:

a) The use of a radome to cover the regions of high intensity radiation near the antenna. As discussed in Appendix II and also observed in Figures 13-14, radiation intensity peaks at a certain distance from the antenna aperture and is a function of the antenna aperture size. The peak of the radiation occurs at a distance of approximately

$$d \approx (1/4)\,(D^2/\lambda)$$

from the antenna aperture. This distance for an antenna with 20-25 dB gain at 30 GHz is in the 5-15 cm range. It may be feasible to enclose this high intensity region within a protective radome.

b) The use of a sensor to detect the presence of objects in the proximity of the radiating antenna and issuing a warning signal and/or possibly turning off the antenna.

In conclusion, due to the proximity of the radiation source (the antenna) to the human head in typical PASS applications, the exposure is at the near field of the antenna and is of a localized nature. Of critical importance is the localized 30 GHz radiation effects on the eyes and the ears. This is a problem that may require additional study. In any case, there are certain measures that may be taken to reduce the effects in the user antenna environment.

REFERENCES

[1] Miles Sue, Editor, Personal Access Satellite System Concept Study, JPL Publication JPL D-5990, February 1989.

[2] American National Standard Safety Levels with Respect to Human Exposure to Radio Frequency Electromagnetic Fields, 300 KHz to 100 GHz, Report No: ANSI C95.1-1982, Prepared by IEEE and US Department of the Navy.

[3] C. H. Durney, et al., Radiofrequency Radiation Dosimetry Handbook, Fourth Edition, Report No: USAFSAM-TR-85-73, Prepared for USAF School of Aerospace Medicine, October 1986.

[4] A. Lakhtakia, M. Iskandar, "Scattering and Absorption Characteristics of Lossy Dielectric Objects Exposed to the Near Fields of Aperture Sources."

[5] USAF Report on Radiation Experiments at 30 and 90 GHz Using Cat's Eyes, to be released in March 1990 by USAF School of Aerospace Medicine.

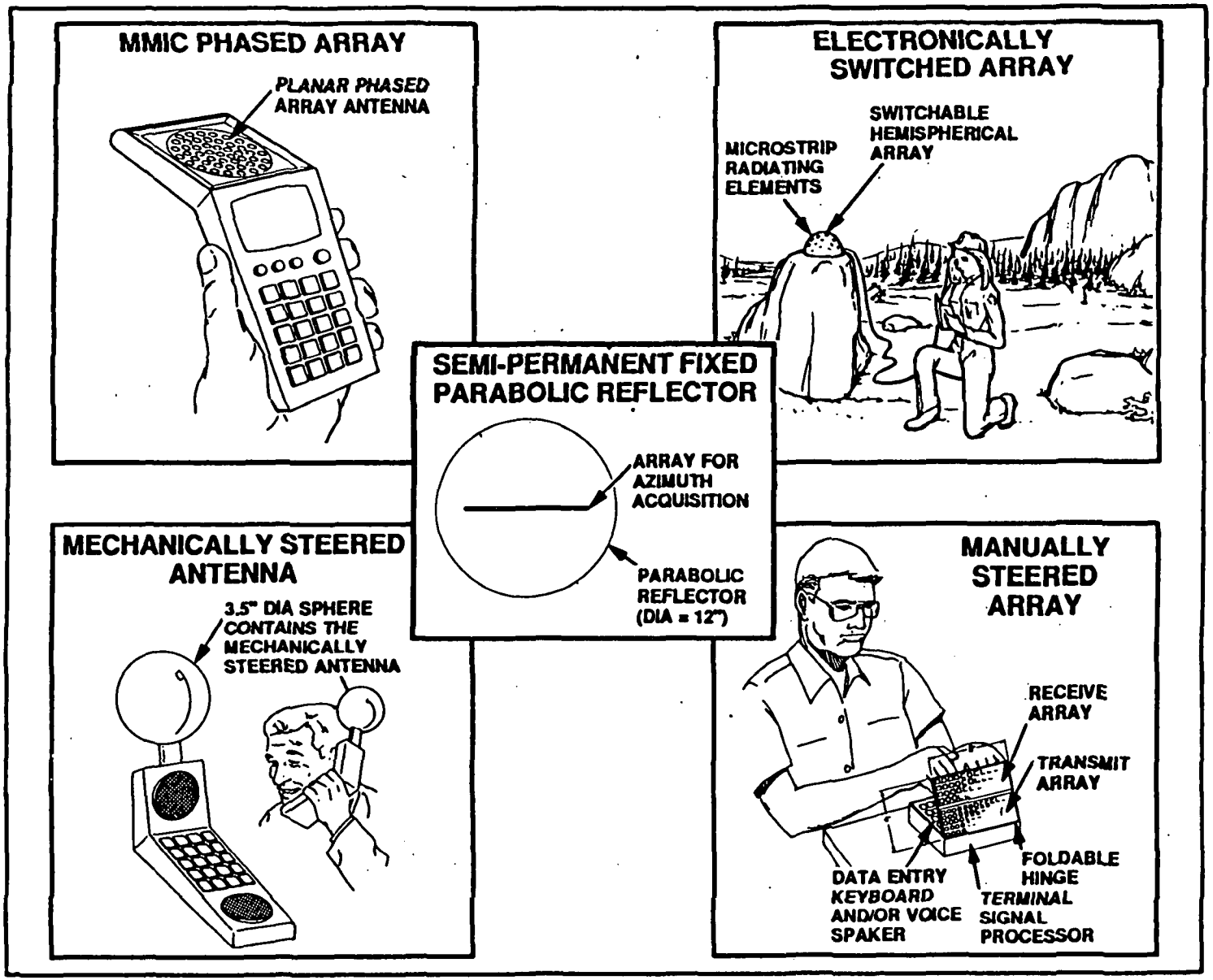

Figure 1. Typical user terminal antenna design concepts (from [1]).

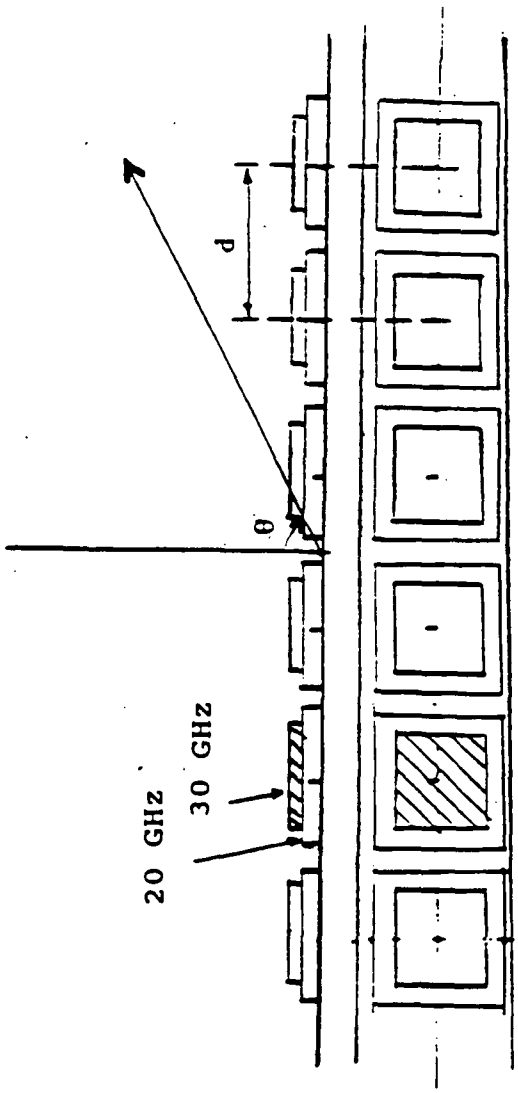

Figure 2. Sketch of a 6-element linear array with collocated elements for 20 and 30 GHz, and inter-element spacing, d.

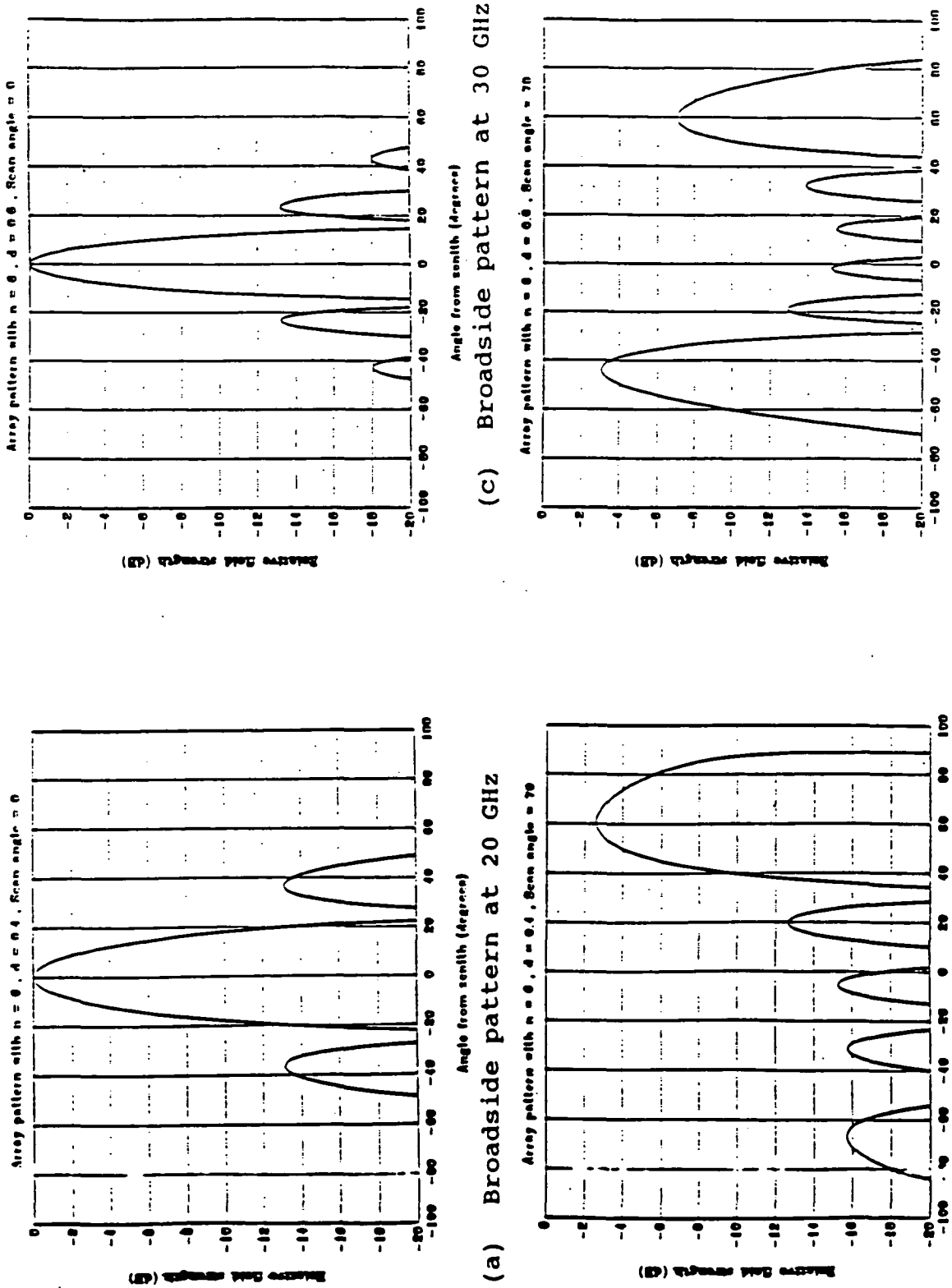

(a) Broadside pattern at 20 GHz

(b) 70° scanned pattern at 20 GHz

(c) Broadside pattern at 30 GHz

(d) 70° scanned pattern at 30 GHz

Figure 3. Patterns of a six element array at 20 and 30 GHz : 0.6 cm inter-element separation.

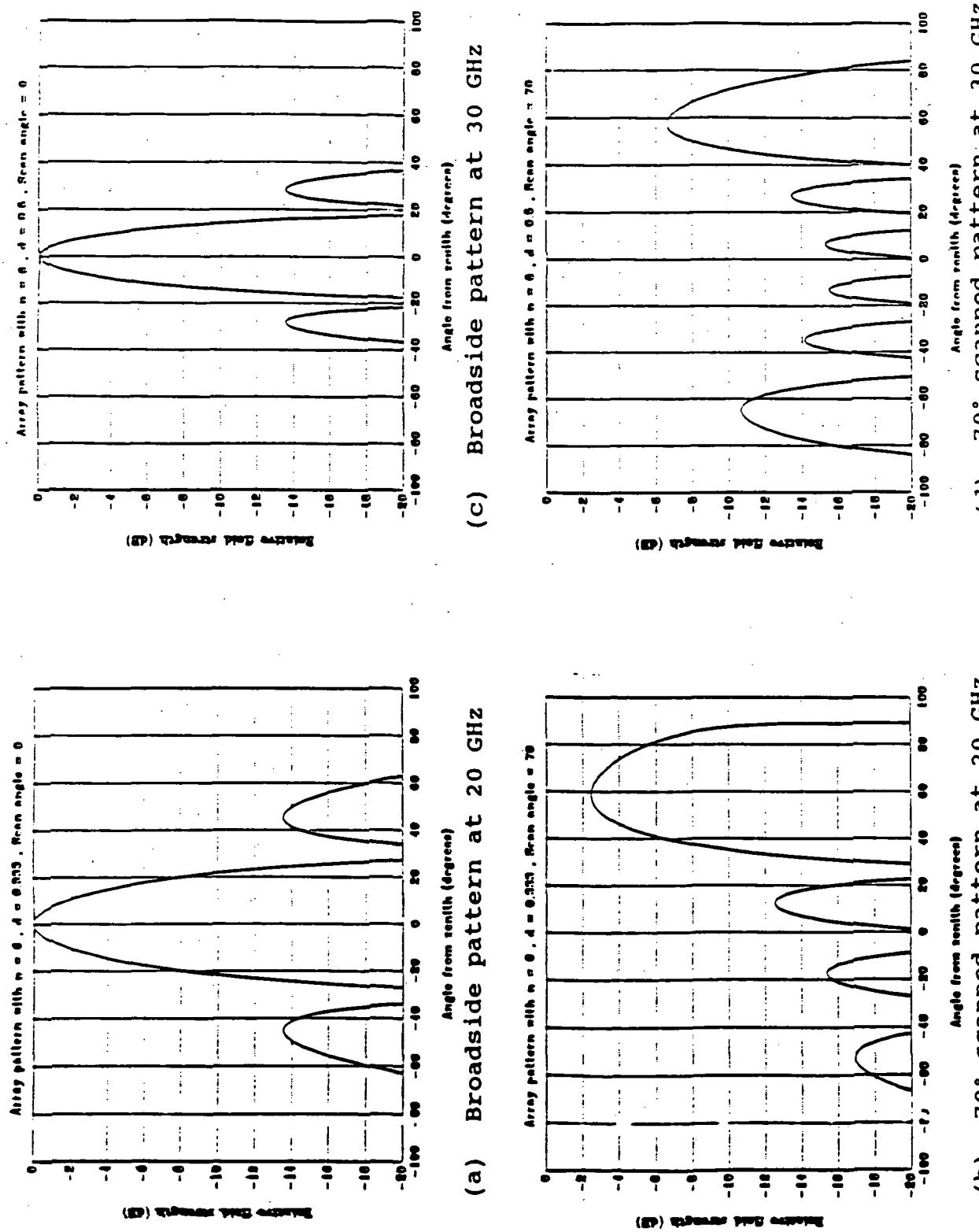

(a) Broadside pattern at 20 GHz

(b) 70° scanned pattern at 20 GHz

(c) Broadside pattern at 30 GHz

(d) 70° scanned pattern at 30 GHz

Figure 4. Patterns of a six element array at 20 and 30 GHz: 0.5 cm inter-element separation.

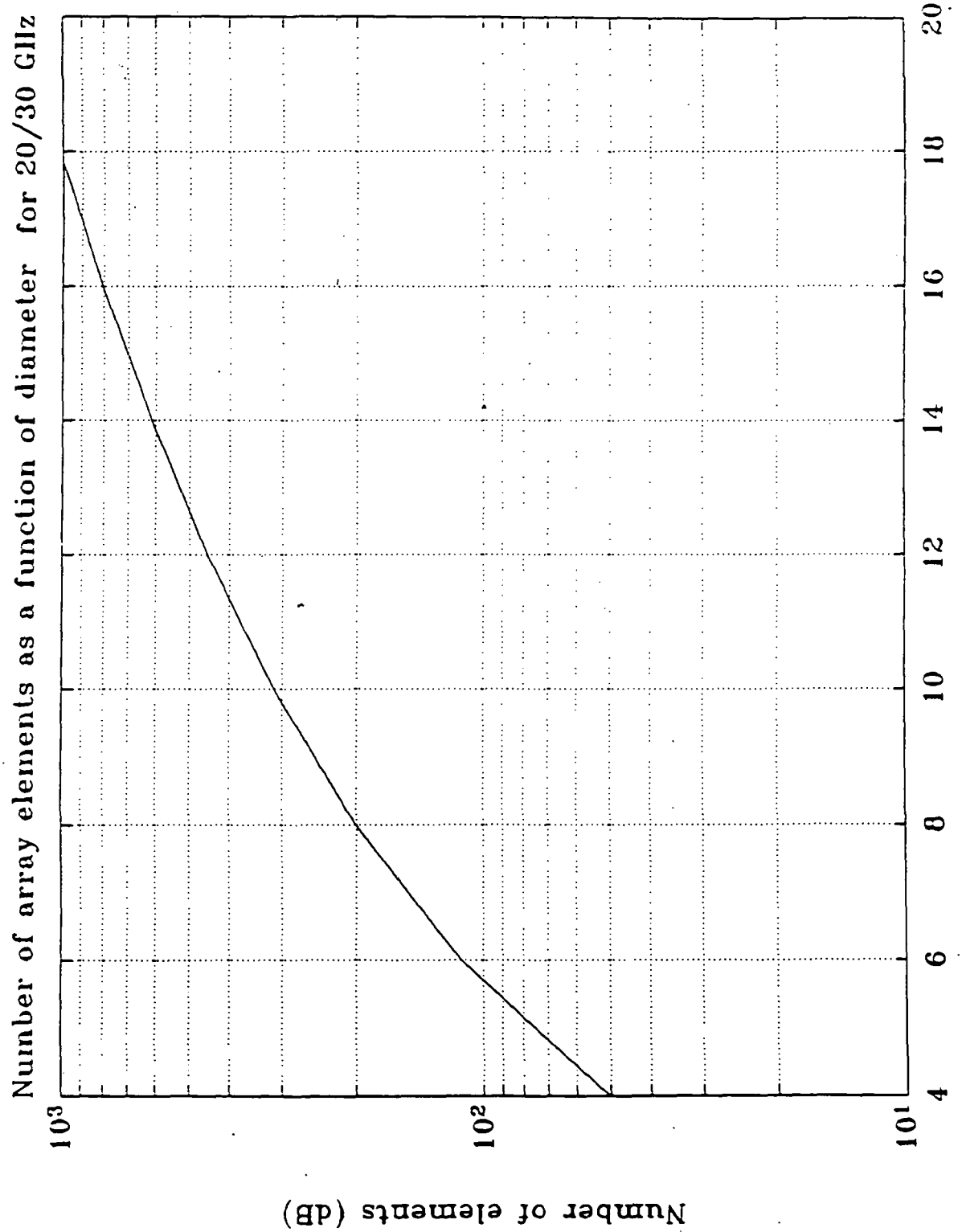

Figure 5. Number of elements versus array diameter in a 20/30 GHz array antenna.

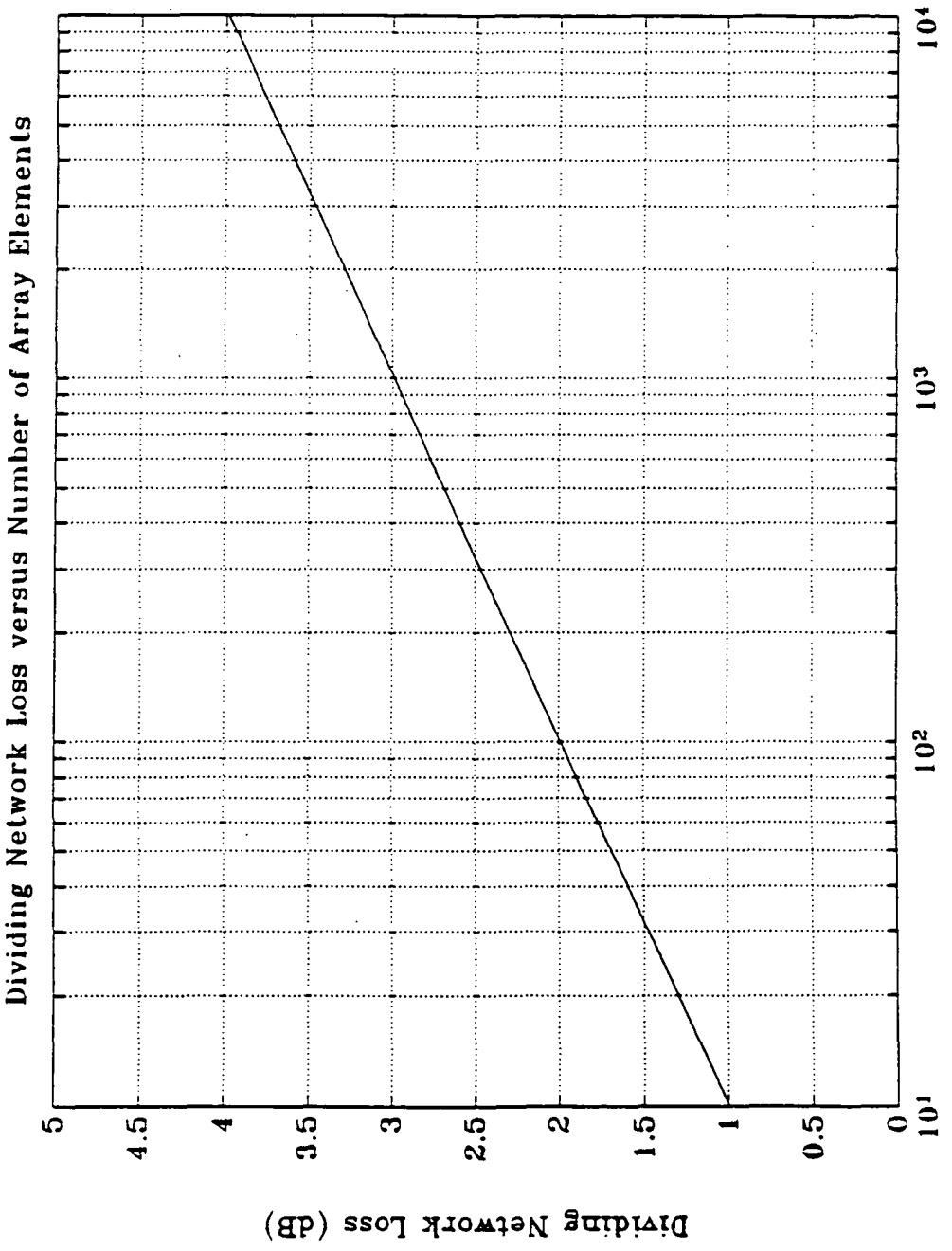

Figure 6. Dividing network loss as function of the number of array elements. 0.3 dB per two-way divider is assumed.

191

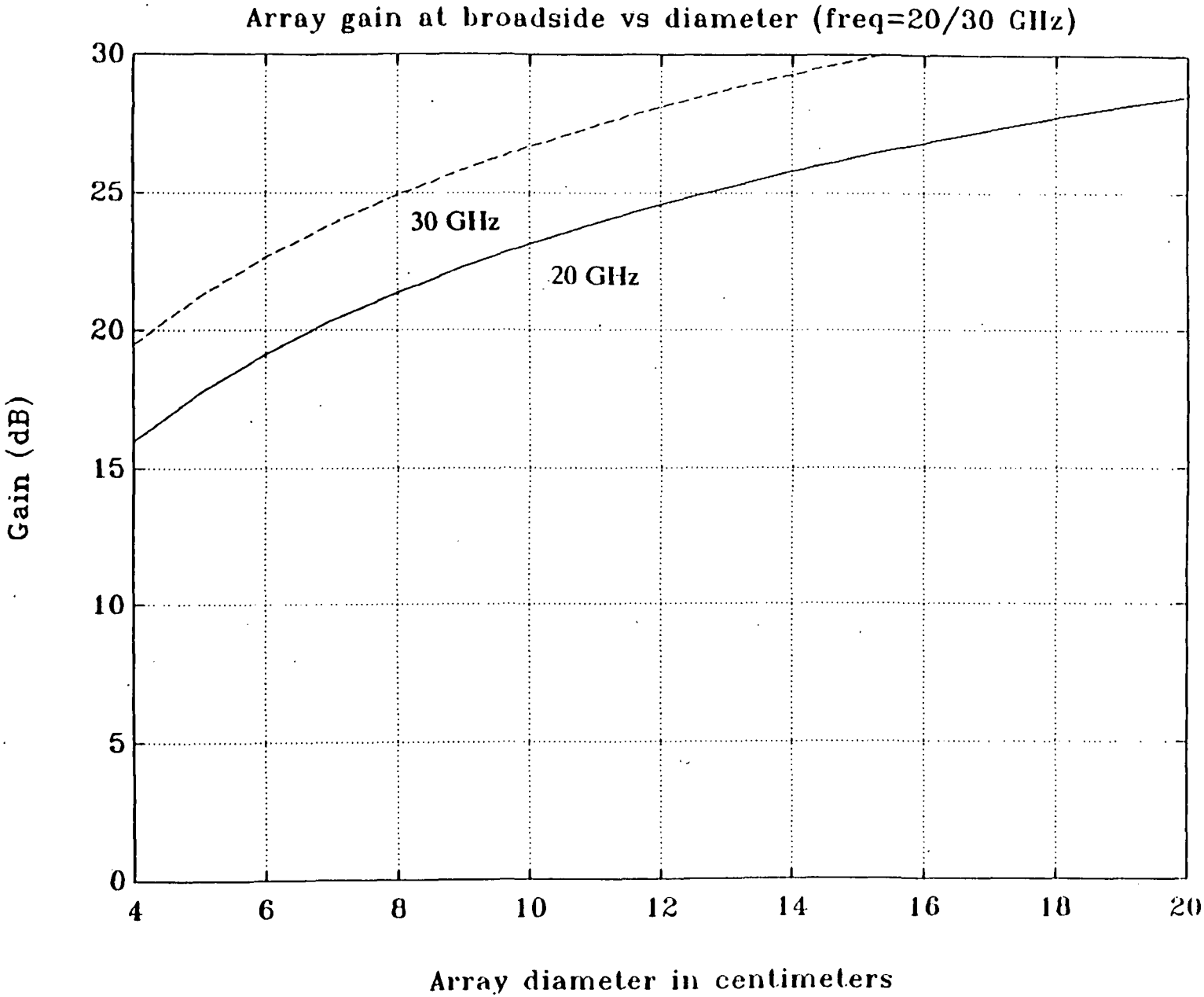

Figure 7. Mechanically steered (in both azimuth and elevation) array gain at 20 and 30 GHz as a function of diameter.

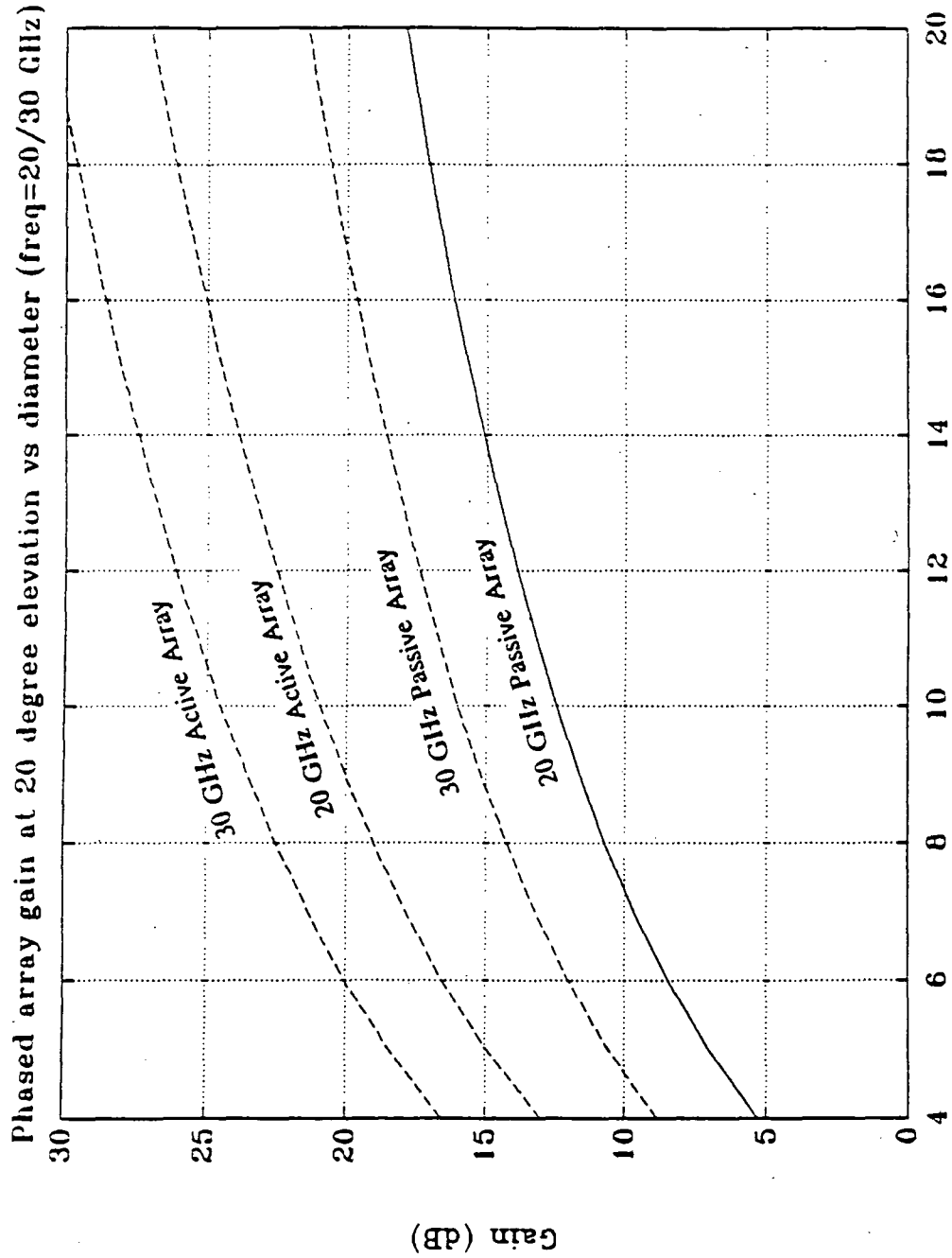

Figure 8. Phased array gain at 20 and 30 GHz as a function of diameter. Both active and passive arrays are considered.

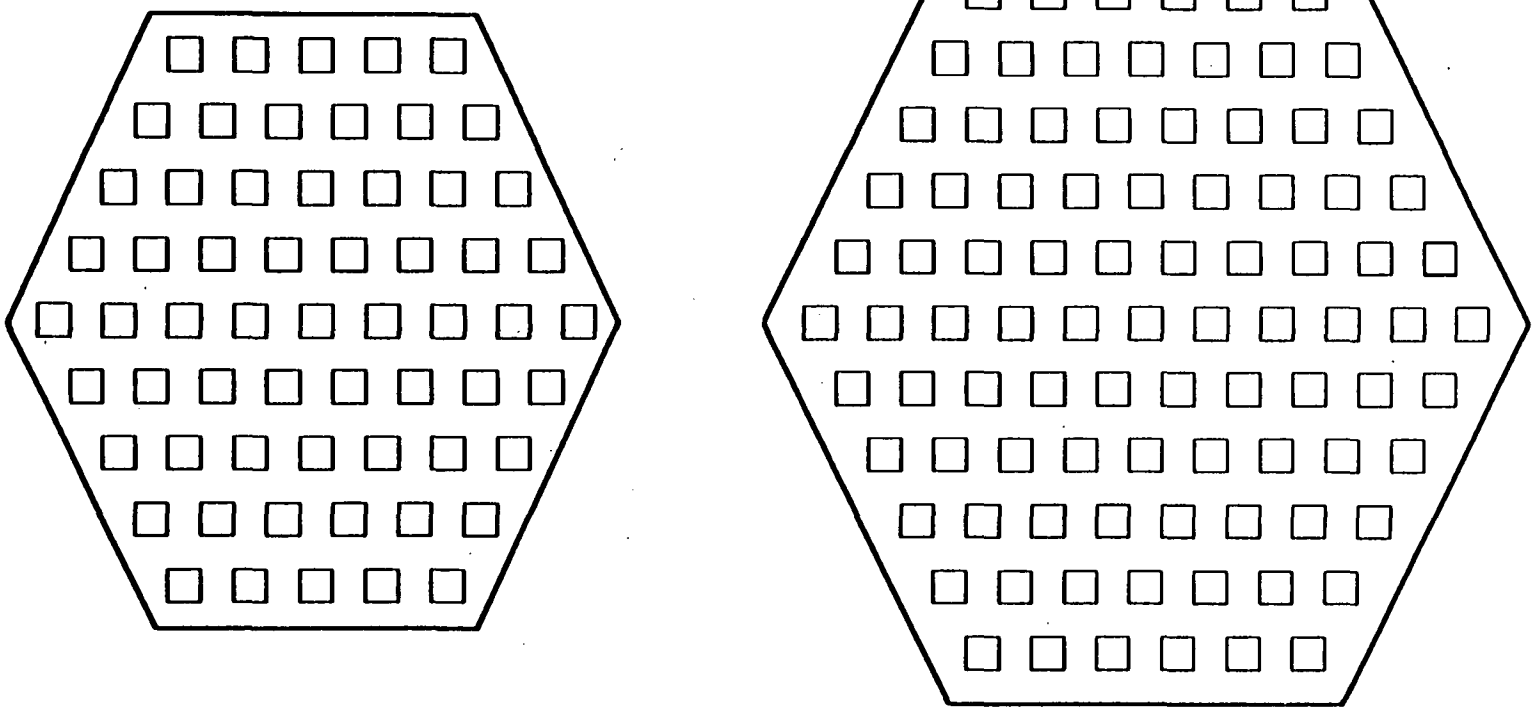

(b) 61 ELEMENTS

(b) 91 ELEMENTS

Figure 9. Hexagonal grid array configuration

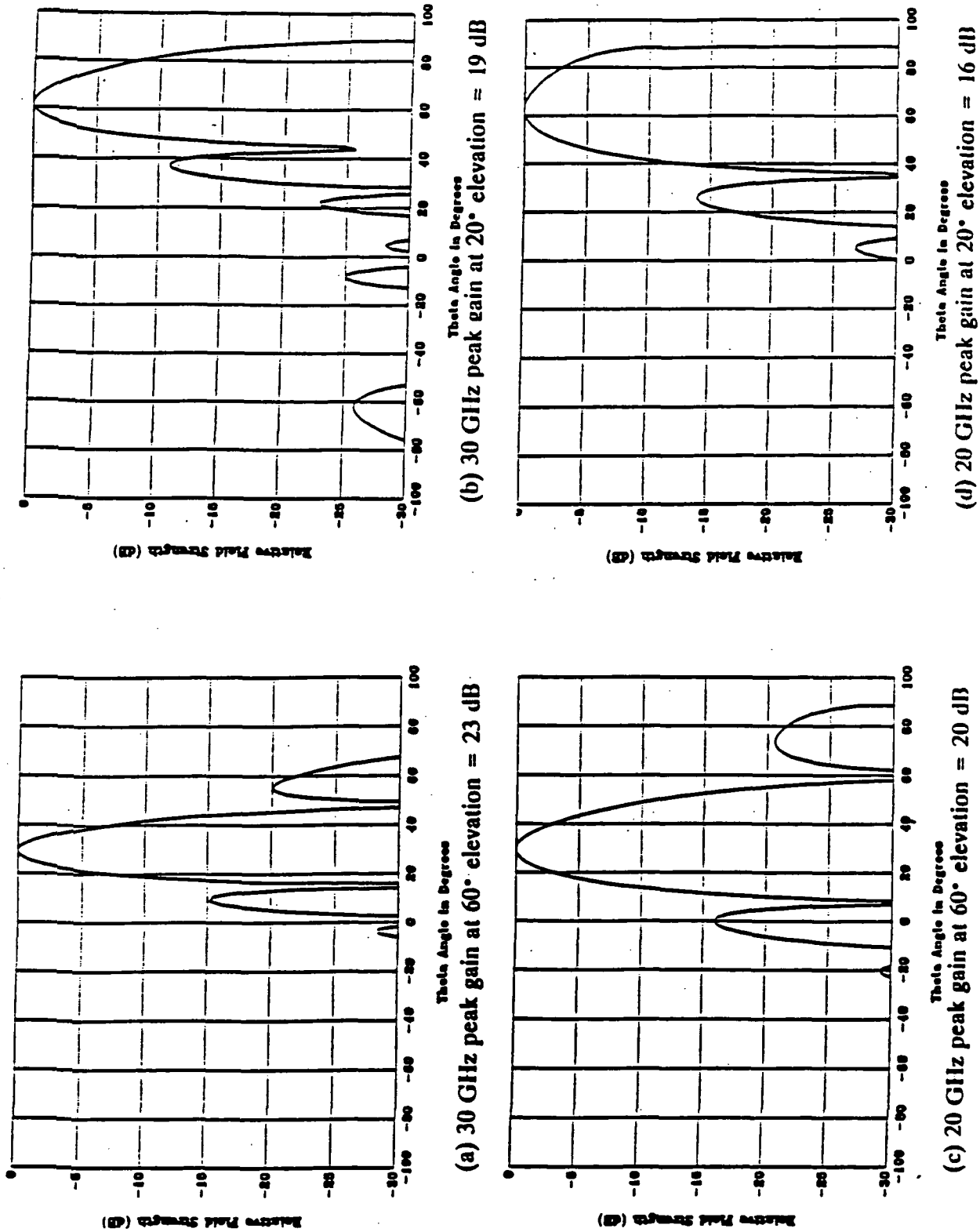

Figure 10. Typical far-field patterns of the 91-element hexagonal grid array for an electronically steered antenna

303

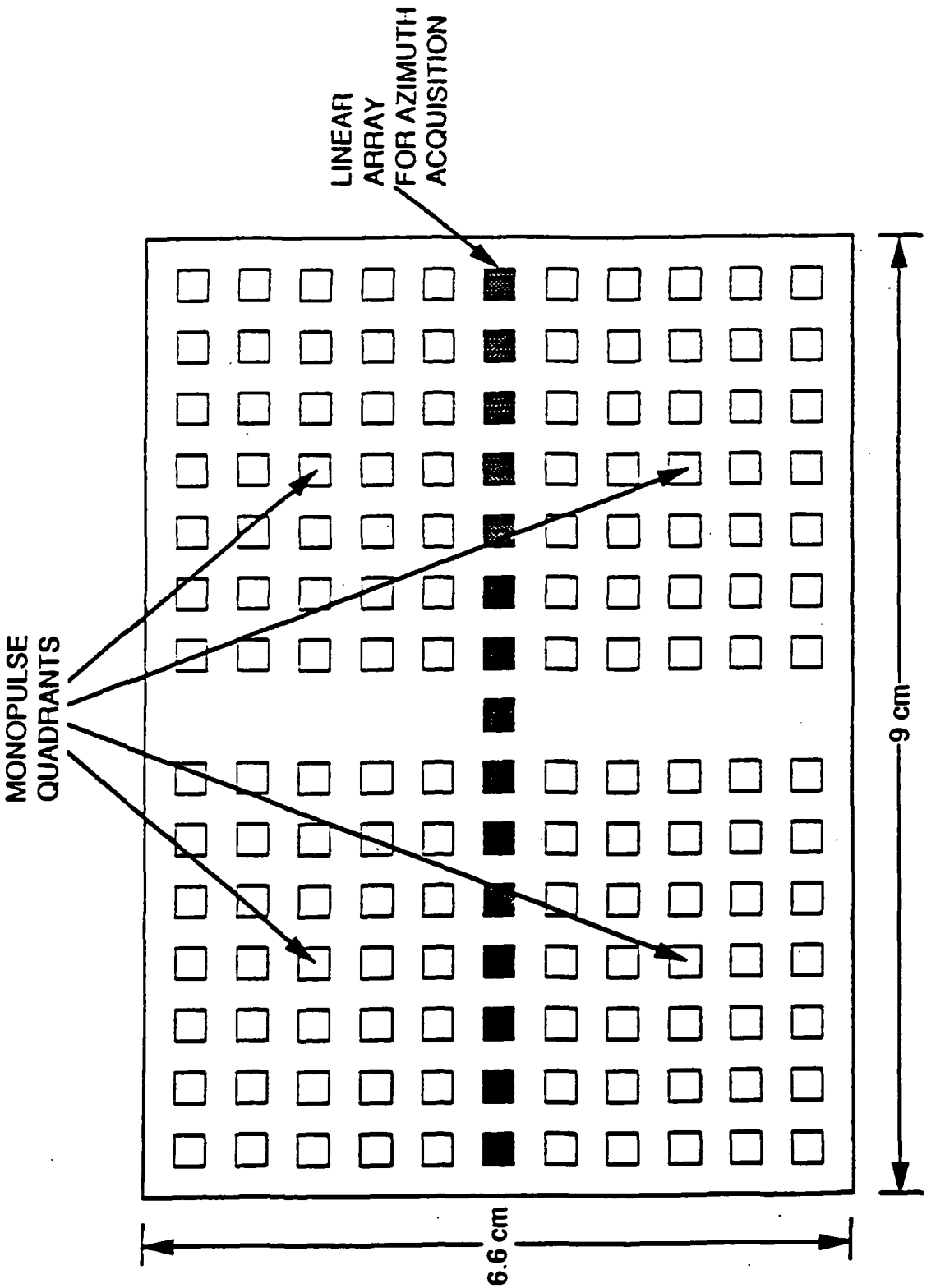

Figure 11. A typical rectangular grid array for a mechanically steered antenna.

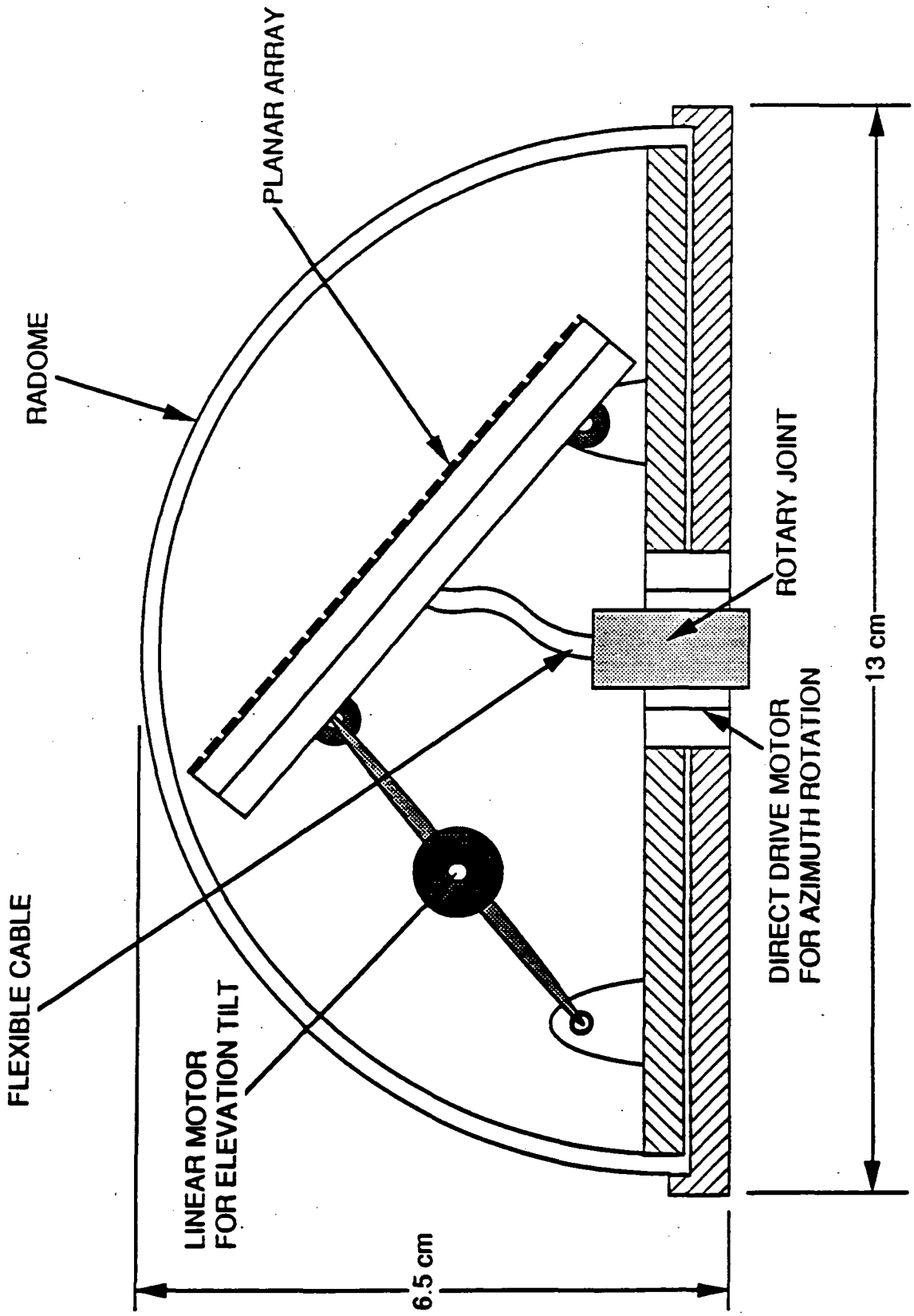

Figure 12. An implementation concept for a mechanically steered antenna.

201

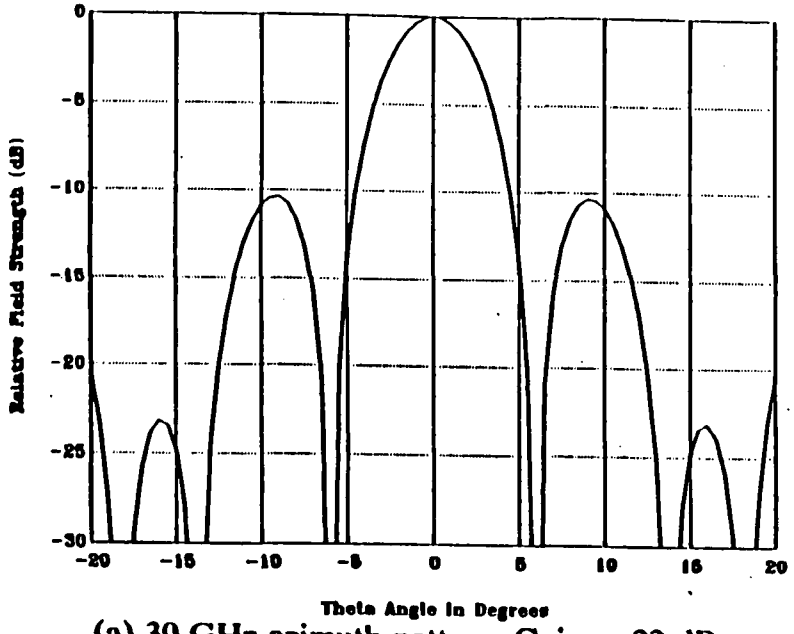

(a) 30 GHz azimuth pattern, Gain = 22 dB

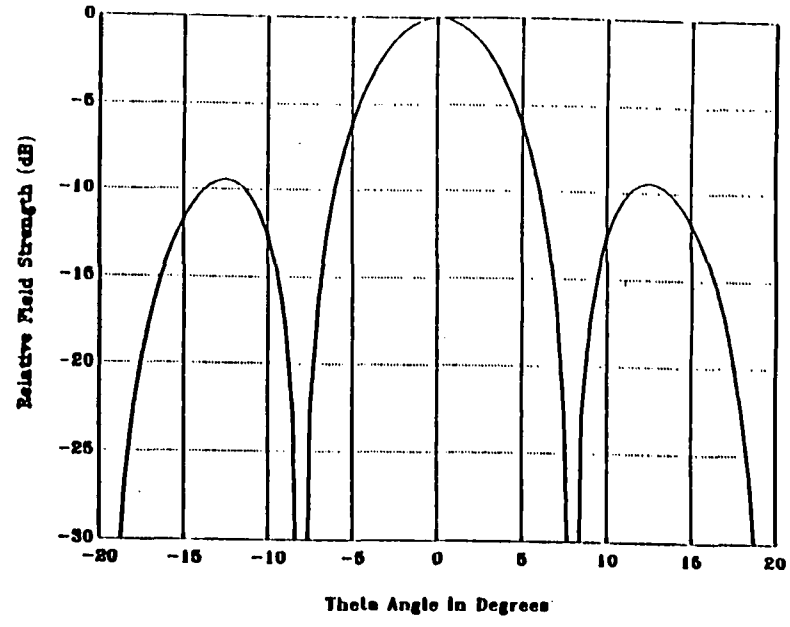

(b) 30 GHz elevation pattern, Gain = 22 dB

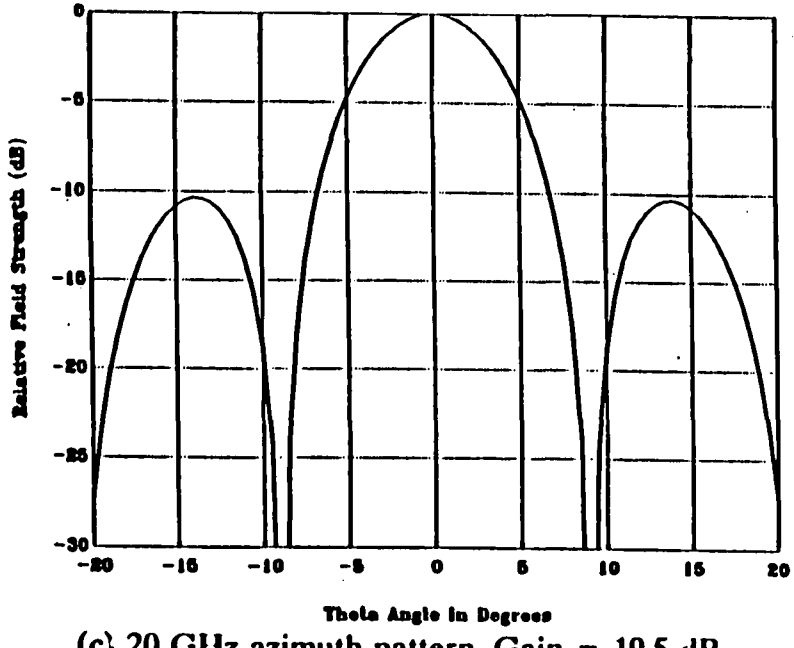

(c) 20 GHz azimuth pattern, Gain = 19.5 dB

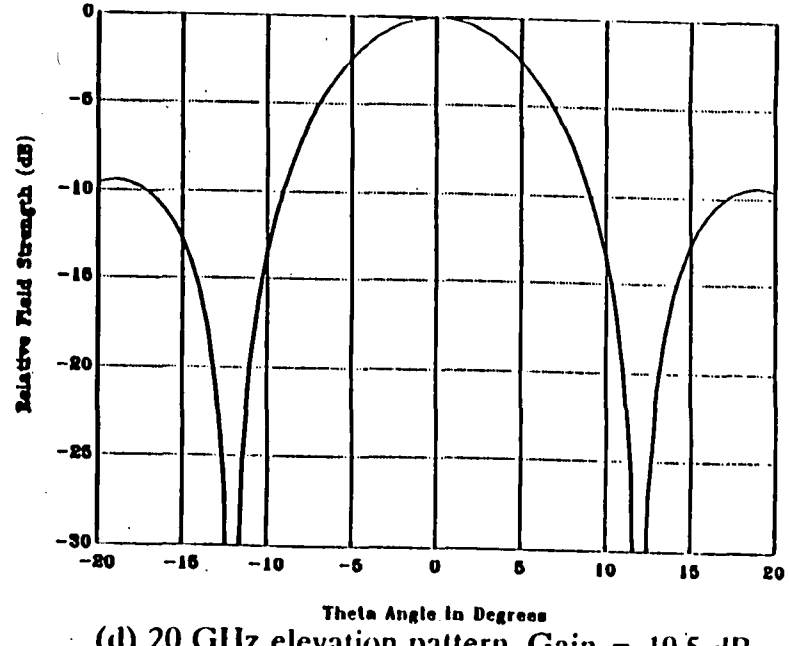

(d) 20 GHz elevation pattern, Gain = 19.5 dB

Figure 13. Typical far-field patterns for a mechanically steered antenna

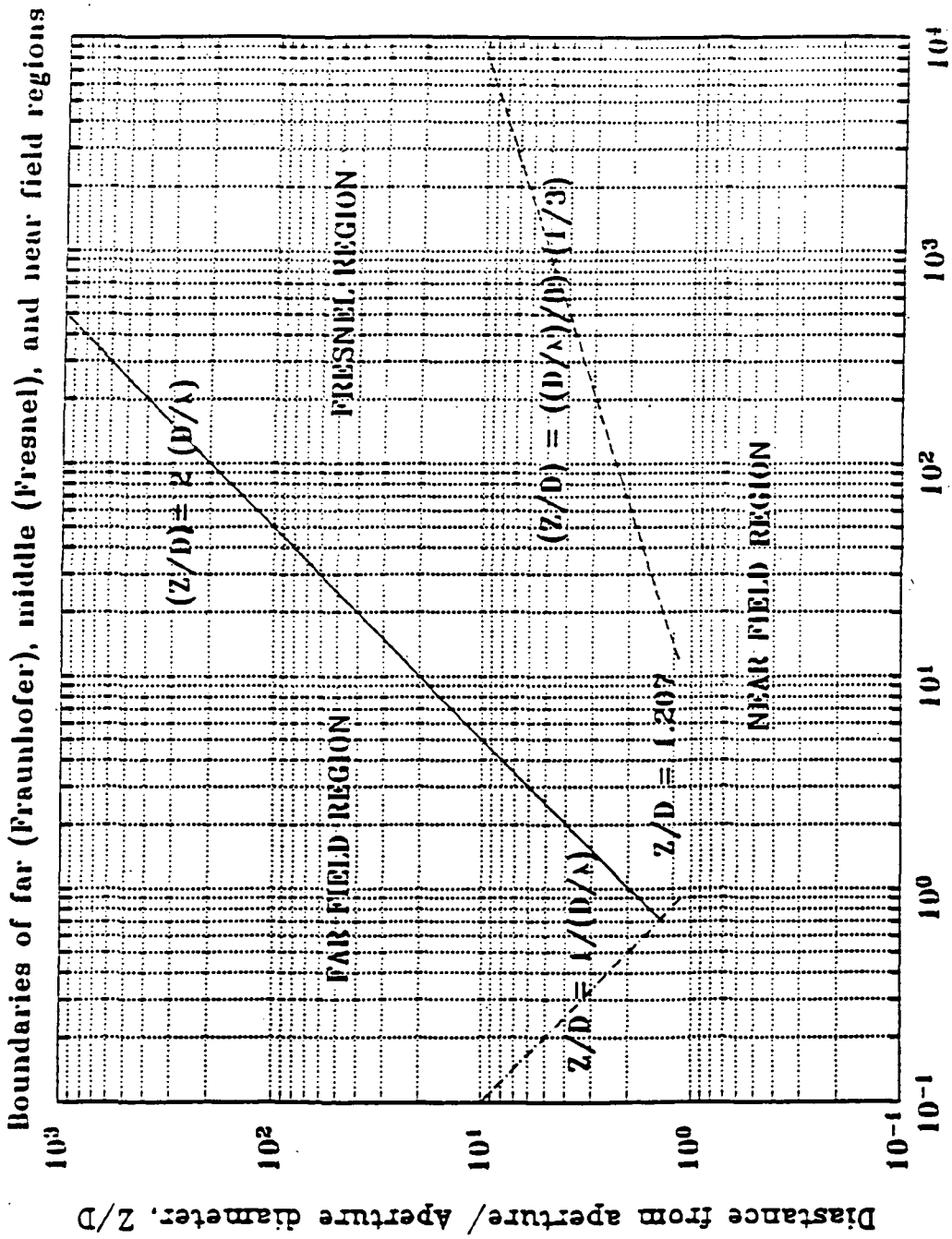

Figure 14. Boundaries of the near, mid(Fresnel), and far (Fraunhofer) field regions of an aperture antenna radiation

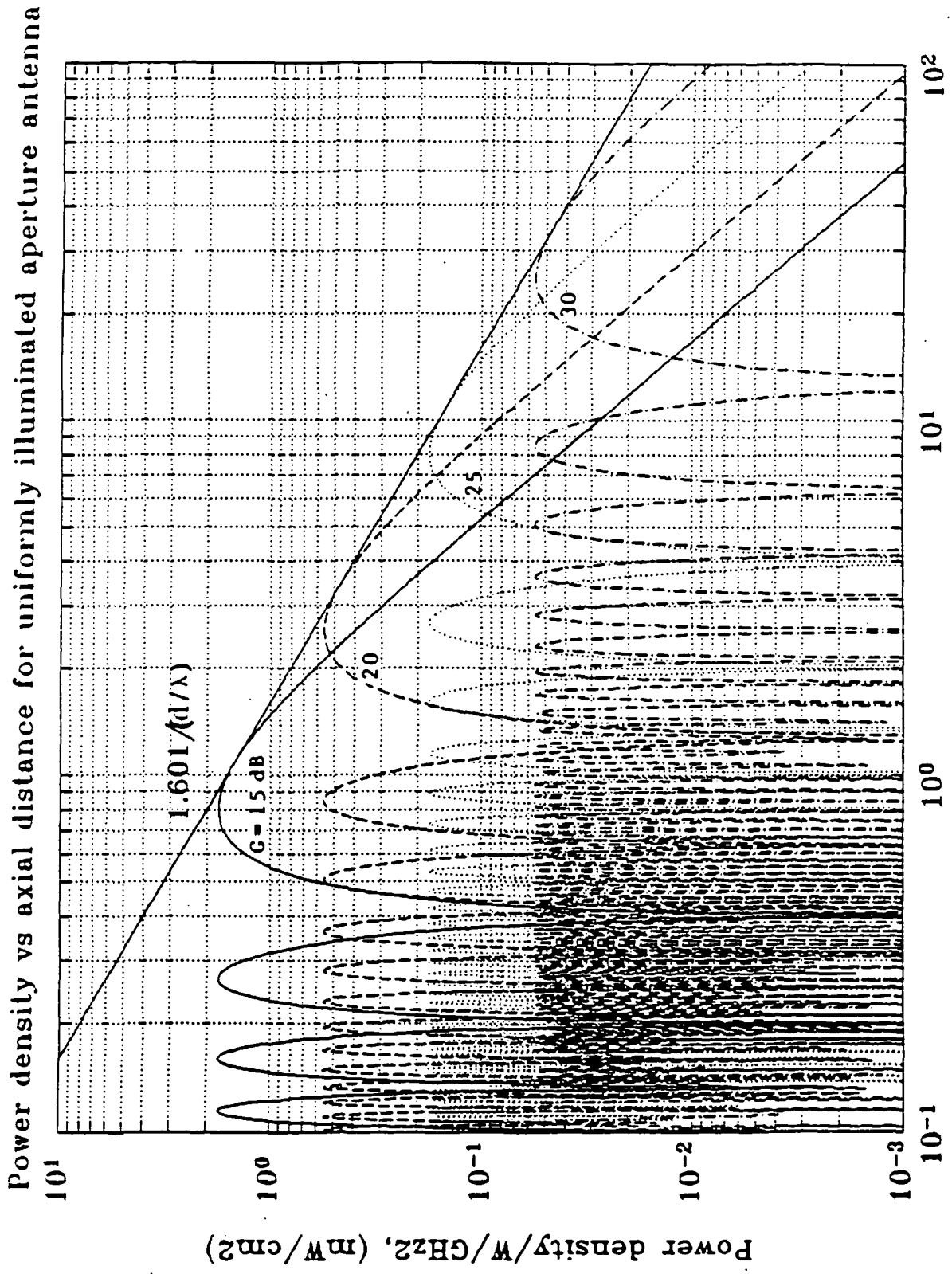

Figure 15. Normalized power density as function of the distance from the aperture for various antenna directivity levels.

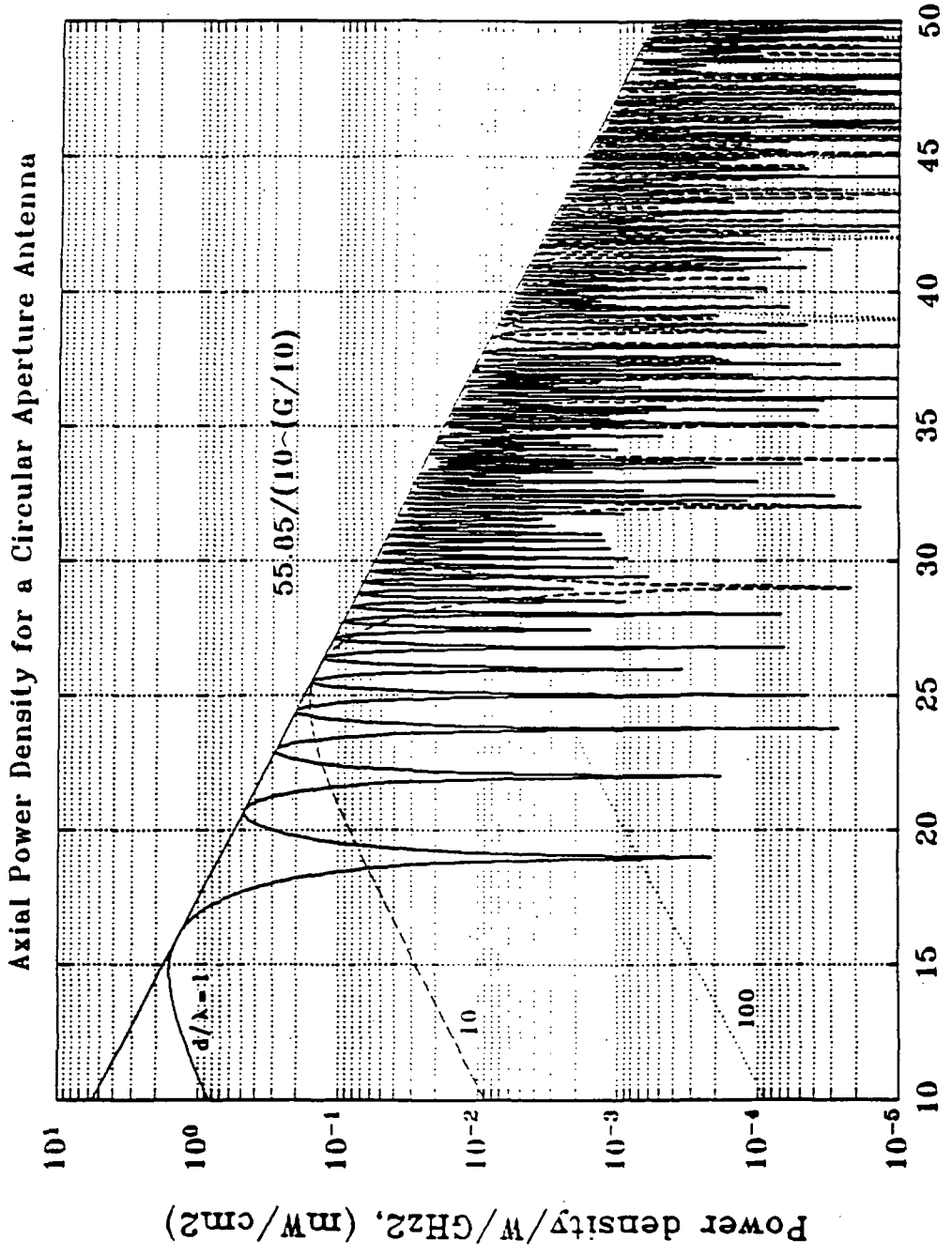

Figure 16. Normalized power density as a function of antenna directivity for various distances from the aperture

APPENDIX I. Gain and figure of merit (G/T) for PASS user terminal antennas (Vahraz Jamnejad)

The performance of the user terminal antennas for Personal Access Satellite System (PASS) can in general be characterized by only two parameters: i) Antenna gain in the transmit mode, ii) Antenna G/T in the receive mode. Indeed, since in principle the antenna may actually utilize two separate radiating apertures or set of radiating elements, different parts of the same aperture, or different subsets of the elements at the two modes of operation, we need to specify only one parameter for each mode of operation.

Thus, the transmit antenna is characterized solely by its gain, G_t and the receive antenna solely by its figure of merit, G_r / T. The concepts of gain and G / T specially when active array antennas are concerned, may not be quite clear and requires some explanation. Here we present a brief description of the gain and figure of merit for receiving antennas. We also take a look at G / T in some typical cases that may occur in actual systems.

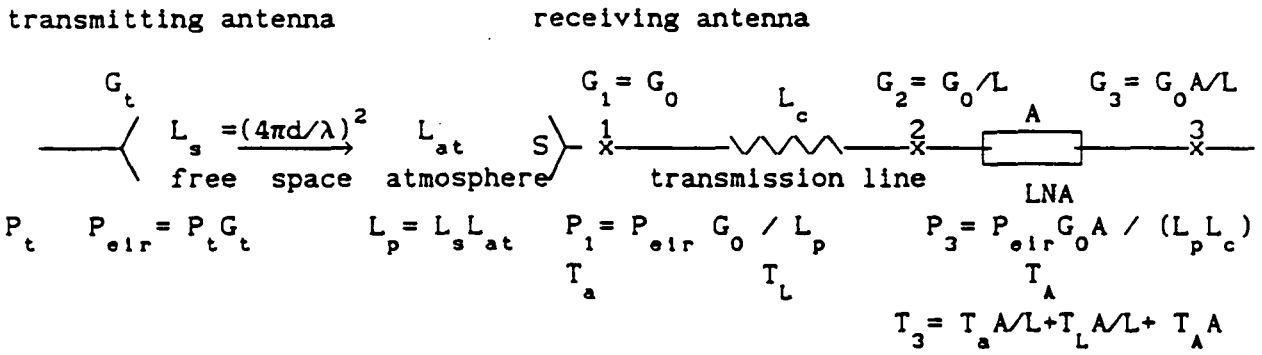

Figure 1. Diagram showing the transmit-receive path

With reference to figure 1, let's define the following parameters:

$G = \eta D = \eta_c G_0$,

$\eta = \eta_c \eta_p$ Beam forming efficiency,

η_p = Polarization efficiency,

η_c = Distribution network(circuit) efficiency,

D = Pattern Directivity,

G_0 = Gain of the antenna directly at the receiving aperture = $\eta_p D$.

Directivity of the antenna, is the ratio of the power density in a

desired direction (usually, the peak direction), to the average power density over the entire space. It includes all the losses associated with forming the antenna beam pattern. For example, we mention the aperture illumination taper and spillover, and surface roughness effects in reflector type antennas, and element tapering loss in arrays. We also include the cross-polarization loss in G_0 which is not usually included in directivity D.

However, we do not include the ohmic losses associated with antenna conducting surfaces, the circuit losses associated with the beam-forming network (such as power dividers and phase shifters), transmission line losses, etc. These losses can be lumped into a single loss figure, here referred to as antenna circuit loss, or beam-forming network efficiency and represented by, η_c, a number smaller than unity. Sometimes circuit loss is represented by the inverse of η_c as

$L_c = 1/\eta_c$ = Circuit Loss Factor (greater than unity).

Here, L_c represents the power lost in the network due to RF absorption and reflection. Strictly speaking, this relation is correct only if the circuit is perfectly matched to the antenna and the receiver, and if the losses are strictly ohmic (in conductors and lossy dielectrics), otherwise it is only an approximation.

Now, for a passive receiving antenna (which does not include any active amplifying elements) the gain, G, is directly measurable at a single physical point, while G_0 is not directly accessible and can only be indirectly deduced, by integration of the theoretically calculated or experimentally measured far field pattern. In an active array antenna where low noise amplifiers are present behind each element or subset of elements, the gain G is not quite meaningful unless one considers the amplifier gain as part of the overall antenna gain. But aperture gain G_0 serves a useful conceptual function in defining the figure of merit, G / T.

The signal power received at the antenna from the spacecraft, directly at input point 1 in Figure 1, is given as:

$$P_1 = \frac{P_t G_t}{4 \pi d^2} S$$

in which,

P_t = spacecraft transmitted power,

G_t = Spacecraft antenna gain,

d = distance from spacecraft to ground antenna, and

S = ground antenna receiving aperture.

Now defining, the Effective Isotropically Radiated Power for the spacecraft transmitting antenna as:

$$P_{eir} = P_t \; G_t,$$

and noting that effective receiving aperture is

$$S = \frac{4\pi}{\lambda^2} \; G_0 \; ,$$

we can rewrite P as:

$$P = \frac{P_{eir}}{(4\pi d/\lambda)^2} \; G_0$$

Defining free space path loss as

$$L_s = (4 \pi d / \lambda)^2,$$

Also representing atmospheric losses by

$$L_a = \text{Atmospheric losses,}$$

we write the total path loss as

$$L_p = L_s + L_a$$

Then The signal power directly at the input to the antenna is

$$P_1 = P_{eir} G_0 / L_p$$

For the arrangement shown in Figure 1, the power at the output of the low noise amplifier (LNA) is given as

$$P_3 = P_{eir} G_0 \; A \; / \; (L_p L_c)$$

The following discussion regarding the noise temperature definitions and calculations are based partially on materials in References [1-3].

The noise temperature directly at the input to the antenna is due to the contributions from space, atmosphere, and ground antenna environment and is dependent on the pattern and directivity of the antenna. It is represented by

$$T_a = \text{Antenna noise temperature}$$

and is in general given by

$$T_a = \frac{1}{4\pi} \iint T_s(\theta,\phi) \; G_0(\theta,\phi) \; \sin(\theta) \; d\theta \; d\phi,$$

in which T_s is the brightness temperature of the discrete or distributed sources in the space around the antenna as function of angle. This integral can be divided over two diffrent regions of space : the upper hemisphere facing the sky (elevation angle $\gamma>0$) and the lower hemisphere facing the ground ($\gamma < 0$). IN the lower half the temperature can be assumed constant and equal to 300° K. In the upper hemisphere this temperature as a function of frequency and for various elevation angles is presented in Figure 2. As can be seen, the temperature in the Ka-band is primarily due to Oxygen and water vapor absorption and peaks at about 20 GHz. Here, we have not considered any localized and/or man-made sources of noise which may be present. The calculation of the above integral is in general requires the actual antenna beam pattern. But in most applications and for relatively narrow beams we can write

$$T_a = \eta_{bl} \times 300 + \eta_{sl} \times T_{sl} + \eta_{ml} \times T_{ml},$$

in which η_{bl} represents the sidelobe efficiency or the percentage of power radiated through the sidelobes. Here by sidelobes we mean all the lobe above the horizon, exclusive of the main beam. Backlobe efficiency refers to the percentage of power radiated below the horizon of the antenna ($\gamma<0$), and finally η_{ml} refers to the percentage of power in the main lobe or beam between the first nulls. T_{sl} and T_{ml} are average temperatures in the main beam and sidelobe directions. For typical directive antennas under consideration we can assume

$$\eta_{ml} \cong 0.8, \ \eta_{sl} \cong 0.1, \ \eta_{bl} \cong 0.1.$$

Consulting Figure 2, the following average temperatures can be assumed at 20 GHz, and for the main beam direction of about 45 degrees above the horizon:

$$T_{ml} \cong T_{bl} \cong 50^\circ \text{ K},$$

The antenna noise temperature is then

$$T_a \cong 0.1 \times 300 + 0.1 \times 50 + 0.8 \times 50 = 75$$

In practice the range of the backlobe with noise temperature of 300 should be extended at least a few degrees above the horizon to account for the hilly terrain, trees and building effects. This may increase the backlobe percentage of power up to 0.2, resulting in the total temperature of

$$T_a \cong 100^\circ \text{ K}$$

The lossy circuit with the loss factor L has a noise temperature which can in general be written as

$$T_L = (F_L - 1) \ T_0$$

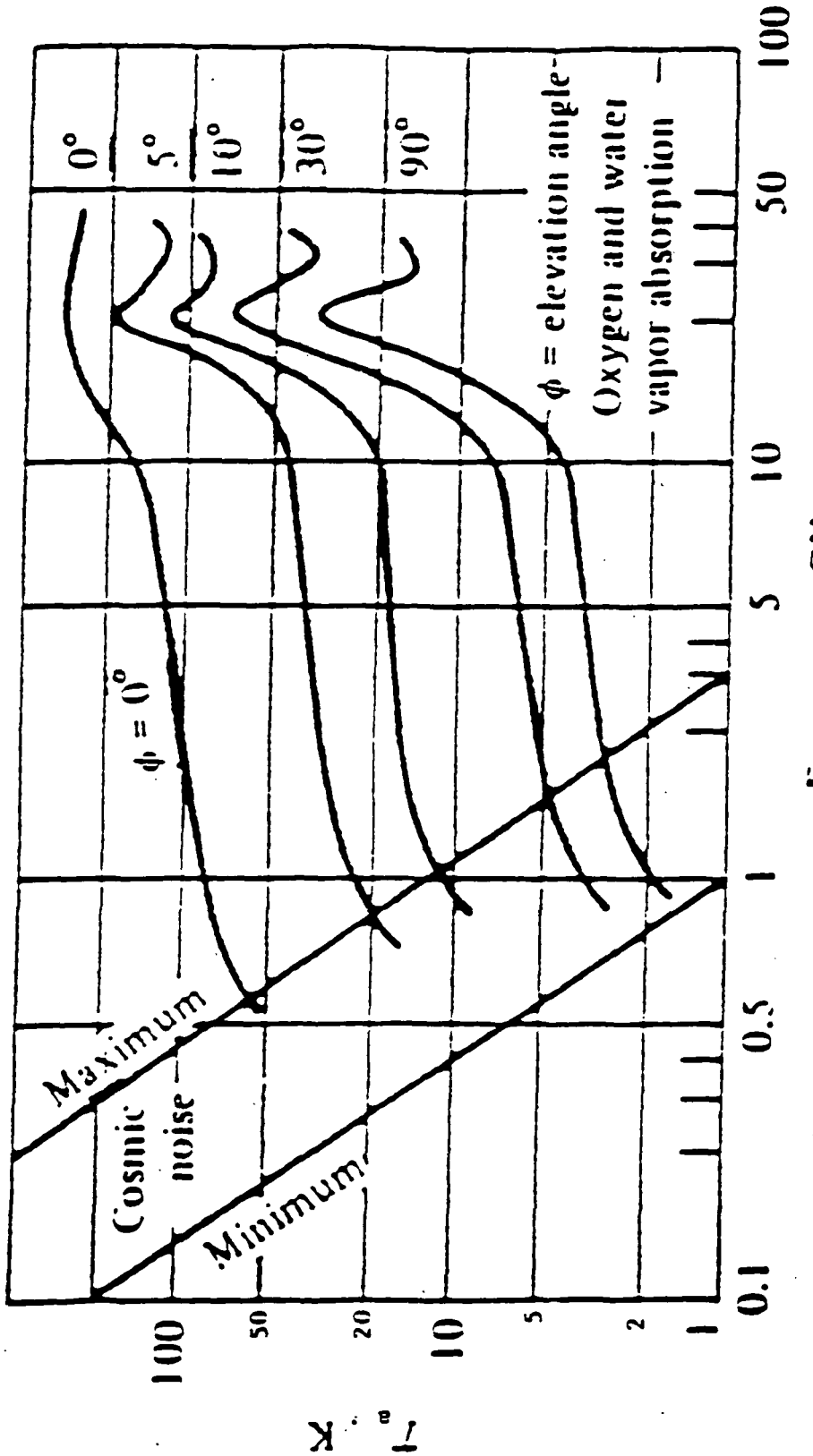

Figure 2. Microwave antenna noise temperature (from Reference 11).

This equation provides a definition for the noise figure F_L. This noise temperature is defined at the input to the lossy circuit.

For a general two-port network as shown in Figure 3, the noise contribution to a load is quite complicated and is given by

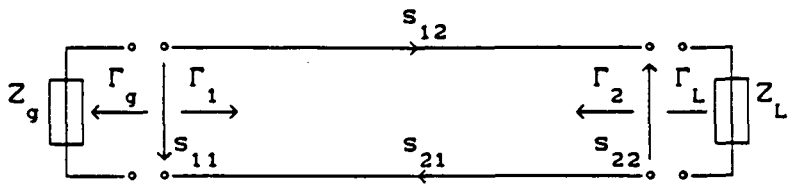

Figure 3. Schematic diagram of a two-port network

$$P_N = \frac{(1-|\Gamma_L|^2)\left\{1-|s_{22}+(s_{21}s_{12}-s_{11}s_{22})\,\Gamma_g|^2-(1-|\Gamma_g|^2)\,|(1-s_{22}\Gamma_L)|^2\,|s_{21}|^2\right\}}{|\,1-s_{11}\,\Gamma_g-s_{22}\,\Gamma_L-(s_{21}s_{12}-s_{11}s_{22})\,\Gamma_g\,\Gamma_L\,|^2}$$

This is in general too complicated to work with. For simplicity we assume this network to be equivalent to a lossy transmission line. Then, the loss for a lossy transmission can in general be given as

$$1 / L = |(1-\Gamma_i\Gamma_o e^{-2\gamma l})|^2\, e^{-2\alpha l},$$

in which Γ_i, and Γ_o are the reflection coefficients towards the input and output sides, γ is the propagation constant, α is the attenuation constant, and l is the line length. for most applications where there is a good match (vswr <2) we can write

$$L \cong e^{2\alpha l}$$

With this approximation, the noise figure is given as

$$F_L = L + (1-M_1)\,(1-1/L)$$

in which M_1 is the mismatch factor at the input junction. It is given by

$$M_1 = \frac{4\,R_l R_r}{|Z_l+Z_r|^2} = 1 - |\Gamma_i|^2,$$

in which Z_l, Z_r, R_l, R_r are impedance and resistance figures to the right and the left of the junction.

The noise figure F_L is ideally under matched conditions ($M_1 = 1$) is

then given as

$$F_L = L$$

In this study an ambient noise temperature of $T_0 = 300^\circ K = 27^\circ C$ is assumed throughout. We think this is a more realistic number than the figure $290^\circ K = 17^\circ C$ used by some in the literature.

The noise temperature of the amplifier is similarly given by

$$T_A = (F_A - 1)\, T_0$$

with

F_A = Amplifier noise figure

Now for a cascaded system with a number of loss and amplification stages as shown in Figure 4, the total noise referenced to the input point is given as

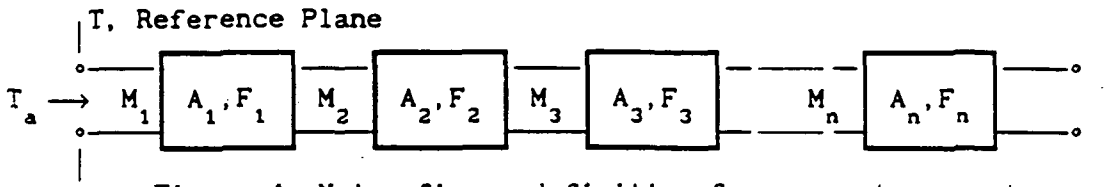

Figure 4. Noise figure definition for an n stage system

$$T = T_a + \frac{(F_1 - 1)}{M_1} T_0 + \frac{(F_2 - 1)}{M_2 (M_1 A_1)} T_0 + \frac{(F_3 - 1)}{M_3 (M_1 A_1 M_2 A_2)} T_0 + \ldots + \frac{(F_n - 1)}{M_n \prod_{i=1}^{n-1} (M_i A_i)}$$

in which F_n is the noise figure of the nth stage, A_n is the amplification or loss at each stage, and M_n is the matching factor at the input to each stage as defined previously.

Now the total noise temperature at point 3 of Figure 1, that is the output of the amplifier, and assuming perfect impedance match throughout, may be written as,

$$T_3 = T_a\, A / L_c + T_L\, A / L_c + T_A A$$

$$= (T_a + T_L + T_A L_c) (A / L_c)$$

In this and following equations we have used L to represent L_c (the circuit loss) for simplicity of notation.

The noise power associated with a temperature T is given by

$$N = K B T$$

K = Boltzman's constant = 1.38×10^{-23} J/ K° = -228.6 dB,
B = receiver bandwidth,
T = total noise temperature at the input to the receiver.

Therefore the carrier power to noise ratio at point 3 of figure 1, i.e., the output of the receiver is given by

$$C / N = (P_{eir} / K B L_s) (G_3 / T_3) = (P_{eir} / K B L_s) (G_1 / T_{31})$$

where $G_1 = G_0$,

and $T_{31} \equiv T$ is the equivalent noise temperature transferred from point 3 to point 1 and given by

$$T_{31} \equiv T = T_a + T_L + T_A L$$

It should be remarked that as long as the final reference point of the G / T specification is fixed the value of this figure of merit calculated at any previous stage remains unchanged. Thus for G/T referenced to the point 3 in Figure 1, we can write

$$G / T\Big|_1 = \frac{G_1}{T_a + T_L + T_A L},$$

$$G / T\Big|_2 = \frac{G_1 / L}{T_a / L + T_L / L + T_A} = \frac{G_1}{T_a + T_L + T_A L}$$

$$G / T\Big|_3 = \frac{G_1 A / L}{T_a A / L + T_L A / L + T_A A} = \frac{G_1}{T_a + T_L + T_A L}$$

However, if the arrangement and location of the amplifier in the system is changed the G/T will change accordingly. To demonstrate this let's consider the following three cases. In all three cases G / T is referenced to point 3.

Case 1) Amplifier after the lossy circuit:

With reference to Figure 5(a), notice that the lossy circuit in this case not only contributes directly to the overall noise temperature, it, in effect, increases the noise contribution of the amplifier. This is consistent with the fact that a lossy circuit stage increases the noise contribution of the later stages.

316

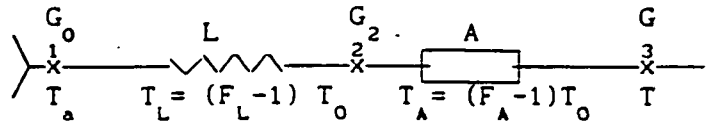

Figure 5(a)

$$G = G_0 \, A / L$$

$$T_3 = T_a A / L + T_L \, A / L + T_A \, A = (T_a + T_L + T_A \, L \,) \, A / L$$

$$G / T = \frac{G_0}{T_a + T_L + T_A \, L}$$

An important fact here is that the power gain of the LNA does not enter this definition. As an example let's assume

$T_a = 100^\circ$, $G_0 = 25\text{dB} \cong 100$,

$L = 5\text{ dB} \cong 3.16$, $F_L = 3.16$,

$A = 20\text{ dB} = 100$, $F_A = 3.5\text{ dB} \cong 2.24$,

Then

$T_L = (3.16-1) \cdot 300 = 648.7$,

$T_A = (2.24-1) \cdot 300 = 371.6$,

$T = 100 + 648.7 + 371.6 \times 3.16 = 1922.9^\circ \cong 32.84$ dB

$G / T = 100 / 1922.9 = 20 - 32.84 = -12.84$ dB

Without the 5 dB network loss the system noise temperature would be

$T = 100 + 371.6 = 471.6 = 26.74$ dB

$G / T = 100 / 472 = 20 - 26.74 = -6.74$ dB

This figure would be even better for an amplifier with lower noise figure. Thus with a no loss BFN and an amplifier noise figure of 2 dB would result in $G / T = -4.4$ dB. Therefore the effect of the network loss on the G / T could be more or less than the loss value in dB, depending on the LNA noise figure. A noisy LNA could completely mask the antenna as well as the network noise temperature effects. While for a good LNA, the network loss could have a very significant effect much larger than its loss value in dB on the overall figure of merit.

Case 2) Amplifier before the lossy circuit:

With reference to Figure 5(b), notice that the contribution of the lossy circuit noise temperature has been reduced by the amplification factor A. This is consistent with the fact that an amplifying stage reduces the noise contribution of the following stages.

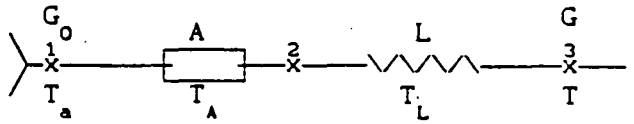

Figure 5(b).

$$G = G_0 \, A / L$$

$$T_3 = T_a \, A / L + T_A \, A / L + T_L / L = (T_a + T_A + T_L / A) \, A / L$$

$$G / T = \frac{G_0}{T_a + T_L / A + T_A}$$

Notice that in this case the power gain of the amplifier does enter the G/T equation. For the example of case 1 we now have:

$T = 100 + 648.7 / 100 + 371.6 = 478.1^{\circ} \cong 26.8$ dB
$G / T = 100 / 478.5 = 20 - 26.8 = -6.8$ dB

As can be seen the G/T is increased by about 3.7. The increase can be higher if the noise figure of the LNA can be further reduced. For example for a noise figure of 2 dB, the G / T is increased to -4.5 dB, a 6 dB improvement compared to the first passive case.

Case 3) Amplifiers before and after the lossy circuit:

With reference to Figure 5(c) which is a compromise case between the previous two cases.

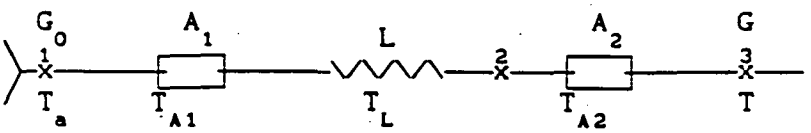

Figure 5(c)

$$G = G_0 \, A_1 A_2 / L$$

$$T_3 = T_a A_1 A_2 / L + T_{A1} A_1 A_2 / L + T_L \, A_2 / L + T_{A2} \, A_2$$

$$= (T_a + T_{A1} + T_L / A_1 + T_{A2} \, L / A_1) \, A_1 A_2 / L$$

$$G / T = \frac{G_0}{T_a + T_{A1} + T_L / A1 + T_{A2} \, L / A1}$$

Now let's consider an example similar to the first case in which the LNA is

218

split into two stages one before and one after the lossy network, each with a 10 dB power gain and a noise figure of 3.5 dB. Then we have,

$T = 100 + 371.6 + 648.7 / 10 + 371.6 \times 3.16 / 10 = 653.9^{\circ} \cong 28.15$ dB
$G / T = 100 / 654.35 = 20 - 28.16 = -8.15$ dB

It is seen that the result falls somewhere in between the previous two cases. The above examples are included in the following table which considers a more general case with two loss and two amplification stages as shown in Figure 6. The relevant formulas are then

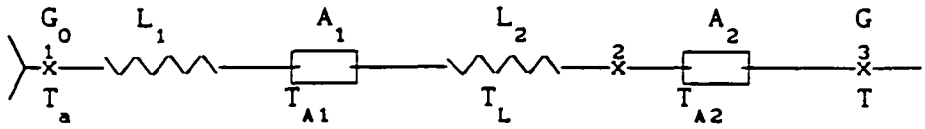

Figure 6

$$G = G_0 A_1 A_2 / (L_1 L_2)$$

$$T_3 = T_a A_1 A_2 / (L_1 L_2) + T_{L1} A_1 A_2 / (L_1 L_2) + T_{A1} A_1 A_2 / L_2 + T_{L2} A_2 / L_2 + T_{A2} A_2$$

$$= (T_a + T_{L1} + T_{A1} L_1 + T_{L2} L_1 / A_1 + T_{A2} L_1 L_2 / A_1) [A_1 A_2 / (L_1 L_2)]$$

$$G / T = \frac{G_0}{T_a + T_{L1} + T_{A1} L_1 + T_{L2} L_1 / A1 + T_{A2} L_1 L_2 / A1)}$$

TABLE 1. SYSTEM NOISE TEMPERATURE AND G/T FOR T= 100° K, G_0= 20 dB

Case	BFN_1 Loss dB	LNA_1 NF, dB	LNA_1 GAIN, DB	BFN_2 Loss dB	LNA_2 NF, dB	LNA_2 GAIN, dB	T, °K	G/T, dB
0a	-	-	-	0	2	20	275.5	-4.4
0b	-	-	-	0	3.5	20	471.6	-6.74
1a	-	-	-	5	2	20	1303.2	-11.15
1b	-	-	-	5	3.5	20	1923.9	-12.84
2a	-	2	20	5	-	-	281.9	-4.5
2b	-	3.5	20	5	-	-	478.1	-6.8
3a	-	2	10	5	2	10	395.8	-5.97
3b	-	3.5	10	5	3.5	10	654.0	-8.15
4a	1	2	20	4	-	-	404.3	-6.07
4b	1	3.5	20	4	-	-	651.2	-8.14
5a	1	2	10	4	2	10	511.2	-7.08
5b	1	3.5	10	4	3.5	10	820.1	-9.14

Based on the cases considered, it is obvious that in antennas with relatively lossy feed distribution networks pre-amplification at the immediate input to the antenna is necessary. This is particularly true in arrays with multiple radiating elements where loss in the distribution network with multiple levels of dividing and combining is quite substantial. The use of amplifiers at the antenna element level as shown in Figures 7(a,b) would then be indeed necessary.

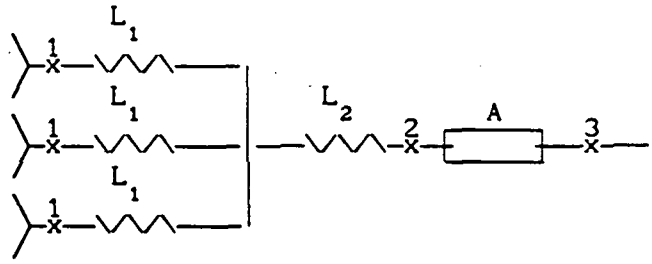

Figure 7(a). Single point amplification in an array

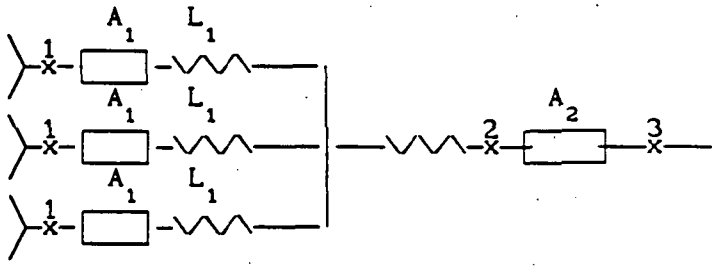

Figure 7(b). Amplification at the radiating element level

REFERENCES

[1] R. E. Collin, *Antennas and Radio Wave Propagation*. Chapter 5.4 McGraw-Hill, 1985.

[2] J. d. Kraus, *Antennas*. Chapter 17. Mcgraw-Hill, 1988.

[3] S. F. Adams, *Microwave Theory and Applications*. Chapter 3. Prentice-Hall, 1969.

330

APPENDIX II
R.F. Radiation Concerns Associated With The PASS User Terminals

P. Cramer

GENERAL PROBLEM

A review was made to determine if the PASS user terminal could present a R.F. radiation safety hazard to users under normal operating conditions. The American National Standards Institute, ANSI, has published the standard ANSI C95.1-1982 [1]. This standard defines the recommended maximum level of RF radiation or electromagnetic fields that would be considered safe for a working environment. This standard was developed under the sponsorship of the IEEE and Naval Electronics Systems Command. The recommendations of this standard were used in evaluating the conditions that need to be met for the safe operation of an user terminal.

Most of the standard is based on the assumption that the user is exposed to an uniform electromagnetic field. This is referred to as whole-body exposure. Figure 1 is a copy of the Radio Frequency Protection Guide for whole-body exposure of human beings from the standard. This guide presents the maximum power density to which an individual can be safely exposed. This guide is based on the assumption that the average specific absorption rate (SAR), the time rate at which electromagnetic energy is coupled to an element of mass of a human body, will not exceed 0.4 W/kg averaged over a 10 minute period. Figure 2 from the standard, contain typical SAR curves for different types of individuals when subjected to a constant power density of 1.0 mW/cm^2 over frequency. The different curves represent measured and empirical cases for individuals ranging in age from infants to adults. The curves shifted to the low frequency end apply to adults and the curves at the highest end apply to infants. Each curve increases rapidly with frequency, reaching a peak and then slowly decreases to a relatively constant level. This variation of energy absorption with frequency is due to the fact that the greatest coupling occurs when the height of an individual exposed to radiation is approximately 0.4 wavelengths and the electric field is oriented along the length of the body. This accounts for the fact that the peak for adults occur at lower frequencies than for infants. The top solid piece-wise curve represents the worst case for a population mix. This curve when normalized to a constant SAR level of 0.4 W/kg, maps approximately into the curve of figure 1 except for the portions of the curve above 1.5 GHz and below 3.0 MHz. These parts of the curve are not allowed to continue to increase, but are held at a constant level and provide an additional safety margin. The time averaged power densities, over a 6 minute period, then must be less than the values in the Radio Frequency Protection Guides of Figure 1. Table 1 is the Protection Guides from the standard in tabular form and also includes levels for the mean squared electric (V^2/m^2) and magnetic (A^2/m^2) field strengths, which are to be used in the near field.

From the Protection Guide, the permissible exposure level at 30 GHz is 5 mW/cm^2. To relate this level to the PASS program, power density patterns were calculated for various sized arrays of patch antenna elements. Patch antenna elements were used since the patch is a strong PASS candidate. 0.3 wavelength wide patches spaced 0.5 wavelengths apart were used. Uniform aperture illumination was assume by assigning the same excitations to each patch element. Five cases ranging from 12 patches to 208 patches were calculated giving a range in gain from 16.4 to 28.4 dB. An input power of 0.1 watt was assume and the antenna dissipative efficiency was 1.0. The transmitter power is equal to the input power divided by the dissipative efficiency. Figure 3, shows the power density calculated along the axis of the antenna. Near the antenna aperture the peak power is not always a maximum on the axis of the antenna as can be seen in Figure 4, which shows the power density pattern in several planes in front of the antenna aperture, the width of the pattern being equal to the size of the antenna aperture. Wherever the off axis level exceeded the on axis level, the level in Figure 3 was corrected to show the maximum off axis level. Therefore, Figure 3 represents the worst case power density in each plane in front of the aperture. For cases where the antenna input power is not 0.1 watt, Figure 3 still can be used by multiplying the power density by the ratio of the desired power to 0.1 watt. The peak or maximum power density for each gain curve varies inversely as the gain, expressed as a power ratio, for gains above 20 dB with an error of less than 6 percent. Therefore, the maximum power density for a given gain can be obtained from Figure 3 by interpolation. For each antenna gain case, it's power density pattern in a plane normal to the antenna axis and at the axial location of it's power density maximum are shown in Figure 5. It can be seen that most of the power lies within one wavelength of the antenna axis. From figure 4, it can be seen that the power density in each plane is lower at a point equivalent to the aperture radius than elsewhere, therefore the maximum or worst case power densities can be considered to be enclosed by a cylinder defined by the antenna perimeter and co-axial with the antenna axis. Figure 6 replots the peak power density points from figure 3, to provide a plot of peak power density as a function of antenna directivity gain.

Of primary interest to the system designer is the effective isotropic radiated power (EIRP). If a program requires a certain EIRP, then the question can be asked, what is the minimum gain antenna that can be used and still meet the safety requirements. Figure 7 is derived from Figure 6 and plots the required gain as a function of EIRP for a power density of 5.0 mW/cm^2. Also included on the same plot is the corresponding input power associated with the indicated gain and the required EIRP.

To get an idea of what restrictions a power density of 5.0 mW/cm^2 might have on the PASS program, consider an antenna gain of 22 dB and an antenna system efficiency of 0.5. From Figure 6, the peak power density is approximately 30.0 mW/cm^2. This would indicate that the 0.1 watt input power would have to be reduced by the ratio of 5/30, or to 0.0167 watts to satisfy the 5.0 mW/cm^2 criteria.

With an efficiency of 0.5, the transmitter power would be 0.033 watts. If an EIRP of 14.0 dBW is required, a transmitter power of 0.32 watts would be needed, which is higher than the allowable 0.033 watts. From Figure 7, however, it can be shown that a gain of 27 dB and a transmitter power of 0.1 watts will satisfy both the EIRP and safety requirements.

ALTERNATE OPTIONS:

The standard recognized that low power devices such as hand-held transceivers where not effectively covered by the standard and therefore provided two "exclusions" for these types of devices. The exclusions were based on the premise that there is a lower likelihood of harm if the exposure is localized such as is the case with the PASS basic user terminals and other handheld transceivers. The first exclusion states that for frequencies between 300 kHz and 100 GHz, the protection guides may be exceeded if the exposure conditions can be demonstrated in laboratory tests to produce specific absorption rates (SAR) below 0.4 W/kg as averaged over the whole body, and spatial peak SAR values below 8 W/kg as averaged over any one gram of tissue. Because of the type of tests specified, it is beyond the scope of this review to take advantage of this exclusion, but could be the basis of a future study. The second exclusion states that for frequencies between 300 kHz and 1 GHz, the protection guides may be exceeded if the total radiated power is seven watts or less. The rationale used to limit the second exclusion to 1 GHz and lower was that antennas at higher frequencies typically had collimated beams, presenting the possibility of exposure to unacceptably high radiation densities. Therefore, the second exclusion does not apply.

The safety standards base their requirements on an average exposure over a 10 minute period of time. This implies that the levels specified in the protection guides can be exceeded as long as the average levels are maintained. It is possible to take advantage of this flexibility if the user terminal radiates power only intermittently. For example, if the user terminal is voice activated, then it is conceivable that the average radiated power would be lower than the instantaneous radiated power. For the 22 dB case, if the instantaneous transmitter power is the proposed 0.32 watts, then the instantaneous aperture power density would be 47.5 mW/cm^2. To meet the protection guide requirements, this would require a 10.5 percent duty cycle over a 10 minute period. Since a hand held terminal is used near or against the head, the question must be raised: are there other hazards to organs such as the eyes if the power density is allowed to increase. This question is address by Om P. Gandhi [2]. He states that in animal experiments, lens opacifications have been noted for power densities greater than 100 mW/cm^2 when applied locally. At lower power densities, he states that no problems have been found and that a chronic far field exposure to 10 mW/cm^2 caused no abnormal ocular changes over a six month period. No safety margins were discussed in relation to the 100 mW/cm^2 test levels, so it is not possible at this point to say that intermittent exposure to 47.5 mW/cm^2 is safe in terms of possible eye damage. It should be pointed out that a safety

margin of at least 10 exists in the values suggested in the protection guide.

If power averaging is considered and it is desired to determine the required antenna gain and input power to provide a given peak or instantaneous EIRP, then additional curves similar to Figure 7 can be derived based on the peak power density to be averaged. However, if a duty cycle of 50 percent is considered giving a maximum power density of 10.0 mW/cm^2, the following approximations can be applied to using Figure 7. First, for a given gain value applied to Figure 7, the corresponding EIRP value read from the figure is increased by 3.0 dB and requires the input power associated with the EIRP value read to be increased by 3.0 dB. Secondly, if a given EIRP value is applied to Figure 7, then the corresponding gain value read from the figure is reduced by 1.6 dB and the corresponding input power is increase by 1.6 dB. This last condition would indicate that for a given EIRP requirement and a 50 percent duty cycle, the required antenna gain could be reduced by 1.6 dB as long as the input power is increased by 1.6 dB. Lastly, if a given input power is applied to Figure 7, then the corresponding EIRP value read from the figure is reduced by 3.3 dB and the gain value associated with the EIRP value read is also reduced by 3.3 dB. These approximations are usable for gains of 20 dB and higher.

From Figure 3, it can be seen that for the lower gain cases, although very high peak power densities result, these peaks are located close to the antenna aperture. The power density then drops off quite rapidly approaching acceptable levels only a short distance in front of the antenna aperture. To take advantage of this fact and to provide protection to a user, a radome could be used to cover the antenna aperture. A radius would have to be selected such that the power density would have reached a safe level by the time the RF fields reach the radome. To get an idea of the size radome that might be needed, the previous example for a 22 dB antenna and an EIRP of 14.0 dBW will be used. An input power of 0.16 watts is required. Using Figure 3, a scale factor of 0.1/0.16 is needed to make it apply to an input power of 0.16 watts. If it is desired to look at the 5.0 mW/cm^2 level, then the 5.0 mW/cm^2 must be multiplied by the scale factor giving a value of 3.1 mW/cm^2. From Figure 3, a 22 dB gain and a level of 3.1 mW/cm^2 corresponds to a distance of approximately 20 wavelengths or at 30 GHz, 20 cm. A radome with a radius this large is not practical, however combined with some of the other techniques discused, a workable design might be provided.

SUMMARY:

A) The most straight forward and safest, if not the most desirable, methods to stay within the safety standards include:

1) The array program was modified to provide the capability to calculate the power density directly on plane surfaces and is available for future calculations. Therefore, each candidate design should be checked for maximum power density to account

for unique properties of each design using the actual element excitations.

2) The standard stated that the mean volts squared per meter squared criteria be used rather than power density in the near field to determine compliance to safety standards. This method was beyond the scope of this review, but should be done with future analysis. A spot check was made and the two approaches appeared to give similar results in the near field. The standard may be recommending the use of the electric field when measuring to determine if a safety hazard exists in the near field rather than as a method of predicting performance.

3) Investigate the feasibility of either increasing the gain of the user terminal antenna or reducing the terminal transmitter power, or both to meet the requirements of the Standard and to satisfy the PASS program requirements.

4) Perform a trade off study of power and gain vs. duty cycle for modest increases in the peak power density above the safe level with the constraint that the average power density does not exceed the safe level.

5) Calculated and plot additional curves similar to Figure 7 for other power densities to support the trade-offs discussed in item 4 above.

6) A trade-off study on the use of radomes should be performed to determine if more favorable designs can be found than the case used as an example in the text above. Also it is recommended that for a given design, sufficient calculations be performed to ensure all unsafe fields are enclosed by the radome

7) Investigate the system, programmatic and technical considerations associated with locating the terminal antenna at a safe distance from the user or other individuals.

B) Approaches requiring more extensive study and development with perhaps less immediate potential might include:

1) Perform a more extensive study of the health safety requirements that would apply to hand held transponders to determine if higher powers can be safely handled. Such studies might include determining what the actual SAR values are to take advantage of the exclusion provisions of the standard, to determine what are safe power density levels for eye exposure and to determine if there are any other limitations to using peak power densities over short periods of time.

2) Investigate and develop techniques: that would constrain the antenna beam from being directed toward the user.

3) Evaluate the use of safety interlocks that would turn off the transmitter power if the unit is not held in a proscribed operating position that has been determine to be safe. An example might be a pressure switch in the ear cup.

References:

[1] ANSI C95.1-1982, "American National Standard Safety Levels with Respect to Human exposure to Radio Frequency Electromagnetic Fields, 300 kHz to 100 GHz", American National Standards Institute, July 30, 1982

[2] Om P. Gandhi, "Biological Effects and Medical Applications of RF Electromagnetic Fields", (Invited Paper), IEEE Trans Microwave Theory and Techniques, Vol. 30, No. 11, November 1982, pp 1831 to 1847.

[3] NIOSH, "Recommendations for a Radiofrequency and Microwave Standard", draft proposal.

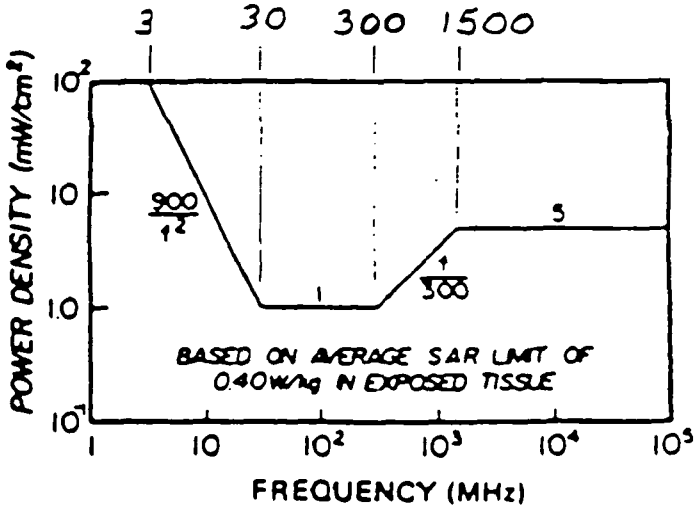

Fig 1
Radio Frequency Protection Guide for Whole-Body Exposure of Human Beings

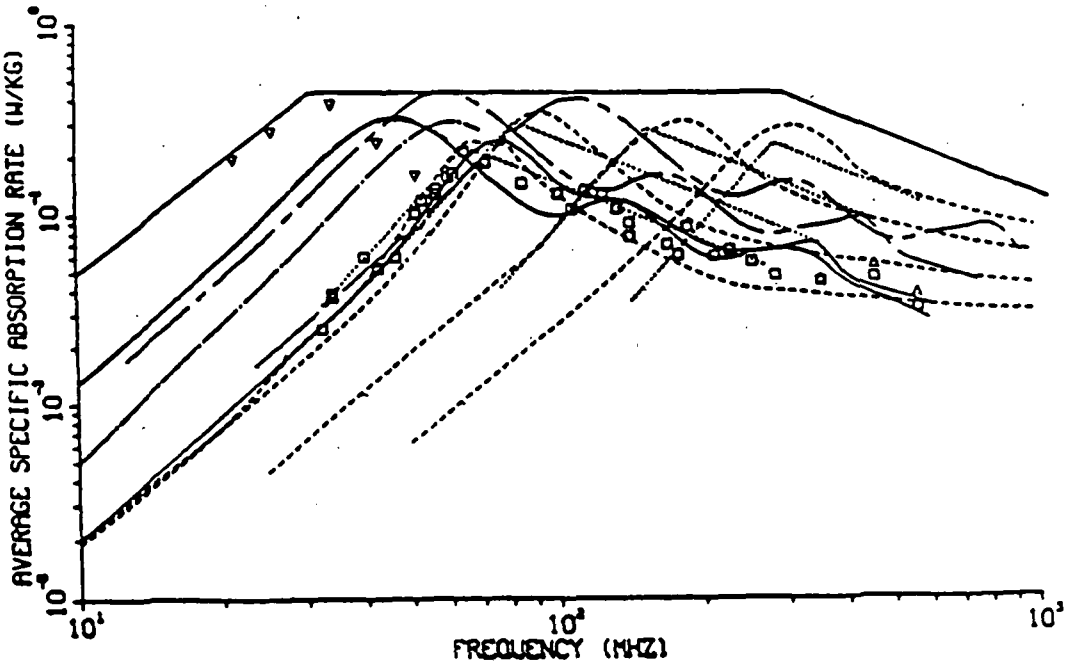

Fig 2

Whole-Body-Averaged SAR

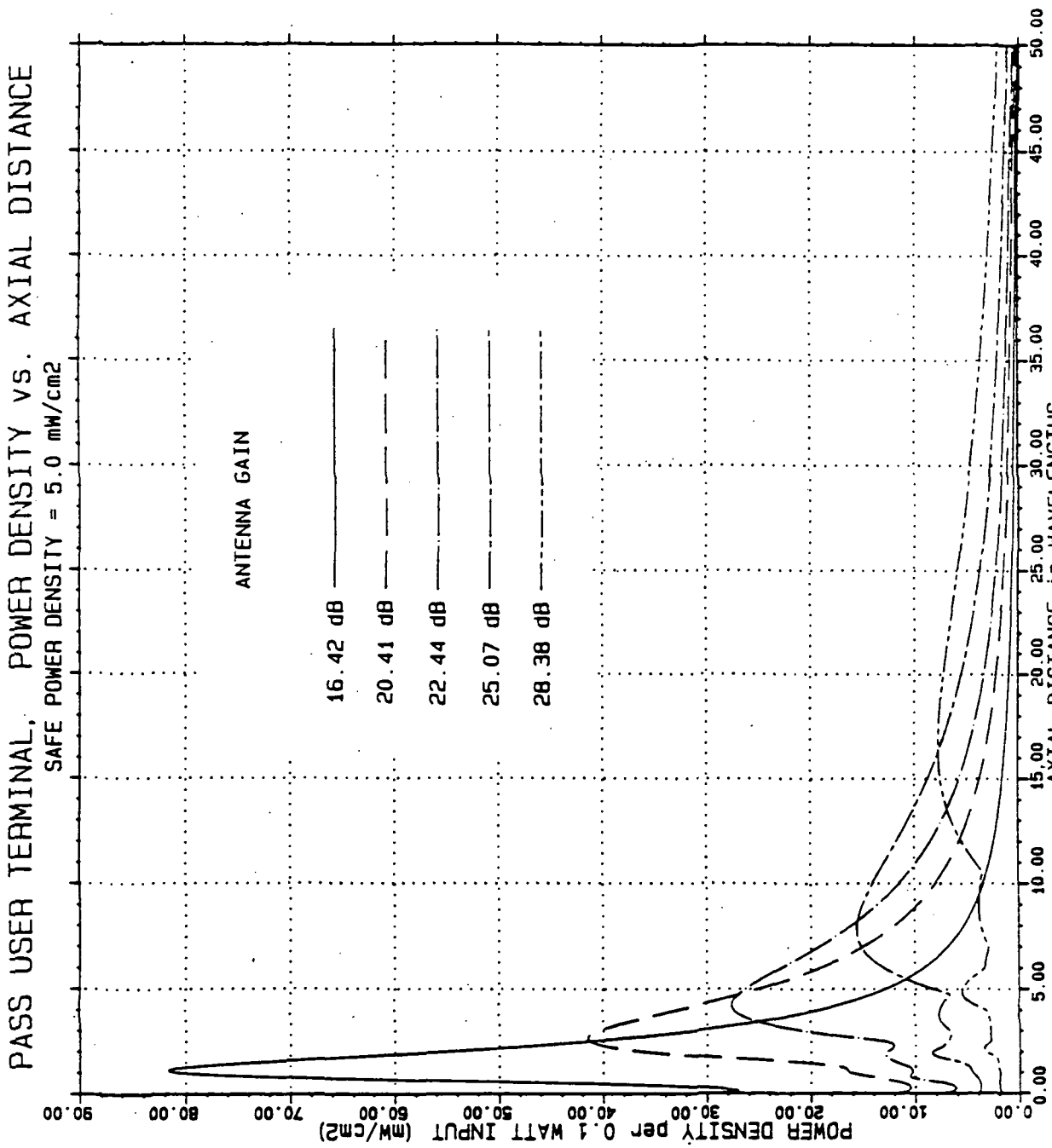
PASS USER TERMINAL, POWER DENSITY vs. AXIAL DISTANCE
SAFE POWER DENSITY = 5.0 mW/cm2
ANTENNA GAIN
16.42 dB
20.41 dB
22.44 dB
25.07 dB
28.38 dB
POWER DENSITY per 0.1 WATT INPUT (mW/cm2)
AXIAL DISTANCE in WAVELENGTHS
0.00
10.00
20.00
30.00
40.00
50.00
60.00
70.00
80.00
90.00
0.00
5.00
10.00
15.00
20.00
25.00
30.00
35.00
40.00
45.00
50.00

Figure 3

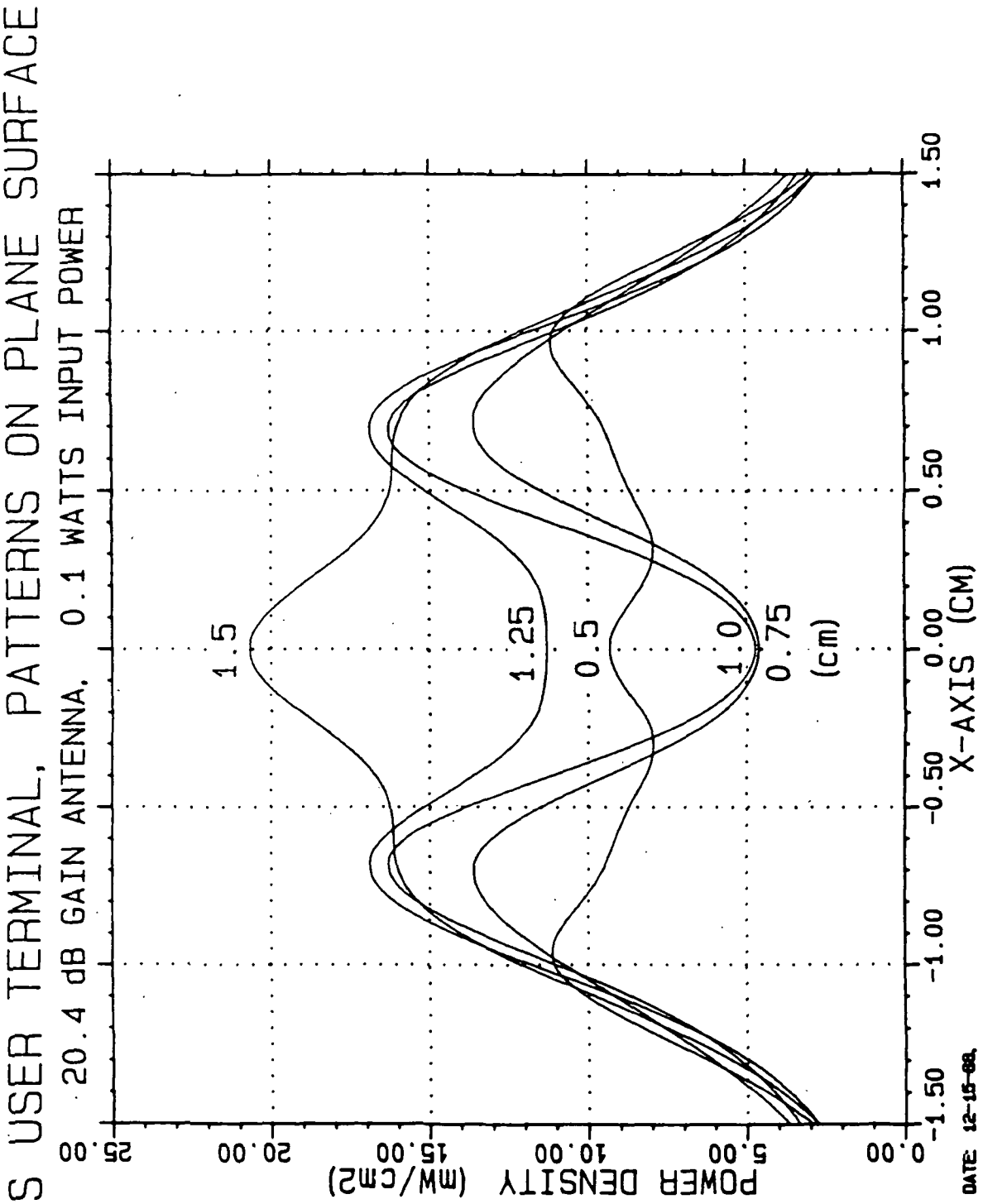
PASS USER TERMINAL, PATTERNS ON PLANE SURFACE
20.4 dB GAIN ANTENNA, 0.1 WATTS INPUT POWER
POWER DENSITY (MW/CM2)
0.00
5.00
10.00
15.00
20.00
25.00
X-AXIS (CM)
-1.50
-1.00
-0.50
0.00
0.50
1.00
1.50
1.5
1.25
0.5
1.0
0.75
(cm)
DATE 12-15-88

Fig. 4

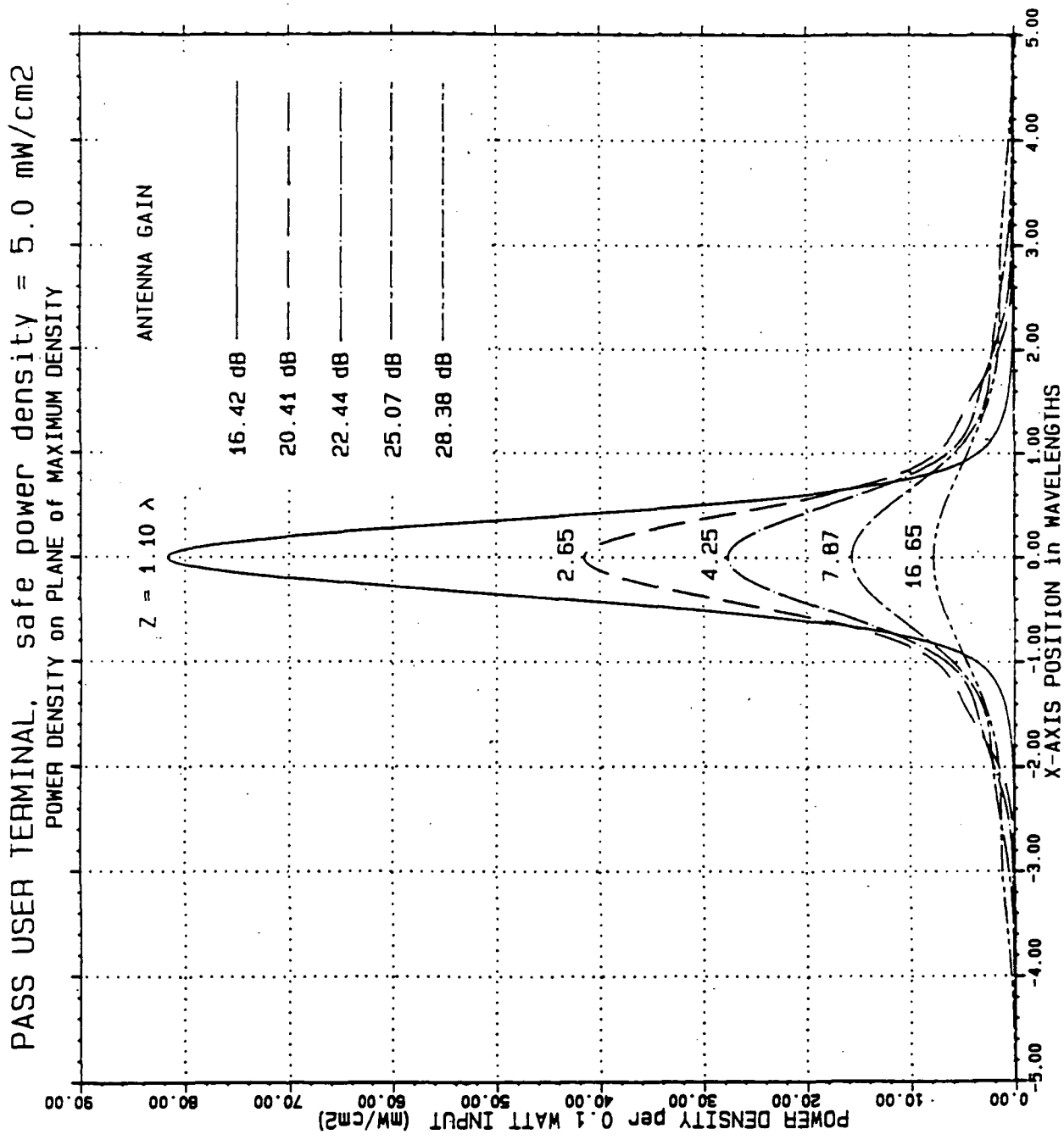
PASS USER TERMINAL, safe power density = 5.0 mW/cm2
POWER DENSITY on PLANE of MAXIMUM DENSITY
ANTENNA GAIN
16.42 dB
20.41 dB
22.44 dB
25.07 dB
28.38 dB
Z = 1.10 λ
2.65
4.25
7.87
16.65
POWER DENSITY per 0.1 WATT INPUT (mW/cm2)
X-AXIS POSITION in WAVELENGTHS

Figure 5

PASS USER TERMINAL

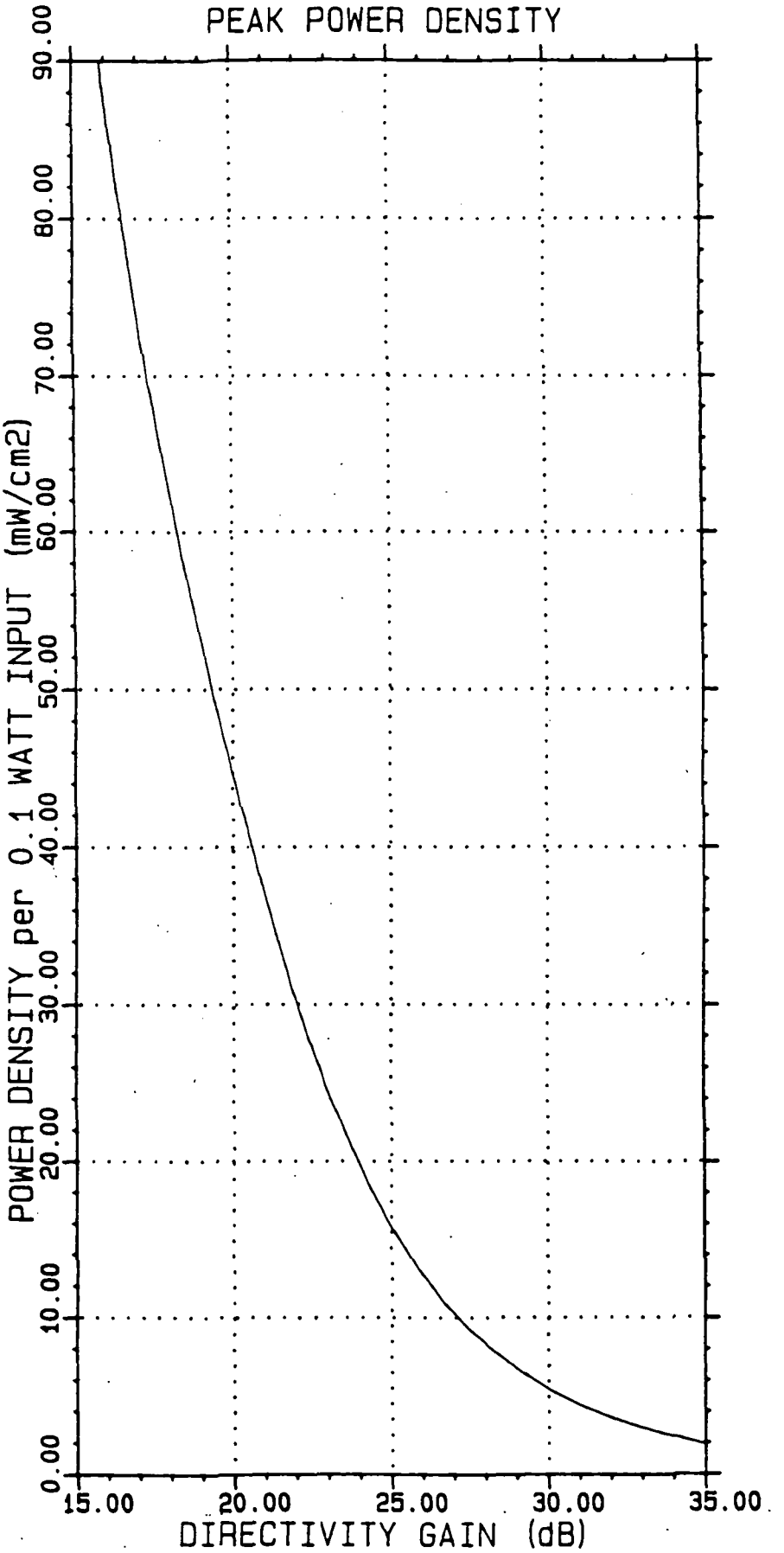

Fig. 6

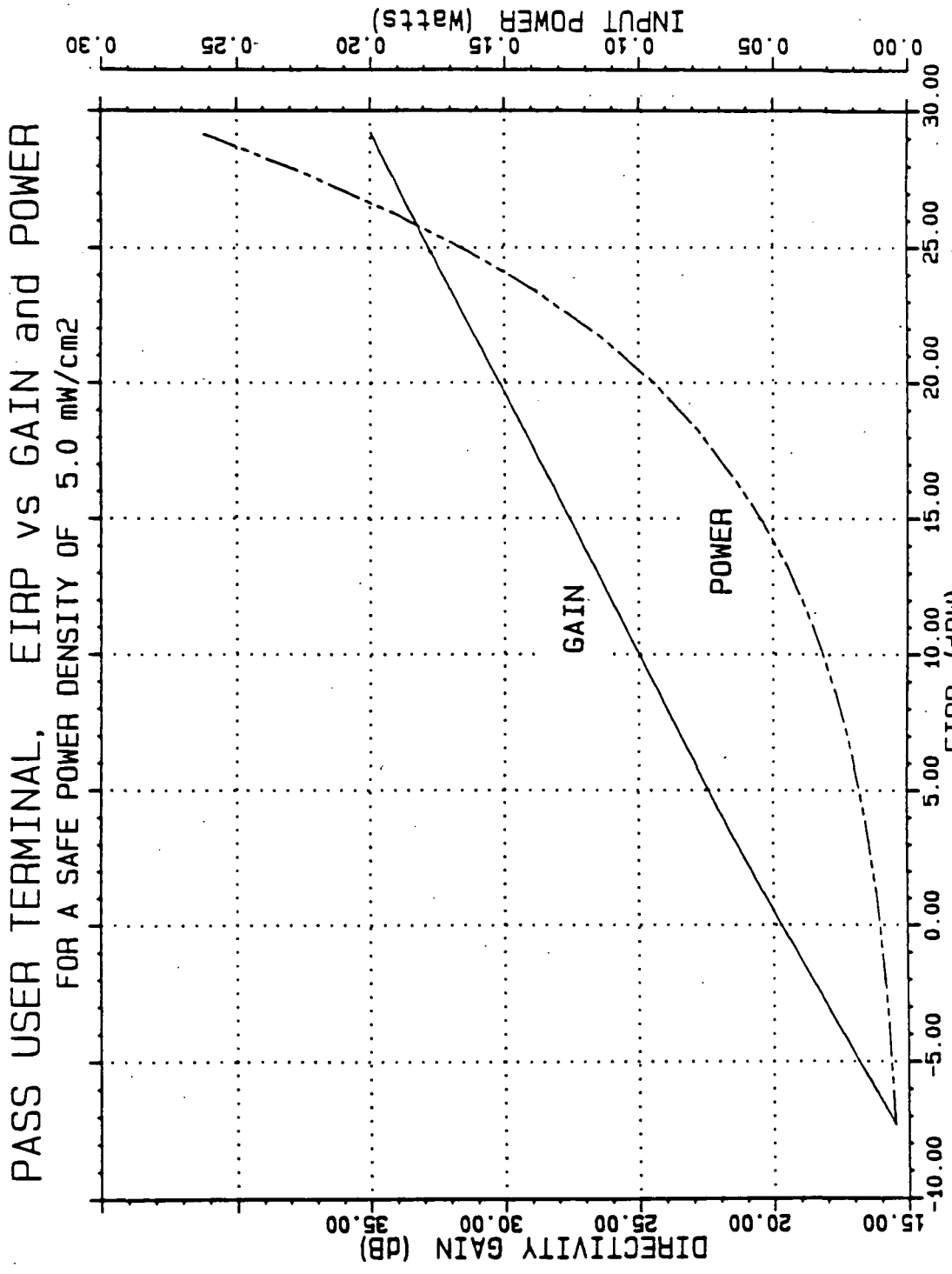
PASS USER TERMINAL, EIRP vs GAIN and POWER
FOR A SAFE POWER DENSITY OF 5.0 mW/cm2
INPUT POWER (Watts)
0.00
0.05
0.10
0.15
0.20
0.25
0.30
DIRECTIVITY GAIN (dB)
15.00
20.00
25.00
30.00
35.00
EIRP (dBW)
30.00
25.00
20.00
15.00
10.00
5.00
0.00
-5.00
-10.00
GAIN
POWER

Figure 7

Radio Frequency Protection Guides

1	2	3	4
Frequency Range (MHz)	E^2 (V^2/m^2)	H^2 (A^2/m^2)	Power Density (mW/cm^2)
0.3 — 3	400 000	2.5	100
3 — 30	4000 ($900/f^2$)	0.025 ($900/f^2$)	$900/f^2$
30 — 300	4000	0.025	1.0
300 — 1500	4000 ($f/300$)	0.025 ($f/300$)	$f/300$
1500 — 100 000	20 000	0.125	5.0

Note: f = frequency (MHz).

Table 1

D-7382

CHAPTER 6: SPACECRAFT ANTENNAS

Dr. Vahraz Jamnejad, Dr. Farzin Manshadi
(with contributions from Dr. Yahya Rahmat-Samii, and Mr. Paul Cramer)

6.0 INTRODUCTION (STUDY OBJECTIVES AND TRADE-OFF CRITERIA)

In the previous report on spacecraft antennas for the Personal Access Satellite system [1], we identified, in a very general manner, various categories of issues that must be considered in the selection and design of spacecraft antennas for such a communication satellite system. Here we consider some of those issues in more detail and provide parametric studies for some of the antenna concepts to help the system designer in making the most appropriate antenna choice with regards to weight, size, complexity, etc.

The question of appropriate polarization for the spacecraft as well as for the User Terminal antenna required particular attention and was studied in some depth. Circular polarization seems to be the favored outcome of this study.

Another problem that has been generally a complicating factor in designing the multiple beam reflector antennas, is the type of feeds (single vs. multiple element and overlapping vs. non-overlapping clusters) needed for generating the beams. This choice is dependent on certain system design factors, such as the required frequency reuse, acceptable interbeam isolation, antenna efficiency, number of beams scanned, and beam-forming network (BFN) complexity. This issue is partially addressed, but is not completely resolved. Indications are that it may be possible to use relatively simple non-overlapping clusters of only a few elements, unless a large frequency reuse and very stringent isolation levels are required.

6.1 PARAMETRIC STUDIES: NUMBER OF BEAMS, GAIN, SIZE, AND WEIGHT

For the coverage of the Contiguous United States (CONUS) a closed form relation was derived that relates the number of beams, N, to the half-power beamwidth of the multiple beam antenna, BW, in degrees. It is given as

$$N = 17.5 / BW^2$$

This equation is based on the solid angle of the coverage region as seen from the satellite and is valid as long as the satellite is in the geostationary orbit at approximately 90 to 100 degrees West Longitude. This relation is graphically presented in Figure 1. Several specific coverage cases were considered and the actual number of beams is also presented in the figure. As can be seen the agreement is quite good, especially for smaller beamwidths.

The actual number of required beams starts to increase for larger beamwidths, since in this case it is hard to match the beam footprints to the contour of the boundary and the area covered by beams becomes larger than the required coverage region. Since

$$BW \approx 70 / (D/\lambda),$$

we can also write

$$N \approx (d/\lambda)^2 / 280$$

Figure 1 also provides the required antenna aperture diameters for the 20 and 30 GHz frequencies corresponding to the various beamwidths.

As for the weight of the antenna system, we concern ourselves only with a reflector antenna system. A full aperture array system is in general too heavy and complex to be considered for this type of application. The weight of the reflector and the support structure depends on the actual implementation and will be discussed in Chapter 7. Here we confine ourselves to the study of the feed array weight for the reflector system. A fixed multiple beam antenna is assumed.

The feed array dimensions depend, in general, mainly on

i) the angular dimensions of the coverage region, and
ii) the focal length of the reflector system.

The feed array dimensions are practically independent of

i) the frequency or wavelength of the operation, and
ii) the number of beams over the coverage region.

Of course, since the focal length is typically of the order of the reflector diameter and should be larger for a larger number of beams, the size of the array becomes indirectly dependent on the reflector dimension, the number of beams and the frequency. A more complete discussion of these issues can be found in Reference [2]. These observations are used in deriving the following formulas for the feed array weight.

The array weight, W, is given by

$$W = S\, W_a + N\, W_{TR}$$

in which S is the surface area of the array feed given by

$$S = \{(1/b)(F/D)[1+(h_c/4F)^2]\}^2\, D^2\, \Omega$$

F is the focal length, D is the reflector diameter, b is the beam deviation factor and approximately equal to or less than unity, h_c is the offset of the reflector center from the main axis (zero for a symmetric configuration), and Ω is the solid angle of the coverage region given approximately by

$$\Omega \approx 0.006 \text{ Steradian.}$$

Then for b=0.9 and F/D=1.5, S is approximated as

$$S \approx D^2/60$$

N is the total number of beams, W_a is the weight per unit of feed area, and W_{TR} is the weight per unit TR module. The latter is based on the assumption that due to the considerable loss in the beamforming network, the feed corresponding to each beam will have its own TR module which consists of a diplexer, a high power amplifier (HPA) and a low noise amplifier (LNA), if the same antenna is used for both transmit and receive operations. The number of the modules could be larger than the number of beams if a more complex feeding system such as an overlapping cluster concept, in which adjacent beams share in a number of radiating elements, is employed.

Of course for separate transmit and receive antennas only an HPA or an LNA will be needed, and the corresponding weight, W_{TR}, will be reduced.

Finally, the overall feed weight can be approximated by either

$$W \approx 4.8 \, N \, \lambda^2 \, W_a + N \, W_{TR},$$

as a function of the number of beams, or

$$W \approx (D^2/60) \, W_a + (1/280)(D/\lambda)^2 \, W_{TR},$$

as a function of reflector diameter. Figure 2 presents a graphical representation of this relation for the transmit and receive antennas. In this figure we have assumed, based on prior experience and the study of a number of cases, that

$$W_0 \approx 1.5 \text{ Kg/m}^2, \; W_{TR} \approx 0.1 \text{ Kg.}$$

Naturally, for specific cases one should make the appropriate changes in the above values for more accurate results.

6.2 ANTENNA POLARIZATION TRADE-OFF (CIRCULAR VS. LINEAR)

An important factor in the design of the PASS system is the choice of the electromagnetic field polarization for the antennas. The design of the spacecraft as well as of the ground user antennas will be affected by this choice. At Ka-band frequencies Faraday rotation in propagation through the atmosphere is not a concern. Therefore, ideally, the linearly polarized antennas should be selected, since this choice simplifies the design of the feeding networks.

However, due to the selection of a multiple beam spacecraft antenna, the linear polarization, at different beam footprints on the ground, will present different levels of cross polarization. This can be seen clearly in Table 1 which presents the variations in the polarization directions from the ideal vertical polarization, at different locations on the ground. This table is based on a program which can solve for any general case in which spacecraft antenna may have any desired position and orientation and can be directed toward any given point on the ground.

The spacecraft feed array can be designed in such a way that the radiating elements for each beam will be polarized differently in order to achieve the best polarization quality within that beam footprint on the ground. However, if for any reason the spacecraft is moved to a different geostationary position, it is possible that the beam polarizations may deteriorate unacceptably.

The movements of the user antenna on the ground may also complicate the situation by not matching the polarization presented by the spacecraft antenna.

The circularly polarized antennas are more robust, however. They are more forgiving of the vagaries of the user antenna movements, and far less sensitive to the relocation of the spacecraft antenna to different geostationary positions.

Appendix I discusses some of these issues in more detail.

6.3 FEED DESIGN TRADE-OFF (OVERLAPPING VS. NON-OVERLAPPING)

The design of the feed and beamforming network for the reflector is perhaps the most challenging aspect of the spacecraft antenna design. This design will affect the overall antenna gain loss, the achievable sidelobe levels which have a direct bearing on the interbeam isolation levels needed for a frequency reuse operation, as well as the polarization of the antenna. This issue has been studied before and documented in [2]. Appendix II provides some additional insight into the choice of simple or multiple element overlapping cluster feed. Overall, it can be said that the choice of the simple non-overlapping feeds is more desirable in most cases.

There are, however, instances in which due to the requirements of a very large number of beams, very low sidelobes, high interbeam isolation, and very large frequency reuse, the introduction of the overlapping cluster design may become necessary. This is particularly true when far scanned beams in a very large multiple beam system will have unacceptably high coma lobes which can be cured by the implementation of a multi-element feed array and/or a much larger focal length/reflector diameter ratio, F/D.

A specific trade-off issue is the choice between a reflector system with a very large F/D and hence large feed array and support booms, or a complex and heavy beamforming network for the overlapping feed clusters. This issue needs further analysis in the context of more specific requirements of the system.

6.4 ALTERNATIVE DESIGN OPTIONS

In this section some alternative design issues are considered. One issue relates to the selection of the most appropriate optics, namely, the number and type of the reflectors and feed arrays and their configuration. A second issue relates to the multiple beam construction and operation and whether they are fixed, switched, or scanned.

And, finally, the issue of beamforming network design in respect to the mechanics of the power distribution is considered and discussed. The beamforming network can be designed to optimize the efficient use of the power amplifiers under conditions of short or long term variable channels allocation and usage by different beams covering different geographic regions.

6.4.1 ALTERNATIVE REFLECTOR/FEED TOPOLOGIES

The last PASS report [1] enumerated some alternative design concepts for the reflector system configuration. The simplest design involves the use of a single offset-fed reflector with a focal plane feed array for fixed simultaneous multiple beam operation. Some numerical results for this design are presented in the next section. Here we look at two alternative concepts.

A promising system involves the use of a near field array in conjunction with a single hyperbolic (as opposed to a typically parabolic) reflector which provides for beam scanning by varying only the phase of the component feed elements (Reference [3]). A theoretical computer study of this concept has been undertaken, but no concrete results have been obtained so far. By using a multi-layer beamforming network (BFN) one can achieve a multiple beam system with independently scanned individual beams with only a single reflector and feed array. We recommend that this concept be further studied in the future since it may be one of the more attractive advanced concepts in the reflector RF design.

Another option considered was mechanical beam scanning by using a small movable array in conjunction with a symmetric parabolic reflector or a spherical reflector antenna. The spherical reflector has the advantage that once the excitation values are evaluated for the on-axis beam, the same excitation values can be used for off-axis or scanned beams, due to the rotational symmetry of the reflector. The results of the mechanical scanning study are presented in Appendix III.

6.4.2 SCANNING / SWITCHED BEAM VS. FIXED BEAM TRADE-OFF

In multibeam satellite systems, scanning/switched beam concepts may be used instead of fixed simultaneous beams. This can reduce the number of components and the weight of the system at the expense of requiring more complex components and beam management systems. The following is a description of the major features of switched or scanned beam systems.

Switched Beams:

1- The number of active beams at any given time is fewer than the total number of beams needed for the entire coverage region.

2- The number of required feed array elements is the same as that needed for a fixed multiple beam system.

3- The number of high power amplifiers (HPA) and low noise amplifiers (LNA) is reduced.

4- To provide the same number of channels as a fixed multiple beam system, using a time division multiplex system, higher power HPAs are required.

5- The system requires complex switching networks including PIN diodes and/or ferrite switches and their driving circuitry.

Scanned Beams:

1- As in the switched beam case, simultaneous coverage is not provided for the entire coverage region.

2- Can be used in a single or dual reflector system with a phased array feed (see section 6.4.3).

3- The number of required feed array elements, if a single reflector antenna is used, is more or less the same as that needed for a fixed beam system.

4- The number of required feed array elements can be substantially reduced if a dual reflector antenna system is used.

5- The number of HPAs and LNAs are reduced.

6- To provide the same coverage as a fixed multiple beam system, higher power HPAs are required.

7- The HPAs and the LNAs may require wider bandwidths.

8- Requires the use of variable (continuous or multiple-bit digital) phase shifters in the beamforming network.

6.4.3 INTERBEAM POWER MANAGEMENT

Multiple beam systems can increase transmission capacity with an increase of satellite antenna gain and reuse of allocated frequency band. However, the implementation of a multiple beam system for contiguous communication requires special considerations to avoid inefficient use of satellite power and to ensure reliable operation. For single beam systems, all the transponders are connected to a single beam, and every Earth station has access to all the transponders. Therefore, traffic variations in a local area are acceptable, provided they do not exceed the total transmission capacity.

On the other hand, in the case of multiple beam systems, the area subtended by each beam is only a part of the total service area, and the transmission capacity of each beam is also a fixed portion of the total transmission capacity. Thus, the fixed allocation of transponder capacity to each beam degrades the flexibility of the system under varying traffic distribution.

In order to cope with these problems, two adaptive schemes are suggested in this section. One is the multiport Hybrid transponder that can be used for a multibeam antenna system, where each beam is generated by separate feed array elements. The other is a full array beam forming network, where each beam is generated by all the feed array elements.

(a) Multiport Hybrid Transponder:

This system, as originally proposed by Egami et al. [4], consists of multiple hybrids and multiple amplifiers and inherently realizes wide-band transmission. Figure 3 shows a 4-port Hybrid transponder where each 4-port box depicts an ordinary 90 degree hybrid. When all the amplifiers are working properly, the information in each beam ends up in one of the antennas only.

Meanwhile, every beam is amplified by all the amplifiers and, therefore, failure of one amplifier does not cause the total loss of that beam's transmission. Hence, this scheme allows for graceful degradation of the multibeam system if one or few of the active elements fail. Moreover, since the amplifiers share a common wide frequency band, the number of carriers transmitted from each beam can be changed from 0 to maximum value, limited only by the total transmitting power. Therefore, this system provides the adaptability needed for the efficient use of satellite power.

Figure 4 shows the 4-port Hybrid transponder used with an offset parabolic antenna system for a simultaneous fixed multibeam transmission. In this configuration, the feed array is placed on the focal plane of the reflector and the reflector is in the far field of the feed array. The hybrid transponder sends each of the beams to a separate feed array element, in the focal plane, and generates the corresponding far field pattern of the reflector.

The disadvantage of this system is that it requires many 90 degree hybrids which increases the size of the feed array assembly. However, it does not need complex phase shifting components and the associated circuitry.

(b) Full Feed Array Beam Forming Network:

In this concept every beam is generated by all the feed array elements. Figure 5 shows a 4-beam, 4-antenna element system. Each beam is connected to the elements of the feed array via phase shifters. The phase shift provided by each phase shifter is determined precisely to point each beam in a specific direction. The amplifiers share a common wideband and each contributes to the amplification of all the beams. Therefore, the failure of one amplifier does not cause a total failure of a beam but only a graceful degradation in the system performance. This concept, like the hybrid transponder method, allows adaptive carrier allocation to each beam. The number of carriers in each beam can change from zero to the maximum, limited only by the total transmission power.

Figure 6 shows two reflector antenna configurations that can be used with the full feed array beam forming network. In Figure 6-a, a single hyperbolic reflector is used in the near field of the feed array [3]. With the feed array outside of the reflector focal region, it is possible to generate multiple far field beams from the multibeam near field pattern of the feed array.

Figure 6-b shows a dual parabolic reflector system where the subreflector is located in the near field of the phased array. In both systems, by proper positioning of the array such that the center of the main reflector and the array are conjugate points, an optimum design can be achieved such that among other things, the reflector surface deformations can be compensated solely by the phase adjustment of the array elements [5].

This system does not require the large number of hybrids which are needed for the hybrid transponder. However, it requires a large number of phase shifters which are relatively complex, lossy and costly.

6.5 DESIGN DATA FOR SELECTED ANTENNA SIZES

For PASS, two separate multibeam satellite antennas are used for receive and transmit to alleviate the potential problem of passive intermodulation (PIM). In order to provide the required antenna gain of over 52 dBi, antenna diameters of the order of 2 to 4 meters at the uplink (receive, frequency of 30 GHz) and 3 to 6 meters at the downlink (transmit, frequency of 20 GHz) are considered.

These antennas produce beams with 3-dB beamwidth of approximately 0.35 degrees for the 2/3 meter system and 0.175 degrees for the 4/6 meter system. Therefore, to cover the CONUS it is necessary to scan the feeds in these antennas by either 10 or 20 beamwidths for the 2/3 or 4/6 meter systems, respectively, as shown in Figures 7 and 8 (reproduced from [1]). Scanning the beam off axis will cause performance degradations which include loss of gain and higher sidelobe levels. However, the severity of these degradations is a function of the reflector geometry and the feed illumination of the reflector.

In this section a parametric study is performed to evaluate the effect of the satellite antenna F/D and the feed edge taper (ET) on the antenna gain and pattern as the feed is scanned. The geometry of the antenna and the location of the feed are shown in Figure 9. In this study two antenna sizes (2 or 4 meters in diameter) are considered at 30 GHz. For the 3 and 6 meter antennas at 20 GHz, the same results will apply since their electrical dimensions (i.e., in terms of the wavelength) are the same. respectively.

To cover the entire CONUS, the feed has to be scanned in both x and y directions as shown in Figures 7, 8, and 9. However, the required scan in the y direction (here assumed to be the East-West direction) is much larger and causes a more severe pattern degradation than in the x direction. Therefore, only the results for the feed scanned in the y-direction are presented here.

The results reported here are generated using a reflector antenna computer program based on the application of the physical optics integration which is evaluated by the Jacobi-Bessel expansion technique [6]. This computer program generates the far field pattern of reflector antennas, with given geometrical dimensions, based on the location and pattern of their feeds.

Table 2 shows the on and off axis gain and efficiency of the 2-meter antenna, as a function of the reflector (F/D) and the feed edge taper, when its feed is scanned in the y direction by 10 beamwidths (the maximum scan in the East-West direction as shown in Figure 7).

Table 3 shows the same parameters for the 4-meter antenna when its feed is scanned in the y direction by 20 beamwidths (the maximum scan in the East-West direction as shown in Figure 8).

As expected, in general, larger F/D (or F, since D is fixed) and higher ET values improve the off-axis gain and efficiency of the reflector, and reduce the sidelobe degradation. However, the larger the F is, the longer and heavier are the supporting booms and the larger is the size of the feed array (see Section 6.1 and References [2] and [7]). Moreover, the values of the ET larger than about -5 dB require overlapping cluster feeds instead of simple feeds.

Overlapping cluster feeds require much more complex beam forming networks (BFN) and are also heavier. Therefore, it is important to keep the ET under -5 dB and the focal length as small as possible.

Figures 10 through 17 show the far field patterns of the 2- and the 4-meter antennas when their feeds are either on focal point or scanned by 10 or 20 beamwidths, respectively. All the patterns are normalized to the on-focus beam maximum and are plotted about their maximum without making corrections for the beam deviation factor. With these figures, the degree of pattern degradation and gain loss can be compared for different values of F/D and ET.

By analyzing the data shown in Tables 2 and 3 the following can be concluded:

For the 4-meter antenna, the supporting boom for the feed has to be very long to avoid high gain loss and poor efficiency. An F/D of 2 requires a focal length of 8 meters for the 4-meter antenna and 12 meters for the 6-meter antenna, focal lengths which are prohibitively large. For an F/D of 1.5, it is necessary to have an ET = -15 dB or higher, which still requires long feed support structures as well as a very complicated BFN.

For the 2-meter antenna, an F/D of 1.5 can be used with an ET=-5 dB to obtain acceptably low gain loss, moderate size for the feed supporting structure, and a simple BFN. For higher ET values, low gain loss and high efficiency can be achieved at the expense of requiring a more complex BFN.

6.6 CRITICAL TECHNOLOGIES AND DEVELOPMENT GOALS

The major challenging technologies for the PASS satellite antennas are described below.

(1) **Monolithic Microwave Integrated Circuit (MMIC)**

The large feed arrays needed for the satellite antennas require very complex electronic circuits. These circuits must be low loss, low weight, and compact in size. MMIC manufacturing technology is a key to implementing such circuits and, therefore, must be developed for use in this system.

(2) **Overlapping Cluster Feeds**

Overlapping cluster feeds are needed to generate closely packed (high cross-over) multiple fixed beams with low sidelobes. This requires developing either MMIC or RF/Optical/RF beamforming networks for the 20/30 GHz region.

(3) **Low Loss Phase-Shifters and Power Dividers/Combiners**

In order to generate time scanned beams, the feed array beam forming network requires phase shifters and power dividers/combiners. At 20/30 GHz frequencies, low loss phase shifters and power dividers/combiners present a formidable challenge and need to be developed using MMIC technology to achieve efficient beam scanning.

(4) **Low Loss Switching Networks**

In order to generate switching beams, the feed array beam forming network requires switching circuits to activate a desired group of radiating elements for each specific beam. Low loss switching networks for 20/30 GHz frequencies are very complex and challenging to develop.

(5) **Time-Delay Beam Forming Networks**

In order to generate scanning beams across the coverage area using the frequency scan approach, true time delay elements (such as filters), in which the phase changes linearly as a function of the frequency, are needed. Development of beam forming networks employing these components is a challenging task.

(6) **Adaptive Reflector Distortion Compensation**

To compensate the effect of the time varying thermal and dynamic distortion on the reflector system in space, adaptive feed arrays can be used. Techniques for compensation of these distortions, by real time change of the array elements phase and amplitude, should be investigated and evaluated for technical feasibility and cost.

(7) **Efficient Feed Array Elements**

Low loss, wideband, and efficient array elements, capable of providing large scan angles, are needed to avoid overall antenna performance degradation. New concepts in array element technology such as scanning or stacked elements should be investigated and their feasibility studied.

REFERENCES

[1] M. K. Sue, Editor, "Personal Access Satellite System Concept Study," Jet Propulsion Laboratory Publication D-5990, February 1989.

[2] M. K. Sue, Editor, "Second Generation Mobile Satellite System: A Conceptual Design and Trade-off Study," Jet Propulsion Laboratory Publication 85-58, June 1985.

[3] G. Bartolucci, et al., "Comparison of Active Phased Array Antennas for Communication Satellite Applications," Proceedings of Symposium on Antenna Technology and Applied Electromagnetics, Winnipeg, Canada, August 1988.

[4] S. Egami, M. Kawai, "An Adaptive Multiple Beam System Concept," IEEE Journal on Selected Areas in Communications, Vol. SAC-5, No. 4, May 1987.

[5] C. Dragone, M. J. Gans, "Imaging Reflector Arrangements to Form a Scanning Beam Using a Small Array," The Bell System Technical Journal, Vol. 58, No. 2, February 1979.

[6] Y. Rahmat-Samii, "Offset Parabolic Reflector Computer Program for Analysis of Satellite Communications Antennas," Jet Propulsion Laboratory Publication D-1203, December 1983.

[7] V. Jamnejad, "Multibeam Feed System Design Considerations for Single Aperture Large Space Antennas," NASA Conference on Large Space Antenna Technology, Dec. 1984.

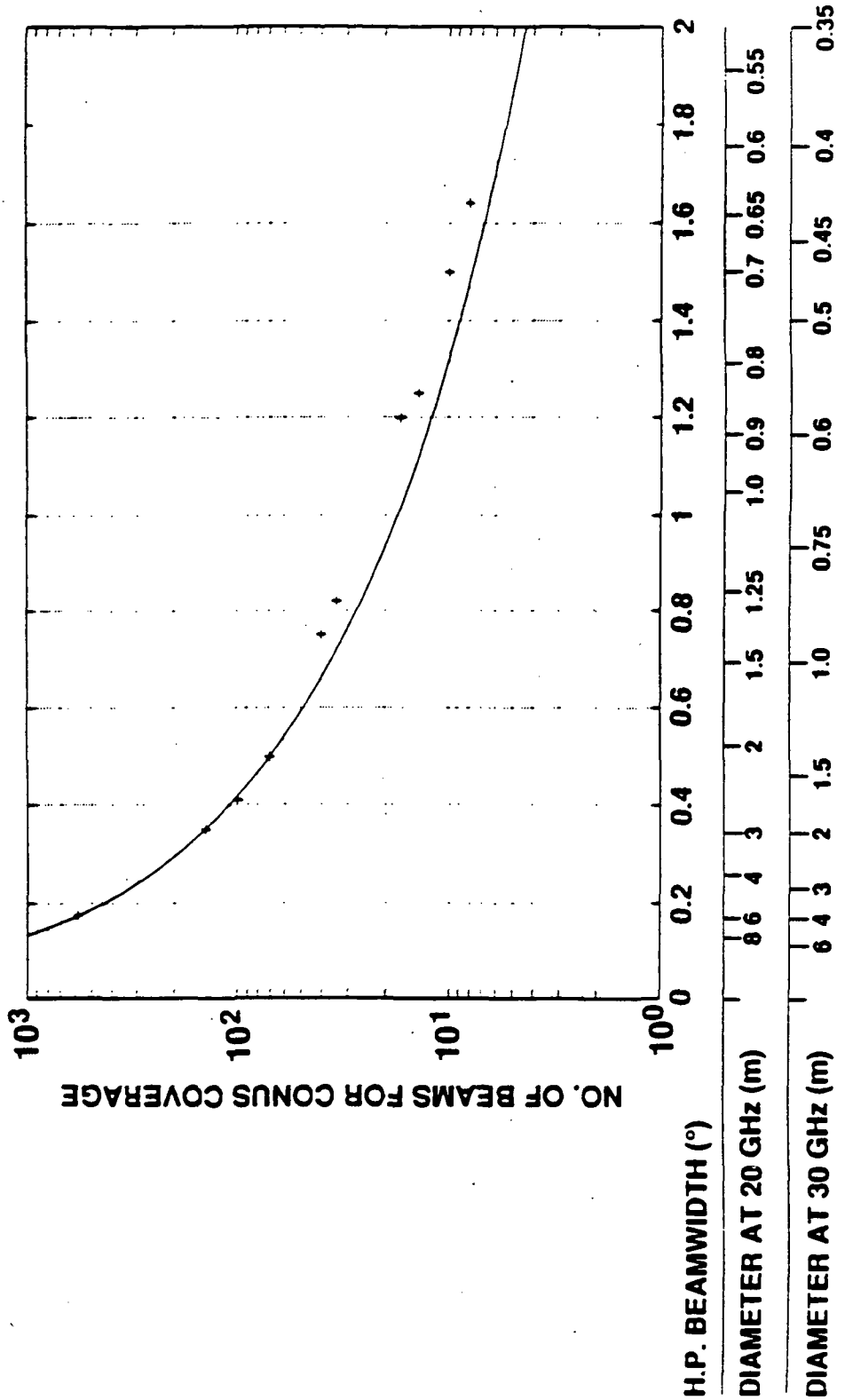

Figure 1. Number of beams as a function of beamwidth for multibeam CONUS coverage.

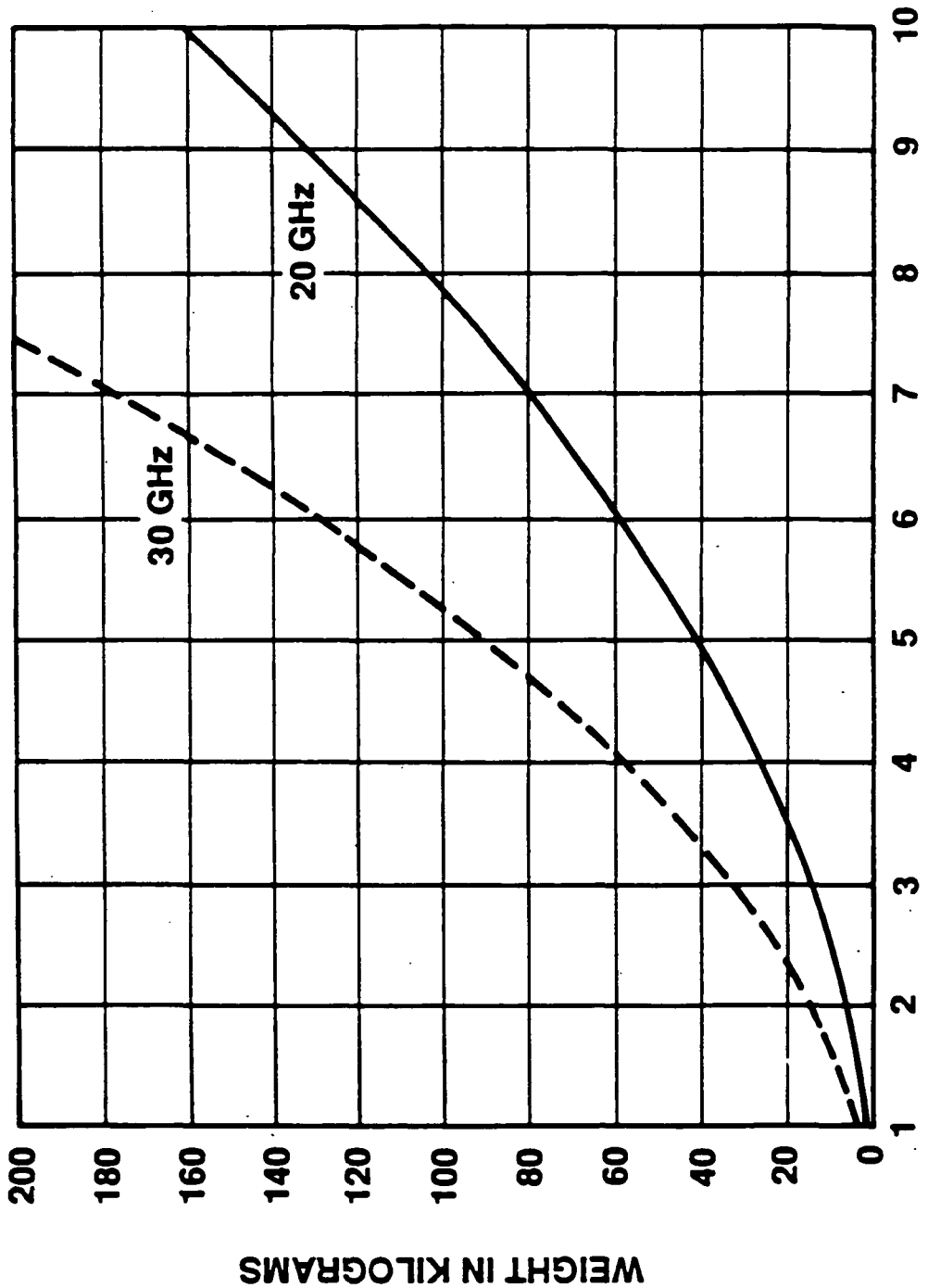

Figure 2. Spacecraft feed array weight as function of reflector diameter for multibeam CONUS coverage.

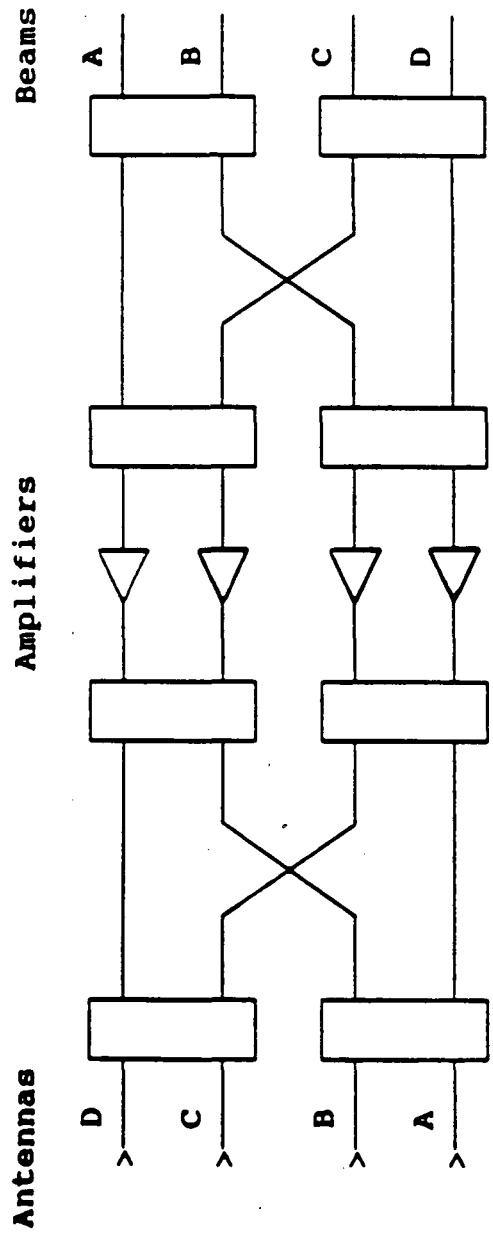

Figure 3. Configuration of a 4-port hybrid amplifier.

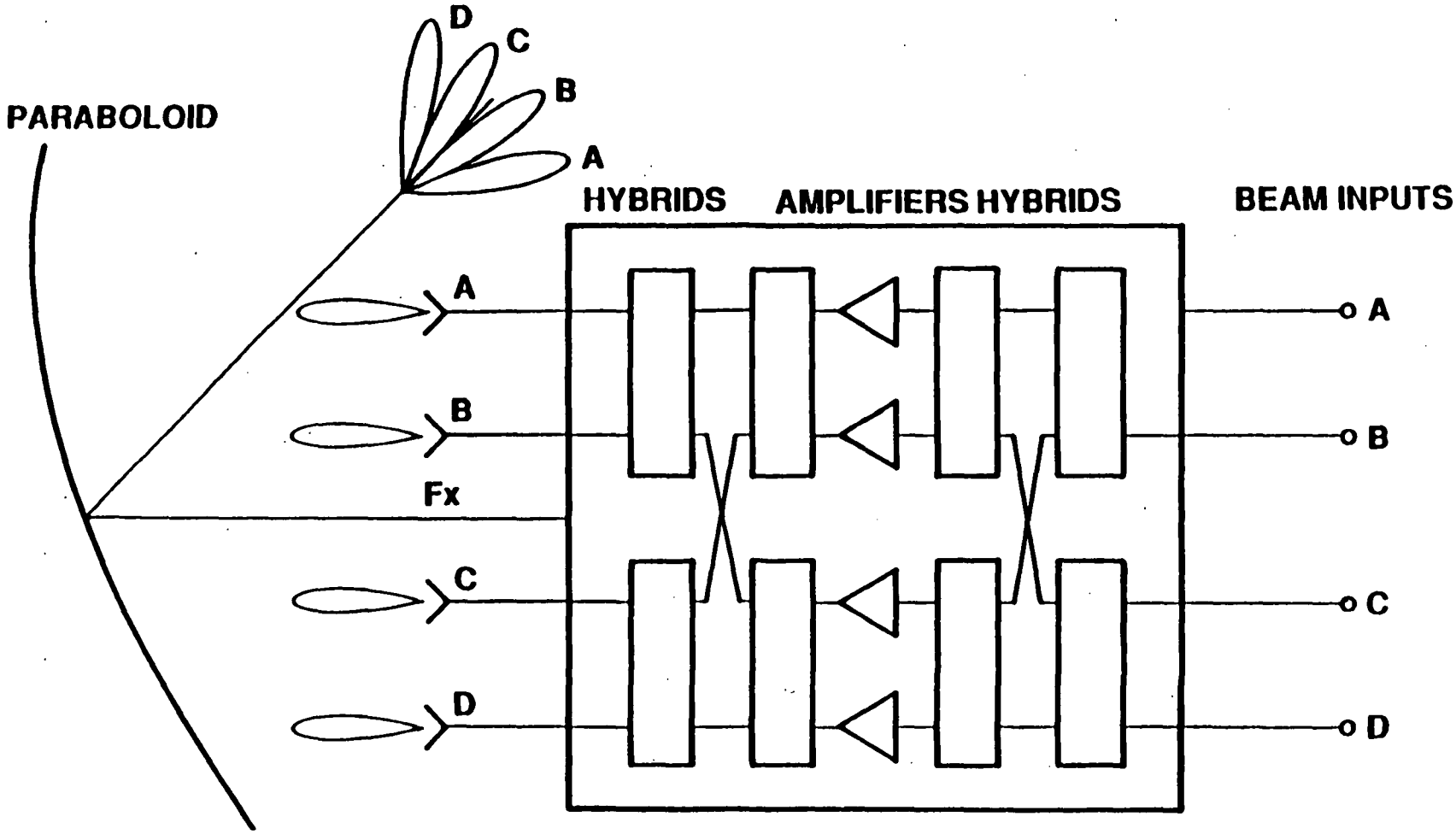

Figure 4. **Hybrid multibeam amplifier concept: Each beam is produced by a separate feed but shares in all the amplifiers.**

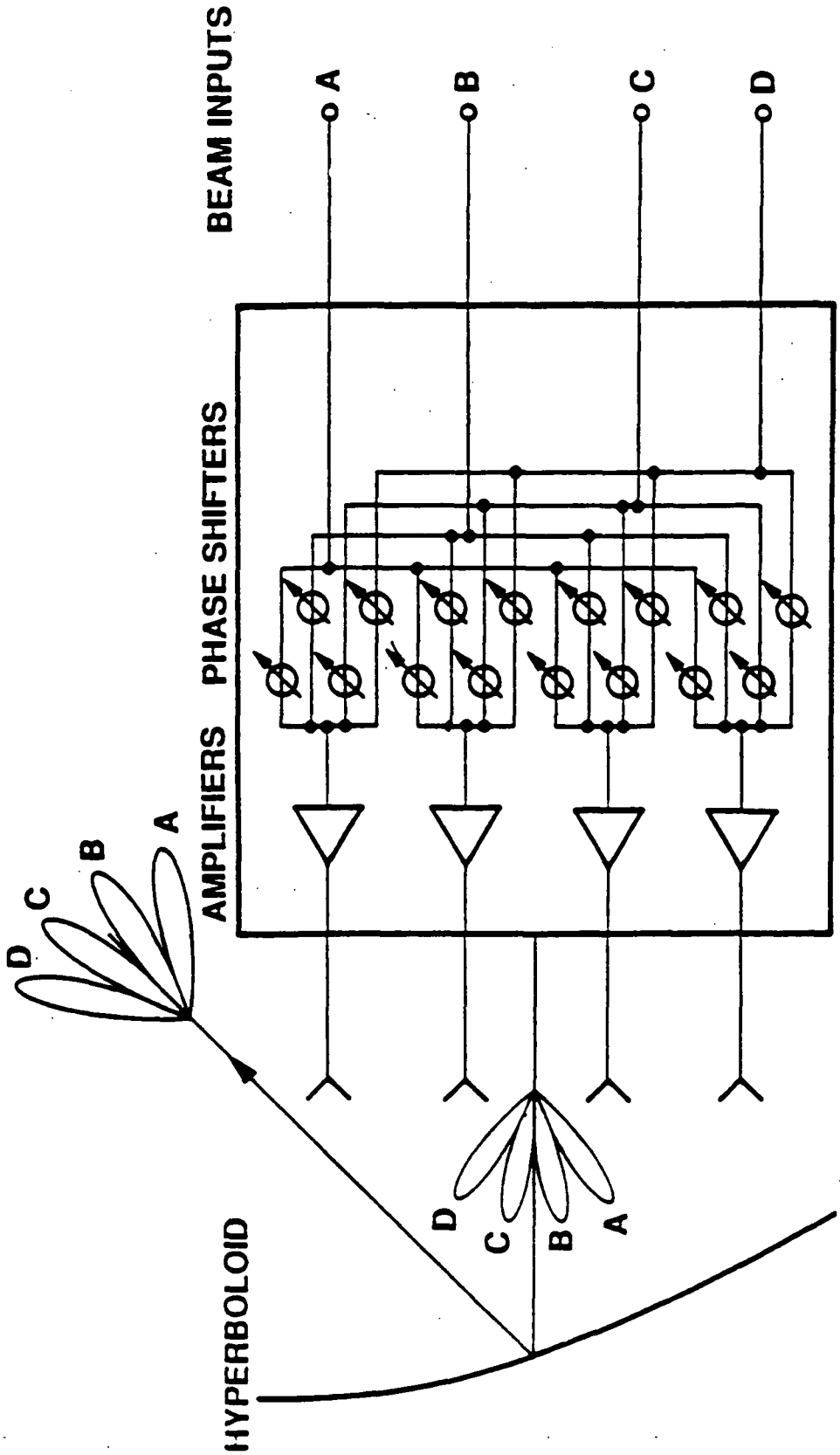

Figure 5. Near-field phased array concept: Each beam is produced by all the feed elements and shares in all the amplifiers.

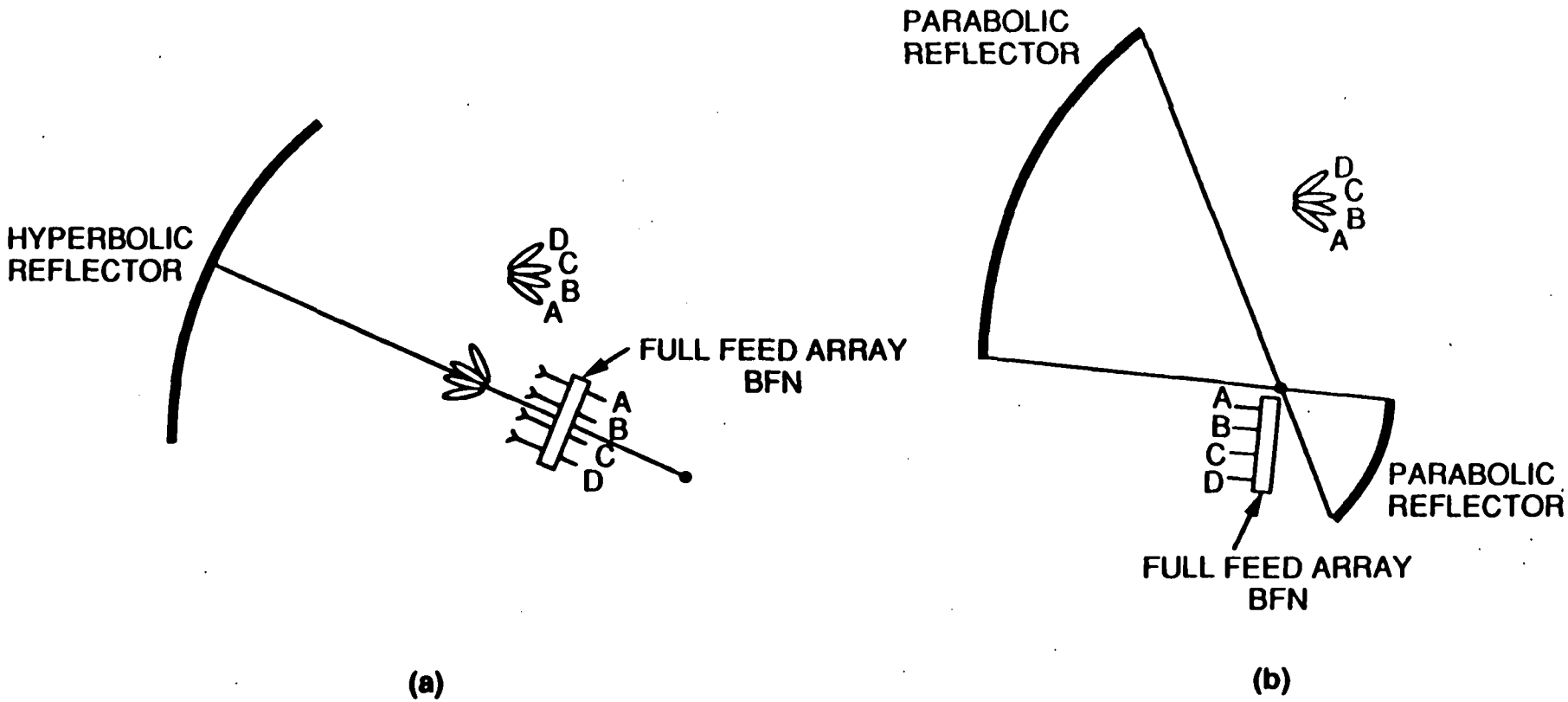

Figure 6. **Simultaneous fixed multibeam antenna using full aperture feed array to provide each beam. a) Single hyperbolic reflector with phased array, b) Dual parabolic reflector with near-field phased array.**

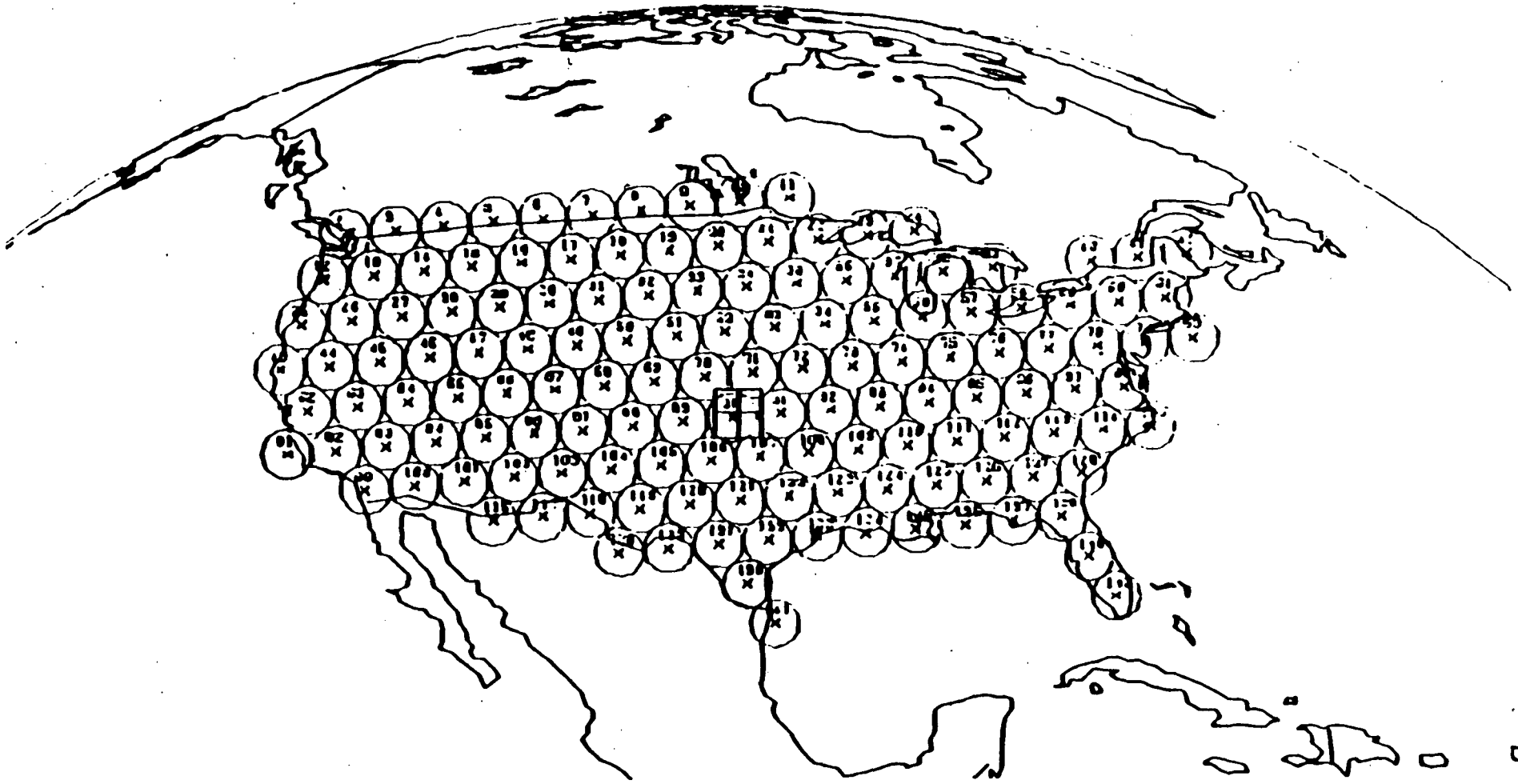

D-7382

Figure 7. **CONUS coverage with 142 spot beams with 0.35° half-power beamwidth using a 2-meter diameter antenna at 30 GHz or a 3-meter antenna at 20 GHz.**

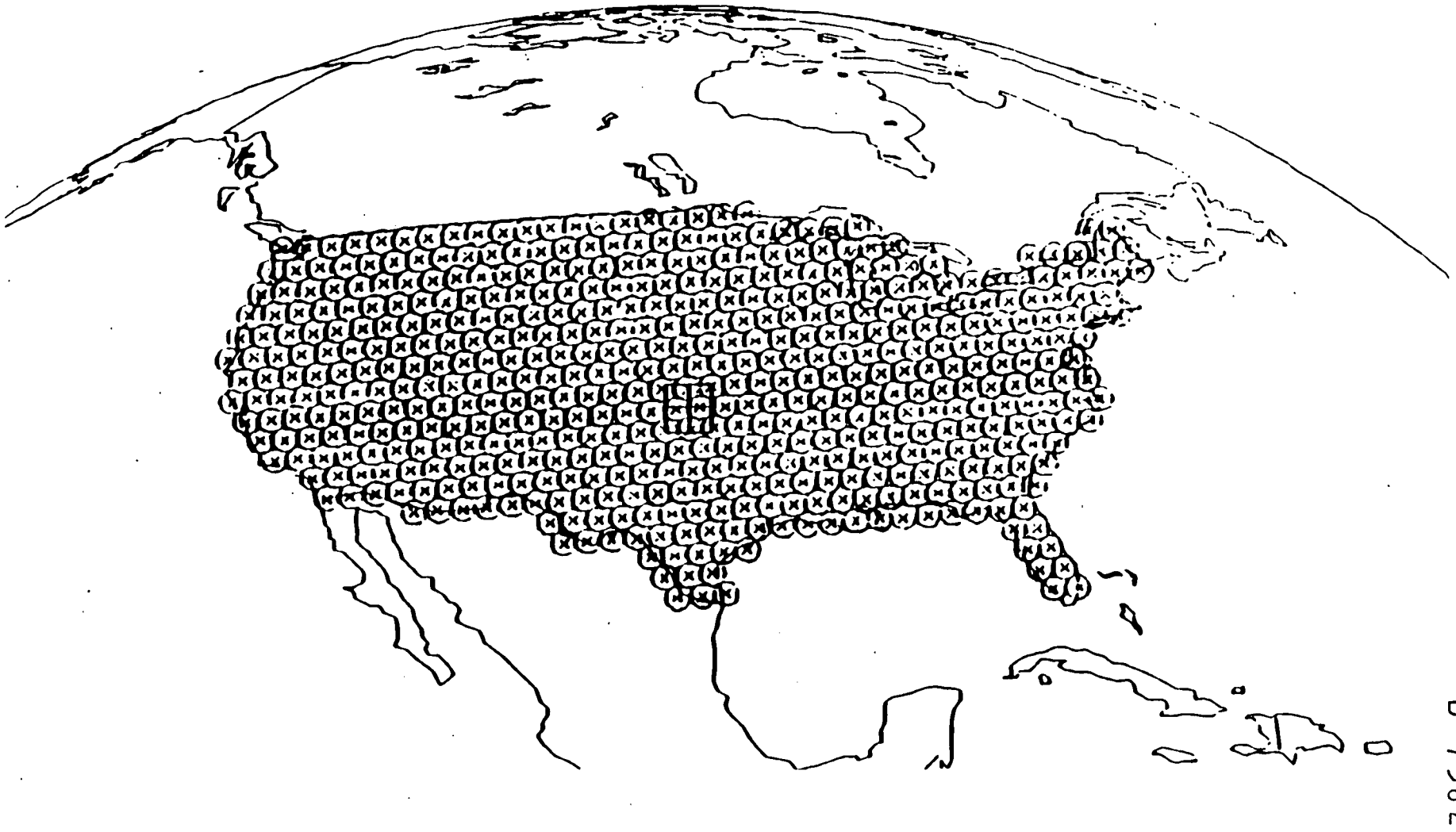

D-7382

Figure 8. **CONUS coverage with 582 spot beams with 0.175° half power beamwidth using a 4-meter diameter antenna at 30 GHz or a 6-meter antenna at 20 GHz.**

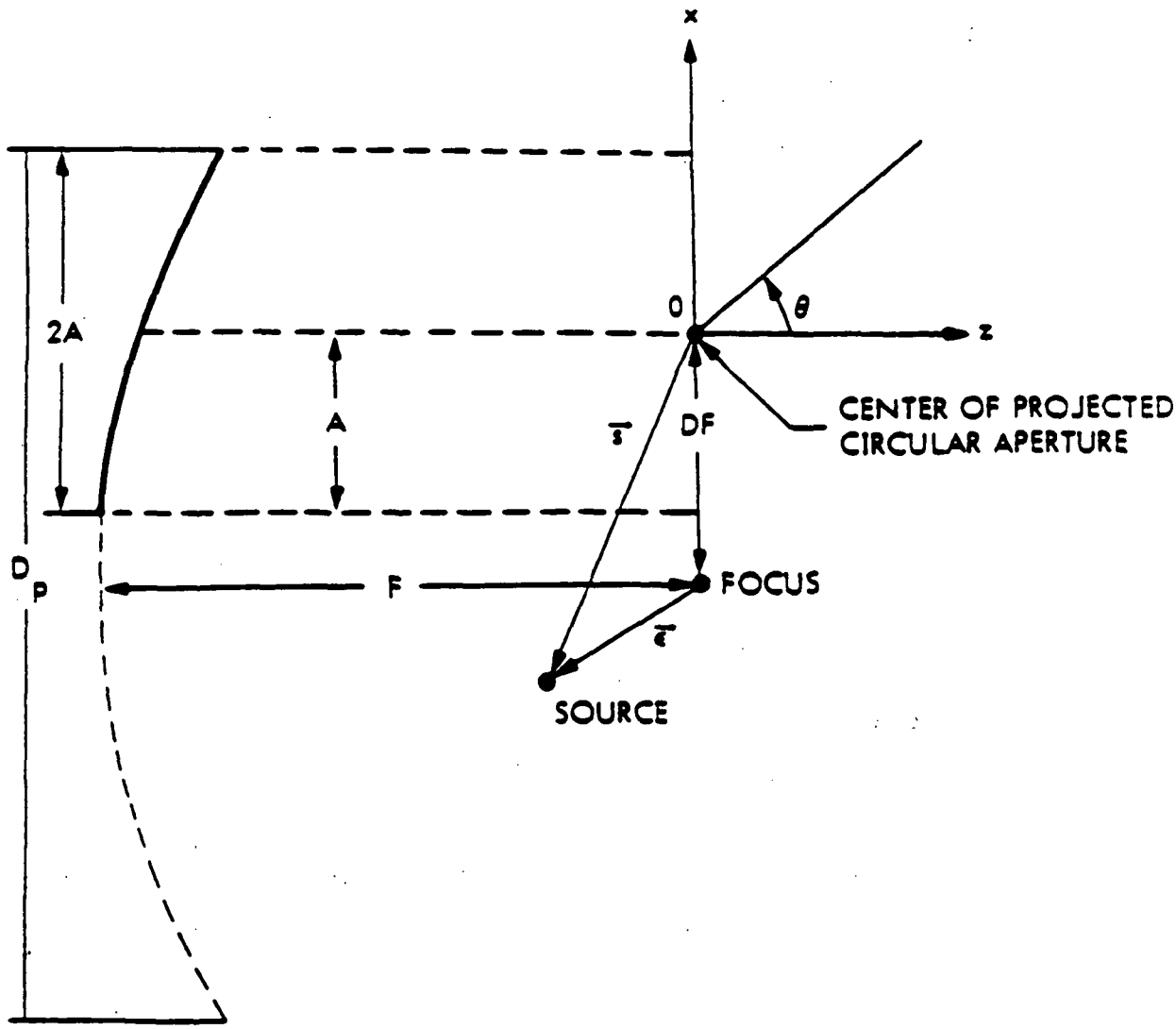

Figure 9. Offset parabolic reflector geometry.

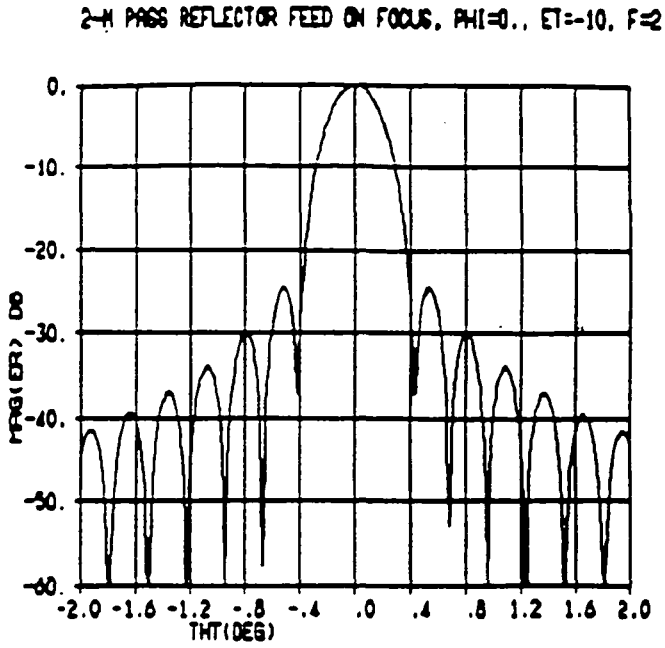

(a)

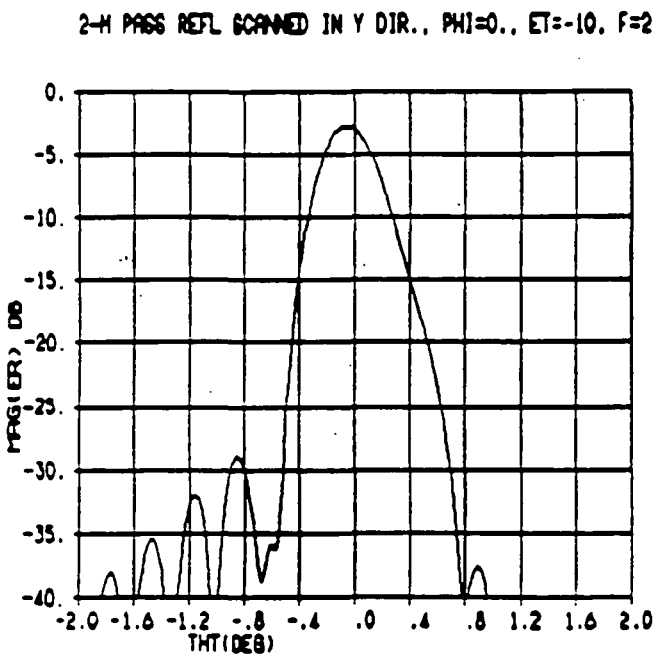

(b)

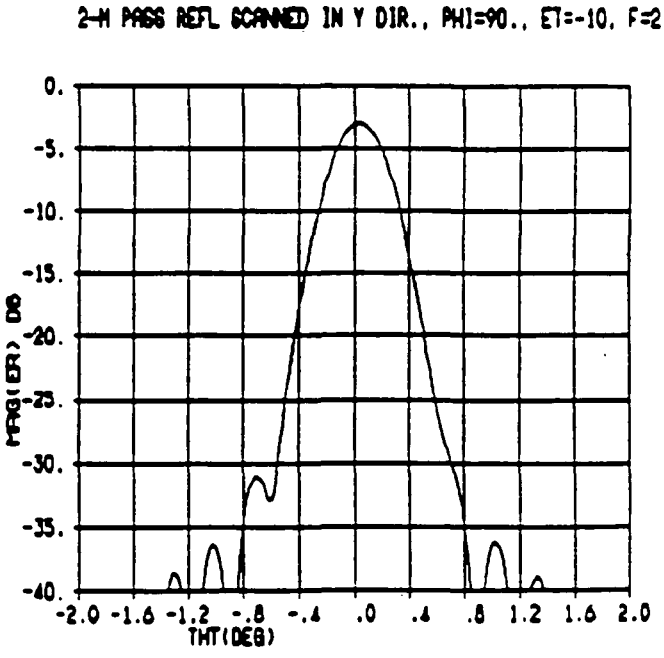

(c)

Figure 10. 2-meter antenna patterns for F/D=1, ET=-10; (a) Feed on focus; (b) and (c) Feed scanned in the Y direction, PHI=0° and PHI=90° cuts.

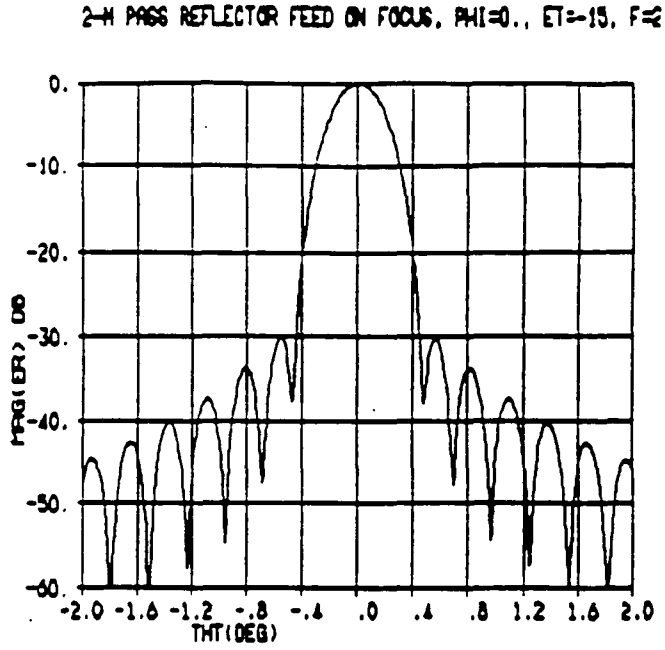

(a)

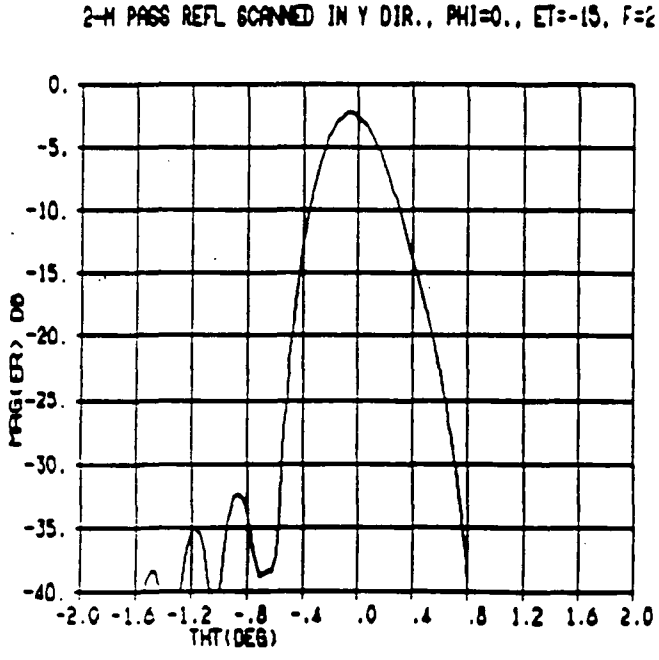

(b)

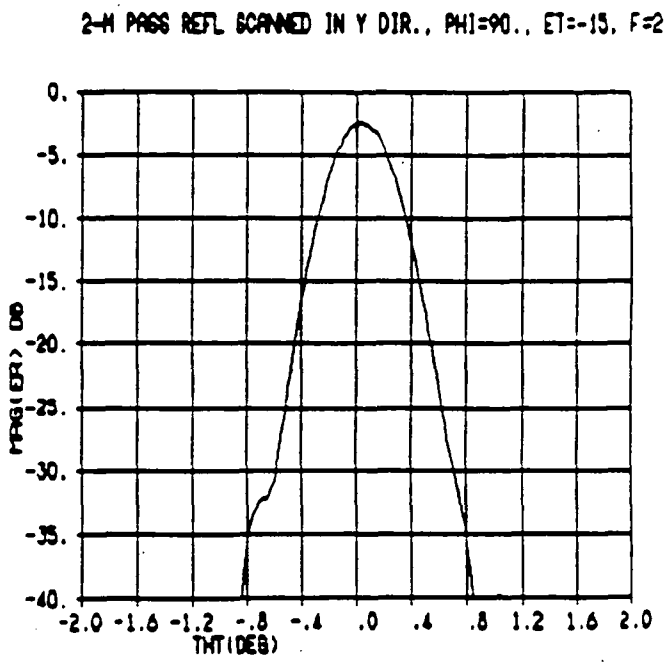

(c)

Figure 11. 2-meter antenna patterns for F/D=1, ET=-15; (a) Feed on focus; (b) and (c) Feed scanned in the Y direction, PHI=0° and PHI=90° cuts.

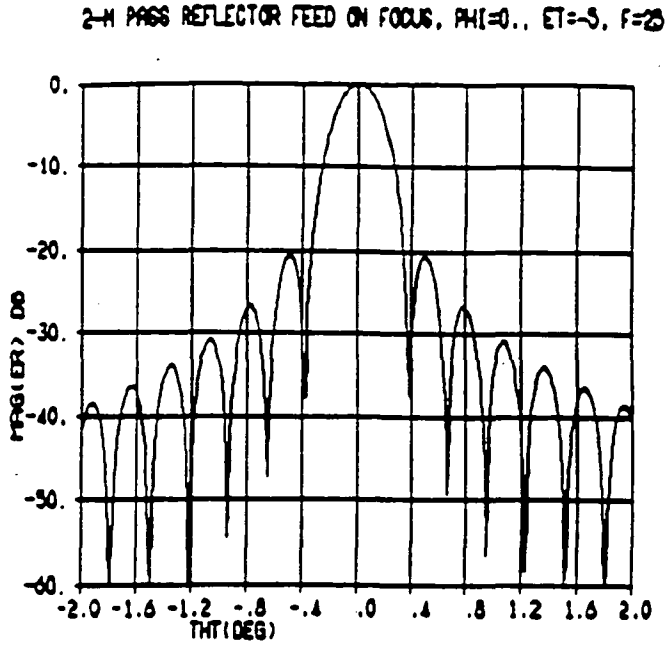

(a)

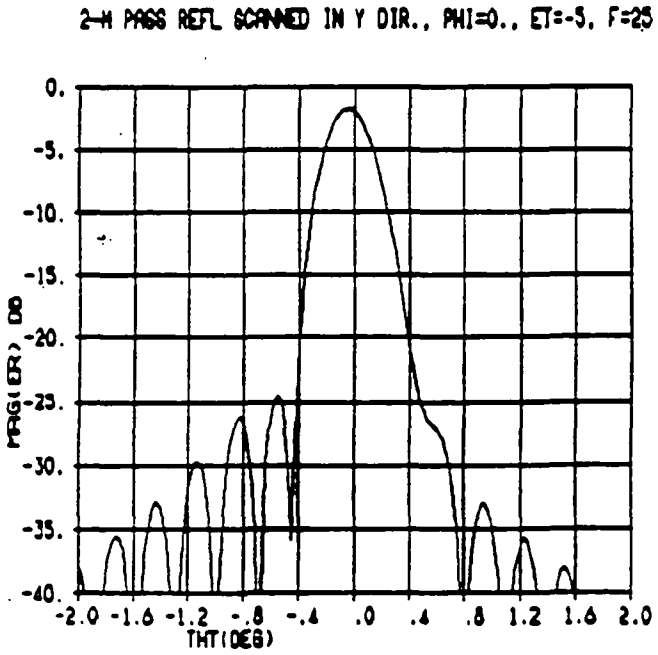

(b)

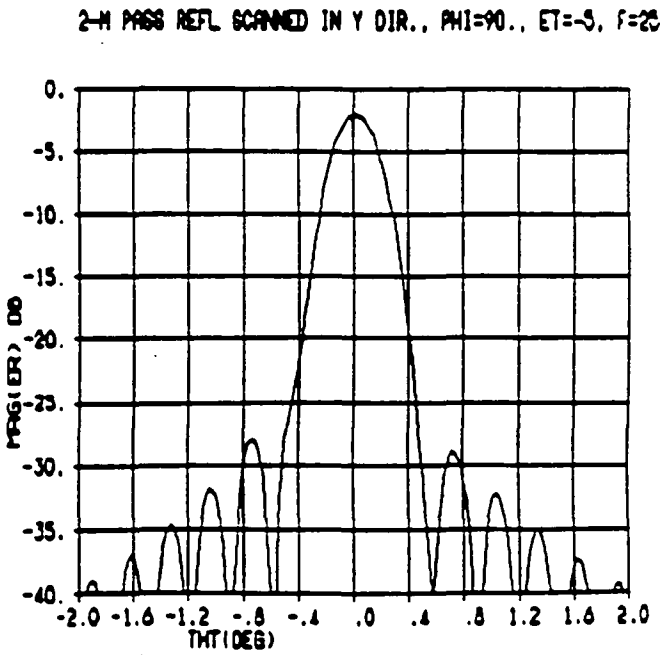

(c)

Figure 12. **2-meter antenna patterns for F/D=1.25, ET=-5; (a) Feed on focus; (b) and (c) Feed scanned in the Y direction, PHI=0° and PHI=90° cuts.**

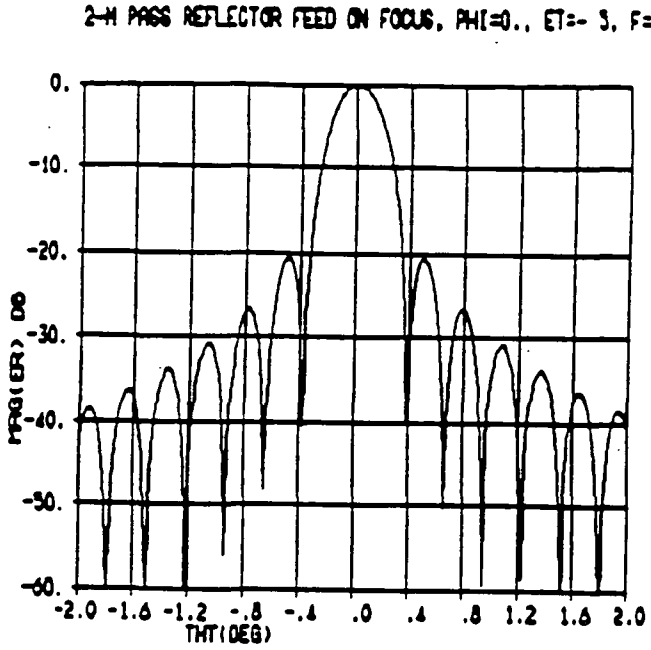

(a)

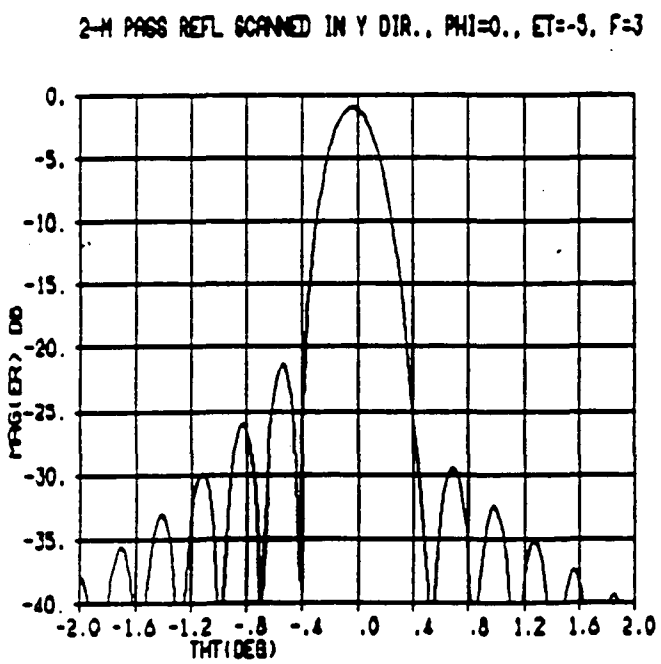

(b)

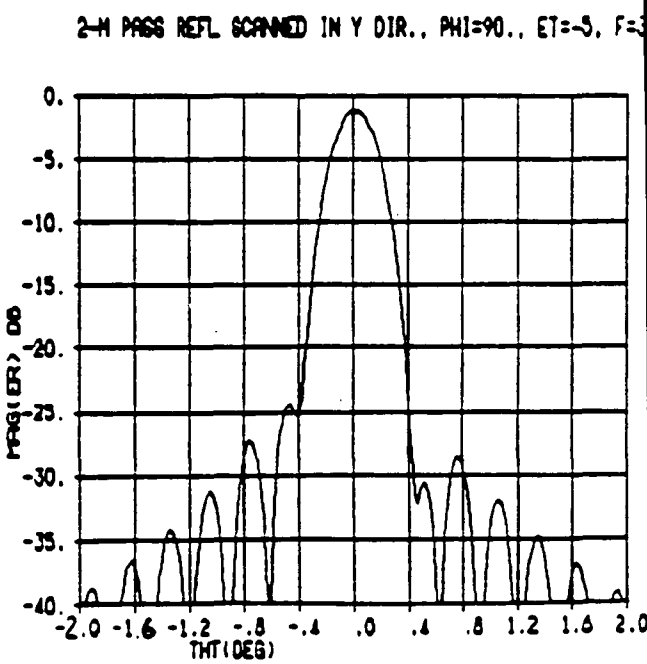

(c)

Figure 13. **2-meter antenna patterns for F/D = 1.5, ET = -5; (a) Feed on focus; (b) and (c) Feed scanned in the Y direction, PHI = 0° and PHI = 90° cuts.**

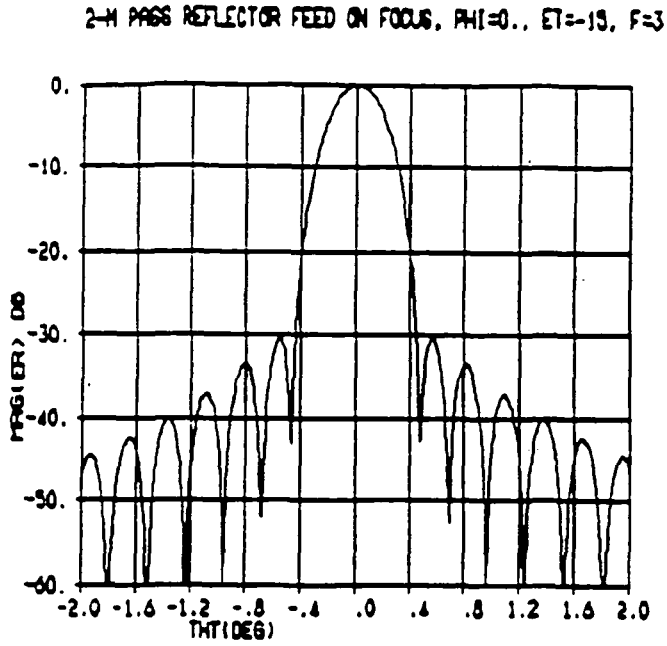

(a)

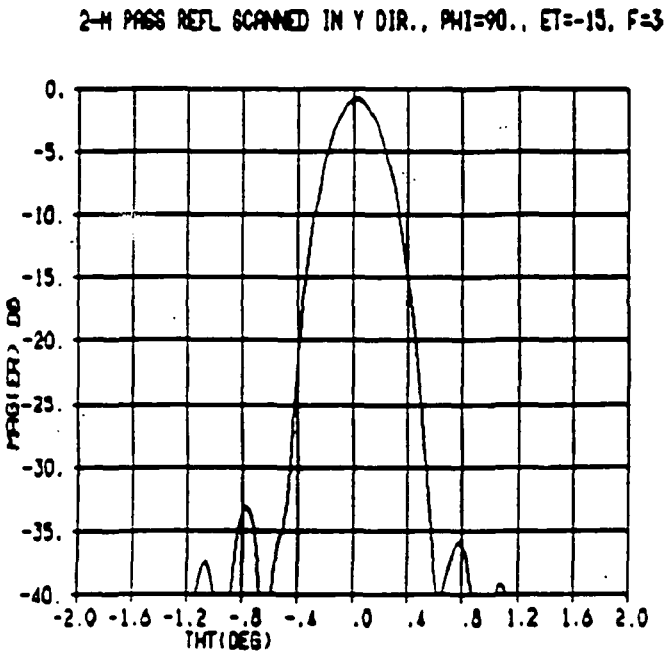

(b)

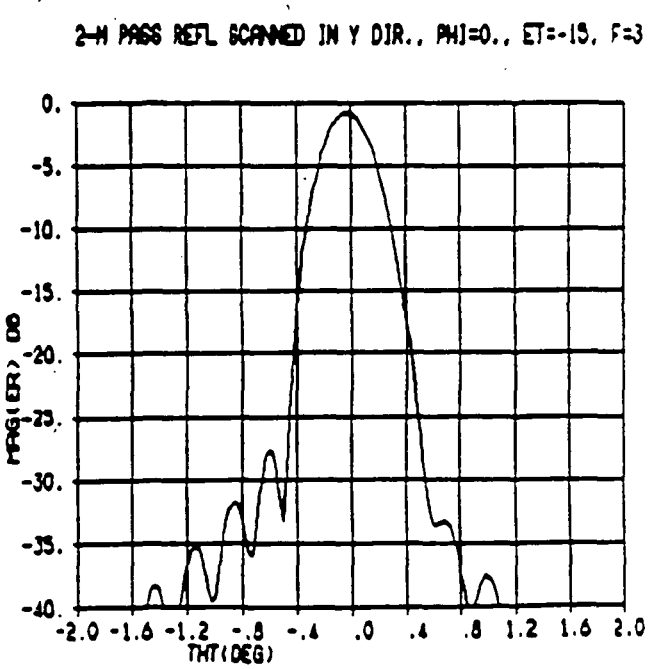

(c)

Figure 14. 2-meter antenna patterns for F/D=1.5, ET=-15; (a) Feed on focus; (b) and (c) Feed scanned in the Y direction, PHI=0° and PHI=90° cuts.

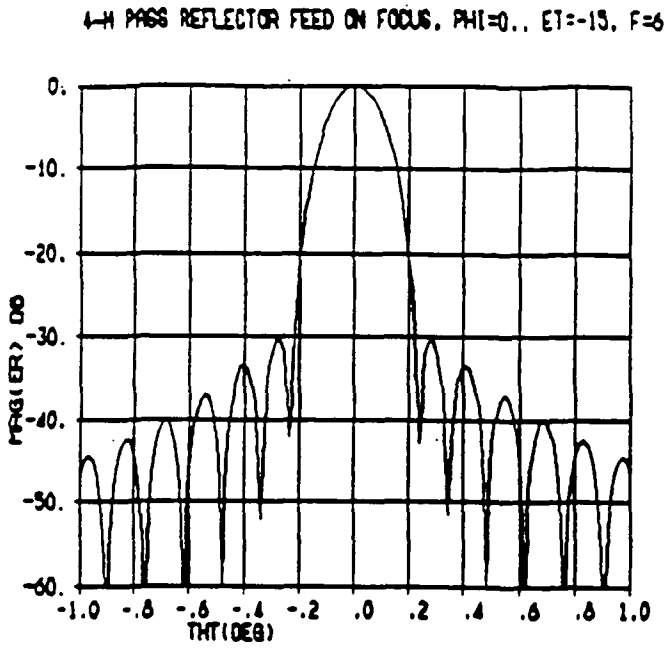

(a)

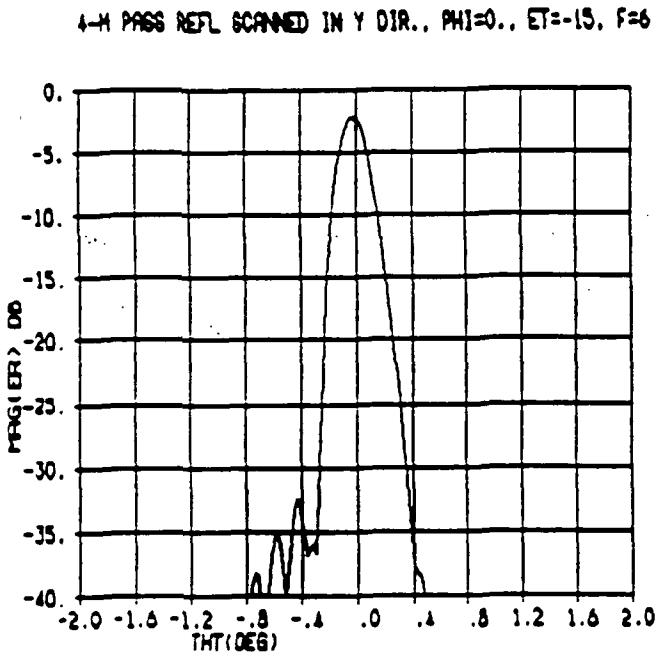

(b)

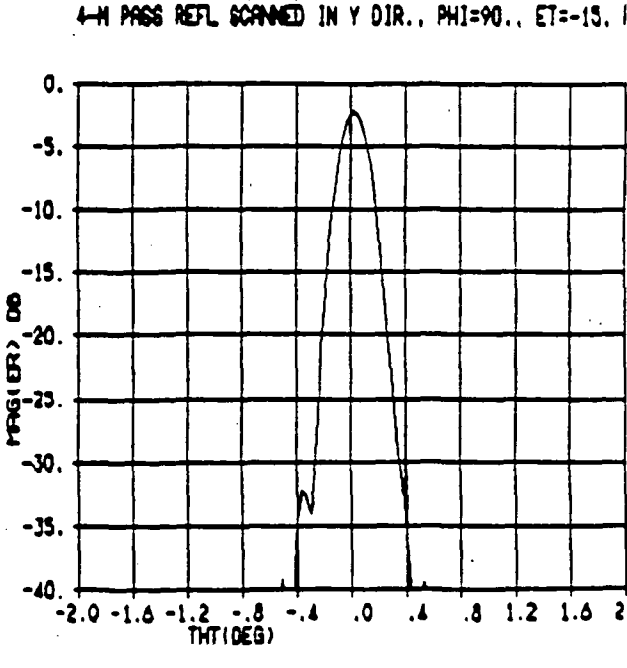

(c)

Figure 15. **4-meter antenna patterns for F/D=1.5, ET=-15; (a) Feed on focus; (b) and (c) Feed scanned in the Y direction, PHI=0° and PHI=90° cuts.**

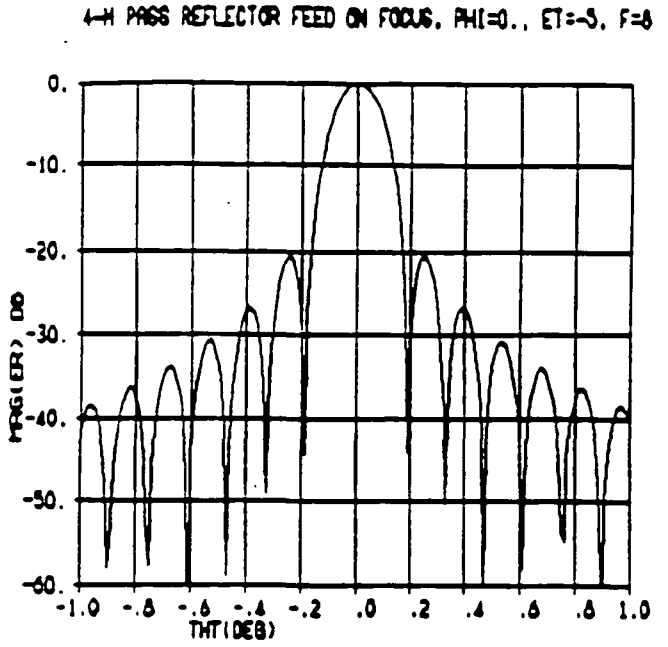

(a)

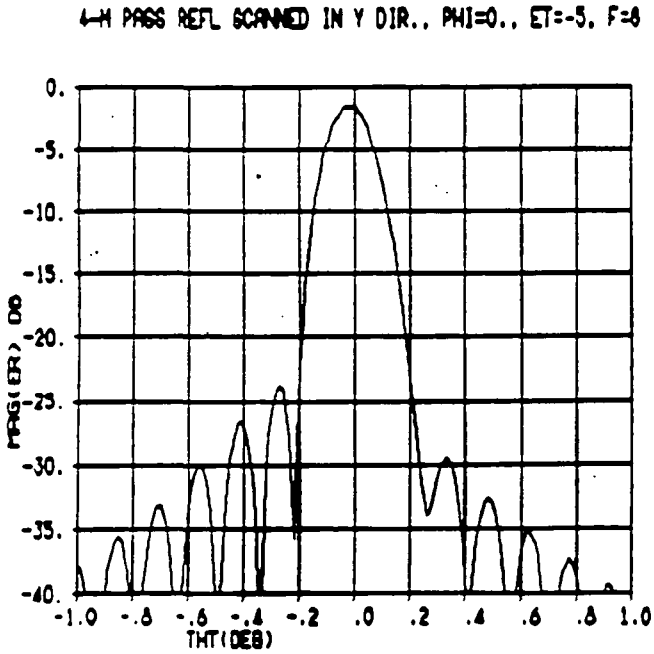

(b)

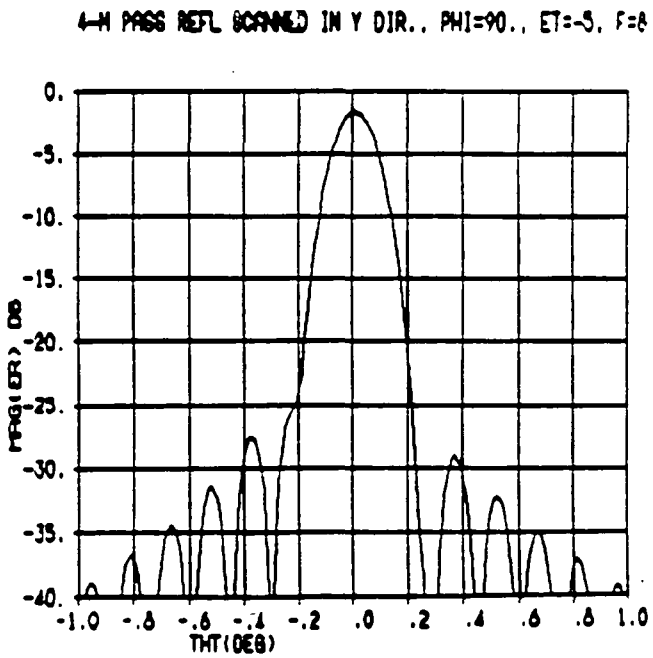

(c)

Figure 16. **4-meter antenna patterns for F/D=2.0, ET=-5; (a) Feed on focus; (b) and (c) Feed scanned in the Y direction, PHI=0° and PHI=90° cuts.**

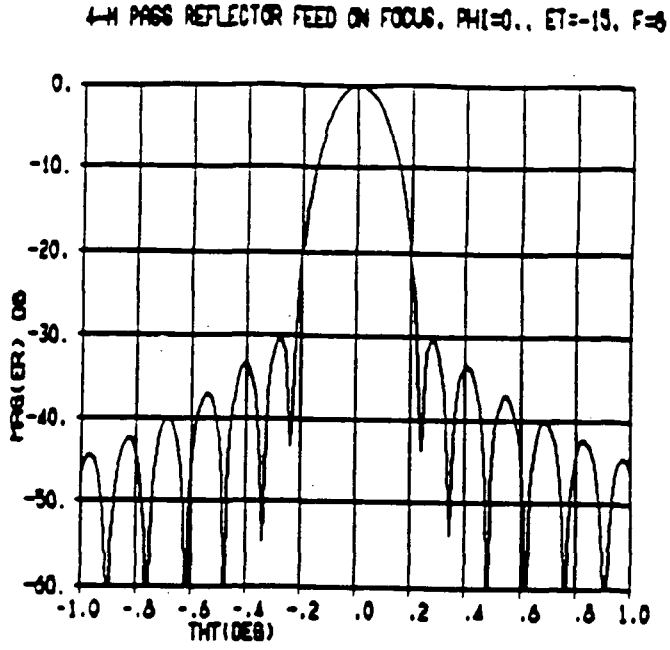

(a)

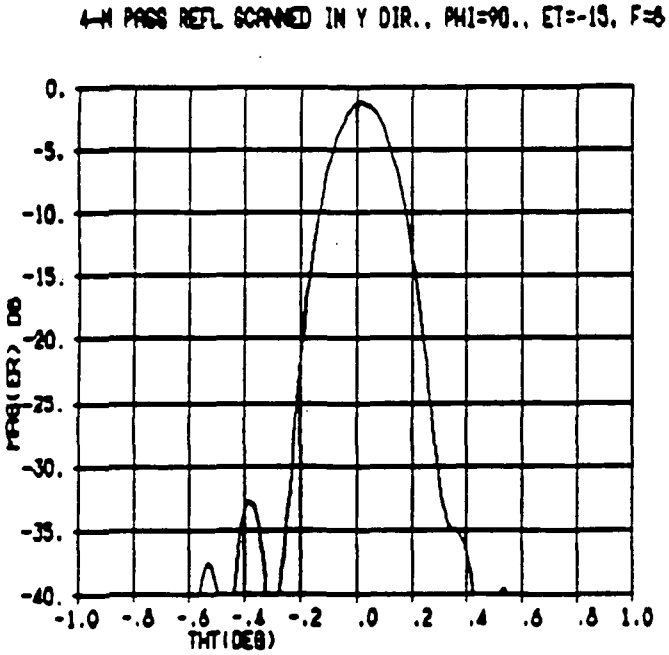

(b)

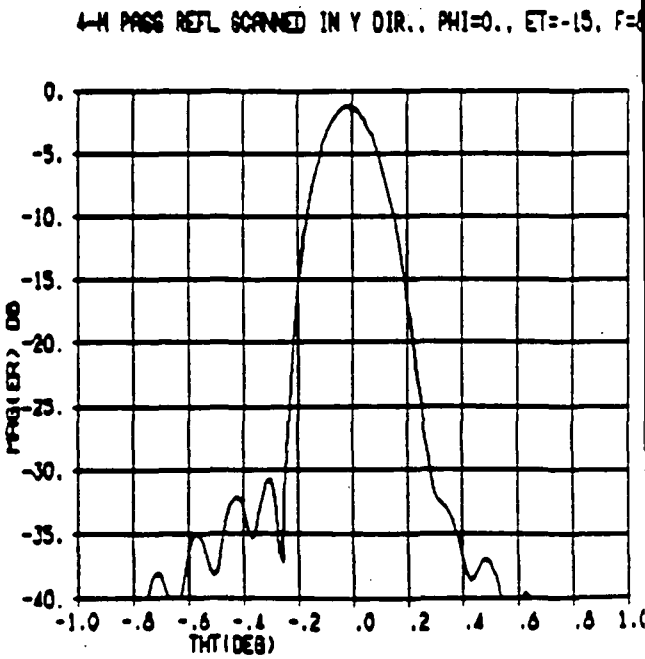

(c)

Figure 17. 4-meter antenna patterns for F/D=2.0, ET=-15; (a) Feed on focus; (b) and (c) Feed scanned in the Y direction, PHI=0° and PHI=90° cuts.

TABLE 1. TILT ANGLE OF VERTICAL POLARIZATION AT SELECTED CONUS LOCATIONS				
LENGTH UNIT: kilometer, ANGLE UNIT: degree				
POSITIVE AZIMUTH: ccw from south, POSITIVE ELEVATION: from ground up				
EARTH RADIUS:	6378			
SATELLITE POSITION:	ALTITUDE	LONGITUDE	LATITUDE	
	35838	-95.00	0.00	
ANTENNA BORESIGHT POSITION		-95.00	36.00	
		GROUND TERMINAL POSITION		POLARIZATION
SITE		LONGITUDE	LATITUDE	TILT ANGLE
ARIZONA		-111.00	31.30	24.27
CALIFORNIA, CAPE		-120.50	34.50	31.89
CALIFORNIA, PASADENA		-118.14	34.15	29.93
CALIFORNIA, SOUTHWESTERN POINT		-117.00	32.50	30.30
CALIFORNIA, WESTERN MOST POINT		-124.50	40.50	29.79
FLORIDA TIP		-80.50	25.00	-28.12
KANSAS, KANSAS CITY		-94.70	38.90	-0.37
LOUISIANA		-90.00	29.00	-8.90
MAINE, NORTHEAST		-68.00	47.20	-22.65
MASSACHUSETTS, CAPE		-70.00	42.00	-24.99
MINNESOTA, NORTHERN BUMP		-95.00	49.40	0.00
MONTANA, MID-NORTHERN BOUNDARY		-110.00	49.00	12.60
NORTH CAROLINA		-75.50	36.00	-24.54
PUERTO RICO, SAN JUAN		-66.00	18.00	-55.94
TEXAS, WESTERN COAST		-97.40	25.80	4.93
TEXAS, WESTERN END		-103.20	29.00	14.37
WASHINGTON D.C.		-77.03	38.89	-20.81
WASHINGTON, NORTHWEST		-124.70	48.40	23.59
ALASKA, ANCHORAGE		-150.00	61.50	23.80
ALASKA, KETCHIKAN		-130.00	55.00	21.73
ALASKA, KODIAK		-152.00	57.50	27.91
ALASKA, LITTLE ISLAND		-180.00	52.00	37.63
ALASKA, NOME		-165.00	64.50	23.96
ALASKA, PRUDHOE		-148.00	71.00	15.26
ALASKA, PT BARROW		-157.00	73.00	14.99
HAWAII, HONOLULU		-157.80	21.40	65.84
CANADA, EASTERN MOST POINT		-53.00	47.00	-31.75
CANADA, WESTERN MOST POINT		-141.00	69.60	14.86

Table 2: 2-meter Antenna On- and Off-Axis Gain and Efficiency as a Function of F/D and ET.

F/D	ET	On-Axis Gain, dB (Efficiency, %)	Off-Axis Gain, dB (Efficiency, %)
1.0	-10	54.9 (78.3)	51.8 (38.3)
1.0	-15	55.0 (80.0)	52.5 (45.0)
1.25	-5	54.3 (68.2)	52.2 (42.0)
1.5	-5	54.3 (68.2)	53.0 (50.5)
1.5	-15	54.9 (78.3)	53.9 (62.2)

Table 3. 4-meter Antenna on- and Off-Axis Gain and Efficiency as a Function of F/D and ET.

F/D	ET	On-axis Gain, dB (Efficiency, %)	Off-Axis Gain, dB (Efficiency, dB)
1.5	-15	60.9 (77.9)	58.5 (44.6)
2.0	-5	60.3 (67.9)	58.5 (44.8)
2.0	-15	60.9 (77.9)	59.6 (57.8)

365

Appendix I. Polarization Options for the PASS System

(P. Cramer)

An open issue for the PASS program is the choice of polarization, linear vs. circular. Linear polarization is the simplest to implement both on the satellite and in the ground terminal and therefore would be the preferred polarization type if it has no performance limitations. The primary limitation would be if the angle (polarization angle) between the effective polarization vectors of the satellite and ground user terminal antennas where of a sufficient magnitude such that the polarization loss exceeded an acceptable level. If the polarization loss is unacceptable, then circular polarization would be required since circular polarization does not suffer a loss associated with a polarization angle.

To resolve this issue, the polarization angle for linear polarization was calculated for typical satellite/ground user terminal geometries. The following definition is used to define the polarization angle. See Figure 1. Two planes, both containing the line of sight between the satellite antenna and the ground user antenna, will be defined with the angle between the two planes being the polarization angle. The first plane will be defined by the line of sight and the polarization vector of the ground user antenna (such as the local vertical for vertical polarization). The user terminal effective polarization vector is in this plane and at a right angle to the line of sight. The second plane will be defined by the line of sight vector and the satellite antenna polarization vector (such as vertical polarization). Again the satellite antenna effective polarization vector is in the second plane and at a right angle to the line of sight. The angle then between the effective polarization vectors and hence the two planes defines the polarization angle. This definition was selected to eliminate the possibility of including pattern directivity effects in the computation of the polarization angle. The polarization power loss would then be equal to the square of the cosine of the polarization angle.

The assumptions were made that the satellite is in a geo-synchronous orbit midway across the continental US (95.0 W longitude) and has the antenna boresighted approximately at the middle of CONUS so that CONUS type pattern coverage could be provided. The polarization angle was then calculated for user ground terminals located around the periphery of the country as this should identify the worst cases. The polarization angles were computed for both vertical and horizontal polarization where the polarization of the user terminal antenna is defined to be either along or normal to the local vertical. Table 1 summarizes the geometry and in the last column, lists the polarization angles associated with each location. The worst cases are along the western and eastern coastlines with the angles getting larger towards the south. With angles ranging from 22 to 30 degrees, this represents polarization losses of from 0.7 to 1.3 dB. However since the ground user terminals must include hand held devices that can not be oriented accurately, the effect of orientation errors must be included in the polarization angle determination. No attempt was made to accurately define what the extent of the orientation errors would be in typical usage, however to get a feel for the effect of such errors, it was assumed that realistic errors would be between 25 to 30 degrees. 27 degrees was specifically selected since this represents a loss of 1.0 dB. Adding this orientation angular error in the worst case direction to the polarization angles in Table 1 gives polarization losses from 3.7 to 5.3 dB. If the orientation errors are any larger, the losses are going to increase rapidly since the cosine of an angle changes rapidly for angles larger than 50 degrees.

Tables 2 and 3 show cases where the satellite is located towards the western and eastern ends of the country to determine the effect of the satellite location on polarization angle. As can be seen the worst case polarization angles are approximately 45 degrees. Orientation errors would have to be held within 12 degrees if losses similar to the centrally located satellite case are to be obtained. However, while the polarization error increased along one coastline, it improved along the opposite coastline. If the satellite antenna is adjusted about its boresight axis, it is possible to balance the polarization angles between each coast and the losses should be comparable to the case for the

centrally located satellite. However, it might not always be possible to adjust the satellite antenna to minimize the polarization angle if redundant or multiple satellites are used in different locations and there is a need to be able to move the satellites to any of these assigned orbit location.

The possibility exists that the polarization orientation of each feed element in the satellite antenna feed array could be adjusted to match the user terminal polarization at the beam direction associated with that feed element. This would eliminate the satellite to user local vertical polarization loss. However, it still does not eliminate the user terminal orientation errors as the 27 degree error equates to a 1.0 dB loss. This solution still has the limitation as to the range in satellite locations that could be supported since it is not feasible to custom design the satellite antenna for each satellite location.

If circular polarization is used, there could be as much as 0.4 dB in increased losses for the user terminal. For a typical patch antenna design, an additional power splitter would be required to generate circular polarization and the additional microstrip circuitry could cut down on the efficiency of the required dual frequency design. The satellite antenna system is to have separate antennas for each frequency and since costs are not as critical for a satellite antenna, it is conceivable that a lower loss solution should be attainable to produce circular polarization, with a loss lower than 0.2 dB.

It is my recommendation that circular polarization be used for the PASS program for the following reasons: Since handheld terminals must be supported by the PASS program, it is not reasonable to expect the average user to be able to control the orientation of their terminal any better than 27 degrees. Assuming that the satellite to user terminal local vertical optimization is used then, polarization losses on the order of 1.0 dB or more can still be expected assuming a terminal orientation error of 27 or more degrees. Even with the circular polarization implementation losses on the order of 0.5 dB, 0.5 dB or more improvement could be obtained with circular polarization. Secondly, if it is not feasible for what ever reason to optimize the satellite antenna

design, then losses as high as 5.0 dB would result, considerably higher than the circular polarization implementation losses. Thirdly it does not seem practical to give up the mission flexibility of being able to locate a given satellite or satellite design in more than one orbit location simply to utilize linear polarization. Commercial satellites in the past have had to live with the fact that in many cases it was not know what their specific orbit location assignments would be until close to launch time. There is no reason to expect that this problem will change in the future. The main argument used in favor of linear polarization is cost and possibly weight. However, with the continual development of integrated and etched antenna circuits and technology, and considering the time frame in which the PASS system would be widely used, there should be very little difference in cost and weight between the two polarization types. The differences in cost will show up primarily as development costs and should be able to be amortized over a large user base and it is part of the technology development activity to make this happen. And lastly, circular polarization leaves open the possibility to take advantage of new antenna concepts or system requirements that might be developed in the future that would not be compatible with linear polarization.

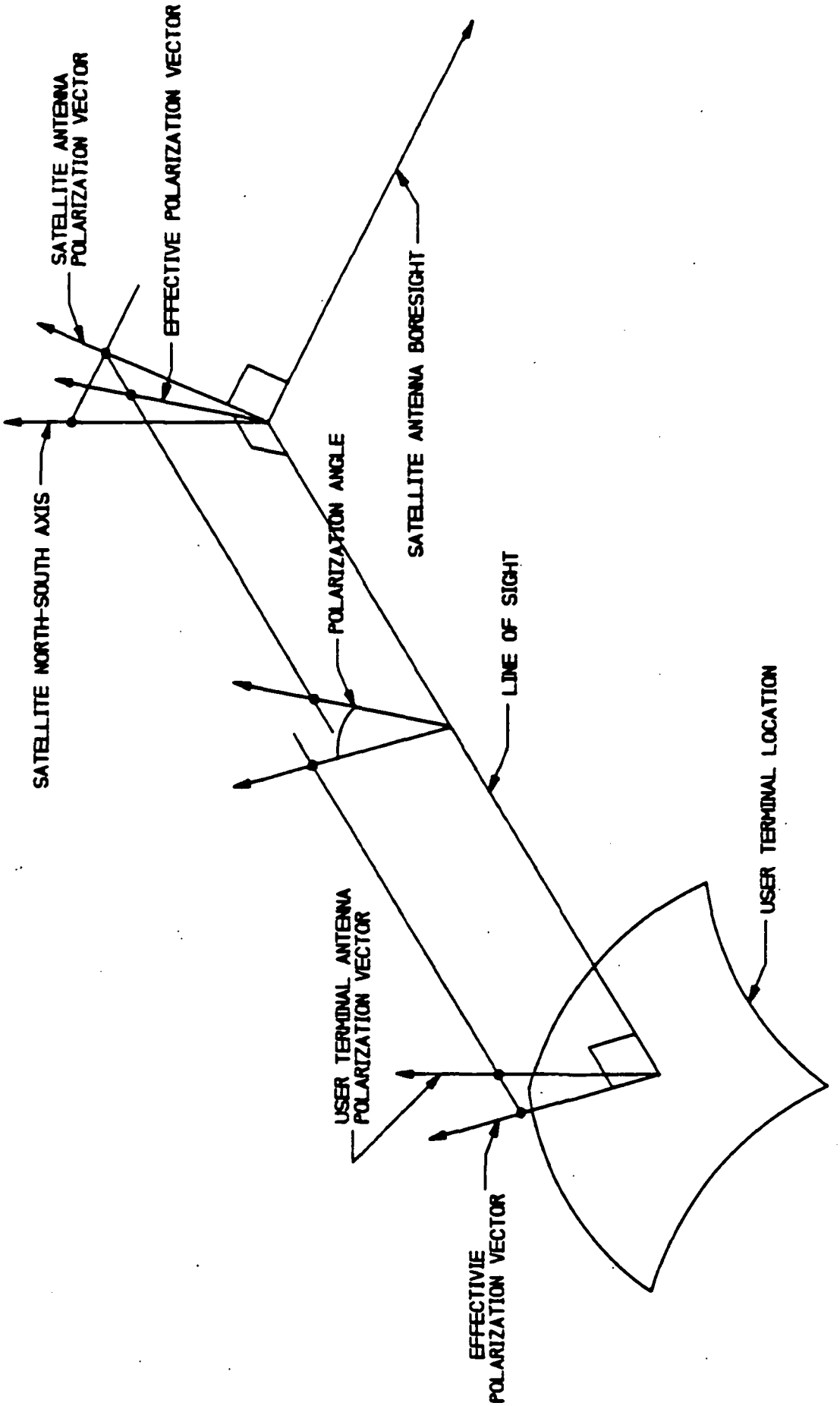

POLARIZATION ANGLE DEFINITION

FIGURE 1

Table 1

SATELLITE/GROUND STATION GEOMETRY

DATE: 11-02-88, TIME: 03:35:13.03 PM

SATELLITE DESCRIPTION:
LATITUDE = .000 DEG ALTITUDE = 35838.052 KM
LONGITUDE = -95.000 DEG EARTH RADIUS = 6378.160 KM

ANTENNA BORESITE LOCATION:
LATITUDE = 36.000 DEG ALTITUDE = .000 KM ELEVATION = 3.777 DE
LONGITUDE = -95.000 DEG AZIMUTH = .000 DE

GROUND TERMINAL LOCATION IN EARTH COORD.				IN ANTENNA COORD NORMAL/TILDE		SATELLITE LOCATION	POLARIZATI ANGLE
SITE	LAT./LONG.	ALT.	RANGE (KM)	POLAR	AZIMUTH	ELEV/AZ	VERT/HORI
Seattle, Wash	47.597	.000	38733.406	3.165	67.422	29.227	22.630
	-122.330			88.785	87.077	145.013	22.568
San Francisco, Calif	37.775	.000	38013.671	3.504	87.822	37.693	30.544
	-122.417			89.867	86.499	139.742	30.536
Los Angeles, Calif	34.058	.000	37589.490	3.197	95.663	43.252	30.114
	-118.250			90.315	86.819	142.506	30.131
San Diego, Calif	32.713	.000	37459.718	3.135	98.975	45.069	30.247
	-117.153			90.489	86.903	143.007	30.273
El Paso, Tex	31.755	.000	37069.400	1.766	109.142	50.981	17.732
	-106.480			90.579	88.331	158.899	17.730
Houston, Tex	29.763	.000	36815.947	.845	176.307	55.301	.630
	-95.362			90.843	89.946	179.271	.631
Miami, Florida	25.775	.000	36797.485	2.708	237.619	55.635	-27.730
	-80.190			91.450	92.287	211.301	-27.808
Norfolk, Va	36.845	.000	37612.656	2.496	271.488	42.934	-23.054
	-76.287			89.935	92.495	209.461	-23.051
Van Buren, Maine	47.158	.000	38688.306	3.150	291.881	29.730	-22.735
	-67.942			88.826	92.924	214.863	-22.695
Detroit, Mich	42.333	.000	37860.493	1.652	296.580	39.640	-12.740
	-83.050			89.261	91.478	197.447	-12.721
Duluth, Minn	46.783	.000	38139.171	1.267	344.883	36.141	-2.696
	-92.113			88.777	90.321	183.959	-2.689
Billings, Mont	45.780	.000	38179.834	1.909	54.762	35.645	12.740
	-108.505			88.899	88.441	161.473	12.710
Kansas City, Mo	39.100	.000	37483.084	.388	351.736	44.737	-.317
	-94.578			89.616	90.056	180.669	-.316

Table 2

SATELLITE/GROUND STATION GEOMETRY

DATE: 11-02-88. TIME: 04:19:23.30 PM

SATELLITE DESCRIPTION:
LATITUDE = .000 DEG ALTITUDE = 35838.052 KM
LONGITUDE = -110.000 DEG EARTH RADIUS = 6378.160 KM

ANTENNA BORESITE LOCATION:
LATITUDE = 36.000 DEG ALTITUDE = .000 KM ELEVATION = 5.746 DEG
LONGITUDE = -95.000 DEG AZIMUTH = -2.054 DEG

GROUND TERMINAL LOCATION IN EARTH COORD.			RANGE	IN ANTENNA COORD NORMAL/TILDE		SATELLITE LOCATION	POLARIZATIC ANGLE
SITE	LAT./LONG.	ALT.	(KM)	POLAR	AZIMUTH	ELEV/AZ	VERT/HORIZ
Seattle, Wash	47.597	.000	38316.020	3.661	68.774	34.013	10.776
	-122.330			88.675	86.587	163.510	10.697
San Diego, Calif	32.713	.000	37058.179	3.105	97.422	51.162	10.710
	-117.153			90.401	86.921	166.927	10.732
Miami, Florida	25.775	.000	37444.799	2.764	237.271	45.282	-45.762
	-80.190			91.494	92.325	232.803	-45.823
Van Buren, Maine	47.158	.000	39382.857	2.442	296.202	22.286	-31.882
	-67.942			88.922	92.191	230.900	-31.842

Table 3

SATELLITE/GROUND STATION GEOMETRY

DATE: 11-02-88. TIME: 04:28:16.40 PM

SATELLITE DESCRIPTION:
LATITUDE = .000 DEG ALTITUDE = 35838.052 KM
LONGITUDE = -80.000 DEG EARTH RADIUS = 6378.160 KM

ANTENNA BORESITE LOCATION:
LATITUDE = 36.000 DEG ALTITUDE = .000 KM ELEVATION = 5.746 DEG
LONGITUDE = -95.000 DEG AZIMUTH = 2.054 DEG

GROUND TERMINAL LOCATION IN EARTH COORD.			RANGE	IN ANTENNA COORD NORMAL/TILDE		SATELLITE LOCATION	POLARIZATION ANGLE
SITE	LAT./LONG.	ALT.	(KM)	POLAR	AZIMUTH	ELEV/AZ	VERT/HORIZ
Seattle, Wash	47.597	.000	39426.153	2.445	62.758	21.841	31.625
	-122.330			88.881	87.826	129.030	31.583
San Diego, Calif	32.713	.000	38232.857	2.874	101.377	35.005	43.174
	-117.153			90.567	87.183	125.497	43.202
Miami, Florida	25.775	.000	36577.959	2.454	235.367	59.876	.597
	-80.190			91.394	92.019	179.563	.548
Van Buren, Maine	47.158	.000	38272.498	3.630	290.705	34.531	-10.705
	-67.942			88.717	93.396	196.243	-10.629

APPENDIX II
Overlapping vs. Non-overlapping Feed Apertures for the PASS Satellite Antenna Concept

P. Cramer

One of the issues that needs to be resolved for the PASS Program satellite antenna design is whether or not overlapping apertures are required. The purpose of this memorandum is to address some of the issues so that a decision can be made.

A single non-overlapping feed aperture is the simplest design since a beam forming network is not required. This is reflected in a lower cost design with lower losses. However, for a design based on a crossover level of 3 dB between adjacent beams, the non-overlapping aperture has a higher illumination efficiency because the feed aperture size available causes the main reflector to be over-illuminated. The negative side of over-illuminating is a low spillover efficiency and a low crossover level between adjacent beams because of narrow beamwidths.

Overlapping aperture designs are not limited by the space available between the feed centers in the reflector focal plane. If the feed elements for one beam are allowed to overlap the feed elements for an adjacent beam, then the feed can be made as large as necessary to optimize the reflector illumination. Typically, the spillover efficiency will improve, but the illumination efficiency will drop as a result of larger edge tapers. The larger edge tapers however, produce lower side lobe levels and therefore the overlapping design is best for frequency reuse applications where high isolation is needed. In addition, the broader beamwidths associated with the lower illumination efficiencies produce higher crossover level between adjacent beams. Overlapping aperture designs require elaborate beam forming networks that are costly and introduce dissipative losses.

For the PASS program, in order to make the proper choice, the constraints must be identified. Frequency reuse is not a requirement. Therefore the high isolation of the overlapping design is not needed. However performance is a critical factor. The PASS concept design indicates that the basic personal terminal must have a gain of 22.8 dB at 30 GHz and provide an output power of 0.3 watt. However it turns out that these performance requirements are not compatible with the requirement that the terminal design not violate RF radiation safety standards [1]. From Figure 7 of reference [1], it turns out that a gain of about 29 dB and a power of only 0.072 watts are needed to reduce the radiated power density to a safe level and still provide the required EIRP. To market an user terminal with 29 dB gain would be prohibitively expensive. In any design, the cost of a ground terminal must be kept low to attract users and to achieve this, system complexity should be shifted to the satellite. Even at an increase cost to the satellite, the overall program costs normally would be lower. To reduce the user terminal gain, the user terminal EIRP must be reduced and the satellite performance

increased accordingly. To satisfy the higher satellite performance requirements, cost of the satellite antenna system is no longer the prime driver. Increasing the satellite antenna size to increase the gain to noise temperature ratio to compensate for the loss of EIRP from the user terminal is not attractive from a cost standpoint until the antenna efficiency has been maximized. Thus the choice between an overlapping feed design and a non-overlapping design should be made based on performance and to a much lesser degree on costs.

To compare the two feed concepts, the antenna configuration presented in the trade-off section of the "Second-Generation Mobile Satellite System" study [2] was used. From part two, section 2.7, the single element cluster with four patches per element is used as a typical example of a non-overlapping feed. The six element cluster with two patches per element is used as a good example of an overlapping feed. In all cases, the same patch size and spacings were used. From the study report, the single element cluster had a peak gain (or efficiency) 0.18 dB higher than the six element cluster. To gain more insight into the relative merits of the two configurations, the patterns of the two configurations were analyzed using the pattern efficiency program. The results are summarized in Table 1 and are identified as the "nominal" cases in the table. Equal excitations were used for all element and patches. The difference in efficiency for the two configurations with the base line F/D of 1.08 is 0.09 dB in favor of the single element cluster. The efficiency program is based on symmetrical reflector designs, while the cases analyzed in the system study are for offset designs. Since the two approaches give differences in efficiencies which are within 0.09 dB of each other (0.18 - 0.09), the efficiency program is still useful in performing trade-offs between various offset designs and provides additional insights since efficiency contributors such as spillover, illumination, phase, cross-polarization, etc are individually identified. Due to the broader secondary pattern of the six element cluster, the six element cluster had an adjacent beam cross-over level of approximately 1.1 dB higher than for the single element cluster. This gives the six element cluster a net improvement of 1.0 dB over the single element cluster.

Table 1 also shows the F/D at which each configuration has the highest efficiency. These cases are identified as the "maximum" cases in Table 1. The results imply that if no changes are made in the feed design and reflector diameter, the antenna would have it's best performance if it had the F/D indicated. The single element cluster would require a F/D of 0.81 which is not attractive since it would have a degraded outer beam performance and a smaller area available for the feed in the focal plane. However, the six element cluster's best F/D is 1.38. If the feed separation that is used for the F/D of 1.08 design is also used for a F/D of 1.38 case, then the adjacent beams would move closer together by about 22 percent. Using equation 2-2 from the study report, the crossover level between adjacent beams for the six element cluster with a F/D of 1.38 would be 1.14 dB higher than for the single element cluster with a F/D of 1.08. This comparison is reasonable

since the illumination efficiency of the two cases are close, implying similarly shaped secondary patterns. Adding the gain improvement associated with the higher efficiency of the six element cluster at a F/D of 1.38 with the efficiency of the single element cluster at a F/D of 1.08 (0.42 dB) gives an overall improvement for the six element cluster of about 1.56 dB. More accurate comparisons should be made by calculating the secondary pattern for the larger F/D case, this type of calculation being beyond the scope of this review. However the size of the improvements (approximately 1.0 dB for F/D of 1.08 and 1.6 dB for F/D of 1.38) indicate that the six element cluster represents a worth while improvement over the single element cluster.

The example above indicates that an overlapping aperture design can provide a significant improvement over a non-overlapping design if it is assumed that there are no network losses associated with the overlapping design. Otherwise a considerable part of the improvement could be lost to dissipative losses, perhaps approaching a wash between the two concepts. If this is the case then a non-overlapping design would be preferable because of simplicity and cost. To make the overlapping design viable, then a method to reduce or eliminate the network losses is required. It is suggested that a low noise preamplifier and a power amplifier stage with diplexer could be placed between the feed elements and the beam forming network to eliminate this loss.

The recommendation for the PASS program then, is to use overlapping feed apertures to obtain higher antenna performance and to locate preamplifiers and power amplifiers behind the feed elements to eliminate the associated network losses. This also opens the possibility of exploring the implementation of the beam forming network at IF frequencies to see if improved performance, packaging size and weight might be found. The enabling technology that would need to be developed would include: 1) low loss linear power amplifier, pre-amplifier and diplexer modules, 2) fabrication methods to make them cheaply and compactly, 3) efficient methods to mount and interconnect each module, and 4) methods to integrate the modules with the feed elements.

References:

[1] Memorandum from P. Cramer to K. Woo, "R.F. Radiation Concerns Associated With The PASS User Terminals", December 30, 1988

[2] M.K. Sue, Y.H. Park, "Second-Generation Mobile Satellite System", JPL Publication 85-58, June 1, 1985, Part Two, Pages 2-51 to 2-74

Table 1
ANTENNA EFFICIENCIES

ELEMENTS PER CLUSTER	PATCHES PER ELEMENT	CASE	EDGE ANGLE DEG	F/D	EFFICIENCIES		
					TOTAL	SPILL	ILLUM
1	4	NOMINAL	25.950	1.085	.7059	.7329	.9633
6	2	NOMINAL	25.950	1.085	.6908	.9248	.7488
3	4	NOMINAL	25.950	1.085	.6221	.8775	.7230
1	4	MAXIMUM	34.492	0.805	.8025	.9041	.8877
6	2	MAXIMUM	20.582	1.377	.7782	.8696	.8960
3	4	MAXIMUM	19.924	1.423	.7237	.8119	.8956

Appendix III. Some Antenna Design Options for 20/30 GHz PASS system

(Y. Rahmat-Samii)

The main objective of this work is to present some new design options for the PASS high gain spacecraft antenna configurations. Usually, most of the studies are focussed on the application of offset parabolic and Cassegrain reflector antennas with large focal lengths (large F/D ratios). See, e.g., Section 6.5, and also Reference [1] for a detailed investigation. One of the key parameters in achieving the design requirements is to generate beams with many beamwidths scan performance. As discussed in section 6, for a complete CONUS coverage the antenna must generate beams with scan capabilities of up to 3.5 degrees off boresight. For example, for a 4.0 meter antenna operating at 30 GHz, over ± 20 BW scan angle is required.

The concepts studied here involve the use of a small movable array to produce an optimized beam. Both symmetric parabolic and spherical reflector antennas are considered. Attention is given to the nature of the excitation coefficients for both on-axis beams and off-axis beams in the 3.5° scan direction.

The geometry of a symmetric parabolic antenna is shown in Figure 1. For this configuration, the antenna performance, using a single feed element as well as a small feed array is studied. Results are summarized in Table 1. Note that the off-axis beams are generated by moving either the single element feed or the small array feed to a proper location in the focal plane of the reflector. Both 7-element and 19-element feed arrays are considered. In order to improve the improve the off-axis performance, the excitation coefficients of the array elements were optimized using the technique presented in [2].

A similar investigation has been performed using a spherical reflector antenna. The geometry of the reflector is shown in Figure 2. It should be noticed that the effective focal point for this reflector is approximately midway between the center of the sphere and the apex point of the reflector. Results of the computer simulation are shown in Table 1. It must be noted that due to the spherical aberration, the single feed configuration does not lend itself to satisfactory results. However , as shown in Table 1, the 19-element array feed does improve the performance considerably. An advantage of using the aberration-corrected spherical reflector is that the same array can be used for the scanned beams. This is due to the rotational symmetry of the spherical reflector. Note that the feed array is positioned in a location with 3.5° tilt angle with respect to the original axis.

Studies need to be conducted for the use of large arrays off the focal plane of the offset parabolic, hyperbolic or other types of reflectors. The purpose of such investigations will be to demonstrate the potential applicability of simple single-reflector electronic beam steering.

The above options should provide new design considerations for the reflector array configurations. More detailed evaluations will be needed to fully characterize the overall advantages of these concepts.

REFERENCES

[1] Final Report 30/20 GHz Lewis Antenna Support, JPL ACC. No. 343-10104-0-3360, February 1981.

[2] Y. Rahmat-Samii, "Improved Reflector Antenna Performance Using Optimized Feed Arrays," Proceedings of 1989 URSI International Symposium, Stokholm, Sweden, August 1989, pp. 559-561.

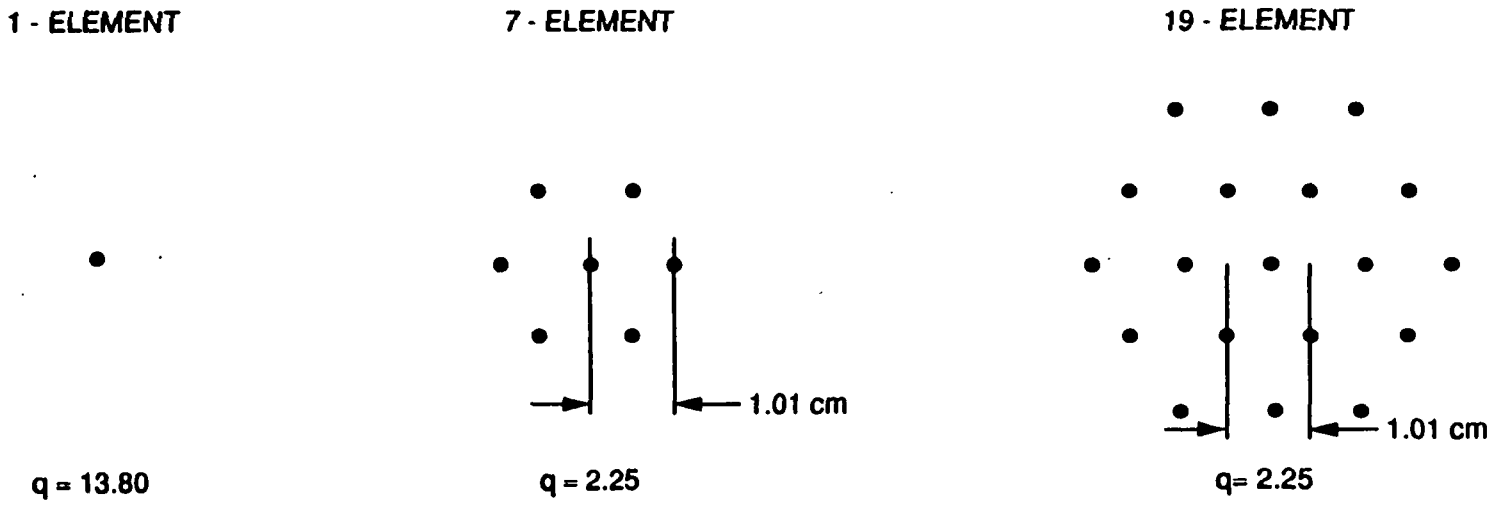

FEED ARRAY WITH ELEMENT PATTERN $\cos^q(\theta)$

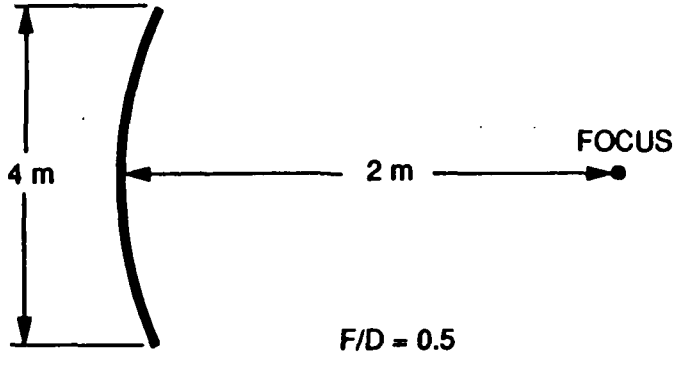

Figure 1. Geometry of a Symmetric Parabolic Reflector

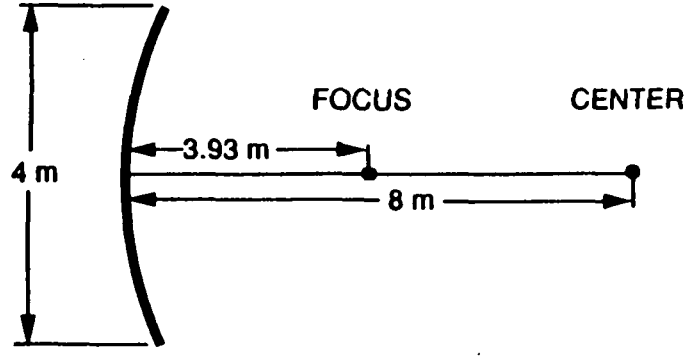

Figure 2. Geometry of a Symmetric Spherical Reflector

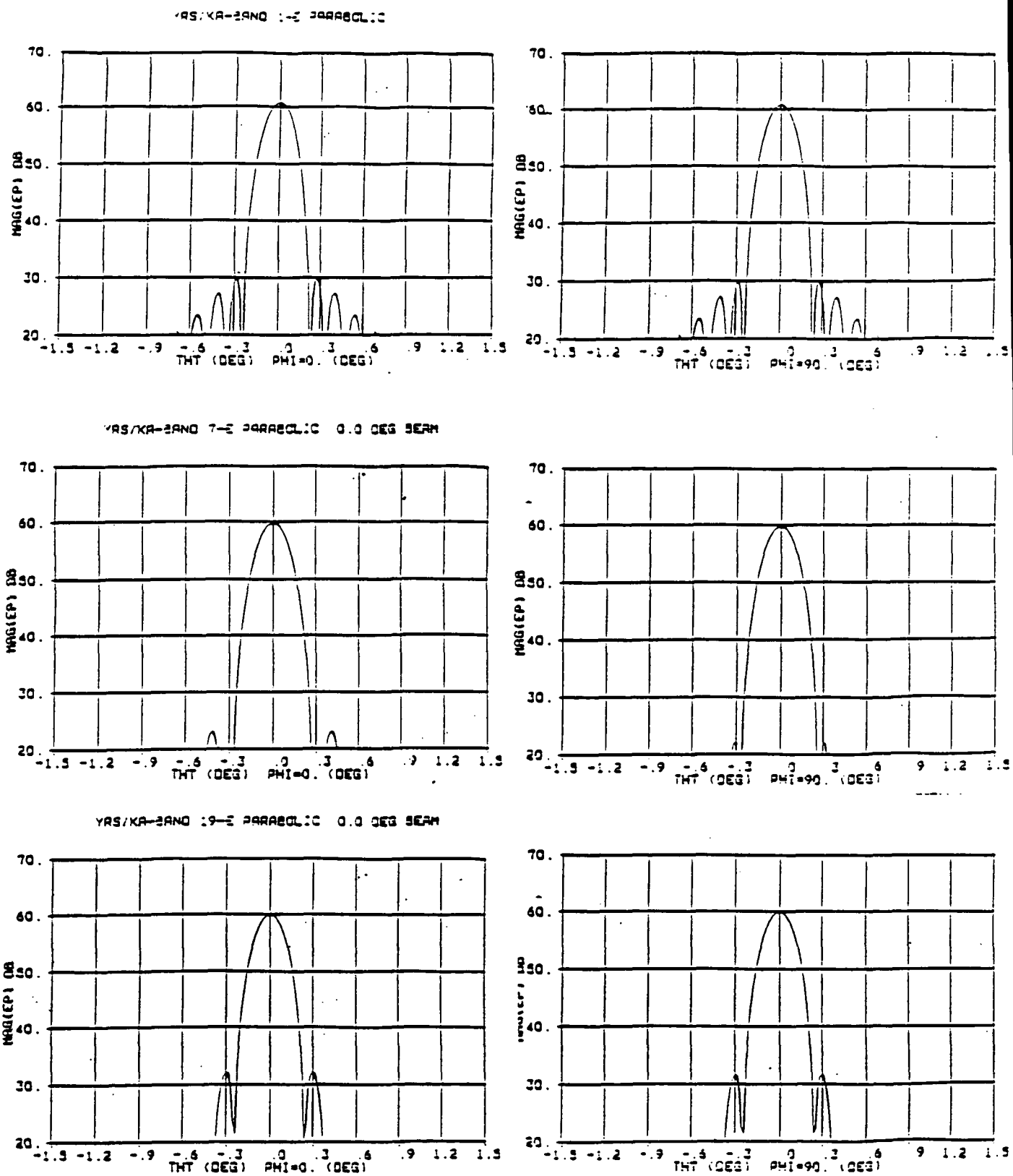

Figure 3. Calculated Patterns of symmetric parabolic reflector with 1,7, and 19 element feed arrays. Scan angle: 0°

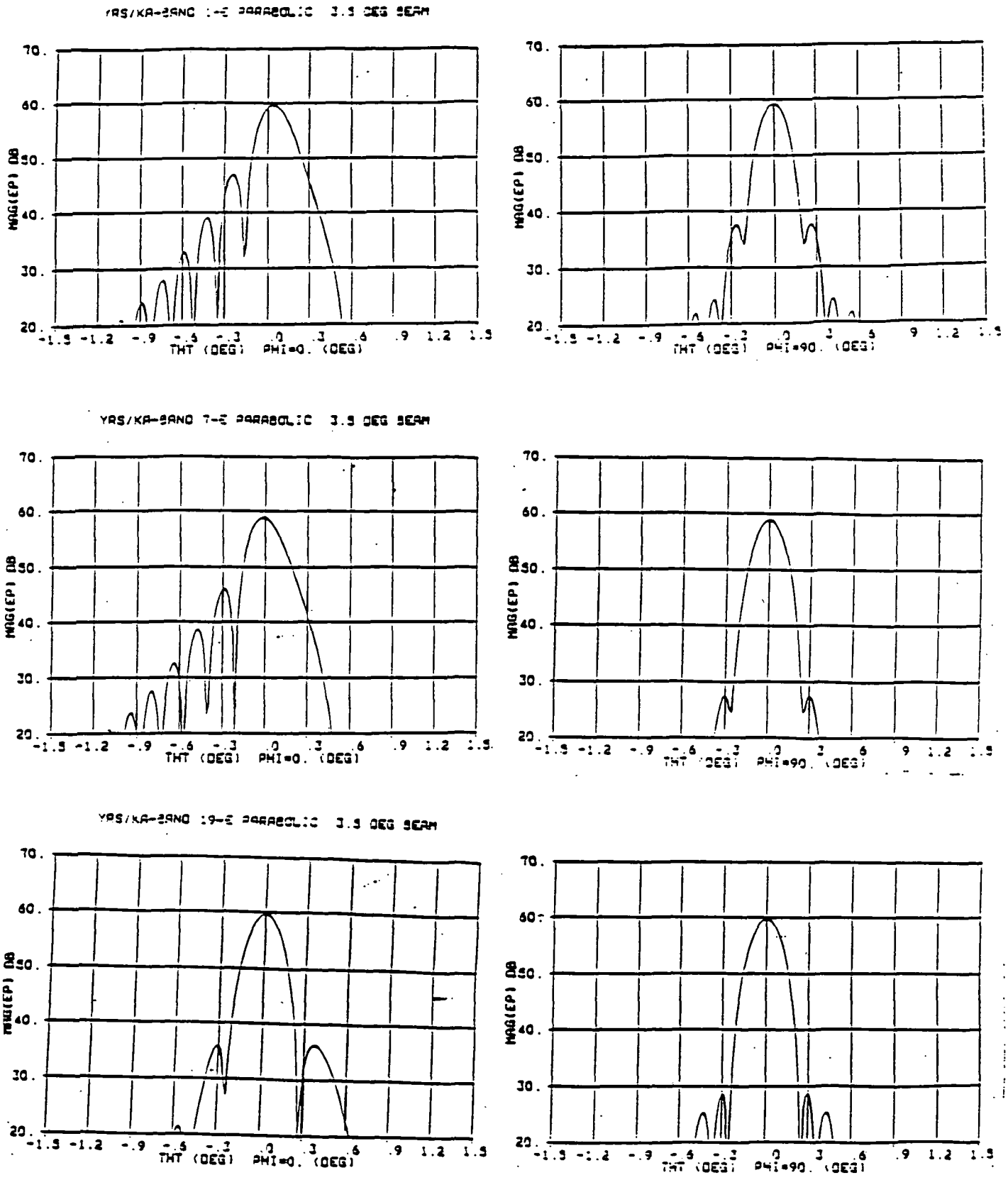

Figure 4. Calculated Patterns of symmetric parabolic reflector with 1,7, and 19 element feed arrays. Scan Anlge: 3.5°

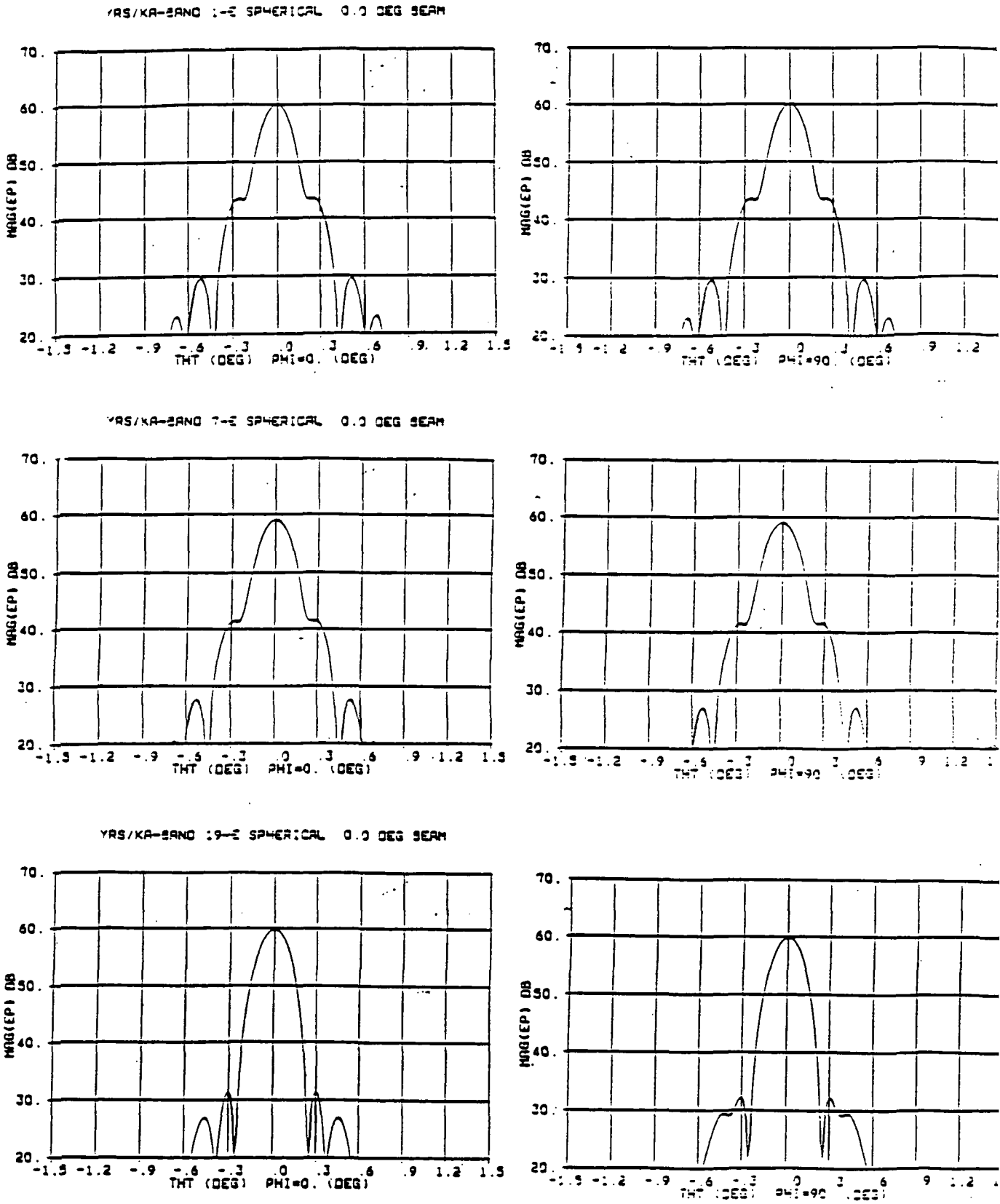

Figure 5. Calculated Patterns of symmetric spherical reflector with 1,7, and 19 element feed arrays. Scan angle: 0°

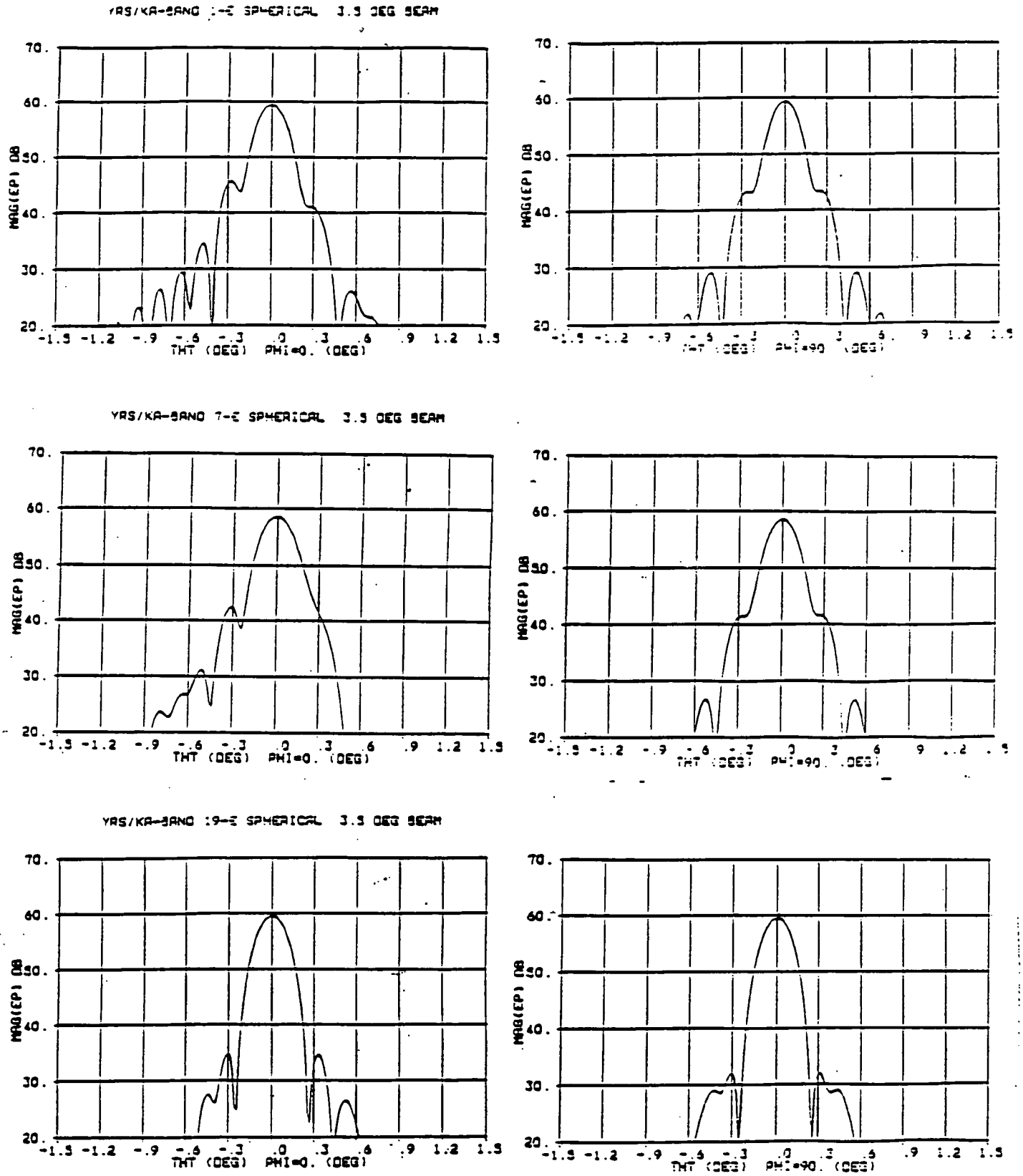

Figure 6. Calculated Patterns of symmetric spherical reflector with 1,7, and 19 element feed arrays. Scan Anlge: 3.5°

Table 1. Summary of pattern calculations for Parabolic and Spherical reflectors with feed arrays.

		Symmetric Parabolic Reflector			Symmetric Spherical Reflector		
Feed Geometry	Beam Direction	Patterns	Directivity dB	Sidelobes dB	Patterns	Directivity dB	Sidelobes dB
1-Element	0°	Figures 3-a,b	60.88	< -30	Figures 5-a,b	60.19	< -17
7-Elements	0°	Figures 3-c,d	59.87	< -38	Figures 5-c,d	59.17	< -18
19-Elements	0°	Figures 3-e,f	60.06	< -27	Figures 5-e,f	59.90	< -27
1-Element	3.5°	Figures 4-a,b	59.30	< -13	Figures 6-a,b	59.49	< -14
7-Elements	3.5°	Figures 4-c,d	58.90	< -13	Figures 6-c,d	58.68	< -15
19-Elements	3.5°	Figures 4-e,f	59.77	< -25	Figures 6-e,f	59.63	< -25

CHAPTER 7

PASS SPACECRAFT ANTENNA TECHNOLOGY ASSESSMENT

R.E. Freeland

I. INTRODUCTION

The purpose of this assessment was to generate estimates of mechanical performance for the classes of spacecraft antenna under consideration for application to PASS. These performance data are needed for the support of trade studies involving antenna system development. The classes of antenna considered by the study included (a) rigid non-deployable antenna structures, (b) mechanical deployable antenna concepts, (c) inflatable deployable antenna concepts, and (d) mesh deployable antenna concepts. Several new industrial developments are in process for mesh deployable antenna technology in both the United States and Japan. They include the development of a high density RF reflector mesh, modifications of existing concepts to accommodate higher frequency applications and the development of new concepts. However, due to the limited data base for this class of structure, with capability for 20 to 30 GHz at this time, they were not included in the assessment. The estimates of mechanical performance are presented in terms of structural weight and cost as a function of the reflector size. Estimates of aperture surface precision are presented for a few discrete antenna sizes. The range of reflector size is 1 to 4 meters for non-deployable structures and 2 to 8 meters for deployable

structures. The range of reflector surface precision is λ /30 to λ /50 for 20 and 30 GHz, respectively.

The data used to generate the performance estimates were obtained from (a) technical reports, (b) technical conference papers, (c) technical interchange meetings, and (d) industrial and government sponsored technical study results (References 1 to 14). The existing technical data base, for the specific antenna concepts, varies considerably with respect to the specific performance data needed for this JPL assessment. Such data are limited because they are based on actual hardware demonstrations, which result from different needs as compared to establishing a generalized performance characterization for the concept. Consequently, extrapolations and judgments were made, based on the available data, to establish the type of performance trends needed to support this system study. The reflector surface precision data represent only the as-manufactured capability and do not include the orbital thermal distortion or deployment repeatability error, for deployable concepts. The orbital thermal distortion is a function of the antenna configuration, materials of construction, spacecraft and mounting configuration, operational orbit and pointing attitude with respect to heat sources such as solar and earth albedo, and the deployment repeatability error is a function of the antenna kinematic configuration. However, all of the antenna concepts under evaluation utilize advanced structural composite materials which are known for their excellent thermal stability.

Therefore, it is reasonable to assume for most applications that the orbital thermal distortion represents only a fraction of the as-manufactured surface error.

The most difficult aspect of the study was to obtain current and well defined hardware cost data because of all the possible variables associated with a single cost figure. For example, the cost for a specific antenna reflector structure is influenced by factors such as (a) the level of technology of the concept, i.e., is the cost associated with the first, second or twentieth piece of hardware ever produced, (b) the number of units produced with the same manufacturing set up and tooling, (c) in addition to the flight unit, is there an engineering model, proof test model or flight spare antenna, (d) for deployable antenna concepts what level of ground based demonstration of deployment reliability is required in addition to delivery of the flight unit, (e) how does the design of the antenna structure vary from previously manufactured antennas, (f) how tight is the scheduling associated with the procurement, and (g) what is the level of qualification testing associated with the procurement?

The mechanical performance projections are intended to accommodate RF system trade type studies. They represent realistic relative differences between types of antenna structures and variations of the same concept. However, they should not be used for estimating specific hardware costs because of all the variables associated with a specific procurement.

II. NON-DEPLOYABLE ANTENNA REFLECTORS

The data presented for solid reflectors represent the manufacturing capability of at least 6 commercial organizations. The reflector size range of hardware utilized for the study is from 1.0 to 4.0 meters. The structural configurations associated with this class of reflectors fall into two categories. One is a honeycomb sandwich shell of uniform thickness (Figure 1). The other is a thin sandwich honeycomb or composite shell that is supported by rings or some type of rib stiffeners. Figure 2 is an example of a rib stiffened structure. This technology is very mature, has extensive flight experience and is "off the shelf" for most "standard" reflector shapes. The materials used for this class of structure include graphite/epoxy, kevlar/epoxy and fiberglass/polymer. Variations of these materials to accommodate specific application requirements are state-of-the-art. A major schedule driver for the production of this class structure is the tooling. An unusual shape or unusually large reflector might take considerably longer to acquire the appropriate tooling.

The non-deployable structure, without question, represents the highest reliability approach structurally for spacecraft antennas. However, there are some drawbacks to using solid antenna reflector structures in the large size ranges of 3 to 4.5 meters. Such large structures tend to dwarf the spacecraft, especially the small size spacecraft often used for communications applications. This situation results in difficulty in (a) access to the spacecraft hardware,

(b) spacecraft ground handling, (c) ground transportation, and (d) launch vehicle integration. Also, due to its size alone, such an antenna is subject to damage from a variety of sources, such as transportation, spacecraft assembly and servicing in the vicinity of the antenna, etc.

The reflector structure as-manufactured surface accuracy, associated with each piece of hardware considered in the survey, represented what was needed for a specific application and usually did not represent the best manufacturing capability for the concept at the time of manufacture. A surface accuracy of 0.2 mm rms, which represents an allowable surface error of λ /50 for 30 GHz, has been demonstrated with a significant number of structures up to 3.5 meters in diameter. This level of surface quality is not expected to be a problem with any of the solid antennas under consideration for PASS. Reflector structure weights and manufacturing cost as a function of size are given by Figures 3 and 4.

III. MECHANICAL DEPLOYABLE ANTENNA REFLECTORS

The data presented for mechanical deployable reflectors are based solely on the TRW Sunflower and the Dornier DAISY structural concepts. Both concepts utilize rigid, high precision, doubly curved, light weight panels that are kinematically connected to accommodate the automated deployment of such stowed elements (Figures 5 and 6, respectively). Both

concepts were conceptualized for reflectors up to about 10 meters in diameter. The Sunflower is intended for operation up to 60 GHz passively for sizes up about 11 meters. Active orbital adjustment capability would increase the upper usable frequency by 50%. The DAISY is designed to operate at wavelengths of a hundred microns at sizes up to 8 meters passively. Neither concept is intended for orbital surface correction at this time. The data base for both of these concepts is very limited because of the small number of detail designs and demonstration hardware models fabricated for either of these concepts. The Sunflower has been developed to the point of (a) 2.5 meter partial deployable antenna consisting of the center panel and 4 out of 16 deployable petals, (b) fabrication of 3 meter panels for a 10 meter antenna, and (c) analytical estimates of orbital thermal performance for all size structures. The DAISY concept was initially developed for FIRST, a European Space Agency (ESA) 8 meter diameter space based submillimeter telescope. This concept has been developed to the point of a 5 meter engineering model with an F/D of 0.64 and an as-manufactured surface precision of 60 μ m rms. It is intended for communications applications at 20 to 30 GHz. The potential surface precision of either concept, especially in the small size range, really exceeds the requirements of PASS. This class of deployable structures, because of its deployed stiffness lends itself to meaningful ground based demonstrations of deployment reliability and surface precision. The Sunflower is currently mature enough to accommodate near term flight applications. The DAISY is expected

to be developed to the point of flight applications within a year or two.

IV. INFLATABLE DEPLOYABLE ANTENNA REFLECTOR

The data base for this antenna concept is based solely on the Contraves Inflatable, Space Rigidized Structural Concept. It is a relatively new and extremely innovative structural concept. This concept development is sponsored by ESA/European Space Research and Technology Centre (ESTEC). The concept is based on using a flexible thin wall structural composite membrane that is assembled on high precision tooling fixturing that simulates the geometry of the deployed structure. This membrane, as a consequence of its flexibility, allows the structure to be folded up and stowed in a variety of configurations, not unlike a life raft or emergency chute on an airplane. The antenna is deployed on orbit by inflation of the membrane structure. Once inflated to the orbital operational configuration, the solar heating causes the rubber-like matrix material to cure and become a rigid shell type structure. The load carrying fibers in this composite material are kevlar. The inflation gas is then released, leaving a permanently rigid space structure (Figure 7). The potential advantages of this concept include (a) excellent mechanical packaging efficiency, (b) high deployment reliability, (c) low weight, especially in the larger sizes, and (d) low cost compared to mechanical concepts. The initial development for this concept was focused on a 15 meter, 22 GHz antenna intended for earth orbiting Very Long Baseline Interferometry (VLBI).

However, recent developments have been focused on an off-axis multiple beam communications antenna application. The current as-manufactured reflector surface precision is on the order of 0.6 mm rms for proof of concept structures up to 6 meters. This number is currently well below the surface precision requirements for PASS, but this concept is still under development and each successive hardware demonstration model has shown significant improvements. Therefore, if the assumption is made that this type of improvement will continue, especially for the small size structures, this concept has real potential for PASS. This new and extremely unique concept should be considered a prime candidate for concept development, specifically for PASS. Figures 3 and 4 represent the latest estimates of performance for this concept in terms of the structural weight and manufacturing cost as a function of size.

V. CONCLUSIONS

1. Rigid, non-deployable reflector structures technology can easily accommodate PASS antenna requirements for structures up to about 4 meters.
2. Current mechanical deployable antenna technology can accommodate PASS antenna requirements for reflectors up to 8 meters but with (a) substantial weight and cost penalties and moderate scheduling penalties as compared to the use of rigid structures in the size range up to 4.5 meters, and (b) weight and cost penalties as compared to inflatable structures in the size range 4 to 8 meters.

3. The inflatable deployable antenna concept evaluated has the greatest potential for accommodating PASS antenna requirements at low cost. However, additional technology development will be required to demonstrate its true value.
4. As technology for PASS matures, it is anticipated that the need for larger size antenna reflectors will materialize.
5. As the size of the antenna reflector increases, especially with respect to small size spacecraft, the importance of working with manageable size spacecraft that require minimal booster payload volume will become even more apparent.
6. When the size of the reflector needed for PASS exceeds the dynamic envelope of the booster payload compartment, then deployable antennas will become mandatory.
7. Since the probability of needing deployable antennas for PASS in the near future is high, serious consideration should be given at this time to (a) adopting existing deployable antenna concepts for PASS, (b) developing new and innovative antenna concepts specifically for PASS, and (c) supporting the innovation of really new antenna concepts for applications not efficiently accommodated by today's technology.
8. Subsequent to this antenna technology assessment a number of industrial sponsored antenna concept developments have been initiated. Consequently, it is recommended that additional evaluation of these "new" developments be made prior to the formulation of a technical development plan for submission to NASA Code E.

It is noted that, subsequent to the completion of the PASS Spacecraft Antenna Technology Assessment, a significantly more in-depth survey was accomplished that focused on commercial IR & D developments of proprietary spacecraft antenna concepts. Consequently, the resulting report, "PASS Spacecraft Antenna Technology Study," is intended only for government use, and distribution will be based on written requests to the authors from authorized government agencies.

REFERENCES

1. Freeland, R. E., Industry Capability for Large Space Antenna Structures, JPL Document 710-12, May 25, 1978 (internal document).

2. Freeland, R. E., "Survey of Deployable Antenna Concepts," Paper, Large Space Antenna Systems Technology - 1982, NASA Conf. Pub. 2269, Part 1, NASA Langley Research Center, Hampton, VA, Dec. 1982, pp. 381-421.

3. Freeland, R. E., "Deployable Antenna Concept Development," AIAA Space Systems Technology Workshop III, Kirkland Air Force Base, Albuquerque, NM, March 1984.

4. Archer, J.S., and Palmer, W.B., "Antenna Technology for QUASAT Application," Paper, Large Space Antenna Systems Technology - 1984 NASA Conf. Pub. 2368, Part 1, NASA Langley Research Center, Hampton, VA, December 1984, pp. 251.

5. Freeland, R. E., "Development of Structural-Composite Reflector Panels for a Submillimeter Space Telescope," 3rd European Symposium on Spacecraft Materials in Space Environment, Paper ESA-SP-232, Noordwijk, The Netherlands, November 1985.

6. Pagana E. and Bernasconi, M. C. 1986, "Prediction of the Electrical Performance of ISRS Offset Antenna Reflectors and Correlation with RF Measurements," Proc 2nd ESA Workshop on Mechanical Technology for Antennas, Noordwijk, The Netherlands, ESA SP-261, 171-177.

7. Abt, Bernd., "Deployable Precision Reflectors," International Astronautical Federation, Paper IAF-86-200, 37th Congress, Innsbruck, Austria, October 1986.

8. Pace, A., LaRosa, I., and Stonier, R., "Development of Lightweight Dimensionally Stable Carbon Fiber Composite Antenna Reflectors For the INSAT-I Satellite," 2nd ESA Workshop on Mechanical Technology for Antennas, ESTEC, Noordwijk, May 1986, ESA SP-261.

9. Bernasconi, M. C., Pagana, E., and Reibaldi, G. G., "Large Inflatable Space-Rigidized Antenna Reflectors," International Astronautical Federation, Paper IAF-87-315, 38th Congress Brighton, United Kingdom, Oct. 1987.

10. Bernasconi, M. C., "Inflatable Space Rigidized Structures Scale-Model Reflector: Flight Experiment Definition," Proc 39th Int Astronautical Congress, Bangalore, India, Paper IAF-88-049, 1988.

11. Kuiper, T.B., "A Mission to Explore the Role of Oxygen In Astrophysics," Investigation and Technical Plan Volumes of a

96

Small Explorer Mission Proposal to NASA, Submitted by JPL, August 31, 1988.

12. Rule, J.E., "Thermal Stability and Surface Accuracy Considerations For Space-Based Single and Dual Shell Antenna Reflectors," Paper by Composite Optics Incorporated, 1988.

13. Gloster, D., "The Technology of Inflatable Space Rigidized Structures: PSDE SAT-2 L-BAND Land Mobile Antenna Reflector - System Study/Final Report," CONTRAVES Final Report SR/SAT2/105(89) CZ, 1989.

14. Bernasconi, M. C., and Gloster, D., "The L-Band ISRS Reflector For SAT-2: A Summary of the Initial System Study," Proceeding ESA Workshop on Antenna Technologies, ESA/ESTEC Noordwijk, The Netherlands, Nov. 1989.

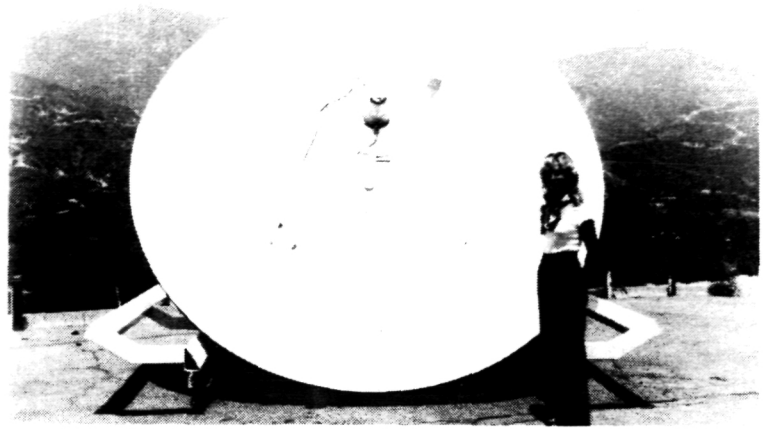

Figure 1. Composite Sandwich Reflector Structure

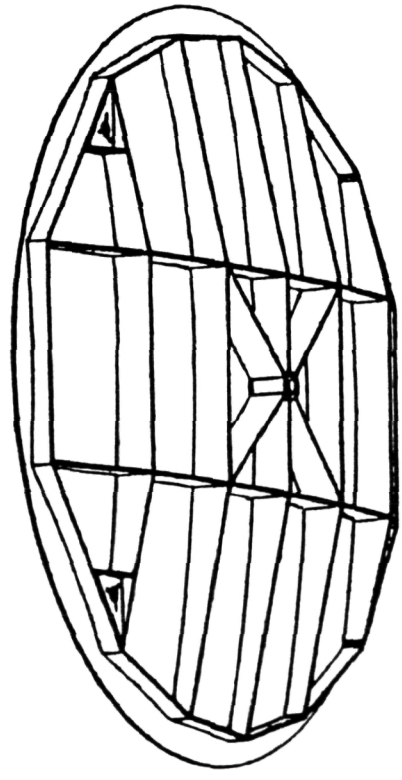

Figure 2. Rib Stiffened Composite Sandwich Reflector Structure

98

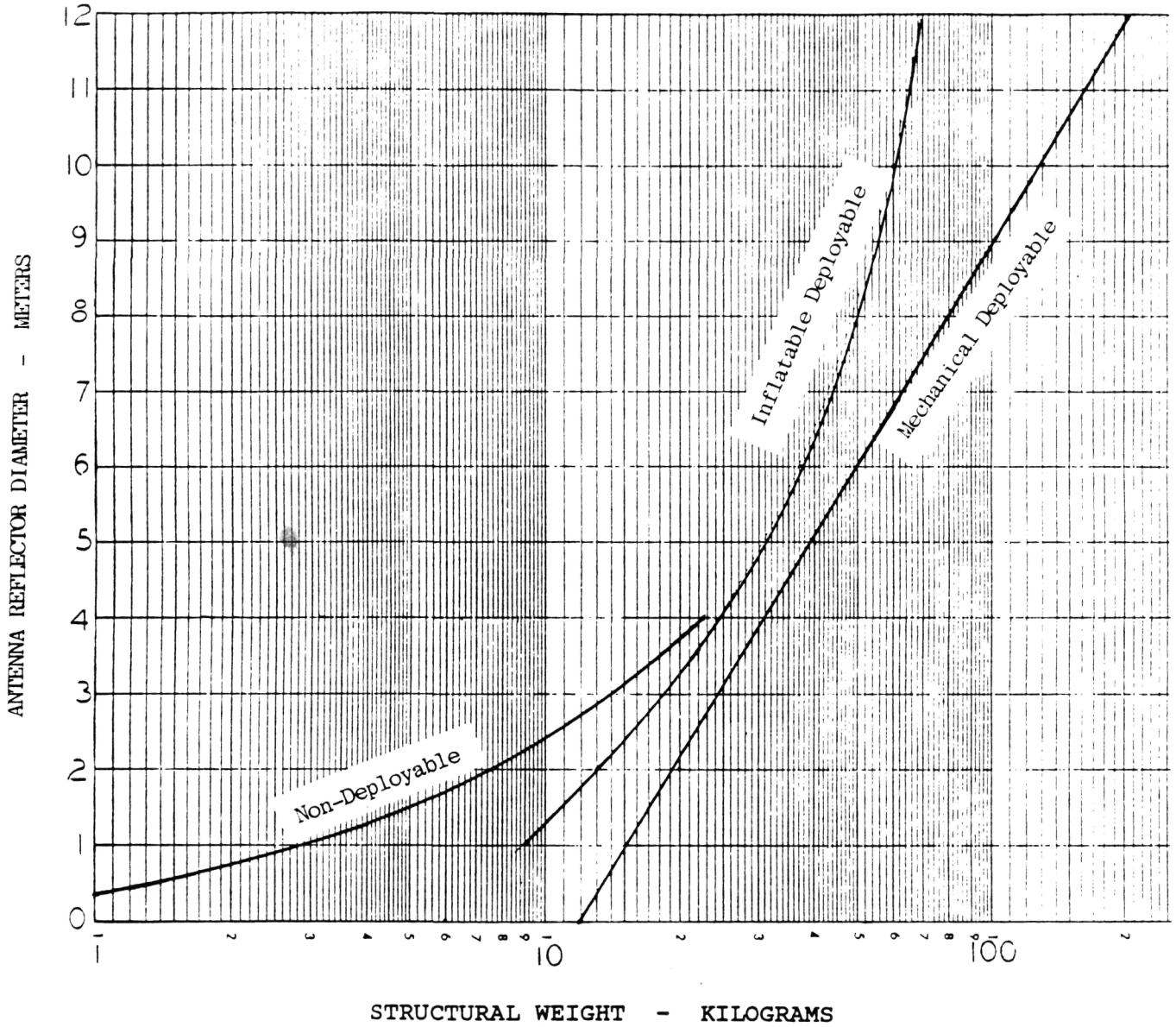

Figure 3. Antenna Weight vs. Size

399

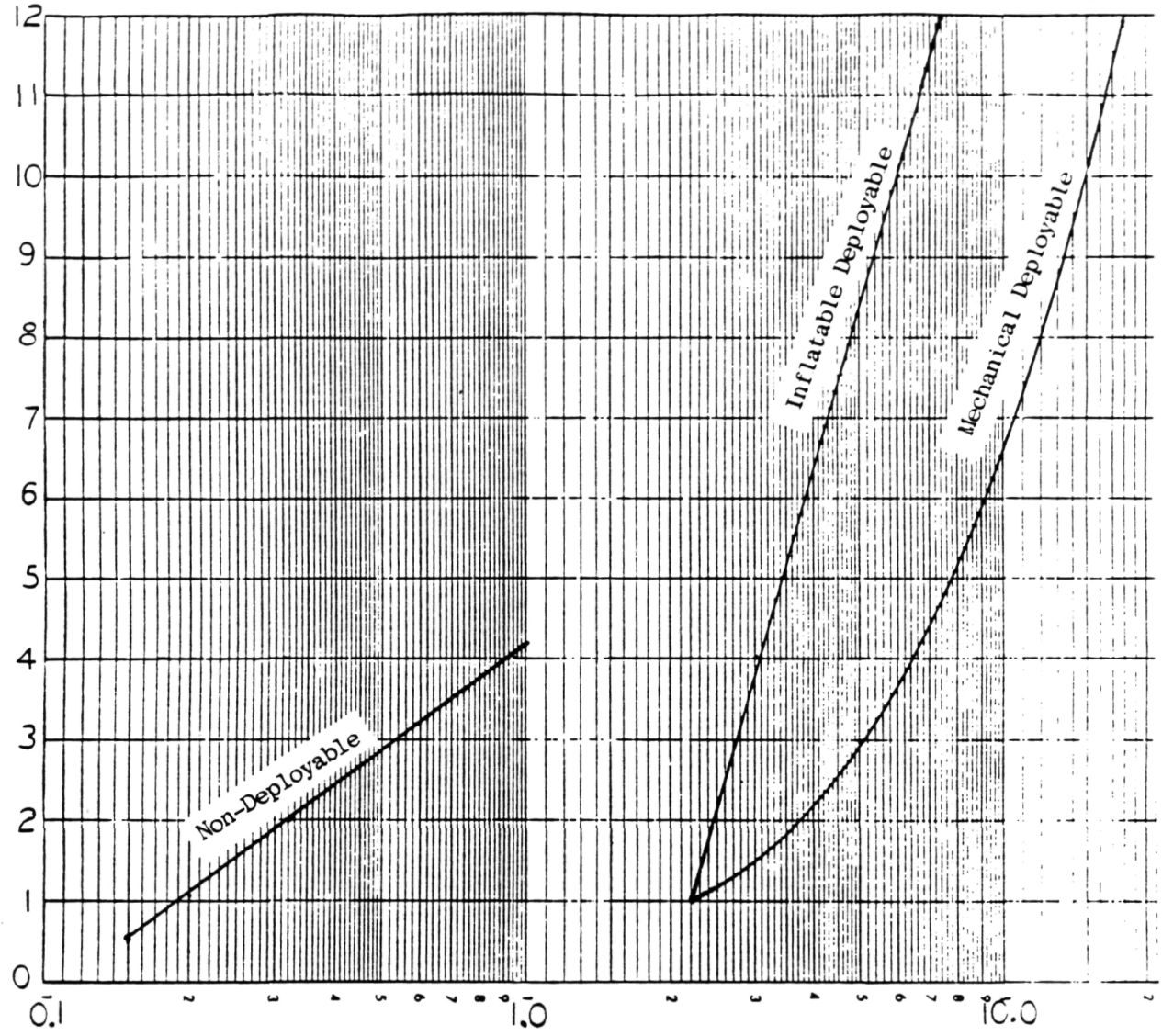

Figure 4. Antenna Cost vs. Size

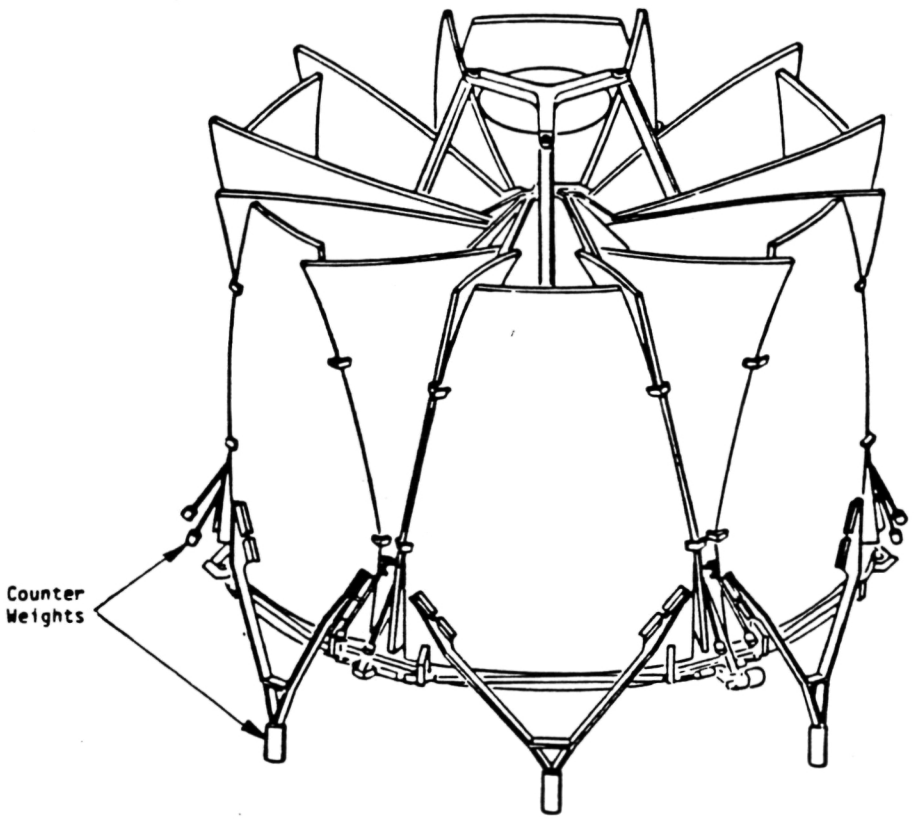

Figure 5. Sunflower Deployable Reflector Antenna

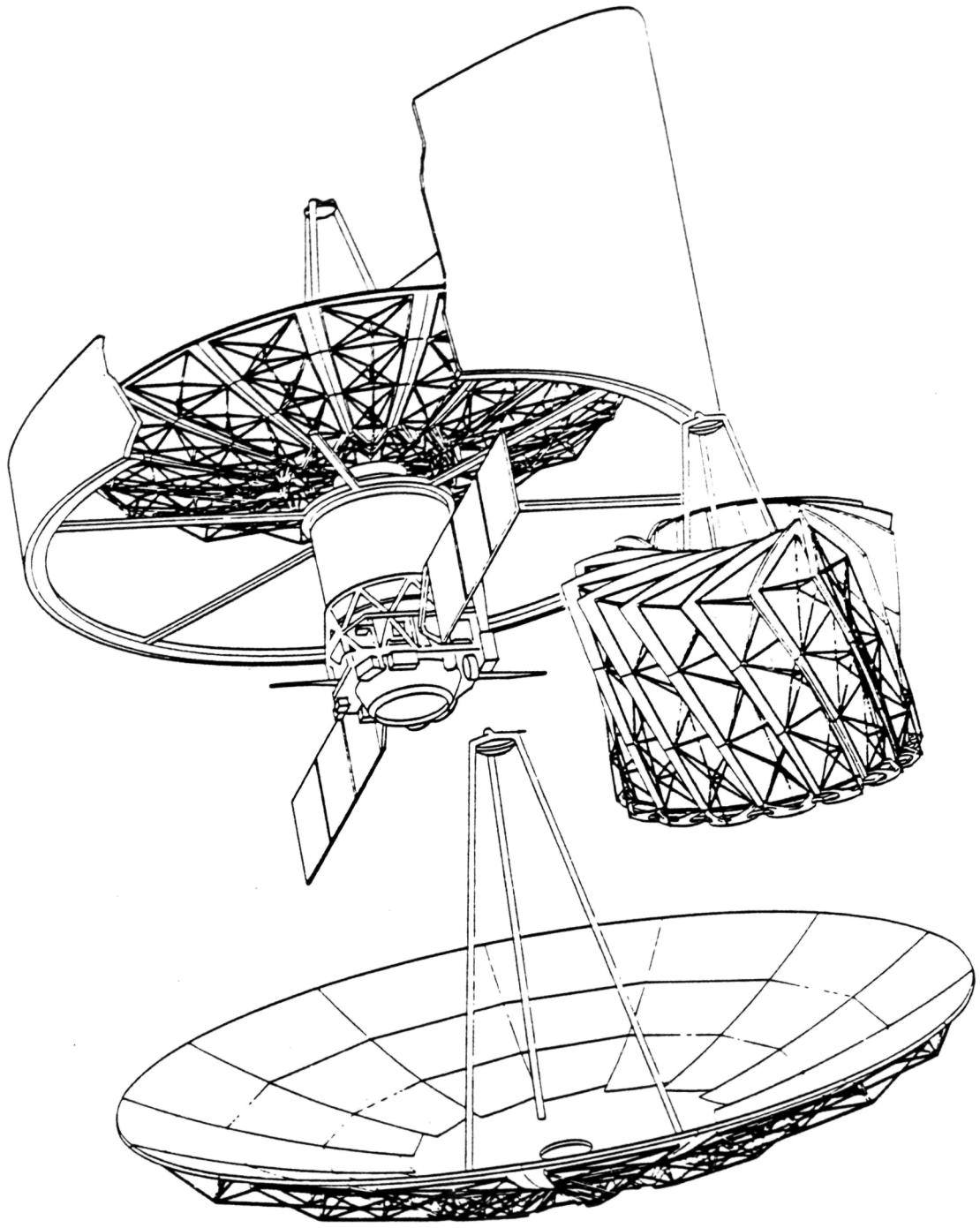

Figure 6. Daisy Deployable Reflector Antenna

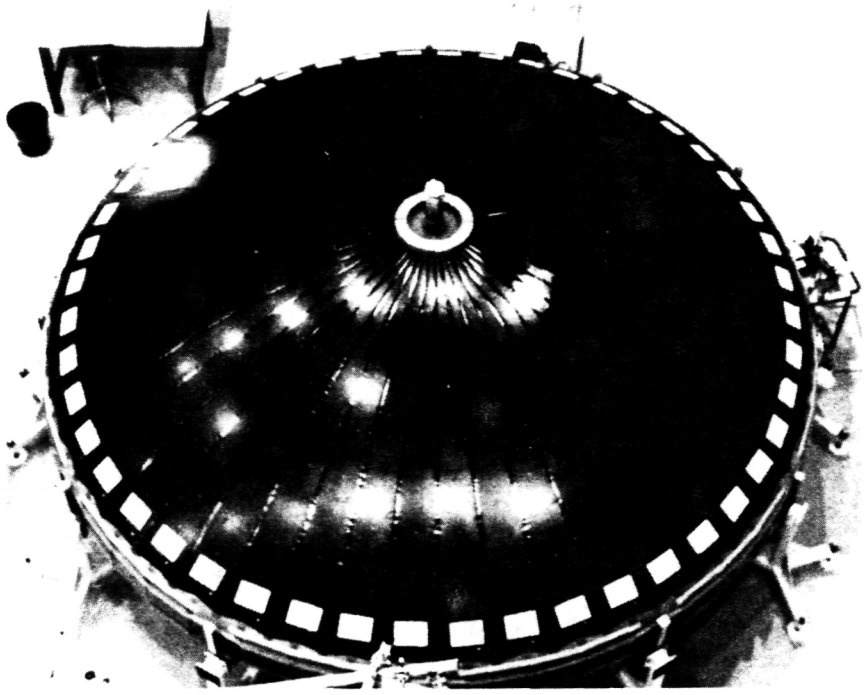

(a) 6-m Axis Symmetric Hardware Demonstration Model

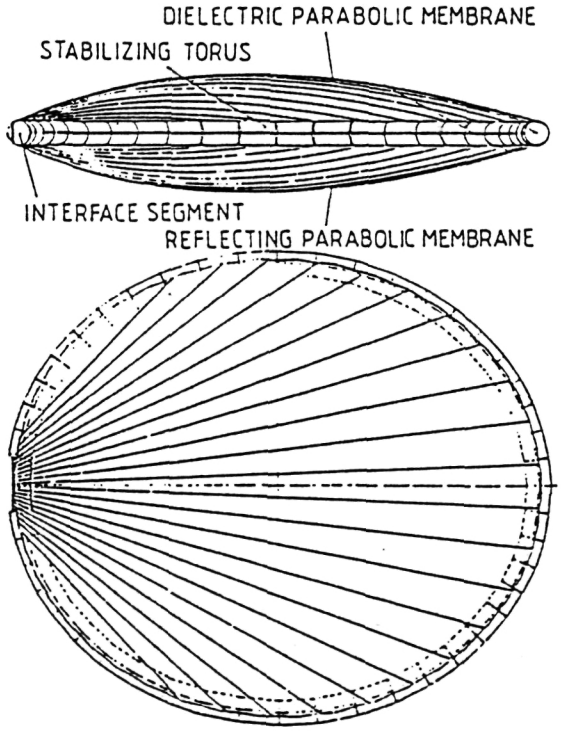

(b) Concept for 5-m Offset Reflector

Figure 7. Contraves Inflatable Space Rigidized Antenna

Chapter 8

Technology Assessment and Experimentation Plan

Dr. Polly Estabrook

8.1 Introduction

This chapter gives an assessment of the critical and enhancing technologies necessary to build the basic personal terminal (BPT), the supplier and the Network Management Center (NMC). The experimentation plan for testing PASS utilizing ACTS is detailed. The experimentation plan gives a list of candidate experiments and describes the proposed experimental set-up. ACTS will be used in the Microwave Switch Matrix (MSM) mode. The Microwave Switch Matrix - Link Evaluation Terminal (MSM-LET) at NASA Lewis Research Center (LeRC) will serve as the microwave front-end for the PASS supplier and the NMC. Link budgets are given for both the forward and return links between the supplier and the basic personal terminal. Finally the equipment required for the experiments is identified.

8.2 Identification of Critical and Enhancing Technologies

Table 8.1 lists the technologies whose development is important to the PASS project due to their role as critical/enabling or enhancing technologies for this project. The table lists the maturity level assigned to each technology based on definitions by the NASA Office of Aeronautics and Space Technology. The definitions for these maturity levels are listed in Table 8.2.

Table 8.1: Relevant Technologies - Space, Ground and Link Segments

Technologies	Importance	Maturity
Space Segment:		
Multibeam antenna and beam forming network	C	2-3
Large deployable antenna (offset-fed)	E	2-3
On-board switching (100s-1000s circuits)	E	3
On-board processing (up to 1000s carriers)	E	3
Efficient solid-state power amplifier (SSPA)	C	3
Efficient high power TWTA	C	4
Low noise receiver	C	4
Reconfigurable multibeam antenna	E	4
Dynamic interbeam power/bandwidth allocation	E	2
Ground Segment		
Low-cost, compact, tracking antenna	C	1-2
Low-cost, accurate frequency source	C	4
High-gain, low noise MMIC receiver	C	3
MMIC transmitter	C	3
Efficient SSPA	C	3
VLSI-based integrated vocoder/modem	C	5
Variable rate modem	E	4
Link Technologies:		
Rain compensation techniques	C	2-4
Efficient multiple access techniques	C	3-4
ISDN compatible networking technology	E	4
Power efficient modulation & coding	C	6
Robust modulation & coding to mitigate multipath, freq. error, and phase error	C	3
LPC voice coding (2.4 Kbps)	E	6

Legends:

C = Critical/enabling technologies
E = Enhancing technologies

Table 8.2: NASA Technology Maturity Levels

Technology Maturity Level	Technology Development Stage
1	Basic principles observed and reported.
2	Conceptual design formulated.
3	Conceptual design tested analytically or experimentally.
4	Critical function/characteristic demonstrated.
5	Component brassboard tested in relevant environment.
6	Prototype/engineering model tested in relevant environment.
7	Engineering model space qualified.

8.3 Experimentation Plan Using ACTS

8.3.1 Candidate Experiments

Three main tests will be performed. First, the communication link between supplier and basic personal terminal will be evaluated. Second, the performance of the variable rate modem and its effectiveness in combatting rain attenuation will be assessed. Third, the impact of the uplink power control schemes implemented at the supplier will be tested and evaluated.

Communication Link Tests

The communication link will be tested to confirm the calculated link budget, to assess terminal EIRP and G/T, and to check the performance of the satellite transponder on the transmitted signal.

The terminal's operational procedures will be verified under various SNR conditions. Specifically the following four features of the terminal will be tested: (1) antenna acquisition, pointing and tracking; (2) time and frequency acquisition of the BPT from the pilot signal generated by the supplier; (3) time for signal acquisition; and (4) call set-up.

The use of a low cost frequency standard in the BPT to set the frequency of the BPT's microwave local oscillators will be quantified in order to verify the noise performance and frequency stability of these local oscillators.

The modem performance will be evaluated according to the following parameters: (1) bit error rate vs. received signal-to-noise; (2) cumulative bit errors vs. time; and (3) Doppler tracking capability.

Finally, the vocoder's performance and sound quality will be assessed. The PASS 4.8

kbps vocoder will utilize the same algorithm as the MSAT-X vocoder but will implemented with VLSI circuits.

Variable Rate Modem Test

The variable rate modem will be used in the BPT and in the supplier station. The supplier station will command a data rate change in the forward link if it is notified by the BPT that rain exists in the BPT's downlink beam. The data rate from the BPT will be decreased if rain attenuation is found in either the BPT's uplink beam or in the downlink beam to the supplier. The algorithm for data rate change is envisioned as operating without network coordination. The modem, therefore, must be able to sense or command a data rate change without receiving information from the network or notifying it.

The design of the algorithm used to control the data rate will depend on the time variation of the rain fade. These second order rain statistics will depend on the location in CONUS and on the time of year; they will be obtained from the propagation community based on the results obtained from the OLYMPUS-1 and ACTS beacons. The data will be used to determine the thresholds at which the data rate should be changed and the number of data rate levels necessary to compensate for rain fades. It will also be used to determine whether changes in the data rate should be ordered apriori or aposteriori to the measurement of these rain fade threshold levels. The design of the algorithm and its implementation must also take into account the level of BER improvement expected, the increased signal delay, and the implementation cost in the modem. The ensuing system availability (for various data rates and voice qualities) will then be assessed.

Once these variable rate modem has been built, it will be tested to assess (1) response time, optimum setting of threshold levels and number of data rate steps; and (2) achieved system availability. These algorithms that control the data rate of the modulator and the vocoder will be implemented in software so that they can be refined in accordance with experimental results and retested.

Uplink Power Control

Uplink power control will be used by the supplier station alone to compensate for rain in the supplier's beam. Power control schemes frequently depend on the reception of a pilot from which fade information is calculated in order to adjust the power in the uplink beam accordingly. Either the beacon is at the identical frequency as the transmit signal, in which case a one for one adjustment of power for beacon fade attenuation may be performed, or the beacon is at a different frequency than the uplink signal, in which case frequency scaling techniques are used to predict the rain attenuation at the uplink frequency.

In the PASS experiment where NASA LeRC's MSM-LET will be used as the supplier, both methods may be tested as the MSM-LET will receive information about the beacons generated from the satellite at 20.185 GHz, 20.195 GHz, and 27.505 GHz. This will be discussed in greater depth in Section 8.3.2.

8.3.2 Proposed Experiment Set-Up

Use of ACTS and ACTS Ground Station

ACTS will be used in the microwave switch matrix (MSM) mode to connect the supplier and the BPT. In the forward link, ACTS will be commanded from the NASA Ground Station at LeRC to connect the Cleveland fixed beam to receiver #1 and IF module #1; the MSM matrix will connect the input from IF module #1 to HPA #1; and the output of this HPA will be connected to the Eastern scan sector hopping beam.[1] This beam will be kept stationary over the LA/San Diego area for the duration of the test. The forward link is shown in Fig. 8.1.

In the return link, ACTS will be commanded from the NASA Ground Station at LeRC to connect the LA/San Diego hopping beam to receiver #2 and IF module #2; the MSM matrix will the input from IF module #2 to HPA #2; and the output of this HPA will be connected to the Cleveland fixed beam for the duration of the test. Thus two of ACTS' possible three wide band transponders will be used for this experiment.[2] The return link is shown in Fig. 8.2.

As mentioned earlier, the NASA LeRC Microwave Switch Matrix - Link Evaluation Terminal (MSM-LET) will be used as the PASS supplier. This terminal is collocated with the NASA Ground Station (NGS) at LeRC. It is one of three terminals intended for use by experimenters - the other two being intended for use with the Baseband Processor (BBP) mode of ACTS, i.e., the BBP Low Burst Rate - 1 terminal and the BBP Low Burst Rate - 2 terminal. The specifications for the NGS, the MSM-LET, and the other two experimental stations are shown in Table 8.3 (taken from [1]).

The NASA Ground Station will be receiving the ACTS generated beacons at 20.185 GHz, 20.195 GHz, and 27.505 GHz. The first two beacons are fade and unified telemetry beacons; 20.185 GHz is a vertical beacon and 20.195 GHz is a horizontal beacon. These beacons are used for spacecraft telemetry using a constant modulation, to point ground terminal antenna, and to measure rain fade. The 27.505 GHz vertical pilot is a rain fade beacon only. The strength of the 27.505 GHz beacon will be monitored by the supplier to determine the necessary uplink power control. Rain fades strength on both the 20 GHz and 30 GHz beacons will be monitored and sent to the BPT so that, upon reception of the supplier generated pilot, it can differentiate between rain in the uplink and downlink beams.

To remain compatible with MSM-LET terminal, the supplier will transmit in the channel centered at 29.634 GHz $\pm$ 166 MHz and receive in the channel centered at 19.914 GHz $\pm$ 166 MHz. The ACTS frequency plan is shown in Fig. 8.3 (taken from [2]).

[1] ACTS is put into the MSM or BBP mode by a 29.975 GHz horizontal command autotrack signal which is transmitted from the NGS.

[2] ACTS possesses four wideband transponders; however, one is used for redundancy so that only three can operate at any one time.

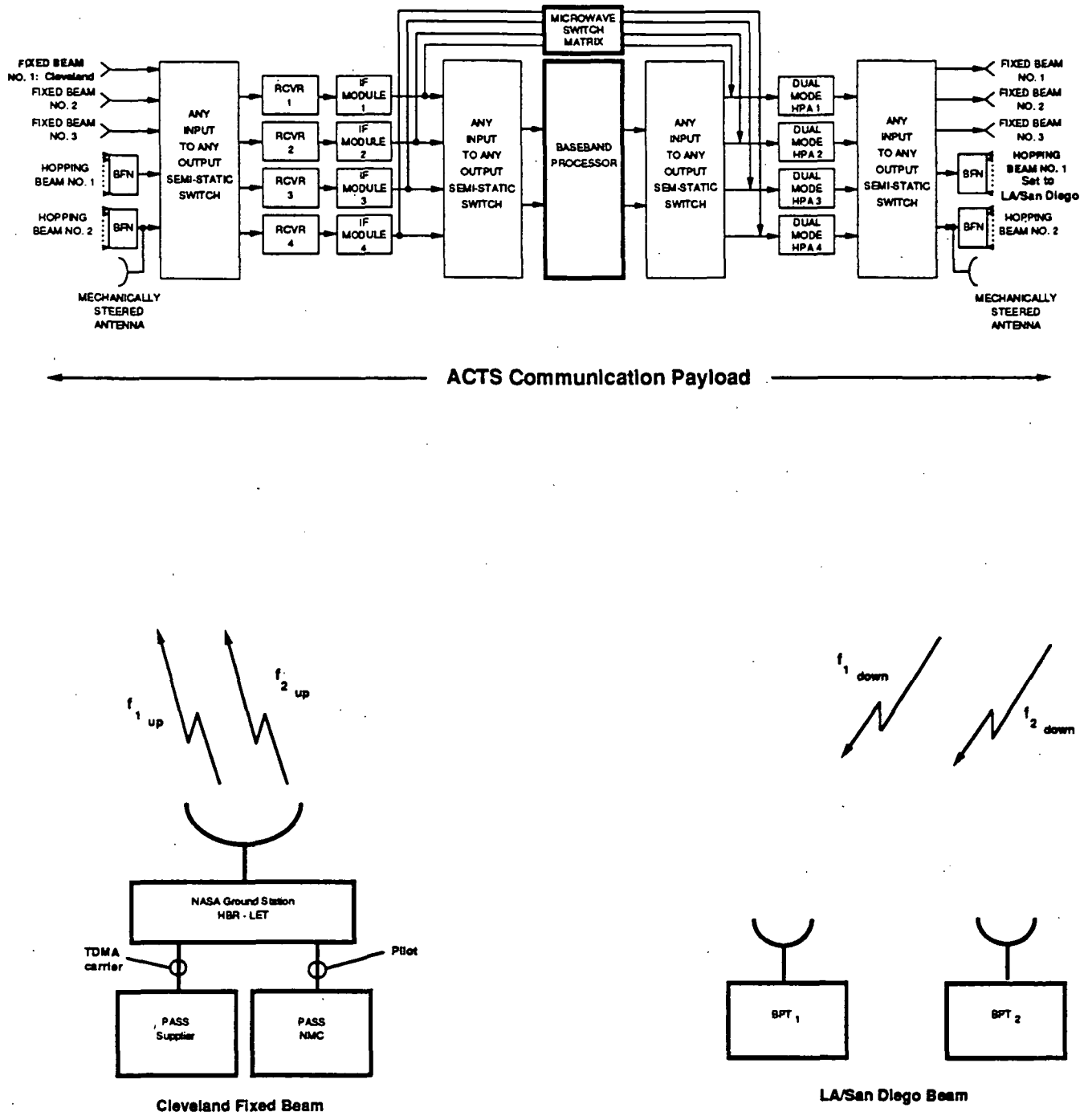

Figure 8.1: Forward link demonstration.

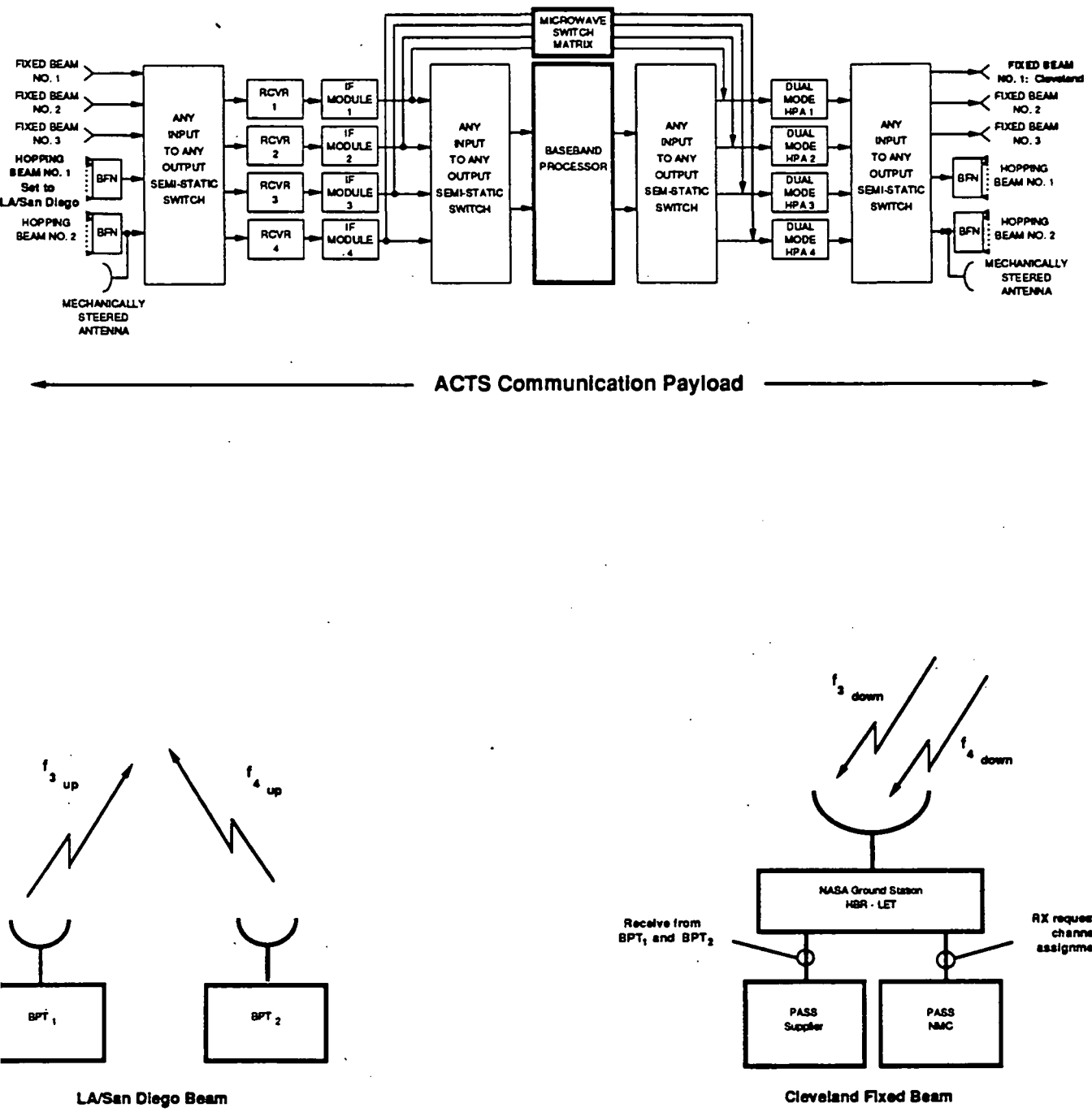

Figure 8.2: Return link demonstration.

Table 8.3: Types of ACTS Earth Stations

	NASA Ground Station	BBP/ LBR-1 (Portable)	BBP/ LBR-2	NASA MSM Link Evaluation Terminal
EIRP	74dBW/68dBW	72dBW/66dBW	66dBW/60dBW	76dBW/68dBW
G/T	>27 dB/K	≈22/16 dB/K	≈22/16 dB/K	>27 dB/K
Antenna Diameter	≈5.0 m	2.4 m	2.4 m/1.2 m	4.77 m
High Power Amplifier	54W/14W	≈65W/16W	≈16W	60W
Uplink Burst ‡ Rate	LBR-1/LBR-2	110/55 Mbps	27.5/13.8 Mbps	220/110 Mbps
Downlink Burst Rate	110/55 Mbps	110/55 Mbps	110/55 Mbps	220/110 Mbps

† Earth station requirements depend on location within the ACTS antenna coverage. 90% of expected experimenter locations can use the lower $EIRP$ and G/T values.
‡ Lower burst rate used to compensate for rain fade.

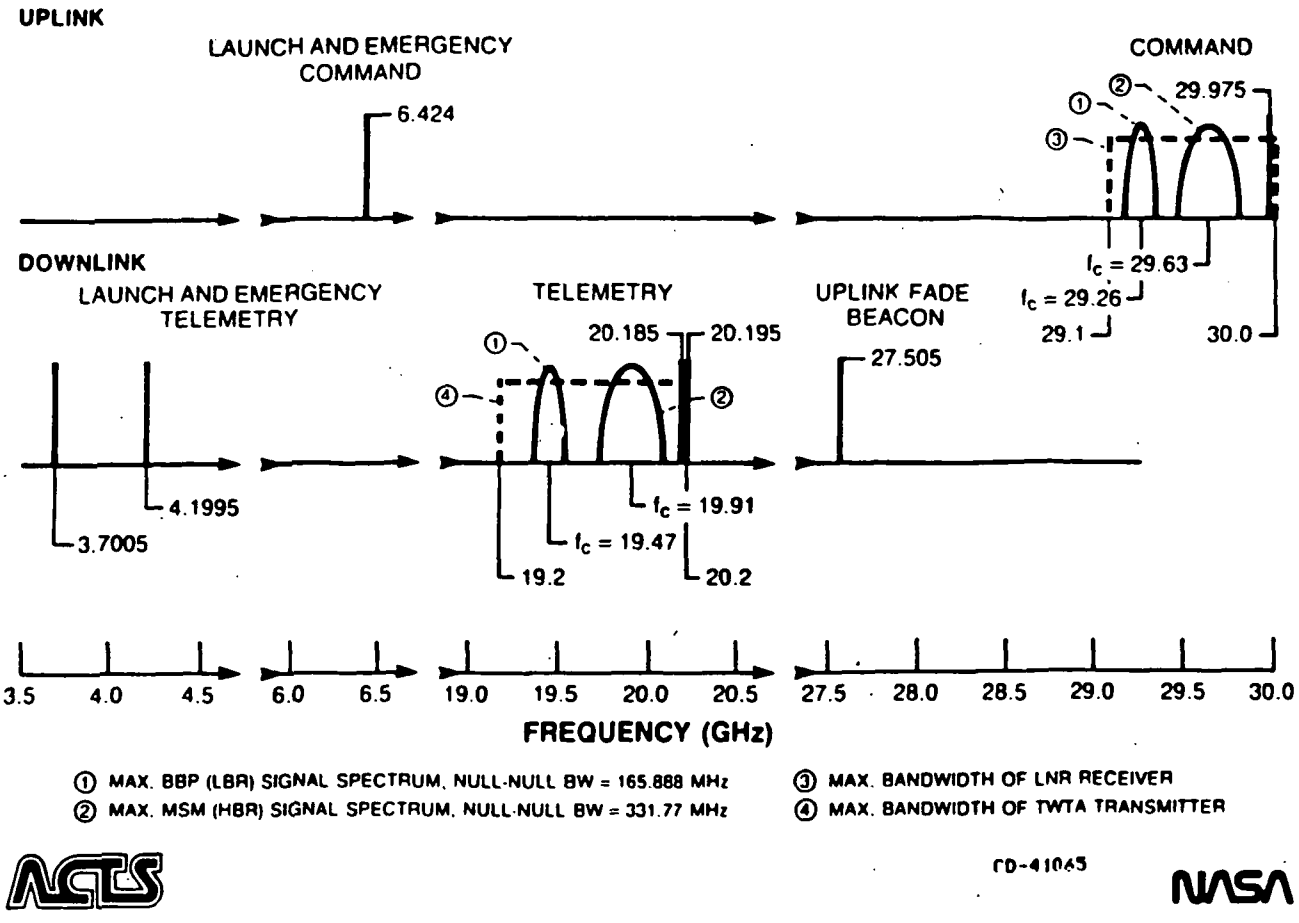

Figure 8.3: Frequency location of ACTS pilots.

Link Budget Assumed for Experiment

The link budget for the forward link is given in Table 8.4. Two equal power signals are assumed to be transmitted from the supplier in the forward link: the supplier generated pilot and the TDMA information signal, nominally set to 100 Kbps. In this plan, the pilot would be used as a beacon for the BPT's antenna to acquire and track the satellite signal, to set the frequency reference for the BPT, and for rain fade information. The performance of the MSM-LET terminal is taken from LeRC's link budgets: transmit losses are due to feed losses of 0.76 dB and waveguide losses of 3.43 dB. The transmit power varies from 10W to 65 W saturated. The $EIRP$ is taken to vary from 68 - 75 dBW depending on the drive level of the TWTA. Satellite multibeam edge of beam gain is taken from NASA's LET link calculation for 220 Mbps SMSK experiment using the Cleveland/Cleveland fixed beam mode. Satellite system temperature is calculated based on a receiver noise temperature of 3.4 dB and an antenna view temperature of 300 K as per the assumptions taken in the G/T calculation in the GE presentation at the ACTS Critical Design Review [2]. The downlink multibeam antenna gain and transmit losses are taken from [3] for the LA/San Diego beam. The effect of the limiter in the ACTS transponder is calculated as in [4]. First, limiter suppression factor, Γ, is calculated. Then, the transmit power is calculated from:

$$P_{TX} = P_{max}\left(\frac{SNR_{in}\,\Gamma}{SNR_{in}\,\Gamma + 1}\right)$$

where P_{max} is the maximum output of the satellite TWT - for two equal power signals transmitted on the uplink, the maximum power in each signal is $P_{max}/2$. The overall C/No is found from:

$$C/N_{overall} = \frac{1}{(C/N_{up}\,\Gamma)^{-1} + (C/N_{down})^{-1}}.$$

$C/No_{overall}$ for the forward link is 63.0 dB-Hz; the required C/No for 100 Kbps operation at a BER of 10^{-5} with a convolutional code with $r = 1/2$ and $K = 7$ is 54.5 dB-Hz. The forward link margin is therefore 8.5 dB.

The link budget for the return link is given in Table 8.5. Only one signal, an SCPC 4.8 Kbps signal, is transmitted from the BPT in the return link.[3] Again, the characteristics of the LA/San Diego beam are taken from [3] and system temperature assumes a receiver of 3.4 dB and an antenna view temperature of 300 K from [2]. To present a conservative link budget, the gain of the multibeam transmit antenna is taken from [3] to be 51.3 dB rather than the 53.1 dB in the LeRC's calculation for the 220 Mbps SMSK experiment. The transmit losses in the multibeam transmit antenna are taken from the above LeRC link calculation to be 4.1 dB rather than the lower 3.8 dB listed in [3]. $C/No_{overall}$ is calculated to be 44.4 dB-Hz as compared with the required C/No 41.3 dB-Hz for a BER of 10^{-5} with a convolutional code with $r = 1/2$ and $K = 7$. The return link margin is therefore 3.1 dB.

[3]This assumption translates into the use of one BPT in the LA/San Diego beam, in fact it may be interesting to simulate operation of a network with several BPT transmitting at once. The effect of several uplink signals upon the ACTS transponder limiter will then have to be taken into account.

Table 8.4: Forward Link Calculation with ACTS

Uplink Supplier to Satellite 30 GHz		Downlink Satellite to BPT 20 GHz	
MSM-LET at LeRC:		Satellite:	
f_{center} (uplink)	29.63 GHz	f_{center} (downlink)	19.91 GHz
Antenna Gain (4.7m)	61 dBi	Antenna Gain (3.3m)	48.1 dBi
TX Power	11.2 dBW/channel	TX Power (46W max)	13.5 dBW
TX Losses	-4.19 dB	TX Losses	-4.7 dB
TX Polarization	HP	TX Polarization	VP
EIRP	68 dBW	EIRP (61.7 dBW max)	56.9 dBW
$L_{pointing}$	-0.39 dB	$L_{pointing}$	-0.5 dB
Propagation Losses (Clear Weather):		Propagation Losses (Clear Weather):	
$L_{Atmosphere}$	-0.61 dB	$L_{Atmosphere}$	-0.92 dB
L_{Space} (Clev. to ACTS)	-213.46 dB	L_{Space} (ACTS to LA)	-209.88 dB
$L_{Polarization}$	-0.5 dB	$L_{Polarization}$	-0.5 dB
$L_{Co-channel\ Interference}$	-1.0 dB	$L_{Co-channel\ Interference}$	-1.0 dB
Satellite:		Basic Personal Terminal in LA:	
$L_{Pointing}$	-0.5 dB	$L_{Pointing}$	-0.7 dB
G/T (Clev. Fixed Beam)	19.6 dB/K	G/T	-9 dB/K
Antenna Gain (2.2m)	50.1 dBi	Antenna Gain	19.3 dBi
System Temperature	30.9 dBK	System Temperature	28.3 dBK
C/T	-128.85 dBW/Hz	C/T	-165.6 dBW/Hz
C/No_{up}	99.75 dB-Hz	C/No_{down}	63.0 dB-Hz
B_T (900 MHz)	89.54 dBHz		
SNR_{in}	10.21 dB		
Limiter Suppression Factor, Γ	2.0		
Overall Link Performance:			
$C/No_{overall}$		63.0 dB-Hz	
$C/No_{required}$ (for 100 kbps operation)		54.5 dB-Hz	
Link Margin		8.5 dB	

Table 8.5: Return Link Calculation with ACTS

Uplink BPT to Satellite 30 GHz		Downlink Satellite to Supplier 20 GHz	
Basic Personal Terminal in LA:		Satellite:	
f_{center} (uplink)	29.63 GHz	f_{center} (downlink)	19.91 GHz
Antenna Gain	22.8 dBi	Antenna Gain (3.3m)	51.3 dBi
TX Power	-5.5 dBW/channel	TX Power (46W max)	-28.4 dBW
TX Losses	-1.0 dB	TX Losses	-4.1 dB
TX Polarization	HP	TX Polarization	VP
EIRP	16.3 dBW	EIRP (64.8 dBW max)	18.78 dBW
$L_{pointing}$	-0.7 dB	$L_{pointing}$	-0.5 dB
Propagation Losses (Clear Weather):		Propagation Losses (Clear Weather):	
$L_{Atmosphere}$	-0.61 dB	$L_{Atmosphere}$	-0.92 dB
L_{Space} (LA to ACTS)	-213.34 dB	L_{Space} (ACTS to Clev.)	-210.0 dB
$L_{Polarization}$	-0.5 dB	$L_{Polarization}$	-0.5 dB
$L_{Co-channel\ Interference}$	-1.0 dB	$L_{Co-channel\ Interference}$	-1.0 dB
Satellite:		MSM-LET at LeRC:	
$L_{Pointing}$	-0.5 dB	$L_{Pointing}$	-0.39 dB
G/T (LA/SD Spot Beam)	17.3 dB/K	G/T	27 dB/K
Antenna Gain (2.2m)	49.2 dBi	Antenna Gain (4.7m)	57.5 dBi
System Temperature	30.9 dBK	System Temperature	30.5 dBK
C/T	-183.05 dBW/Hz	C/T	-167.52 dBW/Hz
C/No_{up}	45.55 dB-Hz	C/No_{down}	61.08 dB-Hz
B_T (900 MHz)	89.54 dBHz		
SNR_{in}	-43.99 dB		
Limiter Suppression Factor, Γ	$\pi/4$		
Overall Link Performance:			
$C/No_{overall}$		44.4 dB-Hz	
$C/No_{required}$ (for 4.8 kbps operation)		41.3 dB-Hz	
Link Margin		3.1 dB	

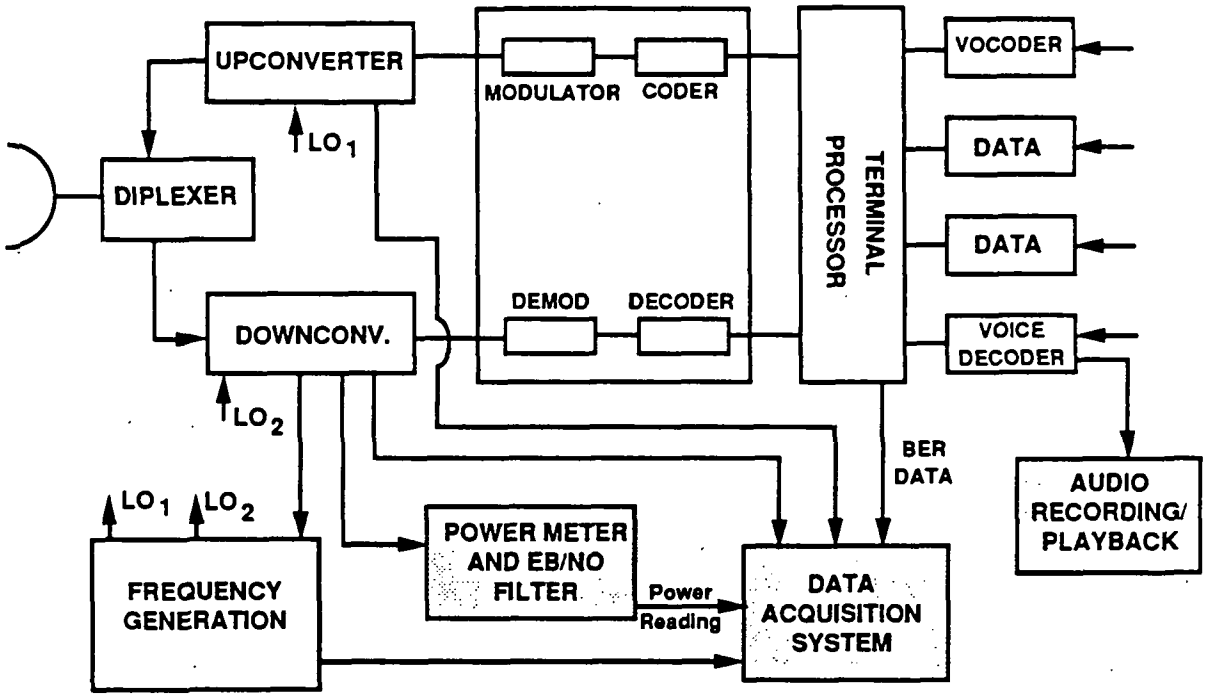

Figure 8.4: Modified user terminal.

From Tables 8.4 and 8.5, it can be seen that the dynamic range required at the output of the BPT is 132 dB, as the BPT transmits a -5.5 dBW signal and receives a -137.3 dBW signal. The dynamic range required at the MSM-LET is greater, 148 dB, as it transmits an 11.2 dBW signal and receives a -137.0 dBW signal.

Equipment Required for ACTS Experiment

For these experiments, it will be necessary to modify the BPT from the prototype specified in the PASS study report [4]. These modifications depend upon the number of BPTs that will be transmitting simultaneously (due to the limiter in the ACTS transponder) and on the certain specifications of the MSM-LET. A block diagram of the modified user terminal is shown in Figure 8.4. The interface equipment to the MSM-LET, which simulates the PASS NMC and the supplier, is shown in Figure 8.5. The measurement and analysis equipment is shown in each figure.

The ACTS experiment will require the following equipment: (1) two BPTs, one for test and one for backup or, possibly, both used simultaneously for network demonstration; (2) a modified NMC station containing only baseband to IF equipment, the NMC's function is to generate the pilot for the LA/SD beam and to handle channel assignment requests from BPTs; and (3) a modified supplier station containing only baseband to IF equipment, it is simplified to transmit one TDM signal to the BPT and to receive one or more SCPC signals

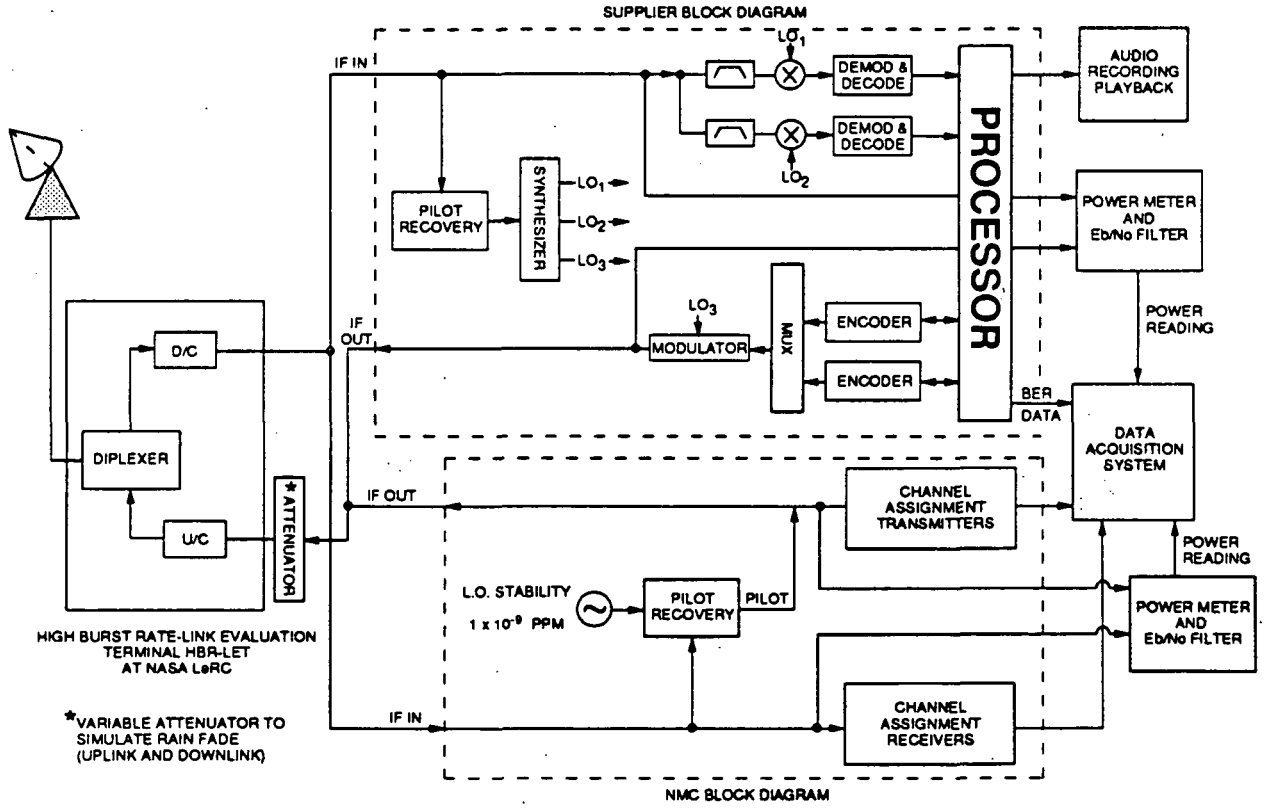

Figure 8.5: Interface equipment to Cleveland Master Station (MSM-LET).

317

from the BPT(s). The NMC and supplier equipment will be located at NASA LeRC; they will utilize the RF up/downconverters and the 4.7m antenna of the MSM-LET terminal. The latter interfaces with the NGS terminal to obtain rain fade information about the 20.185 GHz, 20.195 GHz, and 27.505 GHz beacons.

The following measurement and analysis equipment will be necessary: (1) BER measurement set-ups: one for each BPT and one to be shared by the supplier and NMC; (2) signal-to-noise measurement set-ups: one for the BPTs and one to be shared by the supplier and NMC; (3) data acquisition systems: one for the BPTs and one to be shared by the supplier and NMC; and (4) voice recording/playback equipment: one for the BPTs and one to be shared by the supplier and NMC.

The specifications for the receive portion, the transmit portion and the antenna of the modified user terminal are given in Tables 8.6, 8.7 and 8.8, respectively. Table 8.7 lists the BPT's transmit power as varying from 0.28 Watts to 0.56 Watts - the higher power is necessary to overcome the effects of the limiter if two BPTs were to use the same ACTS transponder.

8.4 Conclusion

The components of a personal access satellite system, i.e., a BPT and the supplier and NMC equipment, can be built in time for a demonstration of PASS using ACTS; however, the construction of certain components will necessitate the development of key technologies. Testing the PASS system on ACTS is feasible. The satellite will be used in the Microwave Switch Matrix mode and the front-end and antenna of the LeRC MSM-LET will be employed for the PASS supplier and NMC stations. Link margins of 8.5 dB and 3.1 dB on the forward and return links, respectively, can be then be achieved. These clear weather margins guarantee that a reasonable test of PASS is possible with ACTS.

8

Table 8.6: Preliminary Specifications for Modified BPT - Receive Side

Center Frequency	19.914 GHz		
RF Bandwidth	1000 MHz		
Max. No. of RX Subbands	9		
Subband Components:	Number/subband	Bit rate	BW
Pilot	1		5 KHz
BPT - TDMA Carrier	1 or more	100 Kbps	410 KHz
EPT - TDMA Carrier	1 or more	300 Kbps	1210 KHz
G/T	-9.0 dB/K		
Data Rates	96 Kbps (nominal) 48, 24 Kbps (fade)		
Modulation, Access	BPSK, TDMA		
Coding	r=1/2, K=7 convolutional code		
Received Signal Power	-137.3 dBW (nominal)		
C/No	63.0 dBHz		
C/No Required	54.5 dBHz (BER=10^{-5} at 100 Kbps)		
Link Margin	8.5 dB		
Noise Floor (kTB)	-144.2 dBW (@ 96 Kbps)		
Dynamic Range	TBD		
Received Pilot Power	-137.3 dBW (nominal)		
Frequency Acq. Time	500 ms (maximum)		
Modem Loss	1 dB		
LO Freq. and Phase Stab.	TBD		
Transponder Freq. Uncertainty	TBD		

Table 8.7: Preliminary Specifications for Modified BPT - Transmit Side

Center Frequency	29.634 GHz
RF Bandwidth	900 MHz
Max. No. of RX Subbands	9
Subband Components:	Number/subband BW
Demand Assigned 4.8 Kbps Channels	1 or more 24.2 KHz
Transmit Power	0.28 Watts (nominal) to 0.56 W
Link Margin	3.1 dB
EIRP	16.3 dBW (nominal)
Data Rates	4.8 Kbps (nominal) 2.4, 1.2 Kbps (fade)
Modulation, Access	BPSK, SCPC
Coding	r=1/2, K=7 convolutional code
Freq. Stability	TBD

Table 8.8: Preliminary Specifications for Modified BPT Antenna

Gain	22.8 dB @ 30 GHz 19.3 dB @ 20 GHz
Coverage	360° Azimuth 15-60° Elevation
Pointing Accuracy	TBD
Polarization	Linear*
Axial Ratio	2 dB (Design Goal)
Antenna Size	TBD
Acquisition Mode	Manual or Automatic
Acquisition Time	<2 sec under nominal conditions

* Linear polarization is assumed for link calculation. Transmit and receive signals from BPT are relayed by the ACTS satellite on orthogonal polarizations (horizontal and vertical).

Bibliography

[1] NASA, Office of Space Science and Applications. *ACTS ... The Blueprint for Future Telecommunications*, Oct. 5, 1989.

[2] NASA, Office of Space Science and Applications. *ACTS - Critical Design Review*, Jan. 22 - 23, 1990.

[3] F. M. Naderi and S. J. Campanella. NASA's Advanced Communications Technology Satellite (ACTS): An Overview of the Satellite, the Network, and the Underlying Technologies. In *AIAA 12th International Communications Satellite Systems Conference*, pages 204 – 224, March 13-17, 1988.

[4] Miles K. Sue, Editor. *Personal Access Satellite System Concept Study.* Jet Propulsion Laboratory, JPL D-5990 Edition, Feb. 1989.